

**SIMULATION AND OPTIMISATION OF PROCESS PARAMETERS IN  
EXPERIMENTAL VERTICAL PNEUMATIC MAIZE GRAIN DRYER**

**MESHACK KIPRUTO KORIR**

**A Thesis Submitted to the Graduate School in Partial Fulfilment of the Requirements for  
the Doctor of Philosophy Degree in Agricultural Engineering of Egerton University**

**EGERTON UNIVERSITY**

**AUGUST, 2023**

## DECLARATION AND RECOMMENDATION

### Declaration

This thesis is my original work and has not been presented in this University or any other for the award of a degree.

Signature.....

Date.....

**Meshack Kipruto Korir**

**BD11/12278/16**

### Recommendation

This thesis has been submitted with our approval as University supervisors.

Signature.....

Date.....

**Dr. Musa R. Njue, PhD**

Department of Agricultural Engineering

Egerton University

Signature.....

Date.....

**Prof. Daudi M. Nyaanga, PhD**

Department of Agricultural Engineering

Egerton University

## **COPYRIGHT**

© 2022, Meshack Kipruto Korir

All rights reserved. No part of this thesis may be reproduced, stored in a retrieval system or transmitted in any form or by any means, photocopying, scanning, recording or otherwise, without the permission of the author or Egerton University.

## **DEDICATION**

This thesis is dedicated to my wife, Marsaline Jepkirui Korir; our children, Mike Kiplagat, Melinda Jepchirchir and Medwin Kiprotich; my parents, Charles and Salina Kosgei; and my siblings, Jane, Dorcas, Emily, Rael, Faith, Rev. Eliud, Josphat and Bilah.

## **ACKNOWLEDGEMENTS**

First and foremost, I am grateful to the Almighty God, Whose Grace, Mercy, and Protection have been my guiding light throughout this journey. Without His divine intervention, I would not have successfully completed this study.

I extend my heartfelt appreciation to the African Development Bank (AfDB) through the Ministry of Higher Education, Science and Technology of Kenya, and Centre of Excellence in Sustainable Agriculture and Agribusiness Management (CESAAM) at Egerton University for the invaluable scholarship and financial support that made this research possible. Their support has been instrumental in bringing this study to fruition. My sincere thanks go to Egerton University for providing me with essential resources, including transport and laboratory services, during the execution of this research project. Your contribution has been pivotal in the achievement of my study's goals.

I am indebted to my supervisors, Dr. Musa R. Njue and Prof. Daudi M. Nyaanga, for their unwavering guidance, encouragement, and constructive criticism. Their scholarly insights and consistent support have steered me in the right direction. Their availability for consultations and their dedication to my academic growth have been invaluable.

A special acknowledgment goes to Dean of the Faculty of Engineering and Technology-Eng. Prof. Japheth Onyando, the Chairman of the Department of Agricultural Engineering, and all the Faculty and Departmental staff members. Your unwavering support and encouragement have been instrumental in my academic journey.

I am grateful to Dr. Frankline Manene for his support during the assembling and installation of sensors in the experimental dryer. His technical expertise has significantly contributed to the successful implementation of this study. I extend my appreciation to Mr. Justus Odhiambo and Mr. Peter Kariba of TECSOLS Limited-Engineering Workshop, Nakuru, for their technical assistance in the development of the experimental dryer. Your expertise has been invaluable in bringing this project to life. Lastly, my heartfelt thanks go to Mr. Alfred Mutua for his steadfast support during the data collection phase of this study. Your contribution has been essential in ensuring the successful completion of this research.

## ABSTRACT

Maize plays a critical role as a staple food and income source in Kenya, yet a significant annual loss of 12% to 20% of the national output occurs due to high moisture content. To mitigate this, drying maize to a safe moisture level of 13.5% (dry basis) before storage is essential. However, drying processes are energy intensive, consuming about 60% of the total invested energy. This emphasizes the need for appropriate technology which is the vertical pneumatic maize grain dryer (PMGD). The objectives of this research were to validate simulation models for mass flow rate (MFR) of maize grain, determine the effect of moisture content (MC), air temperature ( $T_a$ ), and MFR on moisture removal rate (MRR) and energy used (EU) in drying, and optimise energy proportioned for the grain drying ( $E_a$ ) and transportation ( $E_g$ ) to maximise MRR. Furthermore, optimise MC,  $T_a$ , and MFR to enhance MRR and minimise EU through Taguchi's method. The Beverloo (BEV), British Code of Practice (BCP), Tudor (TUD), and New simulation model ( $Q_N$ ) were validated using actual MFR data obtained from maize grain flow through horizontal circular orifices of diameters ranging from 0.040 m to 0.056 m. The experimental conditions included MC levels of 20%, 25%, and 30% (wet basis),  $T_a$  of 60°C, 70°C, and 80°C, and MFR of 720 kg/h, 771 kg/h, and 864 kg/h, while maintaining an air MFR of 547 kg/h during 2 hours drying period for 70.0 kg of the grain. The actual MFR ranged from 720 kg/h to 1735 kg/h, 650 kg/h to 2006 kg/h for BEV, 851 kg/h to 2378 kg/h for BCP, 867 kg/h to 2010 kg/h for TUD and 706 kg/h to 1757 kg/h for  $Q_N$  model. The Student's t-test results showed significant difference ( $P < 0.05$ ) between the actual and models MFR except  $Q_N$  ( $P > 0.05$ ). The effect of MC on MRR was significant ( $P < 0.05$ ). However, MC did not have significant ( $P > 0.05$ ) effect on  $E_a$  and  $E_g$ . The effect of  $T_a$  on MRR and  $E_a$  was significant ( $P < 0.05$ ) except  $E_g$  ( $P > 0.05$ ). The effect of MFR on MRR,  $E_a$  and  $E_g$  was not significant ( $P > 0.05$ ). The optimum  $E_a$  and  $E_g$  for MRR were 7.3 kWh and 2.2 kWh, respectively. Additionally, the optimum MC,  $T_a$  and MFR for MRR were 20%, 80°C and 720 kg/h while that for EU was 20%, 60°C and 720 kg/h, respectively. The Page model with coefficient of determination of 0.99 and root mean square error of 0.0049 was suitable for describing variation of moisture ratio with time in maize grain drying. The availability and use of the optimised PMGD would provide applicable solutions to energy challenges in maize grain drying, ultimately leading to reduced postharvest losses and enhanced food security and income for farmers. This would contribute to the attainment of sustainable development goals, particularly in eradicating hunger and poverty.

## TABLE OF CONTENTS

<b>DECLARATION AND RECOMMENDATION .....</b>	<b>i</b>
<b>COPYRIGHT .....</b>	<b>ii</b>
<b>DEDICATION.....</b>	<b>iii</b>
<b>ACKNOWLEDGEMENTS .....</b>	<b>iv</b>
<b>ABSTRACT.....</b>	<b>v</b>
<b>LIST OF TABLES .....</b>	<b>ix</b>
<b>LIST OF FIGURES .....</b>	<b>x</b>
<b>LIST OF ACRONYMS AND SYMBOLS .....</b>	<b>xi</b>
<b>CHAPTER ONE .....</b>	<b>1</b>
<b>INTRODUCTION.....</b>	<b>1</b>
1.1 Background .....	1
1.2 Statement of the Problem .....	4
1.3 Objectives.....	6
1.3.1 Broad Objective .....	6
1.3.2 Specific Objectives .....	6
1.4 Research Questions .....	6
1.5 Justification .....	6
1.6 Scope and Limitations.....	7
<b>CHAPTER TWO .....</b>	<b>8</b>
<b>LITERATURE REVIEW .....</b>	<b>8</b>
2.1 Grain Flow Rate Through Orifices.....	8
2.1.1 Mathematical Models for Grain Flow Rate Through Orifices .....	8
2.1.2 Parameters Influencing Grain Flow Rate Through Orifices.....	21
2.2 Drying Process Parameters .....	22
2.3 Distribution and Determination of Energy Used in Drying .....	26
2.4 Optimisation Techniques for Process Parameters.....	36
2.4.1 Taguchi’s Method.....	36
2.4.2 Fuzzy Logic Method.....	41
2.4.3 Genetic Algorithm .....	44
2.4.4 Response Surface Method .....	45

2.5 Drying Theory .....	45
2.6 Drying Models.....	46
2.6.1 Theoretical Models .....	48
2.6.2 Semi-Theoretical Models .....	52
2.6.3 Empirical Models .....	58
2.7 Research Gaps .....	59
2.8 Conceptual Framework .....	60
<b>CHAPTER THREE .....</b>	<b>62</b>
<b>MATERIALS AND METHODS .....</b>	<b>62</b>
3.1 Development of Experimental Vertical Pneumatic Maize Grain Dryer .....	62
3.2 Validating Simulation Models for Mass Flow Rate of Maize Grain through Horizontal Circular Orifices .....	67
3.3 Determining Effect of Moisture Content, air Temperature and Mass Flow Rate on Moisture Removal Rate and Energy Used in Drying .....	76
3.3.1 Effect of Moisture Content on Moisture Removal Rate and Energy used for Maize Grain Drying and Transportation .....	76
3.3.2 Effect of air Temperature on Moisture Removal Rate and Energy Used for Maize Grain Drying and Transportation .....	78
3.3.3 Effect of Mass Flow Rate on Moisture Removal rate and Energy Used for Maize Grain Drying and Transportation.....	79
3.4 Optimising Energy Proportioned for Maize Grain Drying and Transportation .....	80
3.5 Optimising Moisture Content, air Temperature and Mass Flow Rate in Maize Grain Drying .....	82
<b>CHAPTER FOUR.....</b>	<b>87</b>
<b>RESULTS AND DISCUSSIONS .....</b>	<b>87</b>
4.1 Validation of Simulation Models for Mass Flow Rate of Maize Grain Through Horizontal Circular Orifices .....	87
4.2 Effect of Moisture Content, air Temperature and Mass Flow Rate of Maize Grain on Moisture Removal Rate and Energy Used for Drying .....	91
4.2.1 Effect of Moisture Content on Moisture Removal Rate and Energy Used for Maize Grain Drying and Transportation .....	92



4.2.2 Effect of air Temperature on Moisture Removal Rate and Energy Used for Maize Grain Drying and Transportation .....	95
4.2.3 Effect of Mass Flow Rate on Moisture Removal Rate and Energy Used for Maize Grain Drying and Transportation .....	98
4.3 Optimisation of Energy Proportioned for Maize Grain Drying and Transportation.....	101
4.4 Optimisation of Moisture Content, air Temperature and Mass Flow Rate in Maize Grain Drying.....	104
<b>CHAPTER FIVE .....</b>	<b>111</b>
<b>CONCLUSIONS AND RECOMMENDATIONS.....</b>	<b>111</b>
5.1 Conclusions .....	111
5.2 Recommendations .....	112
<b>REFERENCES.....</b>	<b>114</b>
<b>APPENDICES.....</b>	<b>141</b>
Appendix A: Detail Drawing of Experimental Vertical Pneumatic Maize Grain Dryer .....	141
Appendix B: Code and Graphic User Interface for Simulation Models .....	142
Appendix C: Key Data and Analysis for Objective One .....	155
Appendix D: Key Data and Analysis for Objective Two.....	165
Appendix E: Key Data and Analysis for Objective Three .....	187
Appendix F: Key Data and Analysis for Objective Four .....	202
Appendix G: Published Paper on Objective One .....	221
Appendix H: Published Paper on Objective Two .....	222
Appendix I: Research Permit .....	223

## LIST OF TABLES

Table 2.1 Coefficients and exponents for selected grains.....	14
Table 2.2 Geometric constants based on product geometry .....	51
Table 3.1 Rewetting and resulting moisture content of maize grain .....	77
Table 3.2 Taguchi's L <sub>9</sub> orthogonal array experimental design with levels of energy proportioned for maize grain drying and transportation.....	81
Table 3.3 Taguchi's L <sub>9</sub> orthogonal array experimental design with levels of moisture content, air temperature and mass flow rate .....	83
Table 3.4 Selected drying models for grains .....	85
Table 4.1 Moisture removal rate for various combinations of energy proportioned for maize grain drying and transportation .....	102
Table 4.2 Moisture removal rate and energy used in drying for various combinations of moisture content, air temperature and mass flow rate of maize grain .....	105
Table 4.3 Constants and performance parameters of selected grain drying models.....	109

## LIST OF FIGURES

Figure 2.1 Schematic notation in cylindrical (a) and conical hopper (b).....	10
Figure 2.2 Flow zones for granular material discharge from funnel outlet .....	17
Figure 2.3 Free flowing zone for a funnel discharge orifice.....	18
Figure 2.4 Distribution of total supplied energy for grain drying.....	26
Figure 2.5 Optimisation process using Taguchi's method.....	38
Figure 2.6 Grey fuzzy logic method .....	41
Figure 2.7 Schematic of thin layer drying for drying process occurring from both sides .....	49
Figure 2.8 Conceptual framework of the research.....	61
Figure 3.1 Section view (a) and actual (b) experimental vertical pneumatic maize grain dryer ..	62
Figure 3.2 Section view of drying chamber.....	63
Figure 3.3 Section view of electric heater .....	64
Figure 3.4 Schematic drying process of maize grain.....	66
Figure 3.5 Schematic transportation process of maize grain during drying .....	67
Figure 3.6 Characteristic dimensions of maize grain.....	69
Figure 3.7 Algorithm for mass flow rate of maize grain through horizontal circular orifices .....	71
Figure 3.8 Experimental set up for validation of simulation models for mass flow rate.....	73
Figure 3.9 Proportioning of total supplied energy for maize grain drying .....	80
Figure 4.1 Effect of horizontal circular orifices diameters on mass flow rate of maize grain for actual and simulation models.....	87
Figure 4.2 Actual and New model mass flow rate of maize grain through horizontal circular orifices.....	90
Figure 4.3 Effect of moisture content on moisture removal rate in maize grain drying.....	92
Figure 4.4 Effect of moisture content on energy used for maize grain drying .....	94
Figure 4.5 Effect of moisture content on energy used for maize grain transportation .....	95
Figure 4.6 Effect of air temperature on moisture removal rate in maize grain drying .....	96
Figure 4.7 Effect of air temperature on energy used for maize grain drying.....	97
Figure 4.8 Effect of air temperature on energy used for maize grain transportation.....	98
Figure 4.9 Effect of mass flow rate on moisture removal rate in maize grain drying .....	99
Figure 4.10 Effect of mass flow rate on energy used for maize grain drying.....	100
Figure 4.11 Effect of mass flow rate on energy used for maize grain transportation.....	101

## LIST OF ACRONYMS AND SYMBOLS

### Acronyms

a	Mean length of the maize grain (m)
$a_1$	Parameter equal to zero for planar geometries
$A_1, A_2$	Geometric constants based on products geometry
ABSMD	Absolute mean difference
$A_d$	Cross sectional area of the air duct ( $m^2$ )
$A_e$	Effective orifice area ( $m^2$ )
AE	Available energy from natural gas (kJ)
AMD	Arithmetic mean diameter (m)
ANOVA	Analysis of variance
ASAE	American Society of Agricultural Engineers
$A_s$	Drying surface ( $m^2$ )
b	Mean width of maize grain (m)
B	Fuel gas consumption ( $m^3/h$ )
BCP	British code of Practice model
BEV	Beverloo model
c	Mean thickness of the maize grain (m)
$C_d$	Friction or discharge coefficient (dimensionless)
$C_o$	Drag coefficient
$C_{pa}$	Specific heat of air (kJ/kg.K)
$C_{pg}$	Specific heat of grain dry matter (kJ/kg.K)
$C_{pv}$	Specific heat of water vapour (kJ/kg $^{\circ}C$ )
$C_{pw}$	Specific heat of water (kJ/kg.K)
$C_{\tau}$	Shear friction correction
d	Dryer pipe diameter (m)
D	Diameter or side length of the orifice (m)
$D_e$	Effective hydraulic diameter (m)
$D_{eff}$	Effective moisture diffusivity ( $m^2/s$ )
$df_i$	Total degrees of freedom
$d_g$	Average size of particles (m)

$D_h$	Hydraulic radius (m)
$D_o$	Diameter of the orifice (m)
$\dot{E}$	Evaporation rate (kg/s)
$E_a$	Energy proportioned for maize grain drying (kWh)
EF	Modeling efficiency residuals
$E_g$	Energy used for maize grain transportation (kWh)
$E_h$	Energy used for heating the grain (kW)
$E_{the}$	Thermal energy supplied (kJ/kg)
EU	Total energy used for maize grain drying and transportation (kWh)
$EU_s$	Simulated energy used for maize grain drying and transportation (kWh)
FAO	Food and Agriculture Organisation
FAOStat	Food and Agriculture Organisation statistical database division
$F_{MC,5\%}$	F-value of initial moisture content of maize grain at 5% level of significance
$F_{MFR,5\%}$	F-value of mass flow rate of maize grain at 5% level of significance
$F_{Ta,5\%}$	F-value of drying air temperature at 5% level of significance
$g$	Acceleration due to gravity ( $m/s^2$ )
GMD	Geometric mean diameter (m)
H	Height of material in the hopper (m)
$h_a$	Specific enthalpy of air (kJ/kg)
$h_{amb}$	Specific enthalpy of ambient air (kJ/kg)
$H_d$	Lower gas heat power ( $kJ/m^3$ )
$h_c$	Convective coefficient of the heat transfer ( $W/m^2K$ )
$h_d$	Specific enthalpy of the dried product (kJ/kg)
$h_h$	Specific enthalpy of heated air (kJ/kg)
$h_i$	Specific enthalpy of the inlet air (kJ/kg)
$H_o$	Enthalpy of the outlet air (kJ/kg)
$h_o$	Specific enthalpy of the exhaust air (kJ/kg)
$h_s$	Specific humidity of air (kg of water/kg of air)
$h_t$	Total coefficient of heat transfer ( $W/m^2K$ )
$h_w$	Specific enthalpy of the wet product (kJ/kg)
j	Level number of experiment parameter

$k_a$	Thermal conductivity of air (W/m <sup>2</sup> K)
$K_p$	Shape factor
$L$	Thickness of the diffusion path (m)
LCD	Fisher's least significant difference
$l_v$	Latent heat of evaporation of free water (kJ/kg)
$m$	Number of experiments in the orthogonal array
$M$	Local moisture content (kg of water/kg of dry matter) or (% , dry basis)
$M_1$	Moisture content of undried maize grain (%)
$M_2$	Moisture content of dried maize grain (%)
$m_a$	Mass of dry air (kg)
$\dot{m}_a$	Mass flow rate of air (kg/s)
$\dot{m}'_a$	Minimum air mass flow rate (kg/s)
MAE	Mean absolute error
MAPE	Mean absolute percentage error
MBE	Mean bias error
MC	Moisture content (%)
$M_{cr}$	Critical moisture content (% , dry basis)
$M_e$	Equilibrium moisture content (% dry basis)
MFR	Mass flow rate (kg/h)
$m_{fr}$	Feed rate in dry basis (kg/kg.h)
$m_g$	Mass of maize grain discharged through horizontal circular orifice (kg)
$M_i$	Initial moisture content (% dry basis)
$m_i$	Quantity of moist material (kg/kg.h)
MR	Moisture ratio
MRR	Moisture removal rate (kg/kg.h)
$MRR_1$	Simulated moisture removal rate with respect to energy proportioned for maize grain drying and transportation (kg/kg.h)
$MRR_2$	Simulated moisture removal rate in maize grain drying with respect to moisture content, air temperature and mass flow rate (kg/kg.h)
$m_{sa}$	Specific air mass flow rate (kJ/kg)
MSE	Mean squared error

$m_w$	Wet mass of grain (kg)
$n$	Number of constants
$N$	Number of observations
$Nu$	Nusselt number
$N_w$	Drying rate ( $\text{kg}/\text{m}^2 \cdot \text{s}$ )
OA	Orthogonal array
$p$	Experiment parameters
$P$	Mean relative percentage error
PMGD	Experimental vertical pneumatic maize grain dryer
$P_h$	Heat power (kW)
PID	Proportional integral derivative
$P_s$	Sensible heat in the dryer outlet air (kW)
$P_t$	Total heat power for drying (W)
PT	Platinum
$P_w$	Energy for evaporation of moisture (kW)
$Q$	Heat transfer rate (W)
$Q_a$	Sensible heat gain by the inlet air (kJ/s)
$Q_{BCP}$	British Code of Practice model mass flow rate of maize grain through horizontal circular orifice ( $\text{kg}/\text{kg} \cdot \text{h}$ )
$Q_{BEV}$	Beverloo model mass flow rate of maize grain through horizontal circular orifice ( $\text{kg}/\text{kg} \cdot \text{h}$ )
$Q_i$	Heat input rate of the air (kJ/h)
$Q_{conv}$	Convective heat for drying (kJ/h)
$Q_d$	Energy output of the dried product (kJ/h)
$Q_h$	Heat for heating of the drying material (kJ/h)
$Q_l$	Heat Losses (kJ/h)
$Q_{l,amb}$	Heat losses to the ambient air (kJ/h),
$Q_{l,exh}$	Heat losses through the exhaust air (kJ/h)
$Q_m$	Heat for moisture evaporation (kJ/h)
$Q_N$	New model mass flow rate of maize grain through horizontal circular orifices ( $\text{kg}/\text{h}$ )
$Q_o$	Heat output rate from the exhaust air (kJ/h)

$Q'_o$	Exhaust heat rate based on a minimum air flow rate (kJ/h)
$Q_q$	Total heat quantity (kJ/h)
$q_s$	Specific energy consumption (kJ/kg)
$Q_{TUD}$	Tudor model mass flow rate of maize grain through horizontal circular orifice (kg/kg.h)
$q_v$	Volumetric air flow rate ( $m^3/s$ )
$Q_w$	Energy input rate of the wet product (kJ/h)
$r$	Coefficient of correlation
$R^2$	Coefficient of determination
$r_f$	Dry basis feed rate (kg/kg.h)
RMSE	Root mean square error
$s$	Standard deviation
SE	Standard error
SLR	Solid loading ratio
S/N	Signal-to-noise (dB)
$S/N_{EUs}$	Simulated signal to noise ratio for energy used for maize grain drying and transportation (dB)
$S/N_{MRR1}$	Simulated signal to noise ratio for MRR with respect to energy proportioned for maize grain drying and transportation (dB)
$S/N_{MRR2}$	Simulated signal to noise ratio for moisture removal rate with respect to moisture content, air temperature and mass flow rate (dB)
$S/N_L$	Signal to noise if the system is optimised when the response is as large as possible (dB)
$S/N_N$	Signal to noise if the objective is to reduce variability around a specific target (dB)
$S_p$	Corrected sum of squares
$SS_e$	Sum of the squared error
SST	Total sum of the squared deviations
$SS_p$	Sum of the squared deviations
$s_y^2$	Variance of observed data
T	Temperature distribution ( $^{\circ}C$ )
t	Time interval (s)
$T_a$	Drying air temperature ( $^{\circ}C$ )



$T_{amb}$	Ambient drying air temperature ( $^{\circ}\text{C}$ )
$t_{crit, 5\%}$	t-critical at 5% level of significance
$T_i$	Air temperature at the inlet of dryer ( $^{\circ}\text{C}$ )
$T_{max}$	Maximum air temperature for maize grain drying ( $^{\circ}\text{C}$ )
$T_o$	Air temperature at the outlet of dryer ( $^{\circ}\text{C}$ )
$t_{stat}$	t-statistics at 5% level of significance
TUD	Tudor model
USB	Universal serial bus
$v_a$	Inlet air velocity of the dryer (m/s)
VFR	Volume flow rate ( $\text{m}^3/\text{h}$ )
$V_n$	Volume of natural gas used ( $\text{m}^3$ )
$V_p$	Variance of the experiment parameter
$V_q$	Quantity of drying air ( $\text{m}^3/\text{h}$ )
W	Quantity of moisture evaporated (kg/kg.h)
$w_c$	Content of the wet material at the inlet of the dryer (%)
$w_f$	Final weight of the sample (g)
$w_i$	Initial weight of the sample (g)
$w_o$	Content of the wet material at the outlet of the dryer (%)
$W_1$	Weight of undried maize grain (kg)
$W_2$	Weight of dried maize grain (kg)
$w_1$	Specific humidity for inlet air (kg of water/kg of air)
$w_2$	Specific humidity for outlet air (kg of water/kg of air)
X	Diffusion path (m)
$X^2$	Reduced Chi-square
$X_d$	Moisture content ratio of the dried product
$x_i^*(k)$	Normalized data
$x_i(k)$	Observed data
$X_w$	Moisture content ratio of the wet product
y	Observed data
$\bar{y}$	Average of observed data

## Symbols

$\alpha$	Angle between the inclined funnel walls and horizontal ( $^{\circ}$ )
$\beta$	Angle between the wall of funnel shaped hopper and vertical line ( $^{\circ}$ )
$\beta_w$	Angle of slide between flowing and non-flowing particles at the orifice edge ( $^{\circ}$ )
$\delta$	Ratio of the height arch to orifice diameter
$\Delta H$	Enthalpy difference (kJ/kg)
$\Delta h_s$	Difference in specific humidity between inlet air temperature and outlet air at temperature
$\Delta_i(k)$	Absolute value of the difference between functions
$\Delta_{max}$	Global maximum value in different data series
$\Delta_{min}$	Universal minimum value in various data sets
$\Delta t$	Temperature difference (K)
$\Delta T_{ml}$	Middle logarithm difference of temperature ( $^{\circ}C$ )
$\varepsilon_r$	Absolute residual error (%)
$\lambda$	Compressibility and density function of the of the material ( $-1.46 \times 10^{-8} m^2$ )
$\eta_j$	Mean signal to noise ratio for the $i^{th}$ experiment
$\eta_{sim}$	Residual error
$\eta_{sim,\mu\%}$	Simulation performance of the models at residual error interval (%)
$\eta_t$	Degree of thermal of utilization (%)
$\phi$	Friction angle of the material on the funnel walls ( $^{\circ}$ )
$\varphi$	Sphericity or shape factor (dimensionless)
$\Psi_{exp,I}$	Experimental value
$\Psi_{sim,I}$	Simulated value
$\rho_g$	Bulk density of maize grain ( $kg/m^3$ )
$\mu$	Sliding coefficient of friction
$\mu_i$	Residual error interval (%)
$\zeta$	Distinguishing coefficient in the range of 0 and 1
$\xi_i(k)$	Relational coefficient for the $i^{th}$ experiment using $k^{th}$ response
$\gamma_i$	Grey relational grade

# CHAPTER ONE

## INTRODUCTION

### 1.1 Background

Maize holds a crucial role as a staple food crop in Kenya and sub-Saharan Africa (Cairns *et al.*, 2013; Food and Agriculture Organization Statistics [FAOStat], 2019; Smale *et al.*, 2011). Globally, it ranks as the third most valuable cereal grain, following wheat and rice (Cardona *et al.*, 2004). This crop significantly contributes to the caloric intake and income generation for numerous households worldwide (FAOStat, 2021; FAOStat, 2019; Rehman, 2006).

Global maize production stands at approximately 10.14 billion metric tonnes (De Groote *et al.*, 2013; García-Lara & Serna-Saldivar, 2019). Africa contributes about 7% to the global output, with Eastern and Southern Africa being prominent (FAOStat, 2021; FAOStat, 2014; Verheye, 2010). In Kenya, annual maize production reaches around 3 million tonnes, while per capita consumption is approximately 88 kg (FAOStat, 2019; Kenya National Bureau of Statistics [KNBS], 2020; Kirimi *et al.*, 2011). Increasing demand for maize is projected in developing nations due to its versatile applications in food processing, animal feed, and ethanol production (Suleiman *et al.*, 2013). Consequently, there's a need to enhance maize production on existing agricultural land to meet growing requirements (Ribaut & Ragot, 2006). The Kenyan government's policy interventions have led to improved production and marketing in the maize subsector (Olwande *et al.*, 2009).

In sub-Saharan Africa, maize grain weight losses of 5% to 45% are attributed to pest infestations (Anankware *et al.*, 2013; Tefera *et al.*, 2011). In Kenya, postharvest losses of maize grain range from 12% to 20% of the national production (Akoko *et al.*, 2021; Onyango & Kirimi, 2017). Major factors contributing to these losses include high grain moisture content, environmental conditions, and biological agents like insect pests and mold (Suleiman & Kurt, 2015).

Maize is typically harvested with a moisture content ranging from 21.9% to 31.6%, on a wet basis (FAO, 1992; Li *et al.*, 2021). This necessitates the drying process to reduce the moisture content to a recommended level of 13.5% on a dry basis for safe storage (Mrema *et al.*, 2012). Drying plays a critical role as it prevents mold growth and aflatoxin contamination, which can render the product unsuitable for human and livestock consumption (Korir & Bii, 2012).

Additionally, drying reduces losses caused by respiration, insect infestations, and pest attacks (Tiwari, 2002; Twidell & Weir, 2015). Moreover, it extends the shelf life and preserves the quality of the product, contributing to the availability of food for the growing global population (Barnwal & Tiwari, 2008). Making food accessible without the need for additional quality improvement resources supports rural development and poverty reduction (Randela, 2003; Rembold *et al.*, 2011).

Despite its significance across agriculture and other sectors, the drying process is energy-intensive (Thakur & Gupta, 2006; Verma, 1993). It is estimated that drying consumes around 60% of the total energy invested in the process (Brooker *et al.*, 1992; Chakraverty *et al.*, 2003).

Open sun drying is a widely practiced method for drying maize grain in tropical and sub-tropical regions, primarily due to economic considerations (Agrawal *et al.*, 1998; Bakker-Arkema *et al.*, 1999). This approach involves spreading the grain on mats or paved surfaces and exposing it to ambient conditions (Bakker-Arkema *et al.*, 1999; Basunia & Abe, 2001). However, open sun drying is labor-intensive and heavily reliant on factors such as solar radiation, ambient air temperature, relative humidity, wind velocity, soil temperature, grain layer thickness, and the type of grain being dried (Jain & Tiwari, 2003). This method faces sustainability challenges due to limited available space for drying, which is further exacerbated by population growth. It also lacks temperature control, leading to potential overheating of the grain. Additionally, the open nature of the process exposes the product to contamination from dust, foreign materials, insects, animals, rodents, and bird droppings (Golob *et al.*, 2002; Jewell *et al.*, 1995).

The utilization of mechanized grain dryers has brought improvements in drying efficiency and product quality compared to open sun drying. However, these dryers consume more energy as drying and transportation of the product are separate processes, resulting in higher drying costs (Ajay *et al.*, 2009). Therefore, there is a pressing need to explore alternative drying technologies that can address the energy related challenges posed by existing methods.

Pneumatic drying is a promising technology wherein grain is dried while being transported within a vertical duct by a heated airstream (Pelegrina & Crapiste, 2000). This method is considered energy-efficient as drying and conveying occur simultaneously. Additionally, recirculating the drying air allows energy recovery from the outlet air that would otherwise be

lost to the atmosphere. The high degree of dispersion achieved through entraining the material in the heated airstream enhances the contact between the drying air and the grain, making pneumatic drying more efficient in terms of energy performance compared to conventional methods (Jayaraman & Gupta, 2014).

Pneumatic drying offers several advantages. It reduces human involvement in the drying process, safeguards the grain from external contaminants, requires minimal space, is not weather-dependent, and achieves high-quality drying with reduced heat damage (Strumillo & Kudra, 1986a; Tanaka *et al.*, 2008). The key characteristics of a pneumatic dryer include concurrent flow, short residence times, small particles, and high temperatures (Pelegrina & Crapiste, 2000). During drying, there's an exchange of heat, mass, and momentum between the air and particles (Hidayat & Rasmuson, 2007). The heat and mass transfer coefficients, as well as the drying rate, are influenced by parameters such as air velocity, moisture content of the product, solid loading, and bend radius ratio. The large surface area for heat and mass transfer contributes to higher drying rates and capacity (El-Behery *et al.*, 2012).

Pneumatic drying is particularly suited for handling high flow rates of solid particles and achieving high moisture removal rates from the particles (Indarto *et al.*, 2007). It's applicable to heat-sensitive materials and for removing external moisture. While inlet temperatures are often high, the product is not unduly overheated, making it a commonly used convective and continuous drying system in industries (Baeyens *et al.*, 1995).

The conveyance of the product in pneumatic drying can be categorized into dilute and dense phase. Dilute phase involves air-suspending materials and transporting them from one location to another by maintaining a sufficient air velocity. This is a continuous process characterized by high velocity, low pressure, and a low product-to-air ratio. In contrast, dense phase relies on a pulse of air to move a slug of material from one location to another. It is a batch process characterized by low velocity, high pressure, and a high product-to-air ratio (Tupkari & Vanalkar, 2015).

A typical pneumatic dryer consists of a heater, product feeder, dryer duct and air-product mixture separator. The product is introduced into the airstream by the feeder, conveyed up upward

through the dryer duct and the air-product mixture is then separated in the cyclone (Bunyawanchakul, 2006).

The main process parameters that significantly influence grain drying include air temperature, relative humidity, air flow rate, and the initial moisture content of the product (Amer, 1999; Bains *et al.*, 1989; Eissen *et al.*, 1985; Filková & Mujumdar, 1995; Fohr & Arnaud, 1992; Meisami-Asl *et al.*, 2010). These parameters play a critical role in determining the efficiency and effectiveness of the drying process.

Simulation, in the context of engineering and research, refers to the imitation or replication of the behavior of a system or process (Frangopoulos *et al.*, 2002). It serves as a valuable tool in the design process, saving time and resources that would otherwise be required for extensive experimentation to achieve optimal system performance. Simulation involves creating a model that mimics the behaviors of interest, experimenting with this model to gather observations, understanding, summarising, and generalizing these behaviours. It's akin to conducting real-world field tests but in a controlled and often computational environment. Simulation is particularly useful for testing and comparing different designs, validating and explaining outcomes, and making recommendations based on the study (White & Ingalls, 2018).

Optimisation, on the other hand, involves the process of maximizing or minimizing a desired objective function while adhering to any prevailing constraints (Belegundu & Chandrupatla, 2019). Optimisation techniques are used across various research fields to determine solutions that either maximize or minimize specific parameters of interest (Alonso *et al.*, 2020). In the context of grain drying, optimisation could be used to find the best combination of process parameters such as air temperature, humidity, and flow rate to achieve the desired drying efficiency or quality outcomes while considering limitations or constraints. This allows researchers and engineers to fine-tune the drying process for better performance and resource utilization.

## **1.2 Statement of the Problem**

The drying process plays a crucial role in reducing the maize grain moisture to a safe storage level of 13.5% (dry basis), which has numerous benefits including extending shelf life, enhancing quality, preventing insect infestations, and minimising mold and aflatoxin

contamination risks (Brooker *et al.*, 1992; Mrema *et al.*, 2012). Based on the energy related challenges associated with existing drying methods, an experimental vertical pneumatic maize grain dryer was developed and tested as a potential solution. This innovative dryer employed horizontal circular orifices to control the mass flow rates of maize grain, indicating that determining the appropriate orifice size is essential when targeting specific mass flow rates for effective maize grain handling.

In pneumatic drying, the critical process parameters involve the moisture content, air temperature, and mass flow rate of the maize grain. However, there remains a knowledge gap regarding how these specific parameters influence the moisture removal rate and energy used in drying. Drying processes are energy intensive, accounting for a significant portion of the total invested cost, as highlighted in previous research (Aghbashlo *et al.*, 2013; Brooker *et al.*, 1992; Chakraverty *et al.*, 2003; Tsotsas & Mujumdar, 2008; Van't Land, 2011). Despite this understanding, there is still a need to bridge the knowledge gap concerning how the energy allocation for grain drying and transportation can be optimised to achieve the highest possible moisture removal rate. The interplay of the moisture content, air temperature, and mass flow rate of the maize grain presents an avenue for improving the moisture removal rate while concurrently minimising energy consumption during drying.

However, determining the optimum combination of process parameters specifically, the moisture content, air temperature, and mass flow rate of maize grain required for achieving the highest moisture removal rate and least energy used in maize grain drying has not yet been definitively established. Although various drying models for grains have been developed and tested, there is still a gap in understanding which of these models is most suitable for accurately describing the drying characteristics of maize grain within the experimental vertical pneumatic dryer. Addressing these knowledge gaps would not only enhance our comprehension of the drying process within the experimental vertical pneumatic maize grain dryer but also potentially lead to more efficient drying method, reducing energy consumption, and improving overall grain quality.

## **1.3 Objectives**

### **1.3.1 Broad Objective**

The broad objective of this research was to establish simulation model for mass flow rate of maize grain and optimise selected process parameters in an experimental vertical pneumatic dryer.

### **1.3.2 Specific Objectives**

The following were the specific objectives of this research:

- (i) To validate simulation models for mass flow rate of maize grain through horizontal circular orifices in an experimental vertical pneumatic dryer.
- (ii) To determine effect of moisture content, air temperature and mass flow rate of maize grain on moisture removal rate and energy used in an experimental vertical pneumatic dryer.
- (iii) To optimise energy proportioned for drying and transportation of maize grain in an experimental vertical pneumatic dryer.
- (iv) To optimise moisture content, air temperature and mass flow rate of maize grain in an experimental vertical pneumatic dryer.

## **1.4 Research Questions**

- (i) What is the best simulation model for mass flow rate of maize grain through horizontal circular orifices in an experimental vertical pneumatic dryer?
- (ii) How do moisture content, air temperature and mass flow rate of maize grain influence moisture removal rate and energy used in an experimental vertical pneumatic dryer?
- (iii) What is the optimum energy proportioned for drying and transportation of maize grain in an experimental vertical pneumatic dryer?
- (iv) What is the optimum moisture content, air temperature and mass flow rate of maize grain in an experimental vertical pneumatic dryer?

## **1.5 Justification**

This study successfully developed a dependable simulation model to predict the mass flow rate of maize grain through horizontal circular orifices within an experimental vertical pneumatic dryer. This crucial mass flow rate data is invaluable for determining the optimum size of orifices to control the flow during maize grain handling. The research also significantly contributed to the understanding of how key process parameters such as moisture content, air temperature, and



mass flow rate of maize grain influence both the moisture removal rate and the energy consumption within the experimental vertical pneumatic dryer.

Furthermore, the research identified the optimum energy distribution required for achieving the highest moisture removal rate during both maize grain drying and transportation processes. This insight is pivotal for making informed decisions regarding the allocation of total energy resources for maize grain drying. Additionally, the research revealed the ideal combination of moisture content, air temperature, and mass flow rate to achieve the dual objectives of maximising moisture removal rate while minimising energy consumption in maize grain drying.

The established drying model serves as a valuable tool for simulating the variations in moisture ratios over time during the maize grain drying process. By doing so, the research provides practical applications in the development of the experimental vertical pneumatic maize grain dryer, enhancing the capacity to address energy related challenges and other issues associated with maize grain drying. This, in turn, leads to a reduction in postharvest losses, contributing to improved food security and increased income for farmers. Ultimately, these outcomes align with the broader goals of achieving sustainable development, including the eradication of hunger and poverty.

## **1.6 Scope and Limitations**

This research investigated the mass flow rates of maize grain through horizontal circular orifices with varying diameters, ranging from 0.040 m to 0.056 m. These determined flow rates were then utilized to validate the simulation models. The research involved employing several key parameters, including the levels of moisture content within the maize grain (set at 20%, 25%, and 30% on a wet basis), the temperature of the drying air (60°C, 70°C, and 80°C), and the mass flow rates of the maize grain (720 kg/h, 771 kg/h, and 864 kg/h).

Additionally, the research explored the energy allocation for both maize grain drying and transportation processes. Three energy levels were considered: 3.5 kWh, 5.5 kWh, and 7.7 kWh for drying, and 2.2 kWh, 2.4 kWh, and 2.8 kWh for transportation. Throughout the experiments, a consistent mass flow rate of drying air of 547 kg/h was maintained. The relative humidity of the drying air was not actively controlled but closely monitored throughout the drying process to evaluate its potential effect.

## CHAPTER TWO

### LITERATURE REVIEW

This chapter provides an overview of relevant literature in several key areas, including simulation models for grain flow rate through different orifices, the impact of process parameters on grain drying, the allocation of total supplied energy for drying, optimization of process parameters, and fundamental drying theories and models. The literature review serves to establish a comprehensive foundation for the research by highlighting existing knowledge and gaps in the field, which will inform the research methodology and findings

#### 2.1 Grain Flow Rate Through Orifices

Understanding the flow rate of grains through various sizes, shapes, and orientations of orifices is crucial for determining the appropriate orifice dimensions in grain handling. Several researchers have investigated the flow rates of grains and other granular materials through horizontal orifices (Beverloo *et al.*, 1961; Chang & Converse, 1988; Chang *et al.*, 1984; Gregory & Fedler, 1987; Moysey *et al.*, 1988). Their studies have revealed that the grain flow rate through an orifice remains unaffected by the depth of the grain above it (Ewalt & Buelow, 1963; Fowler & Glastonbury, 1959). Additionally, it has been observed that the flow rate of granular materials through horizontal orifices increases proportionally with the orifice diameter raised to a power ranging from 2.5 to 3.0 (Chang *et al.*, 1984; Gregory & Fedler, 1987).

##### 2.1.1 Mathematical Models for Grain Flow Rate Through Orifices

The rate at which grains flow through an orifice is influenced by both the orifice area and the hydraulic diameter, which follows a power correlation with an exponent of 0.5 as presented in equation 2.1 (Beverloo *et al.*, 1961):

$$Q = C_d A_e \sqrt{g D_e} \tag{2.1}$$

where,

Q is volume flow rate (m<sup>3</sup>/s)

C<sub>d</sub> is friction or discharge coefficient (dimensionless)

A<sub>e</sub> is effective area computed from D<sub>e</sub> (m<sup>2</sup>)

g is gravitational acceleration (m/s<sup>2</sup>)

D<sub>e</sub> is effective hydraulic diameter (m)

The effective hydraulic diameter ( $D_e$ ) is given by equation 2.2:

$$D_e = D_h - K_p d_g \quad (2.2)$$

where,

$D_h$  is hydraulic diameter (m)

$K_p$  is shape factor (dimensionless)

$d_g$  is average size of particles (m)

Beverloo's law is applicable to granular samples where the diameter of the grains ( $d_g$ ) is greater than 0.5 mm, and the hydraulic diameter ( $D_h$ ) is sufficiently large to ensure smooth grain flow without jamming. Therefore, the application of Beverloo's law for grain flow rate through orifices is valid only when  $D_h$  is significantly larger than  $d_g$ . However, if  $D_h$  falls below a critical value, the flow can be interrupted due to the formation of arches or domes within the material (Zuriguél *et al.*, 2003). For dried maize grain with a moisture content of 11% (wet basis), flowing through a vertical orifice with a diameter equal to or less than 13 cm, the flow rate can be calculated using equation 2.3 (Ewalt & Buelow, 1963):

$$Q = aD_o^b \quad (2.3)$$

where,

$D_o$  is diameter or side length of the orifice (m)

$a$  and  $b$  are constants

The flow rates of granular materials from hoppers have been documented in previous studies (Nedderman *et al.*, 1982). The examination of granular material flow through orifices is commonly conducted using cylinder-shaped and conical-shaped hoppers, as depicted in Figure 2.1 (Nedderman *et al.*, 1982).

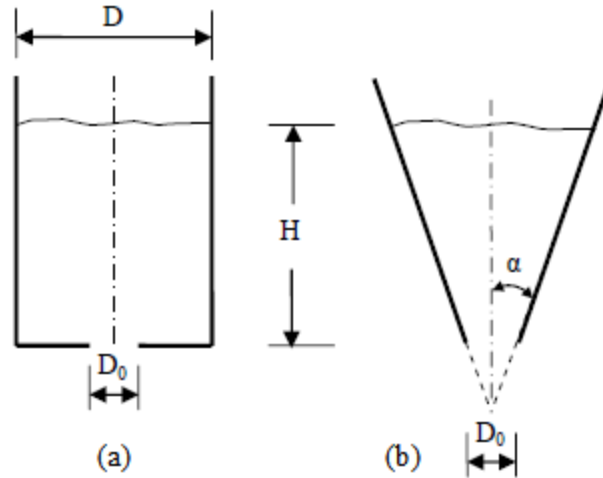


**Figure 2.1** Schematic notation in cylindrical (a) and conical hopper (b)

The quantity of material within the hopper, characterized by its height ( $H$ ), has been studied in relation to its impact on flow rate, revealing that  $H$  has no significant effect on the flow rate (Nedderman *et al.*, 1982). Studies have shown that the mass flow rate (MFR) remains independent of  $H$ . However, there is a proportional relationship between MFR and  $H$  raised to the power of 0.04 (Newton *et al.*, 1945). It has also been observed that MFR remains constant when  $H$  surpasses a critical value. This critical value has been proposed as 2.5 times the orifice diameter ( $D_0$ ) (Xie & Puri, 2006), and during batch discharge, the MFR remains consistent until the material head in the hopper becomes less than the hopper diameter ( $H < D$ ) (Brown & Richards, 1959).

At lower values of  $H$ , the top surface of the material displays a central depression (Nedderman *et al.*, 1982). The MFR remains constant as long as  $H$  at the center line is greater than the orifice diameter ( $D_0$ ) (Myers & Sellers, 1978; Rose & Tanaka, 1959). Consequently, MFR remains independent of  $H$  until the hopper is nearly empty, although the precise value of the critical height is not firmly established (Nedderman *et al.*, 1982). Nevertheless, the mass flow rate of particles has been demonstrated to be unaffected by the vessel diameter ( $D$ ), provided  $D$  is not excessively small (Nedderman *et al.*, 1982). Additionally, MFR remains consistent when  $D > 2.5$  times  $D_0$  (Brown & Richards, 1960; Ketchum, 1919). Correction factors for smaller  $D$  values have been reported (Brown & Richards, 1960). However, a criterion of  $D - D_0 > 30$  times  $d_g$  has been established (Agbetoye & Ogunlowo, 2010). Notably, larger flow rates were observed for smaller  $D$  values, particularly as  $D$  approaches  $D_0$ , and the entire mass of material exhibited

indefinite acceleration under gravity. The correlation for mass flow rate (MFR) has been documented as presented in equation 2.4 (Wieghardt, 1952):

$$\text{MFR} \propto (D_o - K_p d_g)^2 \quad (2.4)$$

where,

MFR is mass flow rate (kg/s)

$D_o$  is orifice diameter (m)

The concept of the empty annulus has also undergone investigation (Brown & Richards, 1960). It has been determined that none of the particle center can approach within a distance of  $d_g/2$  of the orifice edge, leading to all particle centers passing through an orifice of diameter  $(D - d_g)$ . However, this explanation did not account for why the shape factor ( $K_p$ ) would exceed 1. A reduction in the number of particles flow per unit time in the zone adjacent to the orifice edge has been documented (Brown & Richards, 1960). The findings presented by Huntington & Rooney (1971) supported the Beverloo model, yet the values of the flow rate coefficient adjustment (C) and  $K_p$  were consistent across all materials used.

The Beverloo model has been extended for the analysis of fine materials with  $d_g < 500 \mu\text{m}$  (Nedderman *et al.*, 1982). This is attributed to the influence of interstitial pressure gradients (Crewdson *et al.*, 1977). The internal stresses within a bunker containing flowing materials rise from zero on a surcharge-free upper surface to a maximum at greater depths, subsequently dropping to zero again at what is known as the free-fall arch. The interstitial voidage experiences a minimum at some point down the hopper. This indicates compression of the material near the top, with air being released, while above the orifice, air is drawn into the expanding material. Moreover, positive pressure develops in the upper portion of the hopper, while the pressure in the interstitial fluid remains lower than atmospheric pressure immediately above the orifice. Consequently, material approaching the orifice encounters an adverse pressure gradient (Nedderman *et al.*, 1982). Densities around the orifice have been reported to be 30% lower than those in the upper regions of the hopper (Fickie *et al.*, 1989). The influence of interstitial pressure is particularly significant with fine powders. A comprehensive research was conducted, involving numerous experiments on particles of varying sizes, including both fine and coarse particle sizes spanning from  $150 \mu\text{m}$  to  $2,500 \mu\text{m}$ . The research revealed that the flow rate could

be effectively modified using a coefficient (C), as defined in equation 2.5 (Verghese & Nedderman, 1995):

$$C = \sqrt{1 + \frac{\lambda}{d_g^2}} \quad (2.5)$$

where,

C is coefficient adjustment of flow rate (dimensionless)

$\lambda$  is function of compressibility and density of the material ( $-1.46 \times 10^{-8} \text{ m}^2$ )

For orifices with diameters less than six times the diameter of the particle, it was observed that the flow became intermittent and irreproducible (Nedderman *et al.*, 1982). Hence, the applicability of the Beverloo model was limited for cases where the ratio of orifice diameter ( $D_o$ ) to particle diameter ( $d_g$ ) was less than 6. Additionally, assuming that equating  $D_o - K_p d_g$  to zero accurately predicted the point at which flow ceases was not accurate. The critical values were suggested as 2.5 for slots and 4.0 for circular orifices (Brown & Richards, 1959). However, in the case of fine powders, the formation of a stable arch hindered the flow process.

To improve the predictive accuracy of granular solid flow rate through orifices, a model was proposed by Zhang & Rudolph (1991). This model utilized force and momentum balances at the stress-free surface, commonly referred to as the free-fall arch. The study highlighted the significance of shear friction between flowing and non-flowing particles around the edges of the bottom orifice. Shear friction was identified as a crucial factor that needed to be considered. The researchers indicated that shear friction around the periphery of the stress-free surface could be treated as a wall effect. The influence of this wall effect on solid flow rate was minimal when the ratio of  $D_o$  to  $d_g$  was large. However, for smaller values of  $D_o/d_g$ , shear friction played a more prominent role. Consequently, the model introduced a shear friction correction term into the Beverloo model, accounting for the effects of shear friction. The effective orifice diameter ( $D_o - d_g$ ) was also incorporated into the model. The shear friction correction term could be computed using equation 2.6:

$$C_\tau = \left( \frac{3}{2} - \frac{2}{\tan\beta_w} \right) + \left( \frac{2}{\tan\beta_w} - \frac{1}{2} \right) \frac{D_o/d_g}{(D_o/d_g)_{lim}} \quad (2.6)$$

where,

$C_\tau$  is shear friction correction

$\beta_w$  is slide angle between flowing and unflowing particles at the orifice ends

$(D_o/d_g)_{lim}$  is the limiting value of  $(D_o/d_g)$  on  $C_\tau$  taken as 64

The Beverloo, Rose, and Tanak model underwent verification through research involving the flow rate of coarse materials (Verghese & Nedderman, 1995). The study found that materials with diameters of about 600  $\mu\text{m}$  or less exhibited lower discharge rates compared to those predicted by the Beverloo, Rose, and Tanak model. Interstitial pressure gradients were measured, and the gradient near the orifice was determined to be equal in magnitude to the gradient required to account for the observed decrease in flow rate. However, discrepancies in the results were noted, potentially due to pressure variations across the hopper. Actual pressure gradients were found to be independent of orifice size but inversely proportional to the square of particle diameter, which aligns with expectations for materials of similar compressibility but varying size.

For all the tested materials, including kale seed and sands of different diameters, the mass flow rate was proportional to the orifice diameter raised to the power of 5/2. Notably, the proportionality constant was heavily influenced by the particle diameter. Interestingly, the research also demonstrated that hopper angle had a more pronounced effect on the flow rate of coarse materials than on fine materials.

The impact of moisture content within the range of 12.3% to 22.3% wet basis was found to be significant on both the volume and mass flow rates of maize through round and square horizontal orifices (Chang *et al.*, 1984). In the case of corn, the flow rate increased with decreasing moisture content for a given orifice size. However, for sorghum, it was observed that the volume flow rate increased as the moisture content increased from 11.2% to 17.7% wet basis (Chang & Converse, 1988). For wheat, the volume flow rate remained relatively unaffected by moisture content ranging from 12.9% to 15.1%, wet basis.

Research conducted by Chang *et al.* (1991) explored the flow rates of wheat, corn, sorghum, and soybeans through various types of horizontal orifices, including circular, equilateral, and rectangular ones with aspect ratios of 1.0, 1.5, 2.0, and 2.5. The study revealed significant

differences in volume flow rates per unit orifice area among orifices with the same hydraulic diameter. Notably, the volume flow rate per unit orifice area demonstrated an increase with the enlargement of the orifice's hydraulic diameter across all grain types. Additionally, the shape of the orifice had a more pronounced impact on flow rates for orifices with smaller hydraulic diameters, compared to those with larger hydraulic diameters. In accordance with the standard (American Society of Agricultural Engineers [ASABE], 2003), grain and oilseed flow rates through horizontal or vertical orifices can be predicted using equation 2.7:

$$\text{VFR} = C_o A D_h^n \quad (2.7)$$

where,

VFR is volumetric flow rate (m<sup>3</sup>/h)

A is orifice area (cm<sup>2</sup>)

D<sub>h</sub> is hydraulic diameter of the orifice (cm)

C<sub>o</sub> is drag coefficient (dimensionless)

n is exponent with a value ranging from 0.5 to 1.0 (dimensionless)

Table 2.1 presents the drag coefficients and exponents for selected grains namely maize, wheat and flaxseed.

**Table 2.1** Coefficients and exponents for selected grains

Grain	Moisture content (% , wb)	Hydraulic diameter (cm)	C <sub>o</sub>	n
Maize	12-15	13-25	0.028	0.82
	19-22	13-25	0.047	0.65
Wheat	13-15	10-25	0.050	0.69
Flaxseed	4-13	7-20	0.042	0.70

C<sub>o</sub> is drag coefficient and n is exponent

The British code of practice (BCP) model, derived from the Beverloo model, was formulated by Abd-El-Rahman & Youssef (2008) as well as Valentin (1985). This model was extended to predict the flow rate of granular materials through funnel orifices with unspecified shapes, as demonstrated by Tscheuschner (1987). The BCP model is represented by equation 2.8:



$$Q = C_d \rho_g \sqrt{g} (D_o - K_p d_g)^{\frac{5}{2}} \quad (2.8)$$

where,

Q is mass flow rate (g/s)

$\rho_g$  is bulk density of the grain (g/cm<sup>3</sup>)

$D_o$  is orifice diameter (cm)

$K_p$  is shape factor (dimensionless)

If  $\beta < 45^\circ$ ,  $K_p = \tan(\beta)^{-0.35}$  and for  $\beta > 45^\circ$   $K_p = 1$  where,  $\beta$  is angle between the wall of funnel shaped hopper and vertical line.

The influence of the friction coefficient between the funnel wall and granular materials was investigated by the Williams model, as discussed by Abd-El-Rahman & Youssef (2008). This model validated outcomes for funnels equipped with discharge orifices of diameters below 20 mm. The upper limit of the discharged flow rate corresponds to no friction with the wall, while the lower limit of the discharged flow rate can be determined using equation 2.9:

$$Q = K_p \rho_g \sqrt{g} (D_e)^{\frac{5}{2}} \quad (2.9)$$

where,

$K_p$  is shape factor fixed at 1.6 for circular orifice and 2.4 for rectangular orifice

A comprehensive evaluation of the flow rate has been achieved by incorporating the material porosity term and maintaining a fixed value for the shape factor ( $K_p$ ) at 1.5, as depicted in equation 2.10. This approach allows the shape factor to redefine the effective size of the discharge orifice based on the particle size,  $d_g$  (Abd-El-Rahman & Youssef, 2008; Garcimartín *et al.*, 2009):

$$Q = 0.58(1 - \varepsilon) \rho_g \sqrt{g} (D_e - 1.5d_g)^{\frac{5}{2}} \quad (2.10)$$

where,

$\varepsilon$  is material porosity term

When comparing the BCP and Beverloo models, it becomes evident that the form factor in the original meaning proposed by Beverloo leads to a reduction in the flow area through a discharge orifice. Conversely, the  $K_p$  value in the BCP model considers the impact of the funnel's discharge shape and the angle of the funnel's wall inclination.

In theoretical predictions of flow rate, granular materials experience stress reduction and decompression as they move downward in a convergent funnel (Jenike, 1967). If the orifice size at the funnel's base is too small, material won't flow until the tension threshold is exceeded. This contrasts with fluids, where pressure increases continuously due to hydrostatic tension distribution, with the maximum occurring at the bottom (Tudor & Mieila, 2010). To ensure the flow of granular materials without jamming, a minimum orifice size is necessary at the funnel's outlet. Funnel design is based on Jenike's method, accounting for materials tending to form arches that halt the flow. Therefore, the continuous disruption of these arches is necessary to achieve the desired flow (Tudor & Mieila, 2010).

A model for granular material flow through orifices was developed based on the concept of forming and disintegrating unstable arches. These arches of granular material settle above the outlet. The principles of body movement in fluids and the limit of fall speed are employed. The flow is considered continuous unless the conditions for stable arch formation are met. The velocity of flow at the funnel outlet depends on the falling height, described in the profile of the height of granular material arches. The region of free flow (free-falling zone) of granular material through funnel outlets is confined within a dilated zone and bordered by an unstable arch, as depicted in Figure 2.2 (Wu *et al.*, 2003).

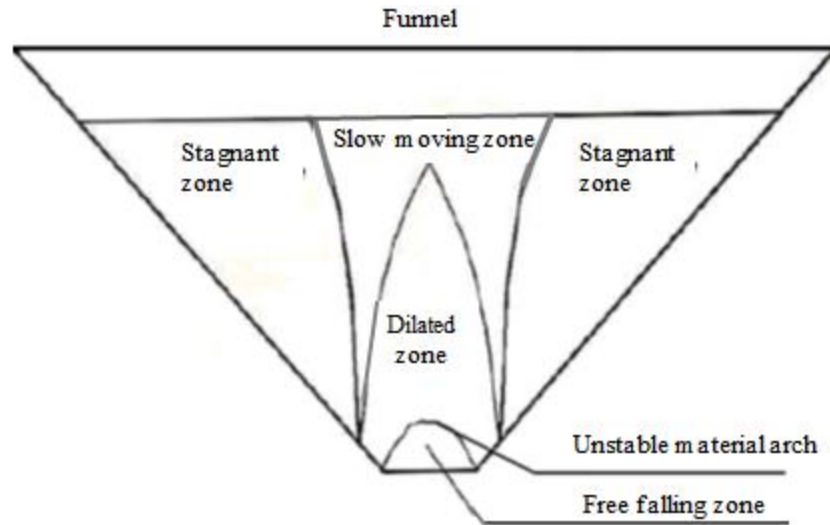


**Figure 2.2** Flow zones for granular material discharge from funnel outlet

Above the outlet, a surface is considered where the normal stress is zero. Under such conditions, the granular material's structure becomes unstable, leading to the formation of an unstable material arch, creating a surface of flow. This region's flow conditions are assumed to mimic those of free fall, regardless of the material's height above this region. These conditions are assumed to remain constant during the discharge process. Key assumptions made during the flow modeling through the outlet include the following: the arching effect is prevalent throughout the flow of granular material through the outlet, whether these arches are stable or unstable in nature. The restriction in the granular flow through the discharge orifice is attributed to this arching effect. Unstable arches are assumed to share similarities in shape and stress properties with stable arches. A dome's shape can be described as a paraboloid, and its characteristics depend on seed properties, funnel shape, and seed-wall friction (Odal, 2005).

The free-flowing zone at the outlet of a funnel is assumed to extend across the entire area of the discharge orifice and is enclosed by a rotated paraboloid resembling the shape of an unstable arch of granular material, as illustrated in Figure 2.3 (Odal, 2005). Based on these assumptions, the flow rate of granular materials through a circular orifice of diameter ( $D_o$ ) can be predicted by evaluating the average velocity of the material passing through the discharge orifice. The surface of the rotating paraboloid is generated by rotating its parabolic axis of symmetry.

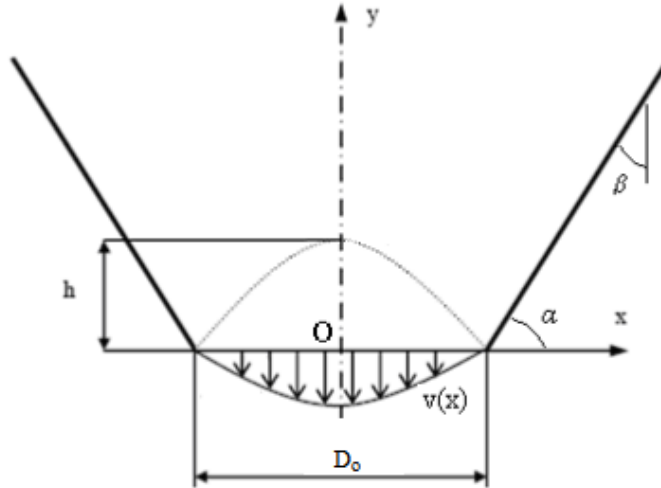


**Figure 2.3** Free flowing zone for a funnel discharge orifice

Using the system of axes XOY (Figure 2.3) the correlation of the generator parabola is given in equation 2.11:

$$y = h \left[ 1 - \left( \frac{2x}{D_o} \right)^2 \right] \quad (2.11)$$

where,

$h$  is the height dome of granular material (m)

The rate of arch height and diameter of outlet for a granular material can be evaluated based on equation 2.12:

$$\delta = \frac{h}{D_o} \quad (2.12)$$

where,

$\delta$  is ratio of arch height to orifice diameter

$h$  is arch height (m)

$D_o$  is orifice diameter (m)

The value of  $\delta$  was 0.40 for wheat seeds, 0.30 for seed maize, 0.46 for poppy seeds, and 0.30 for oat seeds (Odal, 2005). In a vacuum, free-falling bodies experience uniform acceleration, with a speed dependent on the height of the fall and independent of the size, shape, and density of the

body (Tscheuschner, 1987). If the arch of granular material exists above the outlet, the velocity field  $v(x)$  of the discharged seeds for the circular-shaped orifice with diameter  $D_o$  in the plane XOY is given by equation 2.13:

$$v(x) = \sqrt{2gy} \quad (2.13)$$

where,

$v(x)$  is discharged seeds velocity field of the circular orifice (m/s)

When considering equation 2.13, the velocity field of the discharged seeds for the circular orifice with diameter  $D_o$  can be calculated using equation 2.14:

$$v(x) = \sqrt{2g\delta D_o \left[ 1 - \left( \frac{2x}{D_o} \right)^2 \right]} \quad (2.14)$$

Assuming a constant flow speed over circular coroneae of radius  $x$  and width  $dx$ , as given by equation 2.14, the average velocity can be determined using equation 2.15:

$$v_m = \frac{\int_0^{D_o/2} 2\pi x v(x) dx}{\pi \frac{D_o^2}{4}} \quad (2.15)$$

where,

$v_m$  is average flow velocity (cm/s)

Substituting equation 2.14 into equation 2.15 and solving yields equation 2.16:

$$v_m = \frac{2}{3} \sqrt{2g\delta D_o} \quad (2.16)$$

If the bulk density of the seeds near the outlet is assumed to be constant, the mass flow rate can be evaluated using equation 2.17:

$$Q = \rho_b \frac{\pi D_o^2}{4} v_m \quad (2.17)$$

where,

Q is mass flow rate (g/s)

$\rho_b$  is bulk density (g/cm<sup>3</sup>)

Substituting equation 2.16 into equation 2.17 and simplifying, the mass flow rate can be determined using equation 2.18:

$$Q = \frac{\pi\sqrt{2g}}{6} \sqrt{\delta\rho_v} D_o^{\frac{5}{2}} \quad (2.18)$$

When incorporating the inclined walls of the funnel with an angle of inclination ( $\alpha$ ) between the walls and the horizontal, and considering the friction displacement speed of seeds on the walls for a dropping height (h), accounting for the fact that they start moving from a state of rest with a velocity given by equation 2.19 (Tscheuschner, 1987):

$$v = \sqrt{2gh(1 - \mu \text{ctg}\alpha)} \quad (2.19)$$

where,

$\mu$  is the seeds friction coefficient on the funnel wall (dimensionless)

$\alpha$  is angle of inclination between the walls and horizontal (°)

For an angle ( $\alpha$ ) of 45° between the inclined funnel walls and the horizontal, the velocity of seeds on the walls at the lower end of these walls can be calculated using equation 2.20:

$$v = \sqrt{2gh} \sqrt{1 - \mu} \quad (2.20)$$

If  $\mu = \text{tg}\varphi$ , then equation 2.20 is given in equation 2.21:

$$v = \sqrt{2gh} (1 - \text{tg}\varphi)^{\frac{1}{2}} \quad (2.21)$$

where,

$\varphi$  is the friction angle of the material on the funnel walls (°)

Equation 2.21 indicates that if the flow rate of seeds through the orifices is affected by the flow through the funnel, the inclusion of the correction factor  $(1 - \text{tg}\varphi)^{\frac{1}{2}}$  in the mathematical equation for assessing flow rate is justified. In this case, the mass flow rate can be calculated using equation 2.22:

$$Q = \frac{\pi\sqrt{2}}{6} \sqrt{\delta g \rho_g} D_o^{\frac{5}{2}} (1 - \text{tg}\phi)^{\frac{1}{2}} \quad (2.22)$$

Therefore, equation 2.22 serves as a theoretical foundation for the mathematical model of the gravimetric flow rate of seeds through a circular orifice. Furthermore, it provides the basis for the Beverloo model by applying dimensional analysis theory to the examination of the seeds' flow phenomenon through orifices.

### 2.1.2 Parameters Influencing Grain Flow Rate Through Orifices

The key parameters that impact the flow rate of grain through a hopper orifice include hopper diameter, orifice diameter, orifice shape, vertical fill height, particle size, granular mass cohesion, coefficient of mass friction, grain shape, angularity, cone angle of the hopper base, grain size distribution, wall coefficient of friction, and grain angle of repose (Mamtani, 2011).

When the diameter of the container is greater than 2.6 times the orifice diameter, the flow rate remains independent of the container diameter (Brown, 1959; Verghese & Nedderman, 1995). However, this independence doesn't hold if the difference between the hopper and orifice diameters exceeds thirty times the particle diameter (Franklin & Johanson, 1955).

Granular material flow becomes intermittent and unpredictable when the orifice diameter is less than six times the particle diameter (Nedderman & Tüzün, 1979). The critical values are 2.5 for rectangular orifices and 4.0 for circular ones (Brown, 1959). The flow's regularity is disrupted for orifice diameters between 4 and 7 times the particle diameter, depending on the particle shape (Deming & Mehring, 1929). Furthermore, when the hopper diameter or the width of a rectangular hopper is sufficiently large, the hopper walls do not significantly affect the flow near the outlet (Anand *et al.*, 2008).

The cone angle affects the flow rate mainly in mass flow from a hopper (Verghese & Nedderman, 1995). However, this influence is contingent on specific conditions (Harmens, 1963; Rose & Tanaka, 1959).

In various studies, uniform particle size distributions are often assumed, and both analytical and numerical models are based on this assumption. However, real-world situations might involve non-uniform or binary size distributions that challenge this assumption. Finer particles tend to

exhibit higher flow rates compared to coarser ones due to the presence of an empty annulus around an orifice (Anand *et al.*, 2008). This observation is consistent with other findings indicating higher flow rates for finer particles compared to coarser ones (Ostadi, 2019). Numerical research using the discrete element method to study the effect of particle size distribution on granular flow showed that the flow rate increased with a higher mass percentage of finer particles (Anand *et al.*, 2008). An increase in the fine fraction of granular material leads to denser flowing and increased flow rate due to filling of voids between coarse particles (Dias *et al.*, 2004).

The angle of repose, a fundamental property of cohesionless granular materials, defines the maximum slope angle at which a loose packing of material remains stable (Lowe, 1976). However, this parameter might not accurately represent the flow tendency of cohesive and compacted materials (Bell, 1993; Iilejeji & Zhou, 2008). Additionally, the angle of repose might not adequately describe material behaviour in high stress silo conditions, as it doesn't account for variations in shear strength with compaction (Iilejeji & Zhou, 2008). Studies have also indicated that the angle of repose can change with gravitational acceleration variations, showing different static and dynamic angle behavior for all materials (Kleinhans *et al.*, 2011).

## **2.2 Drying Process Parameters**

Grain drying is a complex process influenced by various parameters, with air temperature, air flow rate, and relative humidity playing pivotal roles (Filková & Mujumdar, 1995). Additionally, the initial moisture content of the product is a determining factor, influencing the efficiency and effectiveness of the drying process (Amer, 1999; Bains *et al.*, 1989; Eissen *et al.*, 1985; Fohr & Arnaud, 1992)

Among these parameters, air temperature stands out as the primary influencer of grain drying (Meisami-Asl *et al.*, 2010). The correlation between air temperature and drying rate is well established, with higher temperatures resulting in accelerated drying rates (Filková & Mujumdar, 1995; Kumar *et al.*, 2012; Pandey *et al.*, 2010). This phenomenon is attributed to the increased water-holding capacity of air at higher temperatures, leading to a more efficient moisture removal process (Harold *et al.*, 2013). Notably, elevated air temperatures not only promote faster diffusion within the grains but also trigger a reduction in water activity at the surface, enhancing



both diffusivity and concentration gradients. Moreover, higher air temperatures contribute to energy efficiency by enabling drying with a smaller air mass flow (Chapuis *et al.*, 2017).

Research into various drying scenarios underscores the dominance of air temperature. For instance, investigations into the thin layer drying of prickly pear peels and tunnel drying of potato slices consistently highlighted air temperature as the primary factor governing drying rates (Lahsasni *et al.*, 2004a; Naderinezhad *et al.*, 2016). Furthermore, it's observed that the influence of air temperature surpasses that of air flow rate, as demonstrated in experiments that isolate the effects of these parameters (Delgado & de Lima, 2014). Various studies on the drying of thymus and mint also confirmed the proportional correlation between drying rate and air temperature (El-Sebaei & Shalaby, 2013; Rahmatinejad *et al.*, 2016; Sarker *et al.*, 2012; Slama & Combarous, 2011; Tzempelikos *et al.*, 2014). However, it's worth noting that drying air temperature can influence dryer efficiency. An increase in drying air temperature has been associated with a decrease in dryer efficiency, whereas higher efficiency aligns with greater air flow rates and correspondingly lower drying air temperatures (Aissa *et al.*, 2014; Balbine *et al.*, 2015).

Air flow rate, a crucial parameter in the grain drying process, is defined as the product of air velocity and vent area (Filková & Mujumdar, 1995; Morris, 1981). This parameter exerts a significant influence on the overall drying dynamics of agricultural products (Krokida *et al.*, 2003; Yaldiz *et al.*, 2001). Research has consistently shown that the drying rate is directly proportional to the increase in both air velocity and the quantity of hot air that flows over the product (Filková & Mujumdar, 1995). Notably, the drying kinetics of various crops, such as rice, corn, and potatoes, are largely governed by the air velocity. However, interestingly, studies have demonstrated that air velocity has a limited influence on the drying kinetics of fruits and vegetables (Darıcı & Şen, 2015; Tzempelikos *et al.*, 2014).

The influence of air velocity is intricately tied to the mechanisms of heat and mass transfer, which can involve internal or external resistance (Akpınar *et al.*, 2003a; Krokida *et al.*, 2003; Meisami-Asl *et al.*, 2010; Menges & Ertekin, 2006; Sacilik, 2007; Yaldiz *et al.*, 2001). At lower air velocities, there is a heightened internal resistance, with a notable effect observable at air velocities surpassing 2.5 m/s (El-Beltagy *et al.*, 2007; Guan *et al.*, 2013; Perez & Schmalko,

2009; Reyes *et al.*, 2002). In industrial settings, achieving higher drying rates with minimal drying time is possible by employing elevated velocities and temperatures (Erbay & Icier, 2010). However, it's important to avoid excessive drying temperatures exceeding 80°C and air velocities surpassing 2.5 m/s, as these can detrimentally affect product quality and increase overall energy consumption (Chen *et al.*, 2013; Shi *et al.*, 2008; Sturm *et al.*, 2012).

Higher air velocities contribute to enhanced heat transfer and total energy requirements during the constant drying rate phase. Therefore, extreme drying conditions involving excessively high temperatures and air velocities are not recommended due to potential negative consequences on product quality and energy consumption (Sturm *et al.*, 2012). Additionally, the inlet air velocity plays a crucial role in determining the necessary pneumatic conveying pipe length and overall energy consumption. Reports indicate that air velocity is linked to specific energy consumption, highlighting the importance of this parameter in the overall energy efficiency of the drying process (Chapuis *et al.*, 2017).

In the context of forced convection grain drying, maintaining an appropriate air flow rate is essential for effective drying. This necessitates the use of well-designed fans capable of overcoming the static pressure developed in the drying chamber and ensuring a consistent air flow rate throughout the drying process. The optimization of air flow rate is critical to achieving satisfactory dryer performance, as a lower air flow rate can lead to increased drying air temperature, while a higher air flow rate may result in decreased moisture removal (Murthy, 2009).

Relative humidity is another influential parameter in the drying of products. Higher relative humidity translates to longer drying times, necessitating increased air quantities and elevated temperatures to achieve the desired moisture removal (Filková & Mujumdar, 1995). However, during the drying process, the relative humidity within the drying chamber often fluctuates based on ambient conditions, including temperature and relative humidity of the environment. Despite these variations, the relative humidity's direct impact on the overall drying process is somewhat limited (Aghbashlo *et al.*, 2009a; Misha *et al.*, 2013; Sturm *et al.*, 2012).

The solid loading ratio (SLR) stands as another influential factor impacting drying rate and the ensuing flow regime in pneumatic drying processes. Within the SLR range of 0.1 kg/s to 7.5 kg/s

of solid particles flowing per kg/s, a dilute condition is established, which aligns with the requirements of pneumatic systems (Crowe *et al.*, 2011). Notably, an increase in SLR leads to a decline in drying rate due to a reduction in the driving force. At higher SLRs, the temperature elevation of solid particles is comparatively lower than that observed at lower SLRs, stemming from the lower water vapor pressure at the surface of solid particles. Additionally, higher SLRs result in more humid drying air, causing a decrease in the driving force governing the drying rate. Notably, an SLR value of 0.5 yields favorable operational conditions in terms of both drying rate and capacity (Hidayat & Rasmuson, 2007).

The interplay between air velocity and SLR serves as pivotal process parameters governing flow characteristics and regime within pneumatic systems. Usual operational velocities of pneumatic systems fall in the range of 10 to 30 m/s (Hidayat & Rasmuson, 2007). Enhanced air velocities correspondingly lead to increased drying rates, attributed to the heightened slip velocity. However, elevated air velocities lead to shorter residence times for drying (Hidayat & Rasmuson, 2007). Furthermore, SLR exerts an influence on temperature and moisture profiles during pneumatic drying (Matsumoto & Pei, 1984; Pelegrina & Crapiste, 2001).

In scenarios where the solid to air mass flow ratios are high, the inter-phase drag escalates due to elevated solid concentrations and relative velocities. This escalation culminates in a drop in air pressure, leading to pressure reduction at higher solid-to-air mass flow ratios. Lower SLRs yield rapid decreases in solid moisture content within the acceleration region, consequently decreasing the driving force for mass transfer. Conversely, higher SLRs yield reduced moisture content reduction in the initial sections of the duct, translating to greater driving force in subsequent sections. The amalgamation of amplified driving force and increased solid concentrations augments drying rates, facilitating rapid moisture content reduction in these SLR contexts (Rajan, 2012).

Another significant aspect influencing energy efficiency is the recirculation of exhaust air in drying processes, leading to energy conservation. This practice has been explored in numerous experiments conducted by researchers aiming to ascertain optimal air recirculation ratios for energy savings. Studies reveal that an air recirculation ratio of 70% can yield energy savings of 46%, while 80% recirculation can lead to 50% energy savings in forced convection drying

processes (Lui, 1995). Other instances include energy savings of 28% at an air recirculation ratio of 76%, 30% at 75%, and 53% and 46% at 70% and 80% air recirculation, respectively (Das *et al.*, 2001; Vagenas & Marinos-Kouris, 1991; Walker, 1992).

Noteworthy energy savings of 26% were achieved with an air recirculation ratio of 92%, 30% at 60% in a rotary dryer, and 28% at 80% in a fluidized bed drying setup (Iguaz *et al.*, 2002; Soponronnarit & Prachayawarakorn, 1994; Young *et al.*, 1990). Maize drying experiments showcased energy savings of 26% and 24% at 70% and 86% air recirculation ratios, respectively (Giner & De Michelis, 1988; Soponronnarit & Prachayawarakorn, 1994). Moreover, diverse products achieved energy savings of 30%, 30%, and 28% at 75% air recirculation and 30% at 84% air recirculation (Iguaz *et al.*, 2002; Pelegrina *et al.*, 1999). In the drying processes, the electrical energy consumption by fans escalates with the number of product passes, with operational duration exerting a considerable influence on the extent of electrical energy utilized by fans during the drying phase (Billiris & Siebenmorgen, 2014)

### 2.3 Distribution and Determination of Energy Used in Drying

During the drying process, the allocation of total invested energy follows a division that encompasses the evaporation of moisture, the heating of the drying material, and the residual energy losses (Tolmač *et al.*, 2008). This energy distribution is visually represented in Figure 2.4, which illustrates the estimated breakdown of supplied heat energy within a hot air dryer (Tapani, 2016).

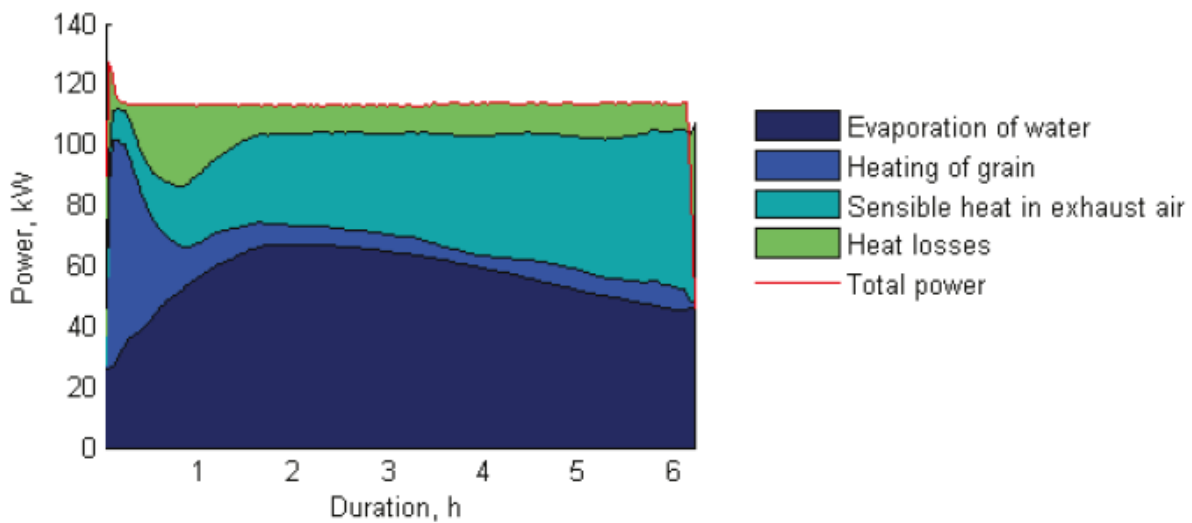


**Figure 2.4** Distribution of total supplied energy for grain drying

Figure 2.4 provides insights gleaned from empirical measurements taken on an industrial-scale farm grain dryer, focusing on key parameters including drying air temperature, relative humidity, grain temperature, and air flow rate. This data-driven analysis reveals that roughly half of the supplied heat energy is allocated to the essential process of moisture evaporation. The balance of the energy distribution sees a significant proportion being dissipated as sensible heat within the exhaust air of the dryer. Energy losses stemming from radiation and conduction through the dryer's structure also contribute to the overall energy expenditure, accounting for approximately 5% to 20% of the total energy supplied (Strumillo *et al.*, 2014).

Moreover, a portion of the energy input is directed toward elevating the temperature of the grain being dried, resulting in an increase in its overall temperature. The metric labeled total power in Figure 2.4 corresponds to the heat power provided to the drying air. This value is determined by assessing changes in the specific enthalpy of the air as it traverses the heating element, coupled with the prevailing drying air flow rate. The specific enthalpy of the air is computed using equation 2.23 (Tapani, 2016).

$$h_s = \frac{C_{pa} m_a T_a + m_a h_s (l_v + C_{pa} T_a)}{m_a} = C_{pa} t_a + h_s (l_v + C_{pv} T_a) \quad (2.23)$$

where,

$h_s$  is specific enthalpy of air (kJ/kg)

$C_{pa}$  is specific heat of air (kJ/kg°C)

$T_a$  is air temperature (°C)

$m_a$  is mass of dry air (kg)

$h_s$  is specific humidity of air (kg of water/kg of air)

$l_v$  is latent heat of evaporation of free water (kJ/kg)

$C_{pv}$  is specific heat of water vapour (kJ/kg°C)

The heat power in the context of this drying process can be expressed as the product of the change in specific enthalpy and the mass flow rate of the drying air. This relationship is captured by equation 2.24 (Tapani, 2016). This equation provides a quantitative understanding of how the energy input contributes to the heating of the drying air, thus facilitating the moisture evaporation process during grain drying.

$$P_h = (h_{amb} - h_h)\dot{m}_a \quad (2.24)$$

where,

$P_h$  is heat power (kW)

$h_{amb}$  is specific enthalpy of ambient air (kJ/kg)

$h_h$  is specific enthalpy of heated air (kJ/kg)

$\dot{m}_a$  is mass flow rate of air (kg/s)

The power required for the evaporation of moisture can be described mathematically using equation 2.25 (Tapani, 2016). This equation embodies the correlation between the latent heat of evaporation of water and the rate at which evaporation occurs. In essence, it quantifies the energy necessary to transform water from its liquid state to vapour during the drying process, shedding light on the energy expenditure associated with moisture removal.

$$P_w = l_v \dot{E} \quad (2.25)$$

where,

$P_w$  is energy for evaporation of moisture (kW)

$\dot{E}$  is evaporation rate (kg/s)

Equation 2.26 (Mujumdar, 2007) provides a method for evaluating the latent heat of evaporation of water within grains. This equation serves as a pivotal tool in determining the amount of energy required for the transition of water from a liquid state to a vapor state during the drying process. By using this equation, researchers and practitioners can gain insight into the thermodynamic properties and energy demands of the moisture evaporation phenomenon within grains.

$$l_g = l_v [1 + k \exp(xMC)] \quad (2.26)$$

where,

$l_g$  is latent heat of vaporisation of moisture in grain (kJ/kg)

$k$  and  $x$  are dependent coefficients for grain

$MC$  is ratio of grain moisture content

Equation 2.27 (Tapani, 2016) offers a means of calculating the evaporation rate during the drying process. This equation plays a fundamental role in understanding the rate at which moisture is

being converted from its liquid state to vapor within the drying material. By employing this equation, researchers and engineers can quantitatively analyze the kinetics of moisture evaporation and its impact on the overall drying dynamics. This information is crucial for optimising drying processes and achieving efficient moisture removal from the material being dried.

$$\dot{E} = \dot{m}_a (w_1 - w_2) \quad (2.27)$$

where,

$w_1$  is specific humidity for inlet air (kg of water/kg of air)

$w_2$  is specific humidity for outlet air (kg of water/kg of air)

Equation 2.28 (Tapani, 2016) provides a methodology for calculating the sensible heat power at the outlet of the dryer. This equation serves as a valuable tool in quantifying the amount of heat energy that is carried away by the exhaust air after it has interacted with the drying material. By utilizing this equation, researchers and practitioners can gain insights into the distribution of heat within the drying system, contributing to a deeper understanding of the energy utilization and efficiency of the drying process. This information is pivotal for enhancing the design and operation of drying systems to achieve optimal energy utilization and product quality.

$$P_s = (C_{pa} + c_{pv} \Delta h_s) (t_o - t_i) \quad (2.28)$$

where,

$P_s$  is sensible heat in the dryer outlet air (kW)

$\Delta h_s$  is specific humidity difference between inlet and outlet air at temperature

The specific heat in the context of grain drying is a crucial consideration. It's composed of the sum of the specific heat in the grain's dry matter and the specific heat of the water contained within the grain. This correlation enables the estimation of energy utilized for heating the grain. This process can be quantified using equation 2.29 (Mujumdar, 2007). This understanding contributes to a comprehensive assessment of energy dynamics during grain drying and aids in optimising the energy efficiency of the entire drying process.

$$E_h = [C_{pg} m_w (1 - MC) + C_{pw} m_w MC] \frac{\Delta t}{t} \quad (2.29)$$

where,

$E_h$  is grain heating energy (kW)

$C_{pg}$  is specific heat of grain dry matter (kJ/kg/K)

$m_w$  is moist mass of grain (kg)

$C_{pw}$  is specific heat of water (kJ/kg/K)

$\Delta t$  is temperature difference (K)

$t$  is time interval (s)

The evaluation of heat losses to the surrounding environment due to radiation and convection is a critical aspect in the energy balance of a dryer. This estimation can be achieved through the utilization of an energy balance equation, as presented in equation 2.30 (Crapiste & Rotstein, 1997). This equation provides a framework for comprehensively calculating the heat losses that occur as a result of radiation and convection during the drying process. By considering factors such as the difference in temperatures and the relevant heat transfer coefficients, this equation offers a method to quantify the energy dissipation due to these loss mechanisms. This is an essential step in gaining a complete understanding of the energy dynamics within the drying system and optimising its efficiency.

$$Q_{l,amb} = (Q_i + Q_w) - (Q_o + Q_d) = (h_i \dot{m}_a + h_w r_f) - (h_o \dot{m}_a + h_d r_f) \quad (2.30)$$

where,

$Q_{l,amb}$  is heat losses to the ambient air (kJ/h)

$Q_i$  is heat input rate of the air (kJ/h)

$Q_w$  is moist product energy input rate (kJ/h)

$Q_o$  is exhaust air heat output rate (kJ/h)

$Q_d$  is energy output of the dried product (kJ/h)

$h_i$  is inlet air specific enthalpy (kJ/kg)

$h_o$  is exhaust air specific enthalpy (kJ/kg)

$h_w$  is moist product specific enthalpy (kJ/kg)

$h_d$  is dried product specific enthalpy (kJ/kg)

$r_f$  is feed rate dry basis (kg/kg.h).



Quantifying heat losses through the exhaust air is crucial for understanding the overall energy balance in a drying system. Equation 2.31 (Kudra, 2008) offers a means to calculate these losses while considering the necessary air flow rate to meet both the heat and hydrodynamic requirements of the process. This equation allows for the estimation of heat losses based on the difference in enthalpies between the incoming and outgoing air streams, as well as the specific heat capacity of the air and the flow rate. By integrating these factors, this equation provides valuable insights into the extent of heat losses occurring through the exhaust air. This information is pivotal in optimising the energy efficiency of the drying process and minimising unnecessary energy wastage.

$$\dot{Q}_{l,\text{exh}} = (\dot{Q}_o - Q'_o) = h_o (\dot{m}_a - \dot{m}'_a) \quad (2.31)$$

where,

$Q_{l,\text{exh}}$  is heat losses through the exhaust air (kJ/h)

$Q'_o$  is exhaust heat rate using a smallest flow rate of air (kJ/h)

$\dot{m}'_a$  is minimum mass flow rate of air (kg/s)

The energy balance plays a crucial role in establishing the relationships between various energy components, including total invested energy, energy usage, and heat losses, throughout the drying process. As noted by Tolmač *et al.* (2008), the energy balance provides a comprehensive view of how energy is distributed and transformed within the system. Equation 2.32 (Holman, 1981; Liu & Baker-Arkema, 1999; Tolmac (1997), enables the determination of the enthalpy difference. This equation serves as a vital tool in quantifying the changes in enthalpy of the drying air as it undergoes the drying process. By considering factors such as temperature and humidity, this equation allows for the assessment of energy changes associated with the air as it interacts with the drying material. This information is instrumental in understanding the energy dynamics within the system and elucidating the factors contributing to heat transfer and transformation during the drying process.

$$\Delta H = h_i - h_o = C_{pa} (T_i - T_o) \quad (2.32)$$

where,

$\Delta H$  is enthalpy difference (kJ/kg)

$h_i$  is enthalpy of the inlet air (kJ/kg)

$h_o$  is outlet air enthalpy (kJ/kg)

$T_i$  is inlet air temperature ( $^{\circ}\text{C}$ )

$T_o$  is outlet air temperature ( $^{\circ}\text{C}$ ).

Equation 2.33 provides a means to quantify the amount of moisture that undergoes evaporation during the drying process. This equation is essential for evaluating the extent of moisture removal from the drying material.

$$W_e = m_i \left( 1 - \frac{100 - w_c}{100 - w_o} \right) \quad (2.33)$$

where,

$W_e$  is amount of evaporated moisture (kg/kg.h)

$m_i$  is quantity of moist material (kg/kg.h)

$w_c$  is moisture content of the wet material at the inlet of the dryer (%)

$w_o$  is moisture content of the wet material at the outlet of the dryer (%).

Equations 2.34 and 2.35 provide methods to determine the total heat quantity involved in the drying process:

$$Q_q = Q_m + Q_h + Q_l \quad (2.34)$$

where,

$Q_q$  is total heat quantity (kJ/h)

$Q_m$  is heat for moisture evaporation (kJ/h)

$Q_h$  is heat for drying material (kJ/h)

$Q_l$  is heat losses (kJ/h)

$$Q_l = BH_d \eta_t \quad (2.35)$$

where,

$B$  is fuel gas used ( $\text{m}^3/\text{h}$ )

$H_d$  is minimum gas heat power ( $\text{kJ}/\text{m}^3$ )

$\eta_t$  is degree of thermal utilization (%)

The quantity of drying air can be determined using equation 2.36:

$$V_q = \frac{Q_t}{\Delta H} \quad (2.36)$$

where,

$V_q$  is quantity of drying air ( $m^3/h$ )

The specific energy consumption is given in equation 2.37:

$$q_s = \frac{Q_t}{W} \quad (2.37)$$

where,

$q_s$  is specific energy used (kJ/kg)

The specific energy consumption can also be given in equation 2.38 (Kudra, 2012):

$$q_s = \frac{m_{sa}(h_i - h_{amb.})}{m_{fr}(X_w - X_d)} \quad (2.38)$$

where,

$m_{sa}$  is specific mass flow rate of air (kJ/kg)

$h_i$  is specific enthalpy of the hot air inlet (kJ/kg)

$m_{fr}$  is feed rate in dry basis (kg/kg.h)

$X_w$  is moisture content ratio of the wet product

$X_d$  is moisture content ratio of the dried product

The thermal energy essential for maize grain drying using natural gas is given in equation 2.39 (Maier & Bakker-Arkema, 2002):

$$E_{the} = \frac{V_n AE}{W} \quad (2.39)$$

where,

$E_{the}$  is thermal energy supplied (kJ/kg)

$V_n$  is volume of natural gas consumed ( $m^3$ )

$AE$  is existing energy from natural gas (kJ)

The degree of thermal utilization is given in equation 2.40:

$$\eta_t = 100 \left( \frac{t_i - t_o}{t_i} \right) = 100 \left( \frac{Q_t - Q_l}{Q_t} \right) \quad (2.40)$$

where,

$\eta_t$  is degree of thermal utilization (%)

The total heat power for grain drying can also be evaluated based on equation 2.41:

$$P_t = h_t A_s \Delta T_{ml} \quad (2.41)$$

where,

$P_t$  is total heat power for drying (W)

$h_t$  is total coefficient of heat transfer ( $W/m^2K$ )

$A_s$  is drying surface ( $m^2$ )

$\Delta T_{ml}$  is middle logarithm difference of temperature ( $^{\circ}C$ )

Equation 2.42 provides the convective heat input required for the drying process when there is no heat loss:

$$Q_{conv} = Q_m + Q_h \quad (2.42)$$

where,

$Q_{conv}$  is convective heat for drying (kJ/h)

Equation 2.43 outlines the method for calculating convective heat transfer during the drying process:

$$Q_{conv} = h_c A \Delta T_{ml} \quad (2.43)$$

where,

$h_c$  is convective heat transfer coefficient ( $W/m^2K$ )

The heat transfer coefficient ( $h_c$ ) through convection can be evaluated using equation 2.44 (Fyhr & Rasmuson, 1997; Tolmac & Lambic, 1997):

$$N_u = \frac{h_c d}{k_a} \quad (2.44)$$

where,

Nu is Nusselt number (dimensionless)

d is dryer pipe diameter (m)

$k_a$  is thermal conductivity of air ( $\text{W/m}^2\text{K}$ )

The energy performance evaluation of a drying process is often quantified by the specific heat consumption, a metric that expresses the energy needed per unit mass of water removed (Mujumdar & Menon, 1995). In pneumatic dryers, the specific energy consumption typically hovers around 4500 kJ/kg of evaporable water, reflecting the energy requirement for effective moisture removal. This range can extend from 4500 to 9000 kJ/kg of evaporable water, encompassing variations in dryer setups (Mujumdar, 2014; Tolmač *et al.*, 2008). In convection drying, specific energy consumption spans from 3850 to 5040 kJ/kg of evaporable water; indicating the energy demand for efficient drying (Islam *et al.*, 2004; Prvulovic *et al.*, 2007).

In a pneumatic dryer, producing 1 kg of dried product necessitates approximately  $3100 \pm 700$  kJ of heat energy, with the specific consumption of energy often associated with the drying process (Precoppe *et al.*, 2015). The total coefficient of heat transfer, a critical factor in the efficiency of the maize starch drying process using a convection pneumatic dryer, is noted as  $308 \text{ W/m}^2\text{K}$  (Prvulovic *et al.*, 2007). The largest share of heat during the drying process is allocated to heating the material and evaporating moisture, as underscored by the energy distribution (Tolmač *et al.*, 2008).

Dryer design characteristics, such as shape, configuration, and heating approach, exert an impact on energy use and efficiency. Convection dryers generally witness higher energy consumption due to the relatively shorter contact duration between drying air and the material, affecting overall efficiency (Kudra, 2004; Kudra, 2012). In the context of a commercial cross-flow dryer with heat recovery, the energy requirement for drying 21590 tonnes of maize that reduces its moisture content from an average initial 18% to 15% (wet basis) using ambient temperature was measured at 3520 kJ/kg of moisture removed (Billiris & Siebenmorgen, 2014). This data showcases the energy demands and efficiency considerations that play a vital role in the optimisation of drying processes.

## **2.4 Optimisation Techniques for Process Parameters**

Optimisation is a crucial technique used to address problems involving the minimisation or maximisation of a function with multiple variables, often subject to equality and/or inequality constraints. This method finds extensive applications in various fields including operations research, management science, and engineering design, enabling the efficient refinement of processes and systems (Sivanandam *et al.*, 2008). Several optimization methods are employed to tackle complex problems in different domains. Some notable methods include: Taguchi, fuzzy logic, genetic algorithm and surface response

### **2.4.1 Taguchi's Method**

The Taguchi method is a systematic approach aimed at enhancing the quality of processes by reducing variation through robust design of experiments. Developed by Genichi Taguchi, this method seeks to identify optimal process parameters that lead to desired performance characteristics. The core idea is to understand how various parameters influence the mean and variance of a process's performance characteristic, which reflects its functionality (Taguchi, 1990).

Taguchi's experimental design employs orthogonal arrays to organize process parameters and their levels. This approach tests pairs of parameter combinations, as opposed to factorial design that tests all possible combinations. As a result, Taguchi method efficiently collects critical data on significant factors affecting performance with a limited number of experiments, saving time and resources (Yang & Tarn, 1998).

The Taguchi method is most effective when dealing with an intermediate number of variables (typically 3 to 50), few interactions between process variables, and a situation where only a few process variables substantially contribute to the outcome. It finds significant utility in manufacturing, aiding in the design of high-quality engineering systems (Ross, 1996; Taguchi, 1990).

The Taguchi approach involves three engineering optimisation strategies for process or product development: System, parameter, and tolerance design: The system design stage applies scientific and engineering principles to create initial functional prototype designs, encompassing both product and process aspects. It includes material selection, component choices, and

tentative parameter values for both products and processes. In the parameter design phase, specific values for system parameters are optimised to enhance performance characteristics. The goal is to identify optimum process parameter values that improve performance and are robust against variations in environmental conditions and noise factors. This step contributes to achieving high quality without increasing costs (Montgomery, 2017). The tolerance design step becomes relevant when determining the best tolerances for parameters. It ensures that the design remains robust even when subjected to variations.

The core of the Taguchi method involves the use of a loss function to quantify how performance characteristics deviate from desired values. This loss function is converted into a signal-to-noise (S/N) ratio, where design parameters are factors controllable by designers, and noise factors are uncontrollable environmental or external factors. The S/N ratio analysis categorizes performance characteristics into smaller is better, larger is better, or nominal is better categories. Regardless of the category, a higher S/N ratio indicates better performance. The optimal process parameter level is the one associated with the highest S/N ratio. Statistical analysis of variance (ANOVA) is then used to identify statistically significant process parameters.

Based on S/N ratio and ANOVA analyses, the optimum combination of process parameters is determined. To confirm these results, a final confirmatory test is conducted. The Taguchi method is a powerful approach to systematically refine processes and achieve high-quality results while managing resources effectively. Equations 2.45, 2.46, and 2.47 represent the S/N ratios for smaller is better, the larger is better, and the nominal is better criteria for performance characteristics, respectively (Nalbant *et al.*, 2007; Singh *et al.*, 2013; Vankanti & Ganta, 2014):

$$S/N_S = -10\log\left(\frac{1}{n} \sum_{i=1}^n y_i^2\right) \quad (2.45)$$

where,

S/N<sub>S</sub> is signal to noise for smaller response (dB)

n is number of observations

y is observed data

$$S/N_L = -10\log\left(\frac{1}{n} \sum_{i=1}^n \frac{1}{y_i^2}\right) \quad (2.46)$$

where

$S/N_L$  is signal to noise for larger response (dB)

$$S/N_N = -10 \log \left( \frac{\bar{y}}{s_y^2} \right) \quad (2.47)$$

where,

$S/N_N$  is signal to noise for reducing variability of a specific target (dB)

$\bar{y}$  is average of observed data

$s_y^2$  is variance of  $y$

The parameter design phase within the Taguchi method encompasses a series of steps that are systematically employed to optimise a process while considering multiple performance characteristics. These steps are depicted in Figure 2.5 (Nian *et al.*, 1999).

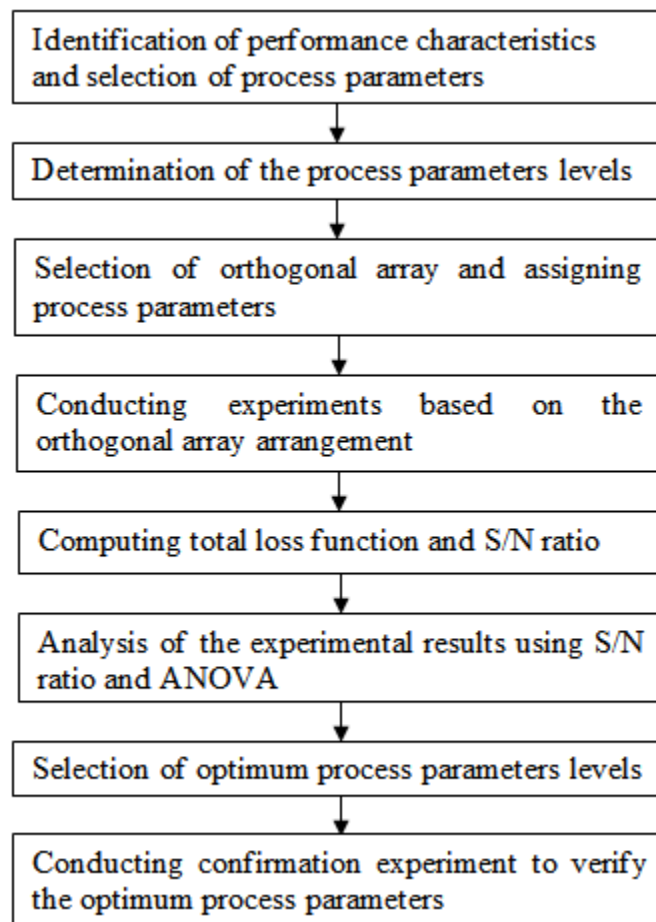


**Figure 2.5** Optimisation process using Taguchi's method



The selection of an appropriate orthogonal array for experimental design involves determining the total degrees of freedom required for the analysis. Degrees of freedom represent the number of independent comparisons between process parameters that are needed to assess the superiority of certain levels and quantify the degree of improvement. The degrees of freedom for the chosen orthogonal array should ideally be greater than or equal to the degrees of freedom associated with the process parameters being studied. To calculate the total sum of squared deviations from the overall mean of the signal to noise, equation 2.48 is used (Lin, 2002; Nalbant *et al.*, 2007):

$$SS_T = \sum_{i=1}^m \eta_i^2 - \frac{1}{m} \left( \sum_{i=1}^m \eta_i \right)^2 \quad (2.48)$$

where,

$SS_T$  is total sum of the squared deviations

$m$  is number of experiments in the orthogonal array

$\eta_i$  is mean signal to noise ratio for the  $i^{\text{th}}$  experiment

The total sum of squared deviations ( $SS_T$ ) can be categorized into distinct sources, including the sum of squared deviations ( $SS_p$ ) attributed to each process parameter, and the sum of squared errors ( $SS_e$ ). The determination of  $SS_p$  is facilitated through the utilization of equation 2.49 (Lin, 2002; Nalbant *et al.*, 2007):

$$SS_p = \sum_{j=1}^t \frac{(s\eta_j)^2}{t} - \frac{1}{m} \left( \sum_{i=1}^m \eta_i \right)^2 \quad (2.49)$$

where,

$SS_p$  is sum of the squared deviations

$p$  is experimental parameter

$j$  is level number of parameter  $p$

$t$  is repetition of each level of parameter  $p$

$s\eta_j$  is sum of signal to noise involving parameter  $p$  and level  $j$

The total degrees of freedom can be calculated using equation 2.50:

$$df_t = m - 1 \quad (2.50)$$

where,

$df_t$  is total degrees of freedom

The degree of freedom of the tested parameter (p) can be computed based on equation 2.51:

$$df_p = t - 1 \quad (2.51)$$

where,

$df_p$  is degree of freedom of the parameter p

The variance of the tested parameter (p) is given in equation 2.52:

$$V_p = \frac{SS_p}{df_p} \quad (2.52)$$

where,

$V_p$  is variance of the parameter p

The F-value for each design parameter can be calculated using equation 2.53

$$F_p = \frac{V_p}{V_e} \quad (2.53)$$

where,

$F_p$  is F-value for the design parameter p

$V_e$  average of the squared error

The corrected sum of squares can be determined based on equation 2.54:

$$S_p = SS_p - D_p V_e \quad (2.54)$$

where,

$S_p$  is corrected sum of squares

The percentage contribution of process parameters to performance characteristics can be computed using equation 2.55 (Nalbant *et al.*, 2007; Vankanti & Ganta, 2014):

$$\rho = 100 \frac{S_p}{SS_T} \quad (2.55)$$

where,

$\rho$  is contribution of each process parameter to the performance characteristics (%)  
 $SS_T$  is total sum of squares

### 2.4.2 Fuzzy Logic Method

Figure 2.6 shows the grey fuzzy logic method reported by Biswajit *et al.* (2016) for identifying optimum process parameters in a multi-response scenario.

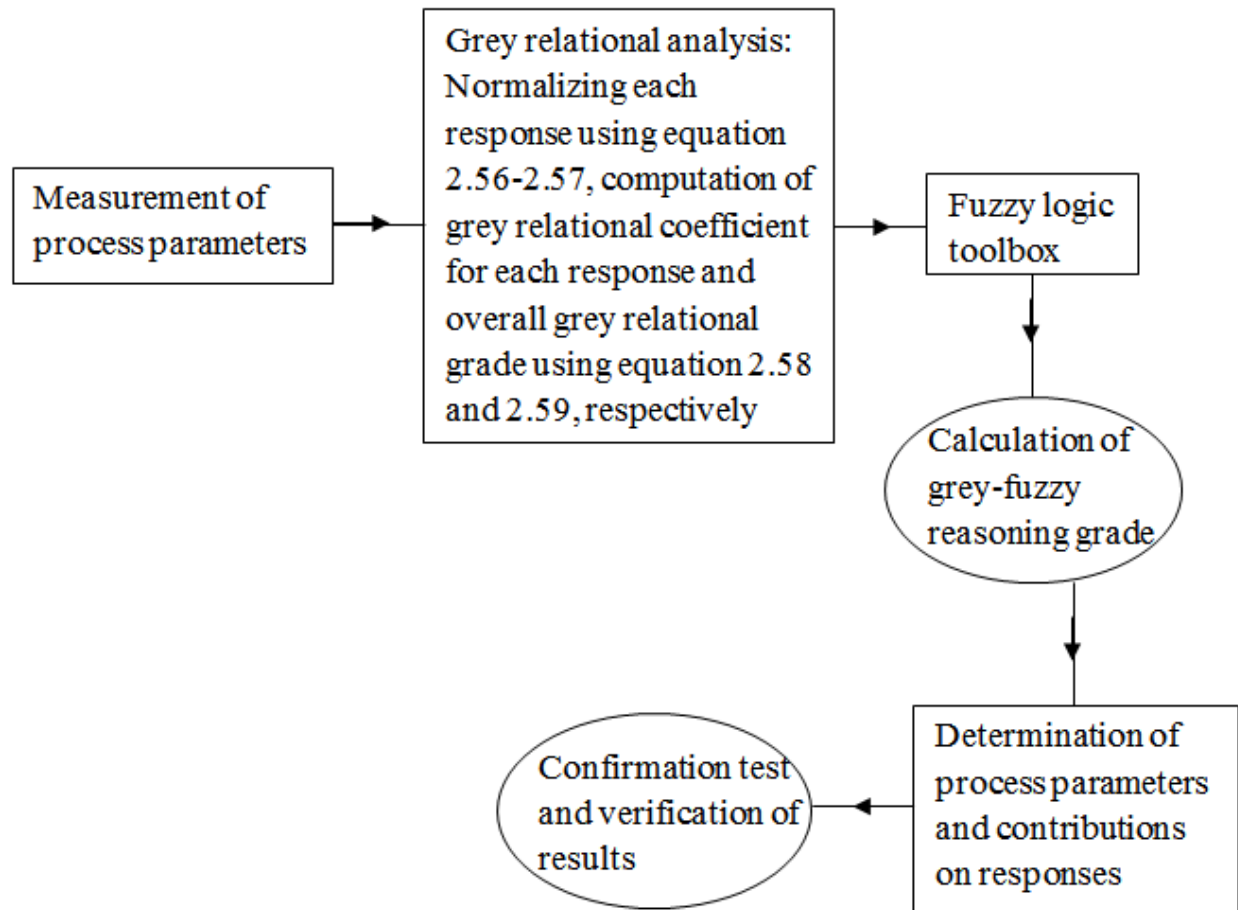


**Figure 2.6** Grey fuzzy logic method

The grey fuzzy logic method involves a series of six operations as outlined by Biswajit *et al.* (2016). These operations include: Selection of process parameters and levels, full factorial experimentation, normalisation of responses, computation of grey relational coefficient and grey relational grade, fuzzification of grey relational coefficient and overall grey relational grade, determination of optimum parameters, contribution analysis, and confirmation tests to validate the obtained results.

In terms of grey relational normalisation, the process parameters are scaled within the range of zero to one. This normalisation is essential due to potential variations in ranges and units across different responses. For responses with higher is better characteristics, normalisation can be performed using equation 2.56:

$$x_i^*(k) = \frac{x_i(k) - \min x_i(k)}{\max x_i(k) - \min x_i(k)} \quad (2.56)$$

where,

$x_i^*(k)$  is normalised data for  $i^{\text{th}}$  experiment using  $k^{\text{th}}$  response

$x_i(k)$  is observed data for  $i^{\text{th}}$  experiment based on  $k^{\text{th}}$  response

If lower is better criterion is used, normalisation can be determined based on equation 2.57:

$$x_i^*(k) = \frac{\max x_i(k) - x_i(k)}{\max x_i(k) - \min x_i(k)} \quad (2.57)$$

The computation of the grey relational coefficient is achieved through the utilization of equation 2.58:

$$\xi_i(k) = \frac{\Delta_{\min} + \zeta\Delta_{\max}}{\Delta_i(k) + \zeta\Delta_{\max}} \quad (2.58)$$

where,

$\xi_i(k)$  is grey relational coefficient for the  $i^{\text{th}}$  experiment using  $k^{\text{th}}$  response

$\Delta_i(k)$  is absolute value of the difference between  $x_i^0(k)$  and  $x_i^*(k)$

$\Delta_{\min}$  is international minimum value in different data series

$\Delta_{\max}$  is global maximum value in different data series

$\zeta$  is distinguishing coefficient within the range of 0 and 1 which expand or compress grey relational coefficient, taken as 0.5

The determination of the overall grey relational grade involves the computation of the average of the grey relational coefficients associated with each performance characteristic. This calculation is performed using equation 2.59:

$$\gamma_i = \frac{1}{n} \sum_{k=1}^n \xi_i(k) \quad (2.59)$$

where,

$\gamma_i$  is grey relational grade

n is number of process responses

The generation of fuzzy rules is accomplished through the formulation of if-then statements. In this process, the two grey relational coefficients, denoted as  $\zeta_1$  and  $\zeta_2$ , are considered alongside a single multi-response output. These rules are established as Rule 1 to Rule n, encapsulating the relationships and dependencies between the grey relational coefficients and the corresponding multi-response output. This step helps in deriving actionable insights from the grey relational coefficients and translating them into meaningful guidelines for optimising the process parameters.

Rule 1: If  $\zeta_1$  is  $A_{11}$  and  $\zeta_2$  is  $A_{12}$ ...and  $\zeta_n$  is  $A_{1n}$  then C is  $D_1$  else

Rule 2: If  $\zeta_1$  is  $A_{21}$  and  $\zeta_2$  is  $A_{22}$ ....and  $\zeta_n$  is  $A_{2n}$  then C is  $D_2$  else

.....

Rule n: if  $\zeta_1$  is  $A_{n1}$  and  $\zeta_2$  is  $A_{n2}$ ...and  $\zeta_n$  is  $A_{nn}$  then C is  $D_n$

where,

$A_{i1}, A_{i2}, \dots, A_{in}$  and  $D_i$  are fuzzy subsets defined by corresponding membership function that is  $\mu_{A_{i1}}, \mu_{A_{i2}}, \dots, \mu_{A_{in}}$  and  $\mu_{D_i}$ .

The fuzzy multi-response output (C) is derived from the fuzzy rules using the max-min interface operation. Through inference, a fuzzy set with a membership function for the multi-response output is generated. This membership function is determined by employing equation 2.60, allowing for the representation of the combined influence of the grey relational coefficients on the multi-response output.

$$\mu_{D_0}(C) = (\mu_{A_{i1}}(\zeta_1) \wedge \mu_{A_{i2}}(\zeta_2) \wedge \mu_{A_{i3}}(\zeta_3) \wedge \dots \wedge \mu_{A_{in}}(\zeta_n) \wedge \mu_{D_1}(C)) \vee \dots \vee (\mu_{A_{n1}}(\zeta_1) \wedge \mu_{A_{n2}}(\zeta_2) \wedge \mu_{A_{n3}}(\zeta_3) \wedge \dots \wedge \mu_{A_{nn}}(\zeta_n) \wedge \mu_{D_n}(C)) \quad (2.60)$$

The fuzzy multi-response output, represented as  $\mu_{Do}(C)$ , is transformed into the grey fuzzy reasoning grade using the fuzzy logic toolbox, employing the centroid defuzzification method. This transformation is governed by equation 2.61 (Biswajit *et al.*, 2016):

$$C_o = \frac{\sum C \mu_{Do}(C)}{\sum \mu_{Do}(C)} \quad (2.61)$$

where,

$C_o$  is grey fuzzy reasoning grade, a non-fuzzy value

The grey fuzzy reasoning grade corresponds to the optimum configuration of input process parameters for multi-response characteristics.

The optimum value of the grey relational grade can be calculated using equation 2.62:

$$\gamma_e = \gamma_m + \sum_{i=1}^q (\bar{\gamma}_i - \gamma_m) \quad (2.62)$$

where,

$\gamma_m$  is total average of grey relational grade value

$q$  is number of input parameters

$\bar{\gamma}_i$  is mean grey relational grade value at the optimum level for the  $i^{\text{th}}$  parameter

### 2.4.3 Genetic Algorithm

Genetic algorithms are rooted in the principles of natural selection and genetics (Goldberg, 1989). The concept of survival of the fittest is emulated by initially generating a population through random selection, followed by iterative improvement through essential operations such as reproduction, crossover, and mutation (Ng and Li in 1994). These genetic algorithms mimic the evolutionary process by manipulating encoded representations of parameter sets to navigate the search for optimal solutions. This approach involves creating and refining a population of potential solutions over successive generations, aiming to arrive at the best possible outcome. The application of genetic algorithms spans various fields, including optimization tasks in engineering, operations research, and other problem-solving domains (Hoffmann & Pfister, 1997; Ng & Li, 1994; Seng *et al.*, 1999).

#### **2.4.4 Response Surface Method**

Response surface methods (RSM) are optimisation techniques that involve fitting a mathematical model to the experimental data within a defined theoretical design (Box *et al.*, 1978; Myers, 1971). These methods are especially useful in multivariate optimisation tasks. The main types of designs used in response surface modeling are central composite designs and Box–Behnken designs, both of which involve three or five levels of input variables.

The central composite designs incorporate a combination of factorial or fractional factorial designs with center points, supplemented by a set of axial (star) points that enable the estimation of curvature within the experimental domain (Hanrahan & Lu, 2006). This design is characterized by having twice as many star points as there are factors in the design, and these star points represent both low and high values for each factor. This allows for the exploration of responses across a range of factor settings, including the extremes, to better understand the relationship between the factors and the response (Otto, 1999).

On the other hand, the Box–Behnken design is a particularly efficient approach within the realm of response surface methods. This design employs three levels for each factor and avoids the corners of the experimental space. It effectively combines a fractional factorial design with incomplete block designs, aiming to create a well-structured and nearly rotatable design that includes a moderate range of factor levels. This design is particularly suitable when the response to be predicted doesn't occur at the extreme levels of the factors, making it a valuable option for predicting responses within a more moderate range (Hanrahan & Lu, 2006; Otto, 1999).

#### **2.5 Drying Theory**

The drying process involves several mechanisms that contribute to the removal of moisture from materials. These mechanisms include surface or liquid diffusion on pore surfaces, liquid or vapor diffusion due to moisture concentration gradients, and capillary action in granular and porous products due to surface forces. Additionally, thermal diffusion, which results from the vaporization-condensation sequence, and hydrodynamic flow, attributed to water flow caused by shrinkage and pressure gradients, can also play a role in the drying process (Özilgen & Özdemir, 2001; Strumillo & Kudra, 1986b).

The dominant diffusion mechanism during drying is influenced by factors such as moisture content and the structure of the material being dried. This dominant mechanism can change over the course of the drying process. Therefore, accurately determining the dominant drying mechanism is crucial for modeling the process effectively.

In general, hygroscopic products undergo drying in two main periods: the constant rate period and the falling rate period, which ends when equilibrium moisture content is reached. During the constant rate period, external conditions like temperature, drying air velocity, air flow direction, air relative humidity, product physical form, agitation, and support method impact the drying process. Surface diffusion is typically the dominant mechanism during this period.

As the constant rate period comes to an end, moisture needs to be transported from the interior of the material to the surface through capillary action. This leads to the appearance of dry spots on the surface and marks the beginning of the first falling rate period or unsaturated surface drying. During this period, although the drying rate per unit wet solid surface area remains constant, the overall drying rate decreases due to the reduction in the surface area with moisture (Mujumdar & Menon, 2020).

Once the surface film of liquid is completely evaporated, the second falling rate period commences. Vapor diffusion becomes the dominant mechanism during this phase, driven by moisture concentration gradients and influenced by internal factors such as moisture content, temperature, and material structure (Husain *et al.*, 1972).

It's worth noting that while some agricultural products like grain or nuts usually experience the second falling rate period during drying, they may not exhibit a constant rate period in their drying processes. In these cases, the entire drying process occurs within the falling rate period (Parry, 1985). The understanding of these mechanisms and their transitions is crucial for efficient drying process design and optimisation.

## **2.6 Drying Models**

Drying models are commonly developed based on the concept of thin layer drying for agricultural products. Thin layer drying involves drying individual particles or slices as a single layer (Akpınar *et al.*, 2006). Because of the thin nature of the sample, the temperature



distribution within the layer is assumed to be uniform. Thin layer drying models are widely used due to their simplicity and the fact that they require less data compared to more complex distributed models like phenomenological and coupling coefficients models (Madamba *et al.*, 1996; Özdemir & Devres, 1999).

These thin layer drying models can be categorized as theoretical, semi-theoretical, and empirical. Theoretical models focus solely on the internal resistance to moisture transfer (Bruce, 1985; Henderson, 1974; Parti, 1993; Suarez *et al.*, 1980). Semi-theoretical and empirical models, on the other hand, consider only the external resistance to moisture transfer between the product and the surrounding air (Fortes & Okos, 1981; Özdemir & Devres, 1999; Parti, 1993; Whitaker *et al.*, 1969). These models are useful for dryer design (Brooker *et al.*, 1974). Theoretical models provide insights into drying behavior across various conditions, but they come with assumptions that can lead to significant errors. Many widely-used theoretical models are based on Fick's second law of diffusion.

Semi-theoretical models also stem from Fick's second law, and some are simplified forms derived analogously from Newton's law of cooling. They are less complex and require fewer assumptions due to the incorporation of experimental data. However, their applicability is limited to the specific process conditions considered (Fortes & Okos, 1981; Parry, 1985).

Empirical models share characteristics with semi-theoretical models. They heavily rely on experimental conditions and may not provide extensive information about drying behavior (Keey, 2013). However, empirical models are often the most dependable for predicting the drying behavior of agricultural materials. They can be confidently used within the range of temperature, relative humidity, air flow velocity, and moisture content for which they were developed (Brooker *et al.*, 1974). Moreover, empirical models are suitable for applications like automatic control of drying processes due to their economy and short computation time (Pabis *et al.*, 1998). Compared to theoretical models, empirical and semi-theoretical models are quicker to apply and do not necessitate assumptions about product geometry, mass diffusivity, or conductivity, making them suitable for automated control processes (Kahveci & Cihan, 2008).

### 2.6.1 Theoretical Models

Under the assumption that heat transfer rates within the product are significantly faster than the rates of moisture transfer, it is possible to consider isothermal conditions that only change over time within the product (Özilgen & Özdemir, 2001). This assumption is rooted in the fact that the heat transfer rate is two orders of magnitude greater than the rate of moisture transfer. Consequently, only equation 2.63 is required to describe mass transfer in this context (Whitaker *et al.*, 1969; Young, 1969).

In equation 2.63, various parameters are involved: M represents the local moisture content in terms of kg water/kg dry matter or (% dry basis), t stands for time in seconds,  $D_{eff}$  denotes the effective moisture diffusivity in square meters per second, x indicates the diffusion path in meters, and  $a_1$  is a parameter. This parameter takes on a value of zero for planar geometries, one for cylindrical shapes, and two for spherical shapes (Ekechukwu, 1999). The solution for equation 2.63 can then be analytically derived, considering the given assumptions and initial conditions, as shown in equations 2.64 to 2.67.

$$\frac{\partial M}{\partial t} = D_{eff} \left[ \frac{\partial^2 M}{\partial x^2} + \frac{a_1}{x} \frac{\partial M}{\partial x} \right] \quad (2.63)$$

$$t = 0, \quad -L \leq x \leq L, \quad M = M_i \quad (2.64)$$

$$t > 0, \quad x = 0, \quad \frac{\partial M}{\partial t} = 0 \quad (2.65)$$

$$t > 0, \quad x = L, \quad M = M_e \quad (2.66)$$

$$t > 0, \quad -L \leq x \leq L, \quad T = T_{amb} \quad (2.67)$$

where,

L is thickness of diffusion path (m)

$M_i$  is initial moisture content (% , dry basis)

$M_e$  is equilibrium moisture content (% , dry basis)

T is temperature distribution (°C)

$T_{amb}$  is ambient drying air temperature (°C)

The boundary conditions for equation 2.63 are outlined in Figure 2.6 (Whitaker *et al.*, 1969; Young, 1969). In this context,  $Q$  represents the heat transfer rate in watts (W), while  $N_w$  denotes the drying rate ( $\text{kg}/\text{m}^2\cdot\text{s}$ ).

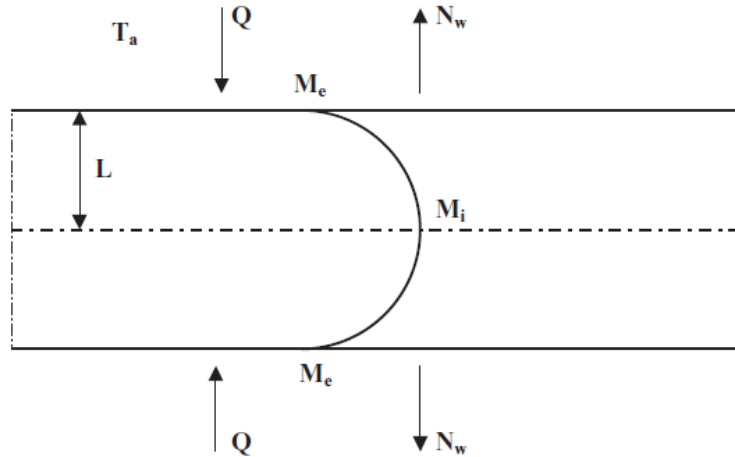


**Figure 2.7** Schematic of thin layer drying for drying process occurring from both sides

Equation 2.63 is underpinned by a set of underlying assumptions that establish the scope and conditions under which it can be effectively applied. These assumptions encompass various pivotal aspects: Firstly, the particle undergoing the drying process is considered to be homogeneous and isotropic. This implies that the particle's properties and behavior are uniform in all directions, allowing for simplifications in the modeling process. Furthermore, the assumption of constant material properties is integral. It posits that the characteristics of the drying particle remain consistent throughout the process, with minimal influence from factors like shrinkage or other variations. Negligible pressure variations within the particle constitute another assumption. This assumption implies that any pressure fluctuations within the particle are negligible and don't play a significant role in shaping the overall drying dynamics. The concept of surface evaporation is also crucial. It dictates that moisture evaporation occurs solely at the particle's surface, and internal evaporation is not considered in the equation's formulation. The assumption of a uniform initial moisture distribution signifies that at the start of the drying process, moisture content is uniformly distributed within the particle, allowing for a standardized starting point in the model. Equilibrium moisture distribution, another assumption, posits that as drying progresses, equilibrium is eventually reached at the particle's surface. This leads to a cessation of surface diffusion and marks a critical phase in the drying process. Uniform

temperature distribution within the particle is another assumption that assumes the particle's temperature is consistent with that of the surrounding drying air, contributing to the equation's applicability. Heat transfer mechanisms are crucial in the assumptions. Conduction within the particle and convection between its surface and the surrounding air facilitate heat exchange. Finally, the constant effective moisture diffusivity assumption implies that this parameter remains unchanging despite variations in moisture content during the drying process (Whitaker *et al.*, 1969; Young, 1969).

The analytical solutions of equation 2.63 for infinite slab or sphere are given in equation 2.68 and 2.69 for infinite cylinder (Crank, 1975):

$$MR = A_1 \sum_{i=1}^{\infty} \frac{1}{(2i-1)^2} \exp\left[-\frac{(2i-1)^2 \pi^2 D_{\text{eff}} t}{A_2}\right] \quad (2.68)$$

$$MR = A_1 \sum_{i=1}^{\infty} \frac{1}{J_0^2} \exp\left[-\frac{J_0^2 D_{\text{eff}} t}{A_2}\right] \quad (2.69)$$

where,

MR is fractional moisture ratio

t is time (s)

$J_0$  is the roots of the Bessel function

$A_1$  and  $A_2$  are geometric constants based on products geometry

Newman's rule finds its applicability in scenarios involving multidimensional geometries, extending its utility beyond simple one-dimensional cases. For instance, this rule can be effectively employed in the context of a three-dimensional slab (Treybal, 1980).

Table 2.2 serves as a valuable resource, delineating geometric constants contingent upon the specific geometry of the products under consideration. This compilation of geometric constants aids in the application of Newman's rule to various scenarios, catering to different shapes and configurations of materials. The table essentially provides a guide for determining the appropriate constants based on the geometry of the system, enabling accurate modeling and analysis in multidimensional cases.

**Table 2.2** Geometric constants based on product geometry

Product geometry	$A_1$	$A_2$
Infinite slab	$8/\pi^2$	$4L^2$
Sphere	$6/\pi^2$	$4r^2$
Three dimensional fine slab	$(8/\pi^2)^3$	$1/(L_1^2 + L_2^2 + L_3^2)$

$A_1$  and  $A_2$  are geometric constants based on products geometry;  $r$  is radius (m);  $L_1$ ,  $L_2$  and  $L_3$  are dimensions of finite slab (m).

The moisture ratio (MR) is a key parameter that can be ascertained by considering the external conditions of the drying process. When the relative humidity of the drying air is maintained at a constant level throughout the drying procedure, the equilibrium moisture content of the material being dried also remains steady. This equilibrium state enables the determination of the moisture ratio using equation 2.70:

$$MR = \frac{(M_t - M_e)}{(M_i - M_e)} \quad (2.70)$$

where,

$M_t$  is the mean moisture content at time  $t$  in dry basis

When the relative humidity of the drying air is subject to continuous fluctuations, this dynamic environment affects the equilibrium moisture content ( $M_e$ ) of the material being dried. Consequently, the moisture ratio (MR) takes on a different form, as represented by equation 2.71 (Diamante & Munro, 1993):

$$MR = \frac{M_t}{M_i} \quad (2.71)$$

If agricultural materials dry without constant rate period then initial moisture content ( $M_i$ ) is equal to the critical moisture content ( $M_{cr}$ ) or moisture content of a material at the end of the constant rate period of drying (% , dry basis). Equation 2.70 simplifies to equation 2.72. This adjustment leads to the moisture ratio (MR) being identified as the characteristic moisture content ( $\phi$ )

$$\phi = \frac{(M_t - M_e)}{(M_{cr} - M_e)} \quad (2.72)$$

### 2.6.2 Semi-Theoretical Models

Semi-theoretical models are developed based on principles such as Newton's law of cooling and Fick's second law of diffusion. Models that stem from Newton's law of cooling encompass the Lewis model, the Page model, and their modified versions. Conversely, models grounded in Fick's second law of diffusion comprise the single-term exponential model and its variations, the two-term exponential model and its variations, as well as the three-term exponential model.

The Lewis (Newton) model, denoted by equation 2.73, postulates that during the falling rate period, the alteration in the moisture content of porous hygroscopic materials is proportionate to the instantaneous disparity between the moisture content and the projected moisture content that the material would attain when achieving equilibrium with the drying air (Lewis, 1921). This model assumes certain conditions, such as the material being thin, the air velocity being high, and the drying air conditions such as temperature and relative humidity remaining constant.

$$\frac{dM}{dt} = -k(M - M_e) \quad (2.73)$$

In thin layer drying theory, the drying constant encompasses a combination of drying transport properties, including moisture diffusivity, thermal conductivity, and interface heat and mass coefficients (Marinos-Kouris & Maroulis, 2020). If the drying constant remains unaffected by the moisture content ( $M$ ), then equation 2.73 becomes equation 2.74, which represents the Lewis (Newton) model:

$$MR = \frac{(M_t - M_e)}{(M_i - M_e)} = \exp(-kt) \quad (2.74)$$

where,

$k$  is drying constant which can be obtained from the experimental data ( $s^{-1}$ )

The Lewis (Newton) model, however, has certain limitations. It tends to underestimate the latter stages and overestimate the initial stages of the drying process (Ghazanfari *et al.*, 2006; Hossain & Bala, 2002; Madamba, 2003; Vijayaraj *et al.*, 2007; Wongwises & Thongprasert, 2000).

Despite these limitations, the Lewis (Newton) model has found application in describing the drying characteristics of various agricultural products, such as strawberries (El-Beltagy *et al.*, 2007), red chillies (Hossain *et al.*, 2007), grape seeds (Roberts *et al.*, 2008), and black tea (Panchariya *et al.*, 2002).

The Page model, represented by equation 2.75, is a modification of the Lewis model aimed at achieving greater accuracy by introducing an empirical constant (Page, 1949). This model has demonstrated successful application in the drying analysis of shelled corn (Page, 1949), tomatoes (Doymaz, 2007), wheat (Rafiee *et al.*, 2008), dates (Hassan & Hobani, 2000), and barberries (Aghbashlo *et al.*, 2009b).

$$MR = \frac{(M_t - M_e)}{(M_i - M_e)} = \exp(-kt^n) \quad (2.75)$$

where,

n is empirical constant (dimensionless)

Modified Page models have been employed to characterize the drying behaviour of soybeans (Overhults *et al.*, 1973). A variant of the Page model, referred to as the modified Page I model, is described by equation 2.76. This particular modification has found application in the drying analysis of sesame hull (Al-mahasneh *et al.*, 2007).

$$MR = \frac{(M_t - M_e)}{(M_i - M_e)} = \exp(-kt)^n \quad (2.76)$$

The modified Page II model, as expressed in equation 2.77, represents a further adaptation of the Page model and offers insights into the drying behaviour of soybeans (White *et al.*, 1980). This model's applicability extends to various drying scenarios, including mint and basil leaves (Akpinar, 2006), aloe vera (Vega *et al.*, 2007), and papaya (Lemus-Mondaca *et al.*, 2009).

$$MR = \frac{(M_t - M_e)}{(M_i - M_e)} = \exp-(kt)^n \quad (2.77)$$

The modified Page II model, a modification of the Page model, finds its application in diverse drying contexts, including the drying of sweet potato slices (Diamante & Munro, 1993). The formulation of this model is provided in equation 2.78:

$$MR = \frac{(M_t - M_e)}{(M_i - M_e)} = \exp - k \left( \frac{t}{l^2} \right)^n \quad (2.78)$$

where,

$l$  is empirical constant (dimensionless)

The Henderson and Pabis (Single term) model, stemming from Fick's second law of diffusion, has found utility in the drying of corns (Henderson & Pabis, 1961). In scenarios where drying times are substantial, employing solely the first term ( $i = 1$ ) from the general series solution of equation 2.68 leads to minimum error. Based on this assumption, equation 2.68 is simplified to equation 2.79:

$$MR = \frac{(M_t - M_e)}{(M_i - M_e)} = A_1 \exp \left( - \frac{\pi^2 D_{\text{eff}}}{A_2} t \right) \quad (2.79)$$

Assuming the constancy of  $D_{\text{eff}}$  throughout the drying process, equation 2.79 can be rearranged through the incorporation of the drying constant  $k$ , yielding equation 2.80, which constitutes the Henderson and Pabis model:

$$MR = \frac{(M_t - M_e)}{(M_i - M_e)} = a \exp(-kt) \quad (2.80)$$

where,

$a$  is empirical constant which indicates shape (dimensionless)

The values of parameters  $a$  and  $k$  in equation 2.79 can be determined through experimental data analysis. While the Henderson and Pabis model is dependable for forecasting the initial stages of the drying process, its reliability diminishes for the later stages (Dissa *et al.*, 2008). This model has found applications in various drying scenarios, including African breadfruit seed (Shittu & Raji, 2011), banana, mango, and cassava (Koua *et al.*, 2009), as well as onion (Sawhney *et al.*, 1999). The gradient of the model ( $k$ ) is correlated to the effective diffusivity when the drying



process exclusively transpires in the falling rate period, governed by liquid diffusion (Panchariya *et al.*, 2002).

The Logarithmic (Asymptotic) model is a logarithmic variation of the Henderson and Pabis model, with an additional empirical term included, as depicted in equation 2.81 (Chandra & Singh, 2017; Erbay & Icier, 2010):

$$MR = \frac{(M_t - M_e)}{(M_i - M_e)} = a \exp(-kt) + c \quad (2.81)$$

where,

c is an empirical constant (dimensionless)

The Logarithmic (Asymptotic) model, expressed by equation 2.81, has been successfully employed in the drying investigations of various materials. This model has found applications in the drying of laurel leaves (Yagcioglu, 1999), green bell pepper (Doymaz & Ismail, 2010), pineapple (Kingsly *et al.*, 2009), barbunya bean (Kayisoglu & Ertekin, 2011), and white mulberry (Doymaz, 2004).

The Midilli model, as presented in equation 2.82, extends the Henderson and Pabis model by incorporating an additional empirical term that includes the drying time t (Midilli *et al.*, 2002):

$$MR = \frac{(M_t - M_e)}{(M_i - M_e)} = a \exp(-kt) + bt \quad (2.82)$$

where,

b is an empirical constant ( $s^{-1}$ )

The Midilli model is essentially a combination of both exponential and linear terms, offering a versatile representation for drying processes. This model has found applications in diverse drying scenarios, including pollen, mushrooms, and shelled/unshelled pistachios, utilizing various drying methods (Midilli *et al.*, 2002).

The Modified Midilli model, as defined by equation 2.83, introduces an adjustment to the shape term, denoted as a, within the Midilli model. In this modification, the shape term is assumed to

be 1.0 at  $t = 0$  (Ghazanfari *et al.*, 2006). Although this model has not been extensively applied to food materials, it has demonstrated favorable outcomes when used with flax fibers.

$$MR = \frac{(M_t - M_e)}{(M_i - M_e)} = \exp(-kt) + bt \quad (2.83)$$

The Demir *et al.* model, as expressed in equation 2.84, shares similarities with the Henderson and Pabis, modified Page-I, Logarithmic, and Midilli models (Demir & colleagues, 2007). This particular model has been employed in the context of drying green table olives.

$$MR = \frac{(M_t - M_e)}{(M_i - M_e)} = a \exp[(-kt)]^n + b \quad (2.84)$$

The Two-Term model, formulated in equation 2.85, takes into account the first two terms of the general series solution of Fick's second law of diffusion, aiming to address the limitations of the Henderson and Pabis model (Henderson, 1974). This model is designed to predict moisture transport and its parameters are indicative of the physical properties associated with the drying process. Notably, the Two-Term model has demonstrated successful applications in various contexts, including grain drying (Glenn, 1978), prickly pear fruit (Lahsasni *et al.*, 2004b) and cladodes (López *et al.*, 2009), sultana grapes (Yaldiz *et al.*, 2001), garlic (Sacilik & Unal, 2005), and pumpkin (Zenoozian *et al.*, 2008).

$$MR = \frac{(M_t - M_e)}{(M_i - M_e)} = a \exp(-k_1 t) + b \exp(-k_2 t) \quad (2.85)$$

where,

$k_1$  and  $k_2$  are the drying constants that can be obtained from experimental data ( $s^{-1}$ )

The Two-Term exponential model, represented by equation 2.86, is a refinement of the Two-Term model achieved by adjusting the constant factor and reconfiguring the representation of the shape constant,  $b$  (Doymaz, 2006; Erbay & Icier, 2010; Sharaf-Eldeen *et al.*, 1980). In this modified version, the value of  $b$  in the Two-Term model is defined as  $(1 - a)$  at  $t = 0$  to ensure  $MR = 1$ . This model has undergone testing in various applications, including pistachio (Midilli & Kucuk, 2003), leek (Doymaz, 2008), and radish (Lee & Kim, 2009).

$$MR = \frac{(M_t - M_e)}{(M_i - M_e)} = a \exp(-kt) + (1 - a) \exp(-kat) \quad (2.86)$$

The Modified Two-Term exponential models encompasses the Verma model and the Diffusion Approach model. The Verma model, represented by equation 2.87, refines the second exponential term of the Two-Term exponential model by introducing an empirical constant,  $g$  (Verma *et al.*, 1985). This modification aims to enhance the model's accuracy in capturing the drying behavior. The Verma model has found application in the drying of rice (Verma *et al.*, 1985), fig (Doymaz, 2005), and coffee (Resende *et al.*, 2009).

$$MR = \frac{(M_t - M_e)}{(M_i - M_e)} = a \exp(-kt) + (1 - a) \exp(-gt) \quad (2.87)$$

The diffusion approach model, described by equation 2.88, is an extension of the Verma model achieved by isolating the drying constant term  $k$  from the empirical constant  $g$  (Erbay & Icier, 2010; Kassem, 1998). This separation aims to provide a more flexible representation of the drying process by individually accounting for these two key factors. The diffusion approach model has been effectively utilized in the drying of various food materials, including tomato (Sacilik *et al.*, 2006), red pepper (Akpınar *et al.*, 2003a), pumpkin, green pepper (Yaldiz & Ertekin, 2001), and yam slices (Sobukola *et al.*, 2008).

$$MR = \frac{(M_t - M_e)}{(M_i - M_e)} = a \exp(-kt) + (1 - a) \exp(-kbt) \quad (2.88)$$

The Verma and Diffusion approach models have found application in the drying of a diverse range of products, showcasing their versatility and effectiveness. These models have been employed in drying apricots (Toğrul & Pehlivan, 2003), apples (Akpınar *et al.*, 2003b), bay leaves (Gunhan *et al.*, 2005), parsley (Akpınar *et al.*, 2006), and olives (Demir *et al.*, 2007), yielding comparable results across these different materials and processes.

The Modified Henderson and Pabis (Three-Term exponential) model is an advancement over the Henderson and Pabis and Two-Term models in the context of drying kinetics. It addresses the shortcomings of these models by incorporating a third term derived from the general series solution of Fick's second law of diffusion. This addition aims to better capture the intricacies of

the drying process and improve prediction accuracy. The model is represented by equation 2.89 (Karathanos, 1999).

$$MR = \frac{(M_t - M_e)}{(M_i - M_e)} = a \exp(-kt) + b \exp(-gt) + c \exp(-ht) \quad (2.89)$$

where,

a, b and c are constants which indicates shape obtained from experimental data

k, g and h are the drying constants obtained from experimental data ( $s^{-1}$ )

In the Modified Henderson and Pabis (Three-Term exponential) model, the primary focus is placed on the three individual terms that constitute the model equation. These terms correspond to different segments of the drying curve and contribute to capturing various stages of the drying process. Specifically, the first term addresses the later stages of drying, the second term pertains to the intermediate part of the curve, and the third term is responsible for representing the initial phase of the drying process.

### 2.6.3 Empirical Models

The Thompson model was formulated through experimentation on the drying of shelled corns within a temperature range of 60 to 150°C. It is represented by equation 2.90 (Thompson *et al.*, 1968):

$$t = a \ln(MR) + b[\ln(MR)]^2 \quad (2.90)$$

where,

a and b are dimensionless constants derived from the actual data

The Thompson model has found application in describing the drying behaviours of various materials, including sorghum (Paulsen & Thompson, 1973), green peas (Pardeshi *et al.*, 2009), and blueberries (Shi *et al.*, 2008).

The Wang and Singh model, an empirical approach designed for intermittent drying of rough rice, is represented by equation 2.91 (Sobukola *et al.*, 2008; Wang & Singh, 1978). This model has demonstrated effective application in describing the drying characteristics of various

products, including banana (Kadam & Dhingra, 2011), parsley leaves (Akpinar, 2011), and bamboo shoot slices (Bal *et al.*, 2010).

$$MR = 1 + bt + at^2 \quad (2.91)$$

where,

a is constant determined from actual data ( $s^{-2}$ )

b is constant derived from experimental data ( $s^{-1}$ )

The Kaleemullah model, an empirical formulation, incorporates moisture ratio, temperature, and time as in equation 2.92 (Kaleemullah, 2002):

$$MR = \exp(-cT + bt^{(pT+n)}) \quad (2.92)$$

where,

T is temperature ( $^{\circ}C$ )

c is drying constant ( $^{\circ}C^{-1}s^{-1}$ )

b is drying constant ( $s^{-1}$ )

p is drying constant ( $^{\circ}C^{-1}$ )

n is drying constant (dimensionless)

The Kaleemullah model has been effectively employed to describe the drying process of red chillies (Kaleemullah & Kailappan, 2006).

## 2.7 Research Gaps

Based on the literature review, the following research gaps were identified:

- (i) A knowledge gap pertaining the appropriate mathematical model to simulate the mass flow rate of maize grain through horizontal circular orifices in an experimental vertical pneumatic dryer.
- (ii) A knowledge gap on how variations in moisture content, drying air temperature, and mass flow rate of maize grain collectively influence two critical aspects: moisture removal rate and energy consumption in experimental vertical pneumatic dryers.
- (iii) A knowledge gap concerning the optimum allocation of energy for both the drying and transportation processes of maize grain, aiming to achieve the highest possible moisture removal rate.

- (iv) A knowledge gap regarding the optimum combination of moisture content, drying air temperature, and mass flow rate of maize grain that would lead to the highest moisture removal rate while minimising energy consumption during the drying process.
- (v) A knowledge gap exists in determining the most appropriate drying model for accurately describing the drying characteristics of maize grain. This gap highlights the need for research that systematically evaluates and compares various drying models to identify the model that best fits the drying characteristics of maize grain.

## **2.8 Conceptual Framework**

The simulation models for mass flow rate of maize grain were subjected to validation using data obtained from experiments involving horizontal circular orifices. These orifices had diameters ranging from 0.040 m to 0.056 m, with intervals of 0.002 m. The research explored the influence of three key parameters: moisture content (MC), drying air temperature ( $T_a$ ), and mass flow rate (MFR) of maize grain, on two critical factors: moisture removal rate (MRR) and energy used for grain drying and transportation (EU).

The experimental variables were set as follows: moisture content (MC) were considered at 20%, 25%, and 30% (wet basis), drying air temperature ( $T_a$ ) were examined at 60°C, 70°C, and 80°C, and mass flow rate (MFR) of maize grain were analyzed at 720 kg/h, 771 kg/h, and 864 kg/h. The energy proportioned for maize grain drying ( $E_a$ ) were 3.5 kWh, 5.5 kWh, and 7.7 kWh while that for transportation ( $E_g$ ) were 2.2 kWh, 2.4 kWh, and 2.8 kWh.

Through experimentation, the optimum values of  $E_a$  and  $E_g$  with respect to MRR during the drying process were determined. Additionally, the optimum levels of MC,  $T_a$ , and MFR were established concerning both MRR and EU. Throughout these experiments, the mass flow rate of the drying air remained constant at 547 kg/h for all conditions.

Figure 2.8 presents the schematic conceptual framework that underpins the entire research. This framework provides a visual representation of the various interconnected components and stages involved in the research. The framework visually conveys the key input variables, experimental setup and output parameters adopted to address the research objectives. Furthermore, the framework provides clear overview of how the research was structured and conducted, facilitating a better understanding of the research process and outcomes.

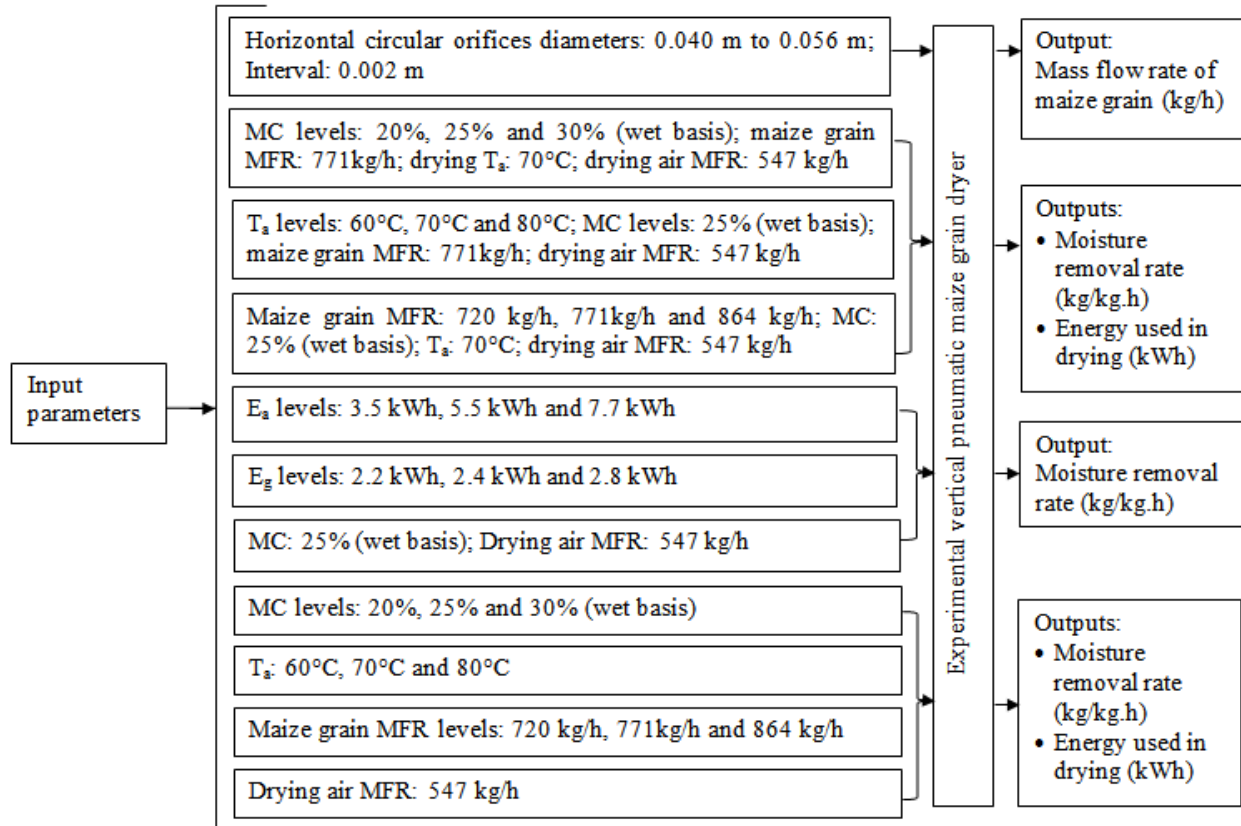


**Figure 2.8** Conceptual framework of the research

**CHAPTER THREE**  
**MATERIALS AND METHODS**

This chapter presents an experimental vertical pneumatic maize grain dryer and outlines research framework. It includes the development and testing of the dryer, validation of simulation models for maize grain flow through horizontal circular orifices, exploration of the effects of moisture content, air temperature, and mass flow rate on moisture removal rate and energy used, optimisation of key process parameters, and evaluation of drying models.

**3.1 Development of Experimental Vertical Pneumatic Maize Grain Dryer**

Figure 3.1 shows both a sectional view (a) and physical representation (b) of the experimental vertical pneumatic maize grain dryer (PMGD) that was developed and tested at Egerton University, Njoro Campus (0°22'11''S, 35°55'58.0''E) within the Department of Agricultural Engineering. Detailed drawing of the dryer is presented in Figure A1, Appendix A.

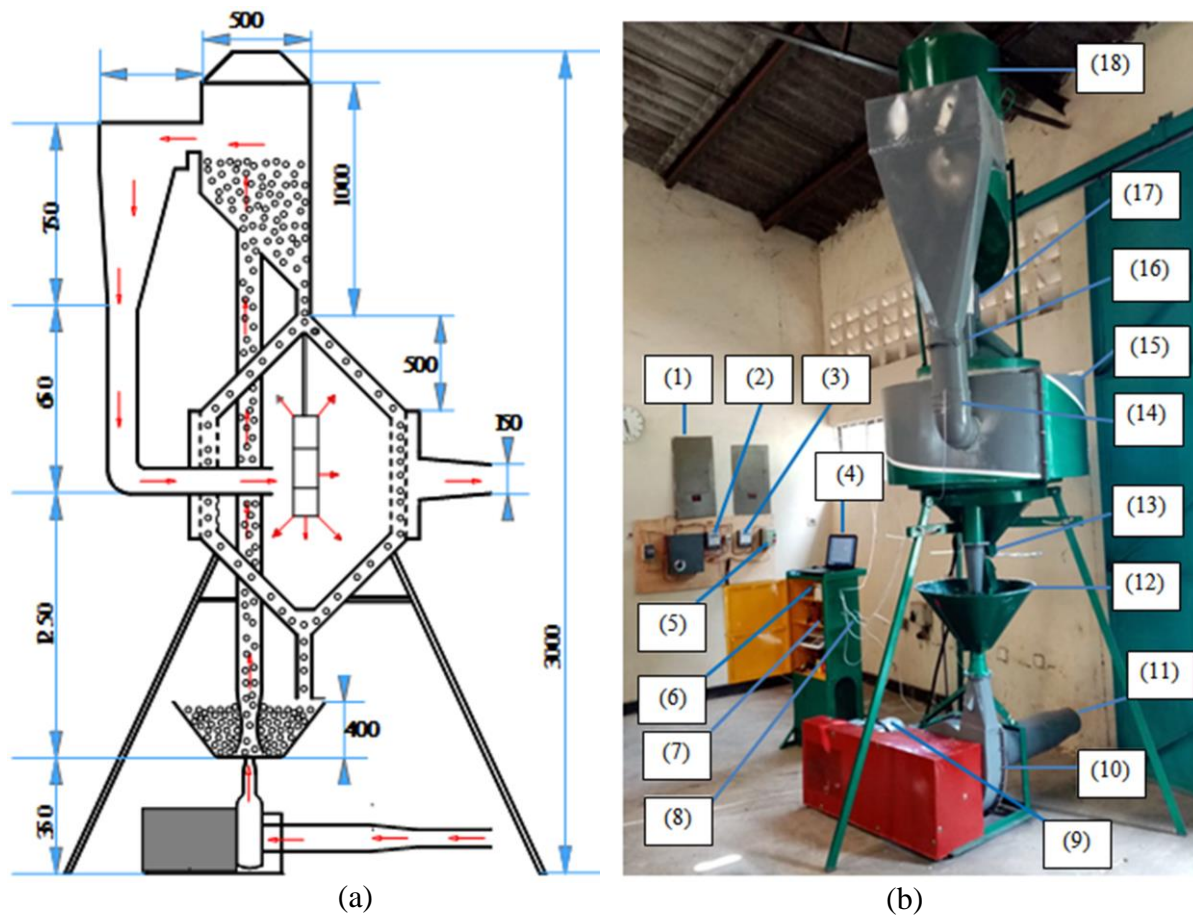


**Figure 3.1** Section view (a) and actual (b) experimental vertical pneumatic maize grain dryer



In Figure 3.1(b), the labelled components include: (1) power supply, (2) electric heater power meter, (3) blower power meter, (4) personal computer, (5) blower power switch, (6) data logger, (7) proportional integral derivative (PID) temperature controller, (8) platinum (Pt)-100 temperature sensors, (9) electric motor, (10) blower, (11) ambient air duct, (12) feed hopper, (13) sliding valve with horizontal circular orifices, (14) separated air duct, (15) drying chamber, (16) air-maize grain mixture duct, (17) separated maize grain duct, and (18) cyclone separator.

The loading unit of the PMGD featured an eight-blade blower, propelled by a single-phase electric motor (Model AMYOL132S, Astramilano, Italy). The motor had a power rating of 5.5 kW and a speed of 2900 revolutions per minute. The drying chamber was designed with two concentric cylinders of varying diameters, allowing for a 0.05 m gap to accommodate the maize grain during drying. The interior cylinder had a diameter of 0.64 m, while the exterior cylinder measured 0.74 m. The two cylinders were constructed using perforated metal sheets with uniform 0.008 m holes, facilitating the flow of heated air from the plenum chamber through the maize grain. The exterior cylinder was enveloped by an imperforated metal casing with a diameter of 0.84 m, directing all exhaust air through the outlet air duct into the atmosphere. The inlet and outlet air ducts were both 0.15 m in diameter. The drying chamber's capacity was 70.0 kg of maize grain. Figure 3.2 shows cross section of the drying chamber.

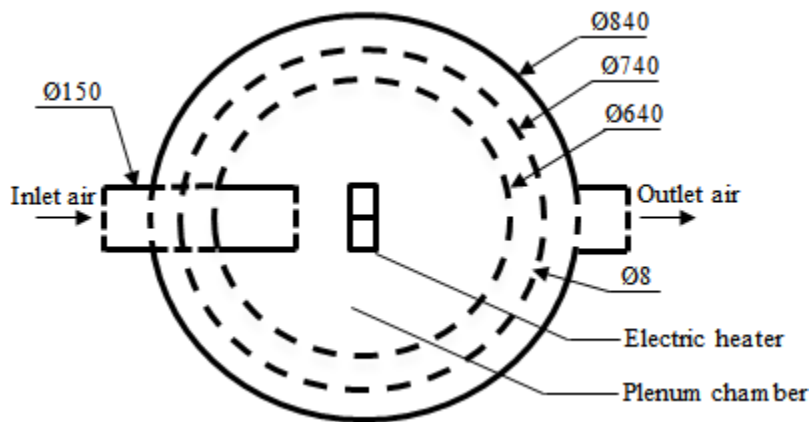


**Figure 3.2** Section view of drying chamber

The plenum chamber of the PMGD was equipped with a 14.4 kW electric heater positioned at the center and oriented perpendicular to the inlet air's flow direction. This heater consisted of eight stainless steel coils, each with a power rating of 1.8 kWh. The coils were affixed to a metallic frame, as depicted in Figure 3.3. To ensure even heating of the inlet air, four coils were

mounted on one side of the metallic frame, while the remaining four were positioned on the opposite side. The coils were spaced uniformly at intervals of 0.7 m.

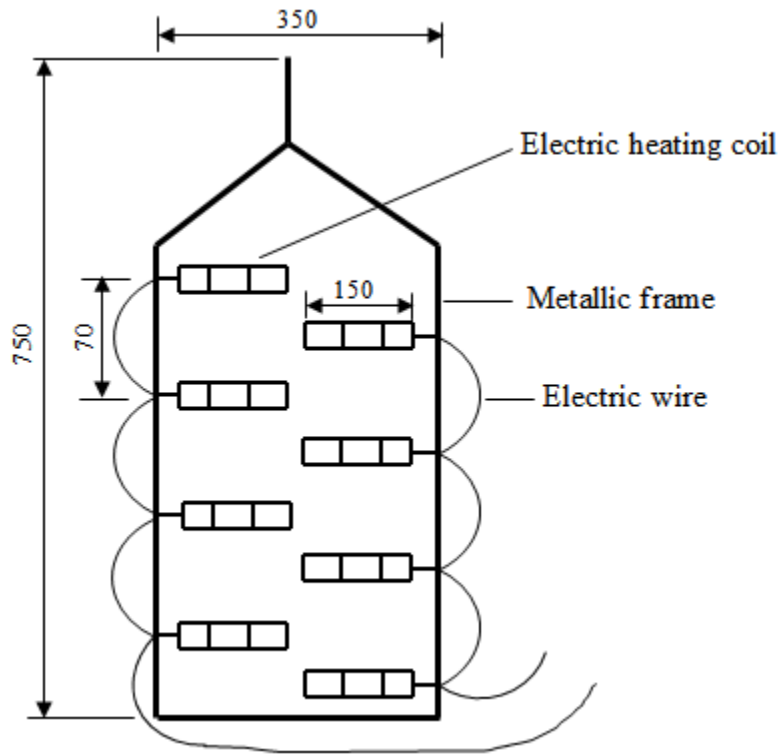


**Figure 3.3** Section view of electric heater

The appropriate number of electric heating coils was determined by comparing the sensible heat gain by the ambient air (inlet air) to the power rating of the heating coil. The calculation of the sensible heat gain by the ambient air was evaluated using equation 3.1:

$$Q_a = \rho_a q_v C_{pa} (T_{max} - T_{amb}) \quad (3.1)$$

where,

$Q_a$  is sensible heat gain by the inlet air (kJ/s)

$\rho_a$  is air density ( $\text{kg/m}^3$ )

$q_v$  is volumetric air flow rate ( $\text{m}^3/\text{s}$ )

$C_{pa}$  is specific heat of air (kJ/kg.K)

$T_{max}$  is maximum drying air temperature ( $^{\circ}\text{C}$ )

$T_{amb}$  is ambient air temperature ( $^{\circ}\text{C}$ )

The ambient air conditions, including temperature, density, specific heat capacity, and velocity, were set at 22°C, 1.2 kg/m<sup>3</sup>, 1007 J/kg·K, and 10 m/s, respectively. The maximum allowable drying air temperature for maize grain was set to 80°C.

The volumetric air flow rate ( $q_v$ ) was evaluated based on equation 3.2:

$$q_v = A_d v_a \quad (3.2)$$

where,

$A_d$  is cross sectional area of the inlet air duct (m<sup>2</sup>)

$v_a$  is inlet air velocity of the dryer (m/s)

Therefore, considering a maximum drying air temperature of 80°C and an inlet air velocity of 10 m/s, the calculated number of required electric heating coils was 7. However, for this research, 8 heating coils were used to account for estimated heat losses ranging from 5% to 20% of the total supplied energy for the drying process (Strumiłło *et al.*, 2014).

The operation of the PMGD involved two main processes: maize grain drying and transportation. In the grain drying process, the desired air temperature was set on the proportional integral derivative (PID) controller, an electronic intelligent device. The electric heater in the plenum chamber was turned on, and the power consumed was measured using a digital power meter. The heating of the air in the plenum chamber constituted the process. Continuous monitoring of air temperature (the controlled variable) in the plenum chamber was carried out using platinum (Pt)-100 sensor. This sensor translated the air temperature into a voltage signal, which was then transmitted to the PID controller. The PID controller had a comparator that compared the feedback signal with the set point. Depending on whether the error was positive or negative, the PID temperature controller made necessary adjustments and sent a forward path signal to the electric heater (actuator) to respond accordingly. Additionally, the ambient and outlet air temperatures were monitored using Pt100 temperature sensors connected to a 16-channel data logger. A personal computer, connected to the data logger via a USB cable, was used to display and record the temperature data. The relative humidity of the inlet and outlet air was also monitored using a digital temperature humidity sensor (Model UT333S, UNI-T Co., China). Figure 3.4 provides a schematic representation of the maize grain drying process.

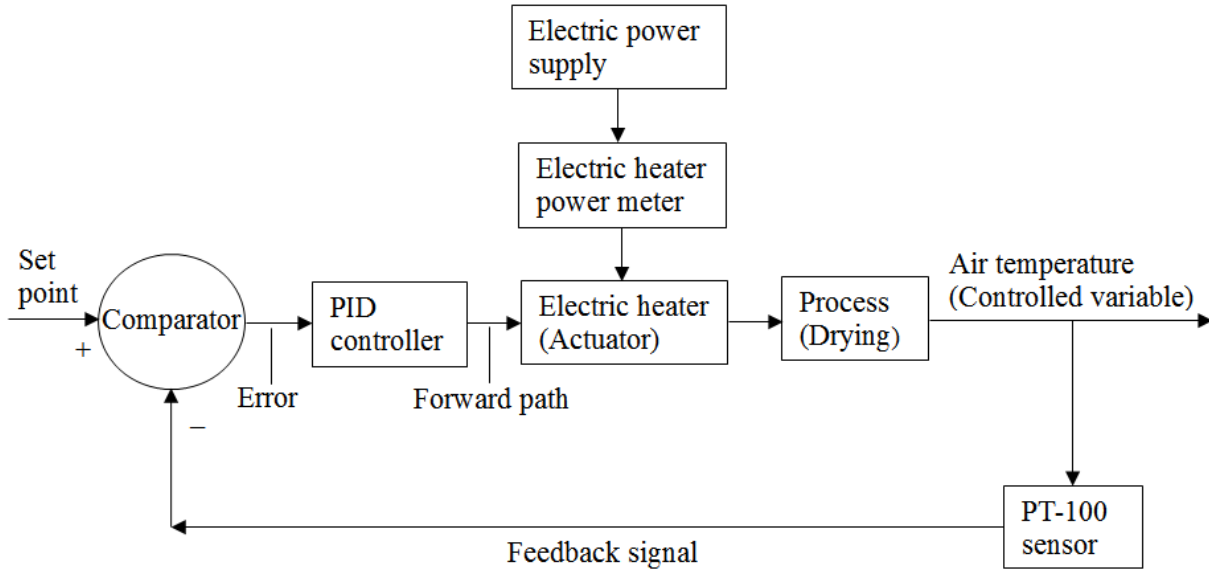


**Figure 3.4** Schematic drying process of maize grain

The maize grain transportation process involved putting on the electric motor coupled to the blower before loading the maize grain. The power consumption of the loading unit was monitored using a digital power meter (Model DDSS28II, Wenzhou linier electric co. Ltd, China). The feed hopper was utilized to introduce the maize grain into the moving airstream, which was drawn from the blower at a velocity of 36.4 m/s. The moving airstream's venturi effect at the intake facilitated vacuum-picking of the grain, which was then transported through a vertical duct to the cyclone. In the cyclone, the air-grain mixture was separated. The separated grain was conveyed to the drying chamber, while the air was directed to the plenum chamber, heated, and utilized in the drying process through a cross-flow mechanism. The maize grain underwent continuous re-circulation from the feed hopper to the cyclone separator and back to the hopper, initiating the process again. The exhaust air was released into the atmosphere. To ensure that the grain discharged from the drying chamber did not exceed the moving airstream's transportation capacity, the mass flow rate of the grain was controlled using horizontal circular orifices. Figure 3.5 shows maize grain transportation process in the experimental dryer.

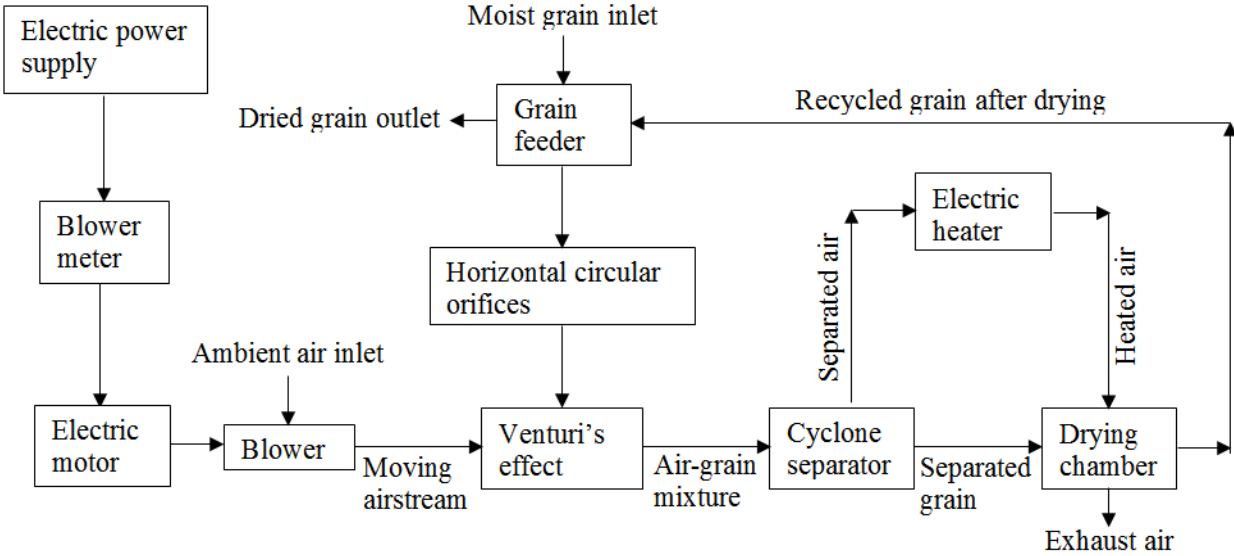


**Figure 3.5** Schematic transportation process of maize grain during drying

### 3.2 Validating Simulation Models for Mass Flow Rate of Maize Grain through Horizontal Circular Orifices

The validated simulation models encompassed Beverloo (BEV), British Code of Practice (BCP), and Tudor (TUD). The modified Beverloo model is given in equation 3.3:

$$Q_{\text{BEV}} = 3600C_d\rho_g A_e (gD_e)^{0.5} \quad (3.3)$$

where,

$Q_{\text{BEV}}$  is Beverloo model mass flow rate (kg/h)

$C_d$  is friction or discharge coefficient (dimensionless)

$\rho_g$  is bulk density of maize grain ( $\text{kg/m}^3$ )

$A_e$  is effective orifice area ( $\text{m}^2$ )

$g$  is acceleration due to gravity ( $\text{m/s}^2$ )

$D_e$  is effective hydraulic diameter (m)

The effective hydraulic diameter ( $D_e$ ) was ascertained using equation 2.2, detailed in subsection 2.1.1 of chapter two. Moreover, in accordance with previous studies (Lewis, 1992; Morrison *et al.*, 1994; Sharma & Fang, 2015),  $D_e$  was equated to the diameter of the orifice:

The effective orifice area ( $A_e$ ) was evaluated using equation 3.4:

$$A_e = \frac{\pi D_e^2}{4} \quad (3.4)$$

The modified BCP model is presented in equation 3.5:

$$Q_{BCP} = 3600 C_d \rho_g g^{0.5} (D_o - K_p d_g)^{2.5} \quad (3.5)$$

where,

$Q_{BCP}$  is British Code of Practice model mass flow rate (kg/h)

$D_o$  is diameter of horizontal circular orifice (m)

$d_g$  is diameter of maize grain (m)

The modified Tudor model is given in equation 3.6:

$$Q_{TUD} = 3600 \left( \frac{\pi \sqrt{2}}{6} \right) \rho_g (\delta g)^{0.5} D_o^{2.5} (1 - \mu)^{0.5} \quad (3.6)$$

where,

$Q_{TUD}$  is Tudor model mass flow rate (kg/h)

$\delta$  is the ratio of dome height of the maize grain to diameter of the orifice

$\mu$  is sliding coefficient of friction

Typically, the input parameters for the simulation models used to estimate mass flow rate encompassed the diameter of the orifice, moisture content of the maize grain, coefficient of friction or discharge, bulk density of the maize grain, acceleration due to gravity, shape factor, ratio of the height of the maize grain dome to the diameter of the orifice, and the coefficient of sliding friction.

The minimum diameter of the horizontal circular orifice for maize grain flow without jamming was evaluated based on equation 3.7 (Aguirre *et al.*, 2014):

$$D_o = R_c d_g \quad (3.7)$$

where,

$R_c$  is critical ratio of minimum orifice diameter to maize grain diameter (dimensionless)

In a flow regime, the probability of the grain jamming is zero provided  $R_c \geq 6$  (Aguirre *et al.*, 2014).

The mean characteristic dimensions (length, width, and thickness) of 100 randomly selected maize grains (hybrid 614) were measured using a digital vernier caliper with an accuracy of 0.01 mm. The mean values were determined based on established methods (Jafari & Tabatabaefar, 2008; Karababa & Coşkuner, 2007; Sangamithra *et al.*, 2016). Figure 3.6 illustrates the characteristic dimensions of the maize grain in both horizontal (a) and vertical (b) orientations.

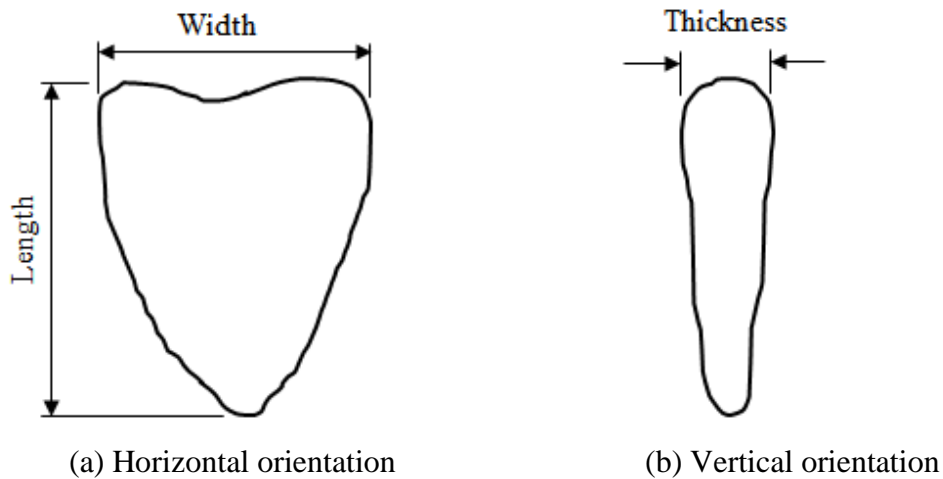


**Figure 3.6** Characteristic dimensions of maize grain

The geometric mean diameter, arithmetic mean diameter, and sphericity (shape factor) of the maize grain were determined using equations 3.8, 3.9, and 3.10, respectively, following established methods (Galedar *et al.*, 2010; Jafari & Tabatabaefar, 2008; Mohsenin, 1986):

$$\text{GMD} = (abc)^{\frac{1}{3}} \quad (3.8)$$

where,

GMD is geometric mean diameter (m)

a is mean length of the maize grain (m)

b is mean width of the maize grain (m)

c is mean thickness of the maize grain (m)

$$\text{AMD} = \frac{(a + b + c)}{3} \quad (3.9)$$

where,

AMD is arithmetic mean diameter of the maize grain (m)

$$\phi = 100 \frac{(abc)^{\frac{1}{3}}}{a} \quad (3.10)$$

where,

$\phi$  is sphericity or shape factor of the maize grain (%)

The mean measurements for maize grain dimensions were  $12.41 \pm 0.12$  mm in length,  $10.50 \pm 0.17$  mm in width, and  $4.96 \pm 0.14$  mm in thickness (Table C1, Appendix C). These values were used to calculate the geometric mean diameter (GMD) of 8.52 mm, arithmetic mean diameter (AMD) of 9.14 mm, and shape factor of 68.7% (Table C1, Appendix C). Adjusting the GMD and AMD using the shape factor yielded modified values of 5.85 mm and 6.28 mm, respectively. Consequently, based on equation 3.7 and utilizing the modified GMD and AMD, the minimum orifice diameters were determined to be 0.035 m and 0.038 m, respectively. However, in this study, the chosen minimum orifice diameter was 0.040 m.

The moisture content of the maize grain was determined through the collection of three random samples, each weighing 25.0 g. These samples were subjected to a constant temperature oven set at  $105^{\circ}\text{C}$  for 24 hours, after which their final weights were measured using a digital balance (Model: Scout Pro SPU6000, Ohaus Corporation, Pine Brook, NJ, USA). The moisture content of each sample was then calculated using equation 3.11 (Bala, 1997), and the mean value was determined:

$$\text{MC} = \left( \frac{w_i - w_f}{w_i} \right) \times 100 \quad (3.11)$$

where,

MC is moisture content of the sample (% , wet basis)

$w_i$  is initial weight of the sample (g)

$w_f$  is final weight of the sample (g)

Thus, the mean moisture content of maize grain was  $11.4 \pm 0.15\%$ , wet basis (Table C2, Appendix C).



In the Beverloo model, the constant input parameters included a friction or discharge coefficient ( $C_d$ ) of 0.75 and a shape factor ( $K_p$ ) of 1.4 (Beverloo *et al.*, 1961). The value of  $K_p$  was an average within the range of 1.3 to 1.5 (Agbetoye & Ogunlowo, 2010). In the British Code of Practice (BCP) model,  $C_d$  was set to 0.58, and  $K_p$  was taken as 1 due to the angle of inclination of the feed hopper wall being greater than  $45^\circ$  (Abd-El-Rahman & Youssef, 2008). In the Tudor model, the values of parameters were as follows: the ratio of dome height of the maize grain to orifice diameter ( $\delta$ ) was 0.3, and the sliding coefficient of friction ( $\mu$ ) was 0.36 (Tudor & Mieila, 2010). The bulk density ( $\rho_g$ ) of the maize grain was established as  $740 \text{ kg/m}^3$  using empirical models (Karababa & Coşkuner, 2007; McNeill *et al.*, 2004; Nelson, 1980). The mean diameter of the maize grain ( $d_g$ ) was 0.0085 m, and the acceleration due to gravity ( $g$ ) was  $9.81 \text{ m/s}^2$ .

Figure 3.7 shows algorithm for determination of mass flow rates of maize grain through horizontal circular orifices based on Beverloo (BEV), British Code of Practice (BCP) and Tudor (TUD) model.

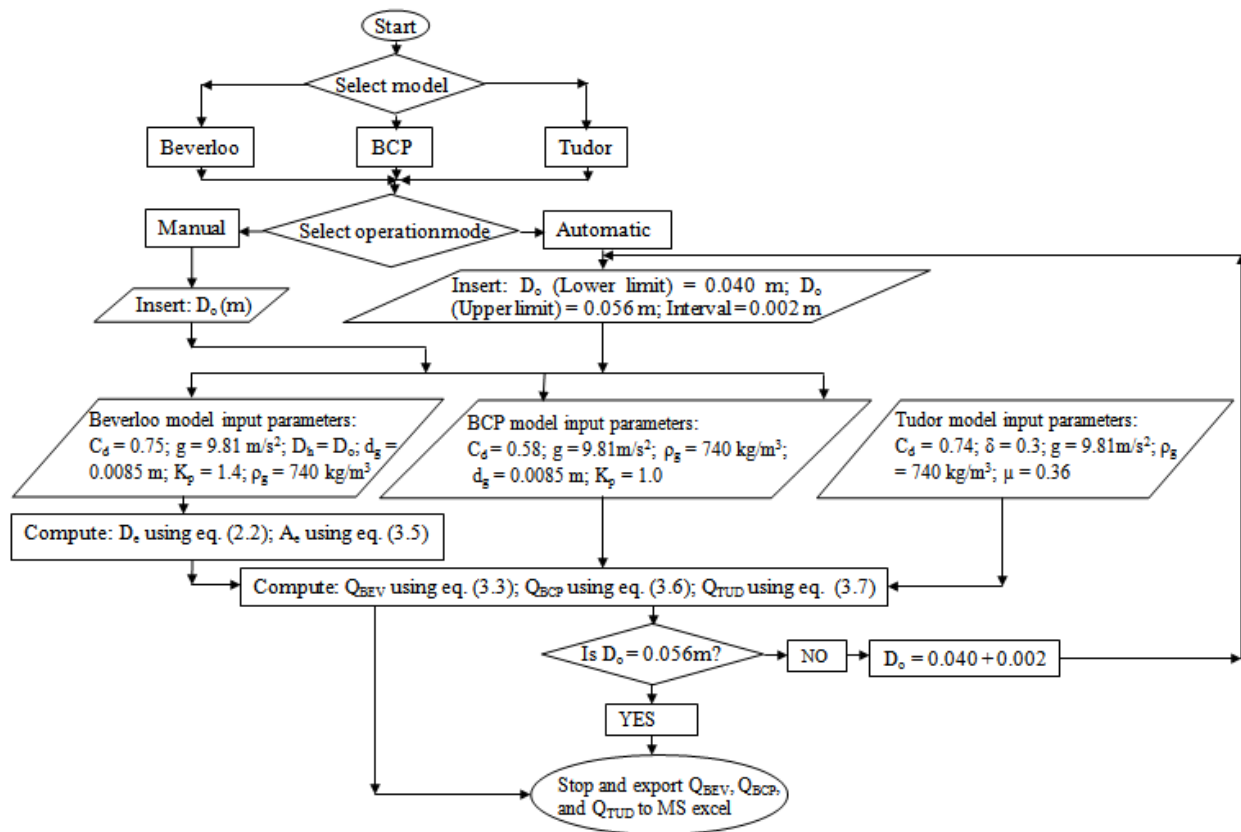


**Figure 3.7** Algorithm for mass flow rate of maize grain through horizontal circular orifices

The algorithm was implemented using the Python programming language and executed through a series of steps outlined in Figure 3.7. The process involved turning on the personal computer, launching the program, selecting the desired model (BEV, BCP, or TUD), choosing between manual and automatic modes, inputting the orifice diameter ( $D_o$ ) and constant parameters ( $C_d$ ,  $g$ ,  $D_h$ ,  $d_g$ ,  $K_p$ ,  $\rho_g$ ,  $\delta$ , and  $\mu$ ) of the selected model, computing the mass flow rates ( $Q_{BEV}$ ,  $Q_{BCP}$ , or  $Q_{TUD}$ ) based on the model, stopping the program, and exporting the computed mass flow rates to Microsoft Excel. For the BEV model, the intermediate parameters of effective hydraulic diameter ( $D_e$ ) and effective orifice area ( $A_e$ ) were determined before computing the mass flow rate.

In manual mode, the program calculates the mass flow rate for a specified orifice diameter without any iteration. Conversely, in automatic mode, a range of orifice diameters is selected, with lower and upper limits. The program conducts multiple iterations and calculates mass flow rates at specified intervals within the diameter range. The program stops and exports the results when the upper limit of the orifice diameter is reached.

In this research, the chosen orifice diameters ranged from 0.040 m to 0.056 m, with calculations performed at 0.002 m intervals. The constant input parameters for the models were determined as described in Section 3.2. The program's output was the mass flow rates of maize grain through horizontal circular orifices, expressed in kg/h. The coding of the program and user interfaces are available in Appendix B, and the simulation model's mass flow rates are discussed in Section 4.1 of chapter four.

The validation of the simulation models involved comparing the simulated mass flow rates with experimental data. Figure 3.8 illustrates the dimensions (a) and actual setup (b) used for data collection during validation. The setup had a height of 0.570 m, upper and lower section diameters of 0.365 m and 0.210 m, respectively.

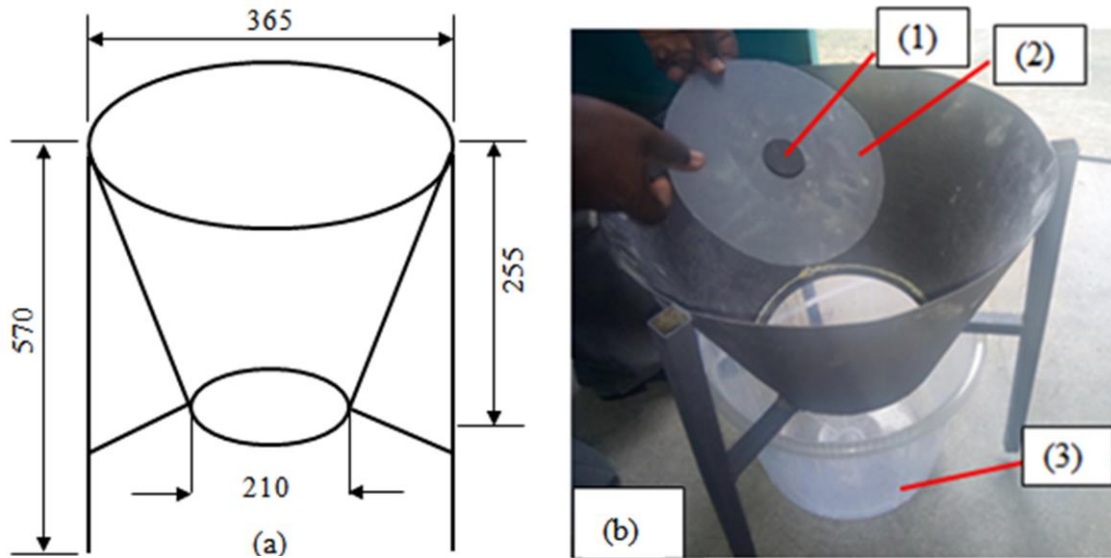


**Figure 3.8** Experimental set up for validation of simulation models for mass flow rate

In Figure 3.8, the components are labelled as follows: (1) represents the horizontal circular orifice, (2) corresponds to the circular cover plate located at the lower section of the experimental setup, and (3) signifies the container used for collecting the discharged maize grains.

To validate the simulation models, the experiment involved placing a circular cover plate with an orifice diameter of 0.040 m at the lower section of the experimental setup, as depicted in Figure 3.8(b). An empty container was positioned beneath the orifice to collect the discharged maize grains. The orifice was sealed, and the setup was loaded with 12.0 kg of maize grain having a moisture content of  $11.4 \pm 0.15\%$  (wet basis). As the grain was discharged through the orifice, a stopwatch was started to record the time taken for the complete discharge. Simultaneously, the weight of the collected grain was measured and documented. This experiment was repeated for varying orifice diameters: 0.042 m, 0.044 m, 0.046 m, 0.048 m, 0.050 m, 0.052 m, 0.054 m, and 0.056 m. Each experiment was replicated three times, and the mean mass flow rates were calculated using equation 3.12:

$$\text{MFR} = 3600 \frac{m_g}{t_g} \quad (3.12)$$

where,

MFR is maize grain mass flow rate through horizontal circular orifice (kg/h)  
 $m_g$  is mass of maize grain discharged through horizontal circular orifice (kg)  
 $t_g$  is time taken for maize grain to flow through horizontal circular orifice (s)

To evaluate the significance of differences between the actual and simulation model results, a student's t-test was employed at a 5% level of significance. The evaluation and selection of simulation models for mass flow rate were carried out using statistical techniques, including the coefficient of determination, reduced chi-square, and root mean square error.

The coefficient of determination was calculated using equation 3.13, which has been widely used in various research (Akpinar, 2006; Dandamrongrak *et al.*, 2002; Gunhan *et al.*, 2005; Jazini & Hatamipour, 2010; Sobukola *et al.*, 2008; Vega-Gálvez *et al.*, 2011).

$$R^2 = 1 - \frac{RSS}{CTSS} \quad (3.13)$$

where,

$R^2$  is coefficient of determination  
 RSS is residual sum of squares  
 CTSS is corrected total sum of squares

The reduced chi-square value was computed using equation 3.14, which has been employed in previous research for evaluation purposes (Doymaz *et al.*, 2004; Sarsavadia *et al.*, 1999).

$$\chi^2 = \frac{\sum_{i=1}^N (\psi_{\text{exp},i} - \psi_{\text{sim},i})^2}{N - n} \quad (3.14)$$

where,

$\chi^2$  is reduced chi-square  
 $\psi_{\text{exp},i}$  is experimental value  
 $\psi_{\text{sim},i}$  is simulated value  
 N is number of observations  
 n is number of constants in the model

The root mean square error was calculated using equation 3.15 (Doymaz *et al.*, 2004; Sarsavadia *et al.*, 1999).

$$\text{RMSE} = \left[ \frac{1}{N} \sum_{i=1}^N (\psi_{\text{exp},i} - \psi_{\text{sim},i})^2 \right]^{\frac{1}{2}} \quad (3.15)$$

where,

RMSE is root mean square error

The repeatability of the experimental data was evaluated by determination of mean and standard errors of the data. The absolute residual error was computed using equation 3.16 (Kanali, 1997; Uluko *et al.*, 2006):

$$\varepsilon_r = 100 \left| \frac{\psi_{\text{sim},i} - \psi_{\text{exp},i}}{\psi_{\text{exp},i}} \right| \quad (3.16)$$

where,

$\varepsilon_r$  is absolute residual error (%)

The simulation performance of the models at  $\mu_i$  (%) residual error interval was evaluated based on equation 3.17 (Kanali, 1997; Uluko *et al.*, 2006):

$$\eta_{\text{sim},\mu\%} = \frac{\beta_i}{\beta_t} \times 100 \quad (3.17)$$

where,

$\eta_{\text{sim},\mu\%}$  is simulation performance at  $\mu_i$  (%) residual error interval (%)

$\beta_i$  is number of data within the  $\mu_i$  (%) residual error interval

$\beta_t$  is total trial data

The actual and simulated mass flow rates of maize grain through the horizontal circular orifices are presented in section 4.1 of chapter four.

### **3.3 Determining Effect of Moisture Content, air Temperature and Mass Flow Rate on Moisture Removal Rate and Energy Used in Drying**

In this section, the influence of moisture content, air temperature, and mass flow rate of maize grain on moisture removal rate and energy consumption during drying is evaluated. The subsection 3.3.1 explores the impact of moisture content, while subsection 3.3.2 investigates the effect of air temperature, and subsection 3.3.3 delves into the influence of mass flow rate. The experiments were conducted using the hybrid 614 maize grain variety, which was obtained from a local farmer in Njoro sub-County, Nakuru County. The analysis of the collected data was performed through analysis of variance (ANOVA) and Fisher's least significant difference (LSD) test at a significance level of 5%.

#### **3.3.1 Effect of Moisture Content on Moisture Removal Rate and Energy used for Maize Grain Drying and Transportation**

To evaluate the influence of maize grain moisture content on moisture removal rate and energy used during drying, a series of experiments were conducted using three moisture content levels: 20%, 25%, and 30%, wet basis. These selected levels were within the typical range of moisture content found in maize grain during harvesting (FAO, 1992). A laboratory experiment was undertaken to precisely determine the moisture content of maize grain at these specified levels. The experiment involved immersing 70.0 kg of maize grain, initially possessing a moisture content of  $11.4 \pm 0.15\%$  on a wet basis, in tap water at a constant temperature of 18°C (Plate D1, Appendix D).

The moisture content of the rewetted maize grain was closely monitored over a span of 9 hours, with measurements taken at 15 minute intervals. During this process, samples of the rewetted maize grain were collected randomly from each container (Plate D1 of Appendix D). These collected samples were blended together and then divided into three equal portions, each weighing 25.0 g. Subsequently, every portion was placed within labelled and empty moisture cans whose weights were known. These moisture cans, along with the moist samples, were placed in a constant temperature oven set at 105°C for duration of 24 hours (ASAE, 1992). Upon extraction from the oven, the samples were allowed to cool, following which the weight of both the moisture cans and the dry samples was gauged using an Ohaus Scout Pro digital balance

(Model: Scout Pro SPU6000, Ohaus Corporation, Pine Brook, NJ USA). The moisture content of the samples was determined based on equation 3.11 in section 3.2.

The results of the laboratory experiment disclosed that a moisture content of 20% (wet basis) was achieved by subjecting the maize grain to rewetting for approximately 0.75 hours. Similarly, a moisture content of 25% was obtained through a rewetting period of about 1.75 hours, while a moisture content of 30% was reached after a rewetting period of approximately 5.75 hours. These findings are detailed in Table 3.1.

**Table 3.1** Rewetting and resulting moisture content of maize grain

<b>Rewetting time (h)</b>	<b>Mean moisture content of maize grain (% , wet basis)</b>
0.00	11.4 ± 0.15
0.75	20.0 ± 0.29
1.75	25.0 ± 0.67
5.75	30.0 ± 0.41

The mean values ± standard error

Furthermore, the laboratory results showing the variation of maize grain moisture content with different rewetting durations are provided in Table D1 and presented in Figure D1 (Appendix D).

Consequently, the influence of varying moisture content levels at 20%, 25%, and 30% (wet basis) on both moisture removal rate and energy used in the drying process was evaluated. To explore this, an initial batch of 70.0 kg of maize grain with an initial moisture content of 11.4 ± 0.15% (wet basis) was subjected to rewetting in tap water at 18°C for 0.75 hours to achieve a moisture content level of 20%, wet basis. The excess surface moisture of the grain was drained before the drying phase commenced. The drying process involved continuous recirculation of the maize grain. The mass flow rate (MFR) of the grain was controlled at 771 kg/h by employing a horizontal circular orifice with a diameter of 0.042 m. Concurrently, the MFR of the drying air was fixed at 547 kg/h. Throughout the experiment, the plenum chamber air temperature was maintained at 70°C. The Pt100 temperature sensors constantly monitored the air temperature, thereby ensuring that the air temperature remained at the designated set point of 70°C through the experiment. This temperature control was achieved by the feedback mechanism of the PID controller, which in turn adjusted the electric heater to maintain the desired air temperature.

Throughout the drying process, both the moisture removal rate and the energy used were systematically monitored at 15 minute intervals. The moisture removal rate was calculated using the equation 3.18 (FAO, 2011):

$$W_2 = W_1 - \frac{W_1(M_1 - M_2)}{100 - M_2} \quad (3.18)$$

where,

$W_2$  is weight of dried maize grain (kg)

$W_1$  is weight of undried maize grain (kg)

$M_1$  is moisture content of undried maize grain (%)

$M_2$  moisture content of dried maize grain (%)

The energy used for both the drying and transportation of maize grain was measured using a digital power meter. This was conducted separately for each process. To ensure accuracy and reliability, three replications of the experiments were performed, and the mean values of the moisture removal rate and energy used for drying were calculated accordingly.

The same experiment was repeated for maize grain with moisture content levels of 25% and 30% (wet basis). To achieve the moisture content level of 25%, dried maize grain with an initial moisture content of  $11.4 \pm 0.15\%$  was rewetted in tap water at  $18^\circ\text{C}$  for 1.75 hours. Similarly, the moisture content level of 30% was obtained by rewetting the maize grain for 5.75 hours. The plenum chamber air temperature, mass flow rate of maize grain, and air conditions were kept consistent with the initial experiment. The results of these experiments, highlighting the influence of different moisture content levels on moisture removal rate and energy used during drying, are presented in subsection 4.2.1 of chapter four.

### **3.3.2 Effect of air Temperature on Moisture Removal Rate and Energy Used for Maize Grain Drying and Transportation**

To determine the influence of air temperature on moisture removal rate and energy used in maize grain drying, three temperature levels ( $60^\circ\text{C}$ ,  $70^\circ\text{C}$ , and  $80^\circ\text{C}$ ) were considered. These temperature levels were selected within the optimum range for maize grain drying (Gao *et al.*, 2021). In the initial experiment, the dryer was loaded with 70.0 kg of rewetted maize grain possessing an initial moisture content of 25% (wet basis). This moisture level was achieved by



rewetting maize grain with an initial moisture content of  $11.4 \pm 0.15\%$  in tap water at  $18^{\circ}\text{C}$  for 1.75 hours. The drying process lasted for 2 hours, with the plenum air temperature set to  $60^{\circ}\text{C}$  using the electric heater. The temperature was maintained consistently at this level throughout the drying process through the use of a PID controller. The mass flow rate of the drying air was maintained at 547 kg/h, and the maize grain underwent continuous recirculation. The grain mass flow rate was controlled at 771 kg/h using a horizontal circular orifice with a diameter of 0.042 m. The moisture removal rate and energy used were evaluated as outlined in section 3.3.1. Similar experiment was repeated for air temperature levels of  $70^{\circ}\text{C}$  and  $80^{\circ}\text{C}$ , while maintaining consistent conditions for grain moisture content and mass flow rates. The results of these experiments, detailing the effect of drying air temperature on moisture removal rate and energy used during drying, are provided in subsection 4.2.2 of chapter four.

### **3.3.3 Effect of Mass Flow Rate on Moisture Removal rate and Energy Used for Maize Grain Drying and Transportation**

To establish the influence of maize grain mass flow rate on moisture removal rate and energy used during drying, three distinct levels were investigated: 720 kg/h, 771 kg/h, and 864 kg/h. These levels were achieved by controlling the grain mass flow through the utilization of horizontal circular orifices with diameters of 0.040 m, 0.042 m, and 0.044 m, respectively. The initial experiment involved loading the dryer with 70.0 kg of rewetted maize grain that had an initial moisture content of 25% (wet basis). The grain was subsequently subjected to a 2-hour drying period. The 25% moisture content level was achieved by rewetting the maize grain with an initial moisture content of  $11.4 \pm 0.15\%$  in tap water at  $18^{\circ}\text{C}$  for 1.75 hours. Throughout the drying process, the maize grain was continuously recirculated. The mass flow rates of the grain and drying air were set at 720 kg/h and 547 kg/h, respectively. The plenum chamber air temperature was elevated to  $70^{\circ}\text{C}$  and maintained at that level for the entire drying duration using the PID controller. The moisture removal rate and energy used were evaluated at 15 minute intervals, as described in subsection 3.2.1. Three replications were carried out, and the average moisture removal rate and energy used were computed. Similar experiments were repeated for maize grain mass flow rates of 771 kg/h and 864 kg/h, maintaining consistent conditions for grain moisture content, drying air temperature, and air mass flow rate. The results of these experiments, describing the effect of maize grain mass flow rate on moisture removal rate and energy used during drying, are presented in subsection 4.2.3 of chapter four.

### 3.4 Optimising Energy Proportioned for Maize Grain Drying and Transportation

The total supplied energy in experimental vertical pneumatic maize dryer was proportioned to energy for maize grain drying and transportation as shown in Figure 3.9.

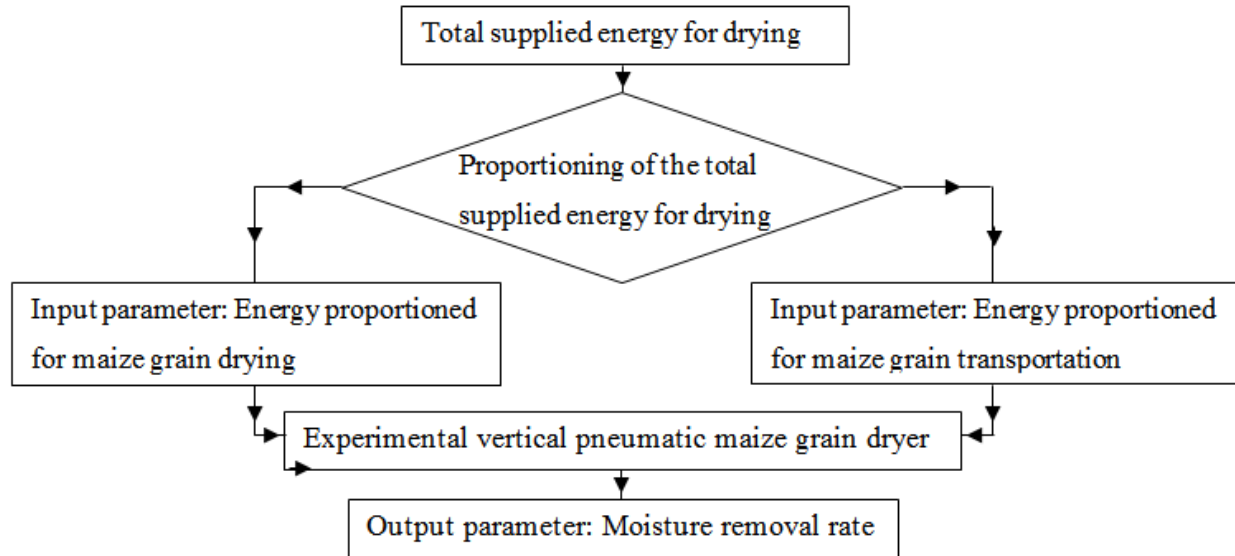


**Figure 3.9** Proportioning of total supplied energy for maize grain drying

The optimisation of energy proportioned for drying and transportation of maize grain, considering moisture removal rate, was conducted using Taguchi method, as detailed in subsection 2.4.1 of chapter two. The energy proportioned for maize grain drying was set at levels of 3.5 kWh, 5.5 kWh, and 7.3 kWh, while for transportation, levels of 2.2 kWh, 2.4 kWh, and 2.8 kWh were considered. The experimental design for Taguchi L9 orthogonal array (OA), along with the energy levels, is shown in Table 3.2.

**Table 3.2** Taguchi’s L<sub>9</sub> orthogonal array experimental design with levels of energy proportioned for maize grain drying and transportation

Experiment	Proportions of energy used for drying	
	Energy for maize grain drying (kWh)	Energy for maize grain transportation (kWh)
1	3.5	2.2
2	3.5	2.4
3	3.5	2.8
4	5.5	2.2
5	5.5	2.4
6	5.5	2.8
7	7.3	2.2
8	7.3	2.4
9	7.3	2.8

The energy proportioned for drying and transportation of maize grain corresponded to the power consumption of the electric heater and blower, respectively. Hence, the energy amounts of 3.5 kWh, 5.5 kWh, and 7.3 kWh for drying were achieved by heating the plenum chamber air to 60°C, 70°C, and 80°C, respectively, and maintaining these temperatures with the PID controller. Similarly, the energy allocations of 2.2 kWh, 2.4 kWh, and 2.8 kWh for transportation of maize grain were established by regulating the grain flow rates at 720 kg/h, 771 kg/h, and 864 kg/h, respectively. These grain flow rates were achieved through the use of horizontal circular orifices with diameters of 0.040 m, 0.042 m, and 0.044 m, respectively.

In Experiment 1, the dryer was loaded with 70.0 kg of maize grain with a moisture content of 25% (wet basis). This moisture level was achieved by rewetting dried maize grain with an initial moisture content of  $11.4 \pm 0.15\%$  (wet basis) in tap water at 18°C for 1.75 hours, as described in subsection 3.3.1. Throughout the 2 hour drying period, the plenum chamber air temperature was maintained at 60°C using the PID controller, while the mass flow rate of the drying air remained constant at 547 kg/h. The maize grain was continuously re-circulated and controlled at a mass flow rate of 720 kg/h. The energy used for drying and transportation of the grain was measured at 15 minute intervals using digital power meters, and the moisture removal rate was also

determined at the same intervals as explained in subsection 3.3.1. A total of three replications were performed, and the average moisture removal rate was computed. Experiments 2 to 9 followed a similar approach, involving different combinations of energy proportioned for drying and transportation of the grain, as outlined in Table 3.2. The moisture content of the maize grain was maintained at 25% (wet basis), and the mass flow rate of the drying air was held constant at 547 kg/h for all these experiments.

The optimisation process utilized Taguchi method, where the signal-to-noise ratio served as the quality characteristic of choice (Taguchi, 1990). The approach followed the larger is better criterion, aiming to maximise the response, which in this case is the moisture removal rate. The signal-to-noise ratio corresponding to a larger response was calculated using equation 2.46 outlined in subsection 2.4.1 of chapter two.

An analysis of variance (ANOVA) was conducted at a 5% significance level to ascertain the process parameters that had a significant influence on the moisture removal rate during maize grain drying. The percentage contribution of energy proportioned for drying and transportation of the grain on the moisture removal rate was computed using equation 2.55, as described in subsection 2.4.1 of chapter two.

The results of optimisation of energy proportioned for maize grain drying and transportation with respect to moisture removal rate are presented in section 4.3 of chapter four.

### **3.5 Optimising Moisture Content, air Temperature and Mass Flow Rate in Maize Grain Drying**

The Taguchi method was employed to determine the optimum moisture content, air temperature, and mass flow rate of maize grain that would yield the highest moisture removal rate and minimise energy used during the drying process. This optimisation process was carried out using the principles of Taguchi method, as detailed in subsection 2.4.1 of chapter two.

The optimisation process involved considering three levels each for moisture content, air temperature, and mass flow rate of maize grain, which were 20%, 25%, and 30%; 60°C, 70°C, and 80°C; and 720 kg/h, 771 kg/h, and 864 kg/h, respectively. The experimental design was

based on Taguchi L9 orthogonal array (OA), which is presented in Table 3.3, outlining the various combinations of the selected process parameter levels.

**Table 3.3** Taguchi’s L<sub>9</sub> orthogonal array experimental design with levels of moisture content, air temperature and mass flow rate

<b>Selected process parameters with level factors</b>			
<b>Experiment</b>	<b>Moisture content (%, wet basis)</b>	<b>Air temperature (°C)</b>	<b>Mass flow rate (kg/h)</b>
1	20	60	720
2	20	70	771
3	20	80	864
4	25	60	771
5	25	70	864
6	25	80	720
7	30	60	864
8	30	70	720
9	30	80	771

In the first experiment (Table 3.3), the dryer was loaded with 70.0 kg of maize grain with an initial moisture content of 20%. The drying process was conducted for 2 hours. The moisture content level of 20% was obtained by rewetting maize grain with an initial moisture content of  $11.4 \pm 0.15\%$  (wet basis) using tap water at 18°C for a period of 0.75 hours, as explained in subsection 3.3.1. Throughout the experiment, the plenum chamber air was heated to 60°C and consistently maintained at that temperature using a PID controller (Model 3300, Cal Controls, United Kingdom). The maize grain was continuously recirculated and controlled to maintain a mass flow rate of 720 kg/h, using horizontal circular orifice with a diameter of 0.040 m. The mass flow rate of the drying air remained constant at 547 kg/h. The moisture removal rate and energy used for maize grain drying were recorded at 15 minute intervals, following the approach outlined in subsection 3.3.1. A total of three replications were performed, from which the average moisture removal rate and energy used in maize grain drying computed.

The experiments 2 to 9 (Table 3.3), were conducted using a similar approach as that of the first experiment (Table 3.3). However, the moisture content levels of 25% and 30% were obtained by rewetting maize grain with an initial moisture content of  $11.4 \pm 0.15\%$  (wet basis) using tap water at  $18^{\circ}\text{C}$  for durations of 1.75 hours and 5.75 hours, respectively, as described in subsection 3.3.1. Additionally, the mass flow rate of the drying air was kept constant at 547 kg/h throughout these experiments. The desired mass flow rates of 771 kg/h and 864 kg/h were achieved by controlling the flow of maize grain using horizontal circular orifices with diameters of 0.042 m and 0.044 m, respectively. The other conditions, such as plenum chamber air temperature and recirculation, remained consistent with those described in the first experiment.

The Taguchi method (Taguchi, 1990) was used to establish the optimum combination of process parameters that would lead to both maximum moisture removal rate and minimum energy used in the drying process. In this method, the signal to noise ratio was used as the quality characteristic for optimisation. The specific characteristics being optimised were the moisture removal rate and energy used during the drying process. The larger is better criterion, which aims to maximise the response, was applied for the optimisation of the moisture removal rate, as detailed in section 3.4 of chapter three. On the other hand, the smaller is better criterion, which aims to minimise the output, was employed when optimising the selected process parameters concerning the energy used for maize grain drying. The signal to noise ratio for the smaller is better criterion was calculated based on equation 2.45 in subsection 2.4.1 of chapter two.

An analysis of variance (ANOVA) was conducted at a significance level of 5% to determine the significance of the selected process parameters, which include moisture content, air temperature, and mass flow rate, on both the moisture removal rate and energy used in the maize grain drying. This analysis helps determine which parameter has a more pronounced influence on the responses.

Additionally, the percentage contribution of each individual process parameter was calculated. This calculation provides insight into the proportion of influence each parameter holds over the final results. The formula used for this determination is given by equation 2.55 in section 2.4 of chapter two. This allows for a quantitative understanding of the relative importance of each parameter in relation to the overall performance of the drying process.

A confirmatory test was conducted using the optimised process parameters to verify whether any improvement was achieved in terms of moisture removal rate and energy used in maize grain drying. This test aimed to validate the effectiveness of the determined optimum conditions by comparing the actual data with the predicted improvements based on the optimisation results.

The results of the optimisation process, including the determined optimum values for moisture content, air temperature, and mass flow rate of maize grain, along with the subsequent effect on moisture removal rate and energy used in the drying, are presented in section 4.4 of chapter four.

Table 3.4 shows selected models that have been used to describe drying characteristics of various grains as presented in section 2.6 of chapter two.

**Table 3.4** Selected drying models for grains

Model name	Model	Grain tested	Source
Single term	$MR = a \exp(-kt)$	Corns	(Henderson and Pabis, 1961)
Logarithmic	$MR = a \exp(-kt) + c$	Beans	(Kayisoglu & Ertekin, 2011)
Modified Page I	$MR = \exp(-kt)^n$	Soybeans	(Overhults <i>et al.</i> , 1973)
Modified Page II	$MR = \exp(-kt)^n$	Soybeans	(White <i>et al.</i> , 1980)
Verma	$MR = a \exp(-kt) + (1-a)\exp(-gt)$	Rice	(Verma <i>et al.</i> , 1985)
Page	$MR = \exp(-kt^n)$	Shelled corns; wheat	(Paulsen & Thompson, 1973; Thompson <i>et al.</i> , 1968)
Thomson	$MR = a \ln(MR) + b[\ln(MR)]^2$	Shelled corns; Sorghum	(Paulsen & Thompson, 1973; Thompson <i>et al.</i> , 1968)
Two-Term	$MR = a \exp(-k_1t) + b \exp(-k_2t)$	Kernel	(Glenn, 1978)
Wang and Singh	$MR = 1 + bt + at^2$	Rice	(Sobukola <i>et al.</i> , 2008; Wang & Singh, 1978)

The models selected for evaluating the variation of moisture ratios with time in maize grain drying (Table 3.4) were tested to determine which one was most suitable for accurately

describing this relationship. The relative humidity of the drying air was not controlled during these tests. As a result, the actual moisture ratios of the maize grain were calculated using the equation 2.71 provided in subsection 2.6.1 of chapter two.

To establish the constants and coefficients of the drying models, the actual moisture ratios were used as input data. This process was conducted using the MATLAB R2019a curve fitting tool. The performance of the different models was then analyzed using two key indicators: coefficient of determination ( $R^2$ ) and root mean square error (RMSE). Generally, if the value of  $R^2$  is higher and the value of RMSE is lower, the goodness of fit is better, signifying that the model's predictions closely align with the actual data (Sacilik & Elicin, 2006; Yaldiz & Ertekin, 2001). Higher  $R^2$  values also indicate a stronger correlation between the actual and model values (Neter *et al.*, 1990).

The result of these analyses helps in determining which model provides the most accurate representation of the moisture ratio variation over time during maize grain drying. This was essential for selecting an appropriate model that could be used for prediction purposes. The results of the model performance analysis are presented in section 4.4 of chapter four.



## CHAPTER FOUR

### RESULTS AND DISCUSSIONS

This chapter focuses on several key aspects related to the validation and analysis of simulation models for the mass flow rate of maize grain through horizontal circular orifices, as well as the effects of various parameters on moisture removal rate and energy used in the drying process. Additionally, the optimisation of selected process parameters and the evaluation of drying models for grains are also discussed.

#### 4.1 Validation of Simulation Models for Mass Flow Rate of Maize Grain Through Horizontal Circular Orifices

The actual mass flow rates of maize grain through horizontal circular orifices with diameters increased from 0.040 m to 0.056 m ranged from 720 kg/h to 1735 kg/h. In comparison, the simulated mass flow rates based on the Beverloo, British Code of Practice (BCP), and Tudor models ranged from 650 kg/h to 2006 kg/h, 851 kg/h to 2378 kg/h, and 867 kg/h to 2010 kg/h, respectively (Table C3, Appendix C).

Figure 4.1 shows the actual, Beverloo, British Code of Practice and Tudor model mass flow rates of maize grain through horizontal circular orifices.

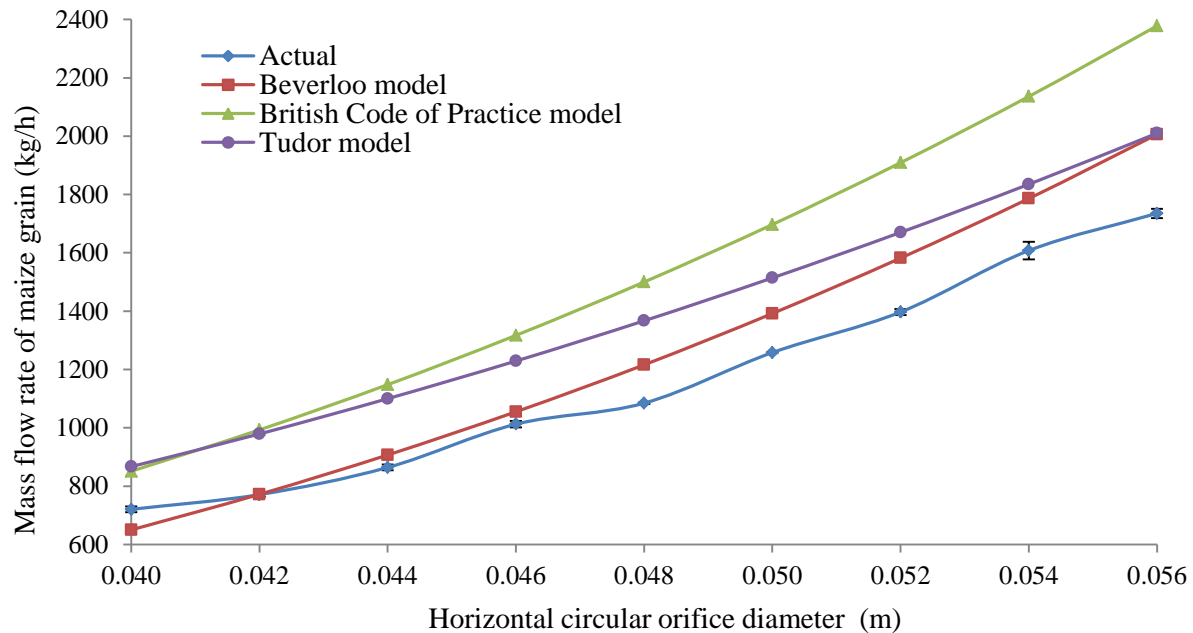


**Figure 4.1** Effect of horizontal circular orifices diameters on mass flow rate of maize grain for actual and simulation models

The mass flow rates of both the actual and simulation models exhibited an upward trend as the orifice diameters increased (Figure 4.1). Notably, the mass flow rate predicted by the Beverloo model closely matched the actual values when the orifice diameter ranged from 0.040 m to 0.046 m. However, the disparity between the Beverloo model's predictions and the actual mass flow rates became more pronounced, ranging from 43 kg/h to 271 kg/h, as the orifice diameter increased beyond 0.046 m. This observation indicates that the Beverloo model accurately simulated the mass flow rate of maize grain for orifice diameters between 0.040 m and 0.046 m, but its predictive accuracy diminished for orifice diameters greater than 0.046 m.

The plots of the mass flow rate simulated by the British Code of Practice (BCP) model and the actual values exhibited similar trends as the orifice diameters increased. However, the deviation between the BCP model and actual mass flow rate grew from 131 kg/h to 643 kg/h as the orifice diameter expanded from 0.040 m to 0.056 m. This discrepancy, with an average deviation of  $387 \pm 52$  kg/h, was higher than the deviations observed between the Beverloo model and actual ( $117 \pm 27$  kg/h) and the Tudor model and actual ( $236 \pm 13$  kg/h). This discrepancy shows that the BCP model tended to overestimate the mass flow rate of maize grain more significantly compared to the Beverloo and Tudor models. This discrepancy might be attributed to the fact that the BCP model was initially designed for predicting flow rates of granular materials through orifices with undefined shapes (Abd-El-Rahman & Youssef, 2008).

The variations in mass flow rates simulated by the Tudor model and the actual values followed a similar trend as the orifice diameter increased. However, the degree of deviation between the Tudor model and the actual mass flow rate displayed significant inconsistency, ranging from a minimum of 147 kg/h observed at an orifice diameter of 0.040 m to a maximum of 282 kg/h at an orifice diameter of 0.048 m.

As the orifice diameter increased, the trends in the mass flow rates simulated by the Beverloo and Tudor models showed similarities. The deviation in mass flow rate between the Beverloo and Tudor models decreased gradually from 217 kg/h to 4 kg/h as the orifice diameter increased from 0.040 m to 0.056 m. This trend indicates that the mass flow rate predictions of the Beverloo and Tudor models tended to converge at an orifice diameter of 0.056 m.

Furthermore, the trends in mass flow rates of the Beverloo and BCP models exhibited similarities as the orifice diameter increased. This similarity can be attributed to the fact that the BCP model was derived from the Beverloo model (Abd-El-Rahman & Youssef, 2008). However, the discrepancy between the two plots gradually grew larger, ranging from 201 kg/h to 372 kg/h, as the orifice diameters increased from 0.040 m to 0.056 m.

Moreover, the trends in mass flow rates of the Tudor and BCP models exhibited similarities as the orifice diameter increased. The plots of mass flow rates for the Tudor and BCP models were comparable when the orifice diameters increased from 0.040 m to 0.042 m. However, the two plots gradually deviated as the orifice diameters increased further, from 0.042 m to 0.056 m. The discrepancy in mass flow rates was 14 kg/h for an orifice diameter of 0.042 m and increased to 368 kg/h for an orifice diameter of 0.056 m.

Therefore, the performance of the Beverloo, BCP, and Tudor models in simulating the mass flow rate of maize grain through horizontal orifices was found to be unsatisfactory. Utilizing the MATLAB R2019a curve fitting tool (Figure C1, Appendix C) and fitting a regression line led to the development of New model for the mass flow rate of maize grain, as presented in equation 4.1:

$$Q_N = 1.903 \times 10^6 D_o^2 - 1.17 \times 10^5 D_o + 2341 \quad (4.1)$$

$$\text{for } \left\{ \begin{array}{l} R^2 = 0.9965; \\ 0.040\text{m} \leq D_o \leq 0.056\text{m}; \end{array} \right\}$$

where,

$Q_N$  is New model mass flow rate of maize grain through horizontal circular orifices (kg/h)

$D_o$  is diameter of horizontal circular orifice (m)

The mass flow rate of maize grain simulated by the New model exhibited a range of 706 kg/h to 1757 kg/h for horizontal circular orifice diameters that increased from 0.040 m to 0.056 m (Table C4, Appendix C). Figure 4.2 depicts the comparison between the actual mass flow rate and the simulated values using the New model for maize grain through horizontal circular orifices. Notably, the trends of the actual and New model mass flow rate plots were similar and exhibited

a close correspondence. This indicated that the actual mass flow rate results were in agreement with the predictions made by the New model.

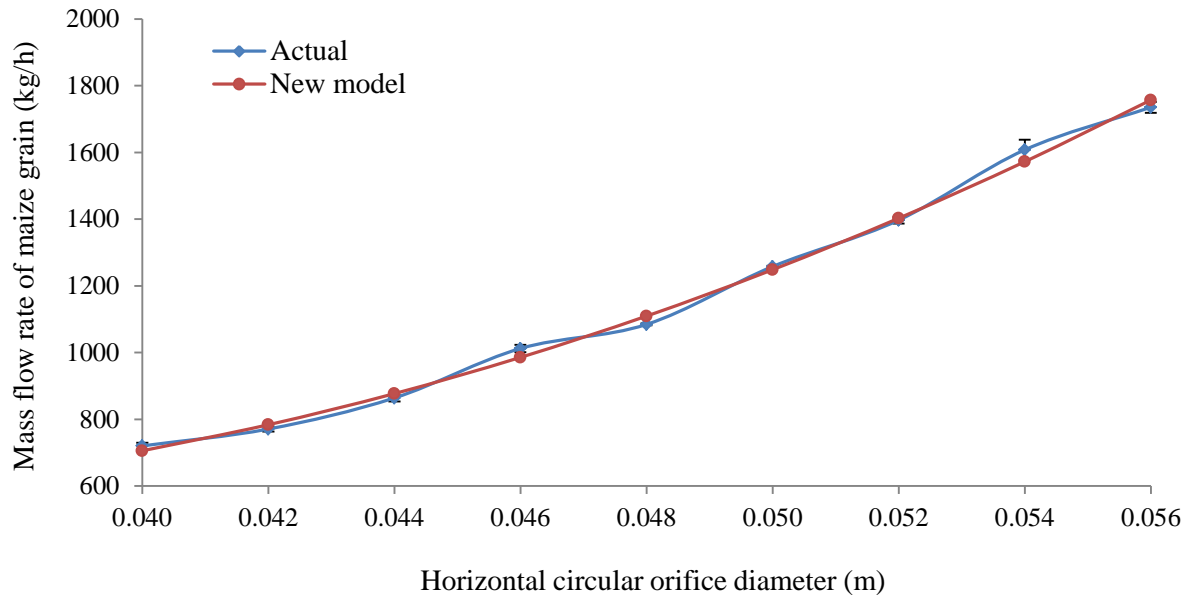


**Figure 4.2** Actual and New model mass flow rate of maize grain through horizontal circular orifices

According to the findings of Beverloo *et al.* (1961), the mass flow rates of green peas and soybeans exhibited a range of 755 kg/h to 2693 kg/h and 812 kg/h to 2820 kg/h, respectively, when passing through orifice diameters within the range of 0.040 m to 0.060 m. Furthermore, the same study reported that the mass flow rates of wheat through orifice diameters between 0.020 m and 0.030 m varied from 107 kg/h to 433 kg/h. Additionally, the Tudor model estimated mass flow rates for wheat seeds through orifice diameters ranging from 0.040 m to 0.060 m to be within the range of 1027 kg/h to 2830 kg/h (Tudor & Mieila, 2010).

The results of the Student's t-test (Table C5, C6, and C7; Appendix C) revealed a significant difference ( $P < 0.05$ ) between the simulated mass flow rates from the Beverloo model (650 kg/h to 2006 kg/h) and the actual mass flow rates (720 kg/h to 1735 kg/h), between the simulated mass flow rates from the BCP model (851 kg/h to 2378 kg/h) and the actual mass flow rates (720 kg/h to 1735 kg/h), as well as between the simulated mass flow rates from the Tudor model (867 kg/h to 2010 kg/h) and the actual mass flow rates (720 kg/h to 1735 kg/h). These results indicate disagreement between the simulated and actual mass flow rates. Therefore, the Beverloo, BCP,

and Tudor models were not suitable for accurately simulating the mass flow rate of maize grain through horizontal circular orifices in the experimental vertical pneumatic dryer (PMGD).

The Student's t-test results (Table C8, C9, and C10; Appendix C) indicated a significant difference ( $P < 0.05$ ) between the mass flow rates simulated by the Beverloo model (650 kg/h to 2006 kg/h) and those simulated by the Tudor model (867 kg/h to 2010 kg/h), between the mass flow rates simulated by the Beverloo model (ranging from 650 kg/h to 2006 kg/h) and those simulated by the BCP model (851 kg/h to 2378 kg/h), as well as between the mass flow rates simulated by the Tudor model (867 kg/h to 2010 kg/h) and those simulated by the BCP model (851 kg/h to 2378 kg/h). These results showed that the simulated mass flow rates from the Beverloo, Tudor, and BCP models did not show any agreement, implying that these models were not compatible with each other in terms of their simulations.

The Student's t-test results (Table C11, Appendix C) revealed that there was no significant difference ( $P > 0.05$ ) between the simulated mass flow rates using the New model (706 kg/h to 1757 kg/h) and the actual mass flow rates (720 kg/h to 1735 kg/h). Additionally, the evaluation results of the simulation models (Table C12, Appendix C) demonstrated that the New model exhibited a higher coefficient of determination ( $R^2 = 0.9965$ ), a lower root mean square error (RMSE = 24.8 kg/h), a lower absolute residual error ( $\epsilon_r = 0.6\%$ ), and a higher simulation performance at 10% residual error ( $\eta_{\text{sim},10\%} = 100\%$ ) in comparison to the Beverloo, BCP, and Tudor models. In general, higher  $R^2$  values and lower RMSE values indicate a better fit, while an  $R^2$  value closer to 1 shows a stronger correlation between actual and simulated values. These results collectively indicate that the New model is more reliable for simulating the mass flow rate of maize grain through horizontal circular orifices in the PMGD, as compared to the Beverloo, Tudor, and BCP models.

#### **4.2 Effect of Moisture Content, air Temperature and Mass Flow Rate of Maize Grain on Moisture Removal Rate and Energy Used for Drying**

The results of effect of moisture content, air temperature and mass flow rate of maize grain on moisture removal rate and energy used for the grain drying and transportation are presented in subsections 4.2.1, 4.2.2 and 4.2.3, respectively.

#### 4.2.1 Effect of Moisture Content on Moisture Removal Rate and Energy Used for Maize Grain Drying and Transportation

The moisture removal rate (MRR) exhibited a range of values across different moisture content levels: from 0.0914 kg/kg.h to 0.0357 kg/kg.h (Table D2, Appendix D) for 20% moisture content, 0.1043 kg/kg.h to 0.0556 kg/kg.h (Table D3, Appendix D) for 25% moisture content, and 0.1185 kg/kg.h to 0.0705 kg/kg.h (Table D4, Appendix D) for 30% moisture content of the maize grain (wet basis).

Figure 4.3 shows the variation in MRR with respect to drying time for maize grain initially having moisture contents of 20%, 25%, and 30% (wet basis). Across all moisture content levels, a common decreasing trend in the MRR plots as drying time progressed was evident. The MRR curves exhibited distinct profiles, gradually decreasing as the drying time increased. Notably, the MRR values for maize grain starting with an initial moisture content of 30% (0.1185 kg/kg.h to 0.0705 kg/kg.h) were notably higher than those for 25% (0.1043 kg/kg.h to 0.0556 kg/kg.h) and 20% (0.0914 kg/kg.h to 0.0357 kg/kg.h). This emphasizes that the initial moisture content of the maize grain had a substantial impact on the moisture removal rate during the drying process.

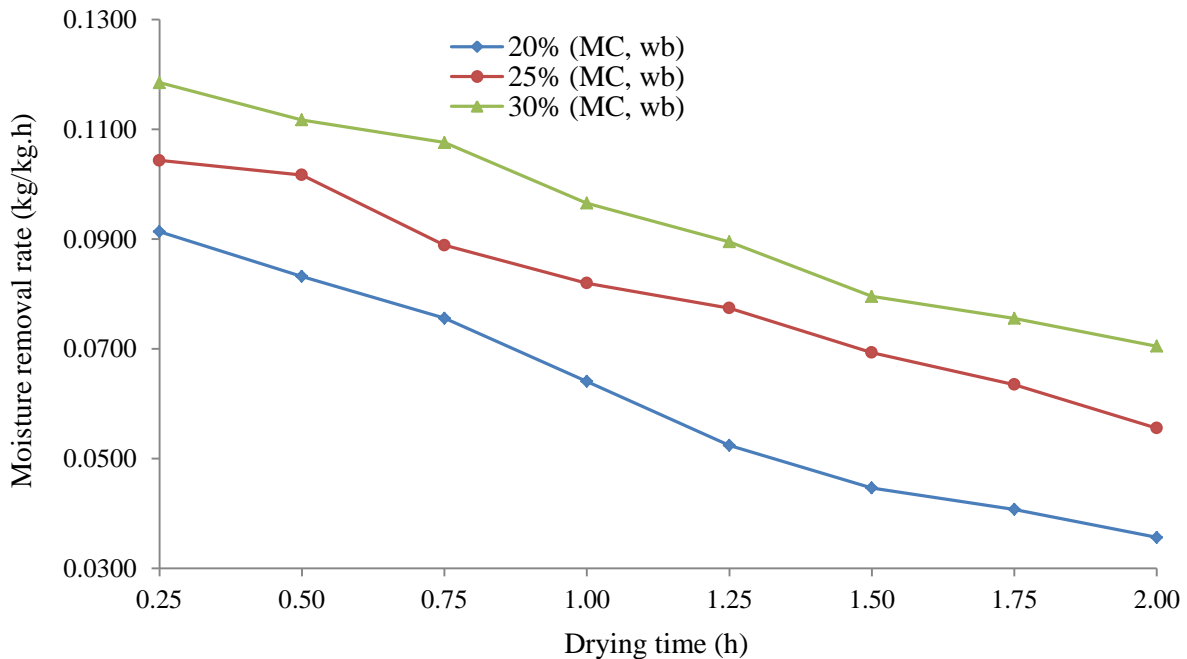


**Figure 4.3** Effect of moisture content on moisture removal rate in maize grain drying

The analysis of variance (ANOVA) results (Table D6, Appendix D) indicated a statistically significant difference ( $P < 0.05$ ) in moisture removal rate (MRR) among all the moisture content (MC) levels of the maize grain. However, when applying Fisher's least significant difference ( $LSD_{5\%}$ ) test results (Table D7, Appendix D), no significant statistical difference in MRR was observed between maize grain samples with an MC of 20% (0.0914 kg/kg.h to 0.0357 kg/kg.h) and those with an MC of 25% (0.1043 kg/kg.h to 0.0556 kg/kg.h). Similarly, there was no significant difference in MRR between maize grain samples with an MC of 25% (0.1043 kg/kg.h to 0.0556 kg/kg.h) and those with an MC of 30% (0.1185 kg/kg.h to 0.0705 kg/kg.h).

However, a statistically significant difference in MRR was observed between maize grain samples with an MC of 20% (0.0914 kg/kg.h to 0.0357 kg/kg.h) and those with an MC of 30% (0.1185 kg/kg.h to 0.0705 kg/kg.h), as indicated by the  $LSD_{5\%}$  test results (Table D7, Appendix D). This shows that the MRR influenced by the moisture content of the maize grain, and significant differences was observed between the extreme moisture content levels (20% and 30%).

The energy used for drying maize grain ( $E_a$ ) at moisture content (MC) levels of 20% and 25% (wet basis) was 10.5 kWh (Table D2 and Table D3, Appendix D), while at MC of 30%, it was 10.6 kWh (Table D4, Appendix D). When observing the variation of  $E_a$  with drying time for maize grain with initial MC of 20%, 25%, and 30% (wet basis) as depicted in Figure 4.4, it is evident that there is an increasing trend in the energy used over time for all MC levels. Furthermore, the  $E_a$  plots for all MC levels seem to overlap and not show distinct differences. This indicated that the initial moisture content of the maize grain did not have a significant influence on  $E_a$ .

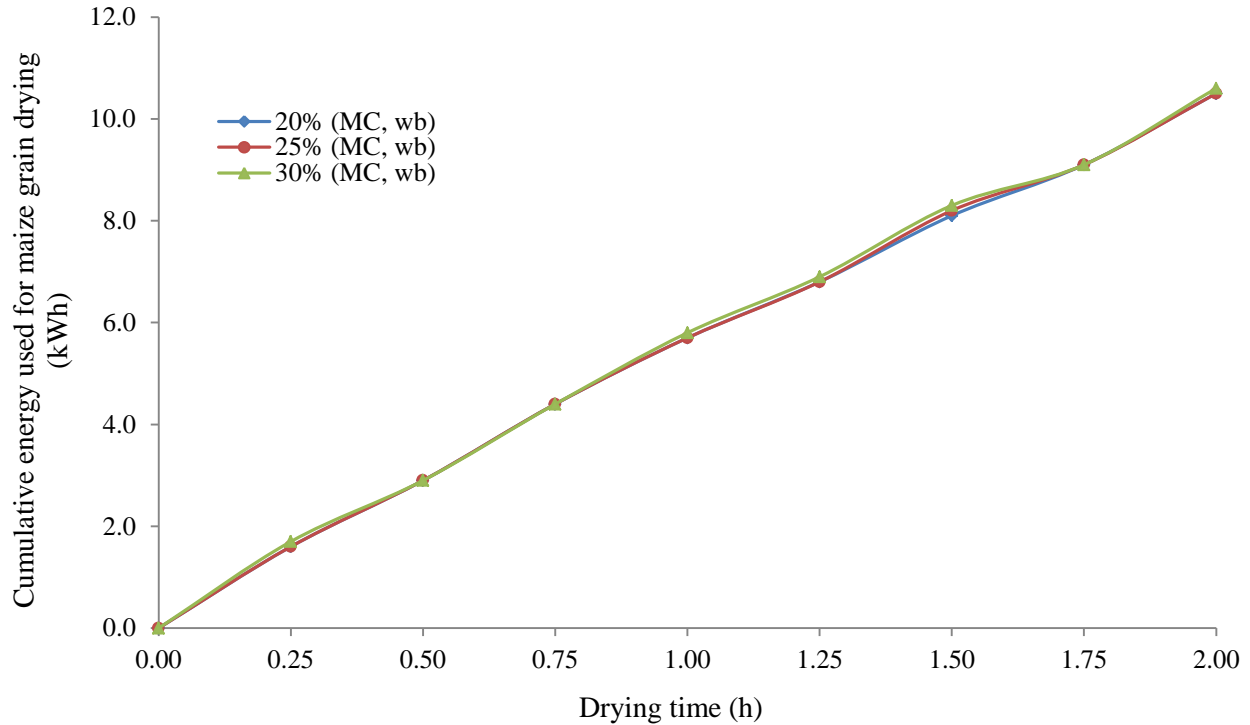


**Figure 4.4** Effect of moisture content on energy used for maize grain drying

The ANOVA results (Table D9, Appendix D) did not indicate any significant effect ( $P > 0.05$ ) of the moisture content (MC) of maize grain on  $E_a$ . Furthermore, the Fisher's least significant difference ( $LSD_{5\%}$ ) results (Table D10, Appendix D) did not demonstrate any statistically significant differences in  $E_a$  between the different moisture content levels, namely 20%, 25%, and 30%, wet basis.

The energy used for transportation of maize grain ( $E_g$ ) during drying varied with different moisture content levels. For maize grain with initial moisture content (MC) of 20%, the  $E_g$  was 4.6 kWh (Table D2, Appendix D). Similarly, for MC levels of 25% and 30%, the  $E_g$  was 4.8 kWh (Table D3, Appendix D) and 5.0 kWh (Table D4, Appendix D), respectively.

As shown in Figure 4.5, the plots of the  $E_g$  had similar increasing trends with drying time for maize grain with initial MC levels of 20%, 25%, and 30%, wet basis. The plots were distinct but followed a similar trend. Additionally, the  $E_g$  for maize grain with an initial MC of 30% was higher by 0.4 kWh and 0.2 kWh compared to that for 20% and 25%, respectively. This indicates that the energy consumption for transportation increased as the initial moisture content of the maize grain increased.



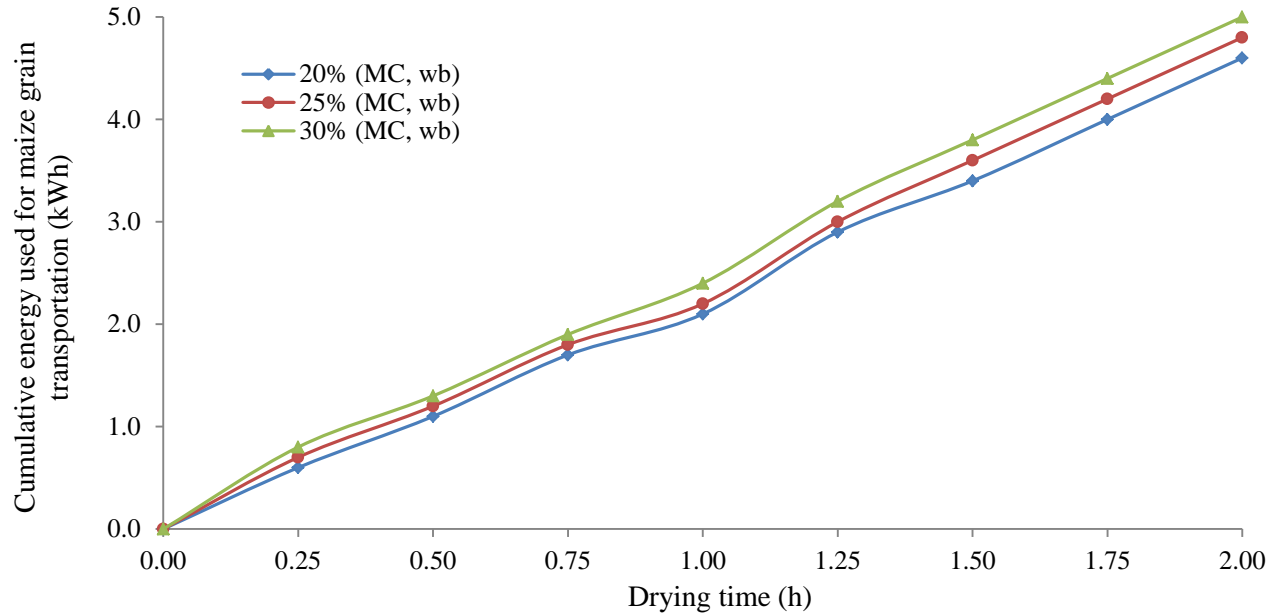


**Figure 4.5** Effect of moisture content on energy used for maize grain transportation

The ANOVA results (Table D12, Appendix D) did not reveal any significant differences ( $P > 0.05$ ) in the  $E_g$  among all the moisture content (MC) levels. Furthermore, the Fisher's least significant difference ( $LSD_{5\%}$ ) results (Table D13, Appendix D) did not show any statistically significant differences in the  $E_g$  between the different MC levels, including 20% (4.6 kWh), 25% (4.8 kWh), and 30% (5.0 kWh).

#### 4.2.2 Effect of air Temperature on Moisture Removal Rate and Energy Used for Maize Grain Drying and Transportation

The moisture removal rate (MRR) showed different ranges for different air temperatures ( $T_a$ ) during maize grain drying. Specifically, at an air temperature of  $60^\circ\text{C}$ , the MRR ranged from 0.0702 kg/kg.h to 0.0556 kg/kg.h (Table D14, Appendix D). At an air temperature of  $70^\circ\text{C}$ , the MRR ranged from 0.1043 kg/kg.h to 0.0556 kg/kg.h (Table D15, Appendix D). Finally, at an air temperature of  $80^\circ\text{C}$ , the MRR ranged from 0.1379 kg/kg.h to 0.0556 kg/kg.h (Table D16, Appendix D).

Figure 4.6 shows how the moisture removal rate (MRR) varies over the drying time for maize grain drying at different  $T_a$  of  $60^\circ\text{C}$ ,  $70^\circ\text{C}$ , and  $80^\circ\text{C}$ . Across all the  $T_a$  levels, there was a noticeable decreasing trend in the MRR as the drying time progressed. The MRR was found to be higher for maize grain dried at  $T_a$  of  $80^\circ\text{C}$  compared to that for  $70^\circ\text{C}$  and  $60^\circ\text{C}$ . This

observation reveals that the MRR tends to increase as the air temperature rises. This phenomenon can be attributed to the elevated latent heat of vaporization and enhanced mass transfer at higher temperatures, factors that promote the moisture removal process (Coradi *et al.*, 2016; Filková & Mujumdar, 1995; Kumar *et al.*, 2012; Pandey *et al.*, 2010).

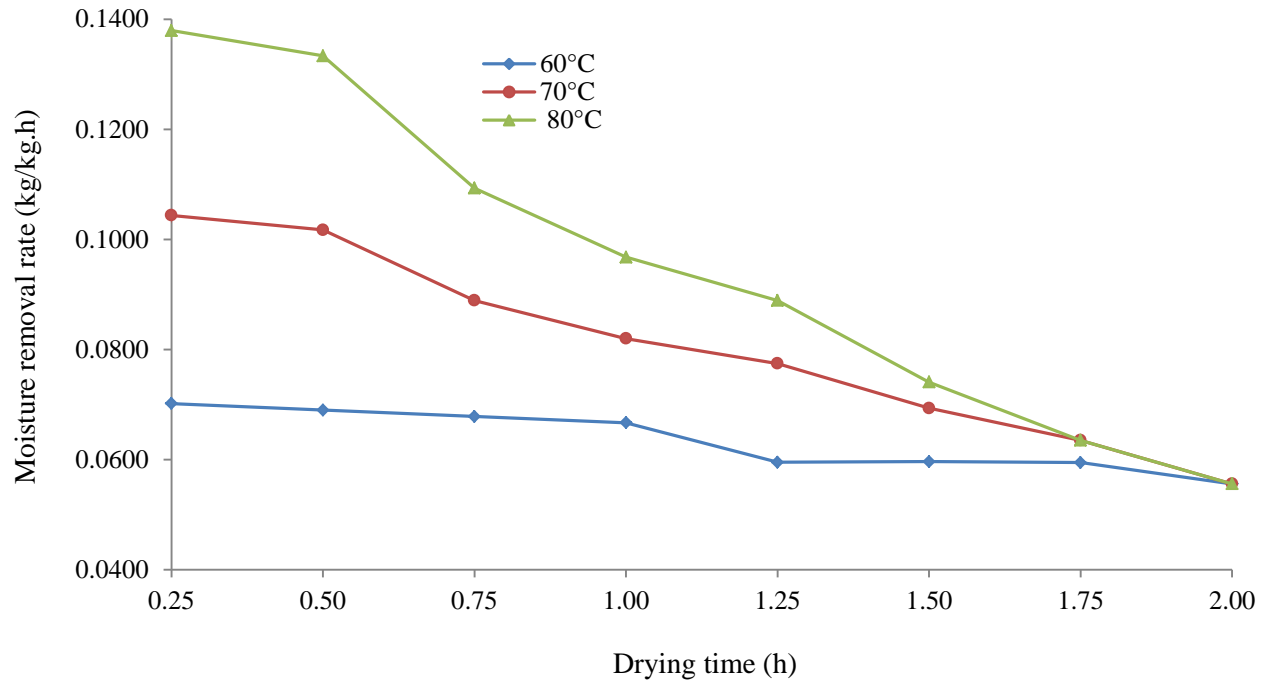


**Figure 4.6** Effect of air temperature on moisture removal rate in maize grain drying

The ANOVA results (Table D18, Appendix D) pointed to a significant difference ( $P < 0.05$ ) in the moisture removal rate (MRR) among all the tested  $T_a$  levels. However, the Fisher's least significant difference ( $LSD_{5\%}$ ) results (Table D19, Appendix D) indicated statistically significant difference in the MRR between maize grain drying at 60°C (0.0702 kg/kg.h to 0.0556 kg/kg.h) and 70°C (0.1043 kg/kg.h to 0.0556 kg/kg.h), as well as between drying at 70°C and 80°C (0.1379 kg/kg.h to 0.0556 kg/kg.h). However, the MRR for maize grain drying at 60°C (0.0702 kg/kg.h to 0.0556 kg/kg.h) and 80°C (0.1379 kg/kg.h to 0.0556 kg/kg.h) did exhibit a statistically significant difference (Table D19, Appendix D).

The energy used for maize grain drying ( $E_a$ ) was observed to be 6.6 kWh (Table D14, Appendix D) at an air temperature ( $T_a$ ) of 60°C, 10.5 kWh (Table D15, Appendix D) at 70°C, and 13.8 kWh (Table D16, Appendix D) at 80°C. The graphical representation in Figure 4.7 shows the variation in  $E_a$  over time during maize grain drying at  $T_a$  levels of 60°C, 70°C, and 80°C. A

consistent upward trend in the  $E_a$  with drying time was observable across all the  $T_a$  levels. As drying progressed, the plots began to diverge from one another. The  $E_a$  at a  $T_a$  of 80°C exceeded that at 60°C and 70°C by 7.2 kWh and 3.3 kWh, respectively. These results indicate that the selection of the  $T_a$  significantly influenced the  $E_a$ .

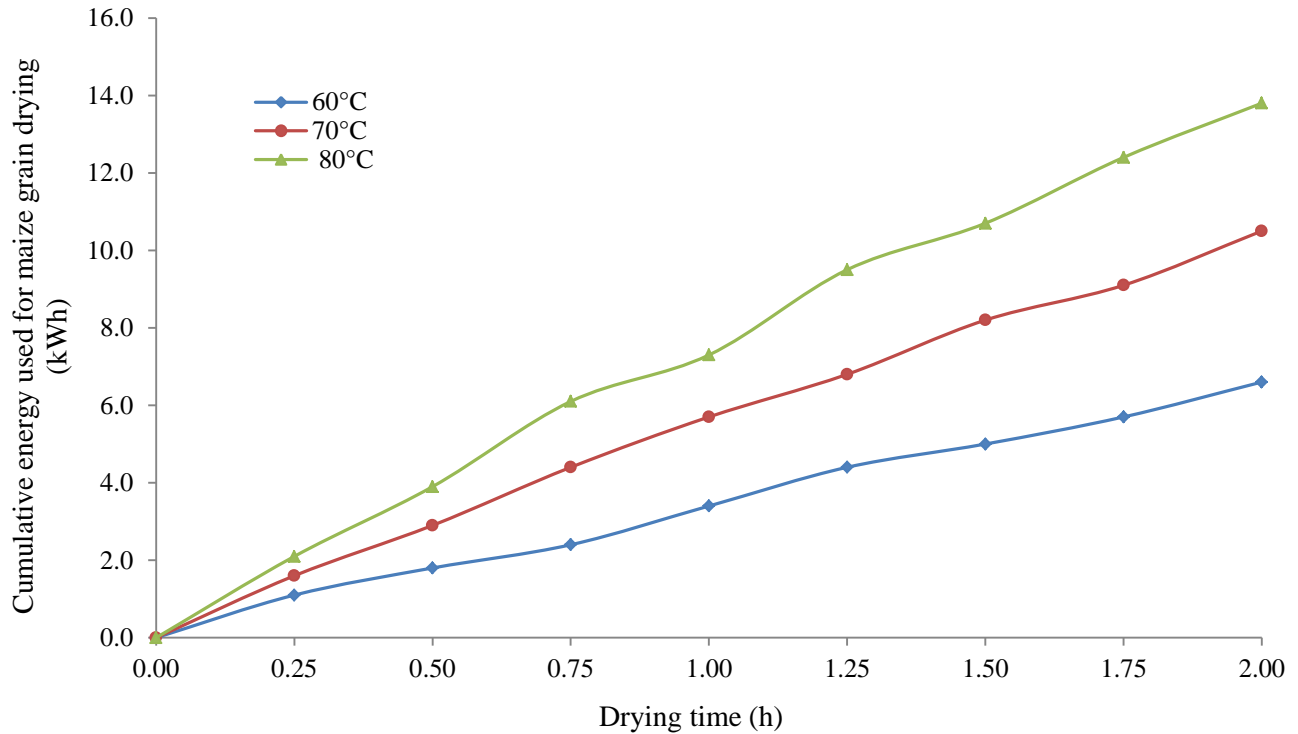


**Figure 4.7** Effect of air temperature on energy used for maize grain drying

The ANOVA results (Table D21, Appendix D) indicated a statistically significant difference ( $P < 0.05$ ) in the  $E_a$  across all the tested  $T_a$  levels. However, according to the Fisher's  $LSD_{5\%}$  results (Table D22, Appendix D), there was no significant statistical difference in  $E_a$  between the  $T_a$  of 60°C (6.6 kWh) and 70°C (10.5 kWh), nor between a  $T_a$  of 70°C (10.5 kWh) and 80°C (13.8 kWh). Conversely, the  $E_a$  at  $T_a$  levels of 60°C (6.6 kWh) and 80°C (13.8 kWh) was found to be statistically different (Table D22, Appendix D).

The energy used for transportation of maize grain ( $E_g$ ) during drying remained consistent at 4.8 kWh across all drying air temperature ( $T_a$ ) levels (Table D14, D15, and D16, Appendix D). As shown in Figure 4.8, the variation of  $E_g$  with time for  $T_a$  levels of 60°C, 70°C, and 80°C resulted in comparable plots. This implies that variation in  $T_a$  levels did not significantly influence the  $E_g$  during the drying process.

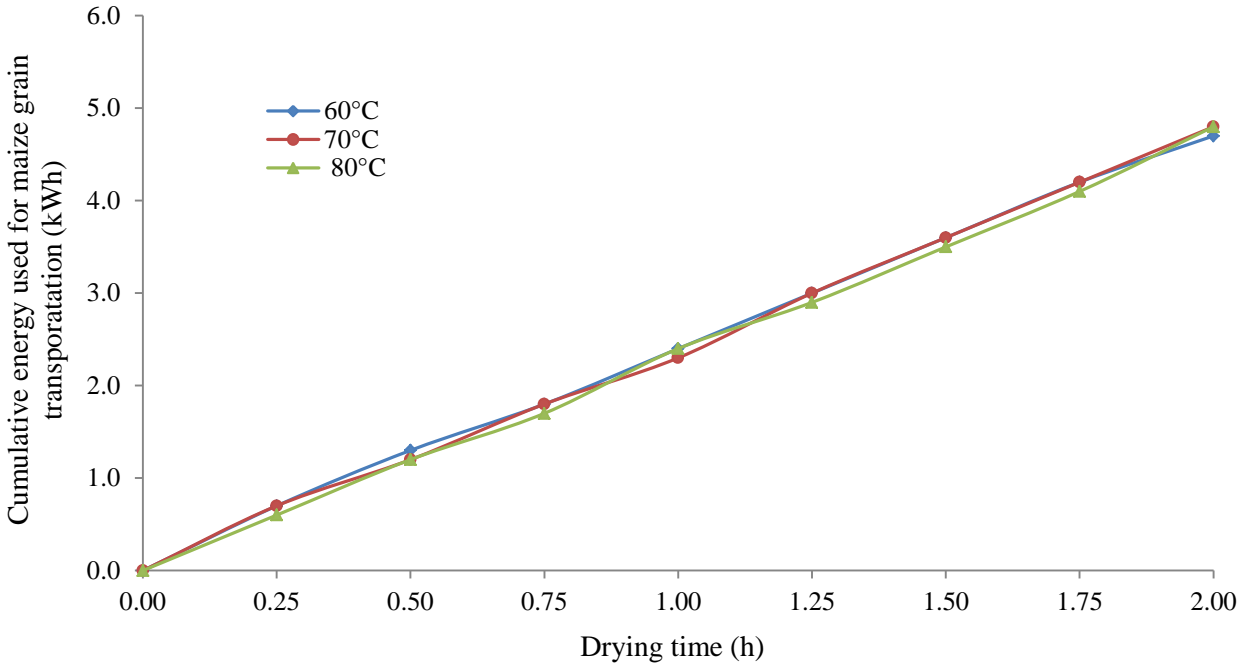


**Figure 4.8** Effect of air temperature on energy used for maize grain transportation

The ANOVA results (Table D24, Appendix D) indicated that there was no significant difference ( $P > 0.05$ ) in the energy used for transportation of maize grain ( $E_g$ ) across all the drying air temperature ( $T_a$ ) levels. Similarly, the Fisher's least significant difference ( $LSD_{5\%}$ ) results (Table D25, Appendix D) showed that there was no statistical difference in  $E_g$  between the  $T_a$  levels of 60°C and 70°C, 60°C and 80°C, and 70°C and 80°C.

#### 4.2.3 Effect of Mass Flow Rate on Moisture Removal Rate and Energy Used for Maize Grain Drying and Transportation

The moisture removal rate (MRR) ranged from 0.1379 kg/kg.h to 0.0556 kg/kg.h (Table D26, Appendix D), 0.1043 kg/kg.h to 0.0556 kg/kg.h (Table D27, Appendix D) and 0.0908 kg/kg.h to 0.0556 kg/kg.h (Table D28, Appendix D) for maize grain drying at controlled mass flow rates (MFR) of 720 kg/h, 771 kg/h and 864 kg/h, respectively.

Figure 4.9 shows variation between moisture removal rate (MRR) and drying time for maize grain drying at controlled mass flow rates (MFR) of 720 kg/h, 771 kg/h, and 864 kg/h. The trend observed is that as drying time increases, the MRR decreases for all MFR levels. Additionally, the MRR for maize grain drying at an MFR of 720 kg/h was higher compared to that at MFRs of 771 kg/h and 864 kg/h. This is attributed to the fact that at a lower MFR, there is increased

contact time between the maize grain and the drying air, leading to a higher moisture removal rate.

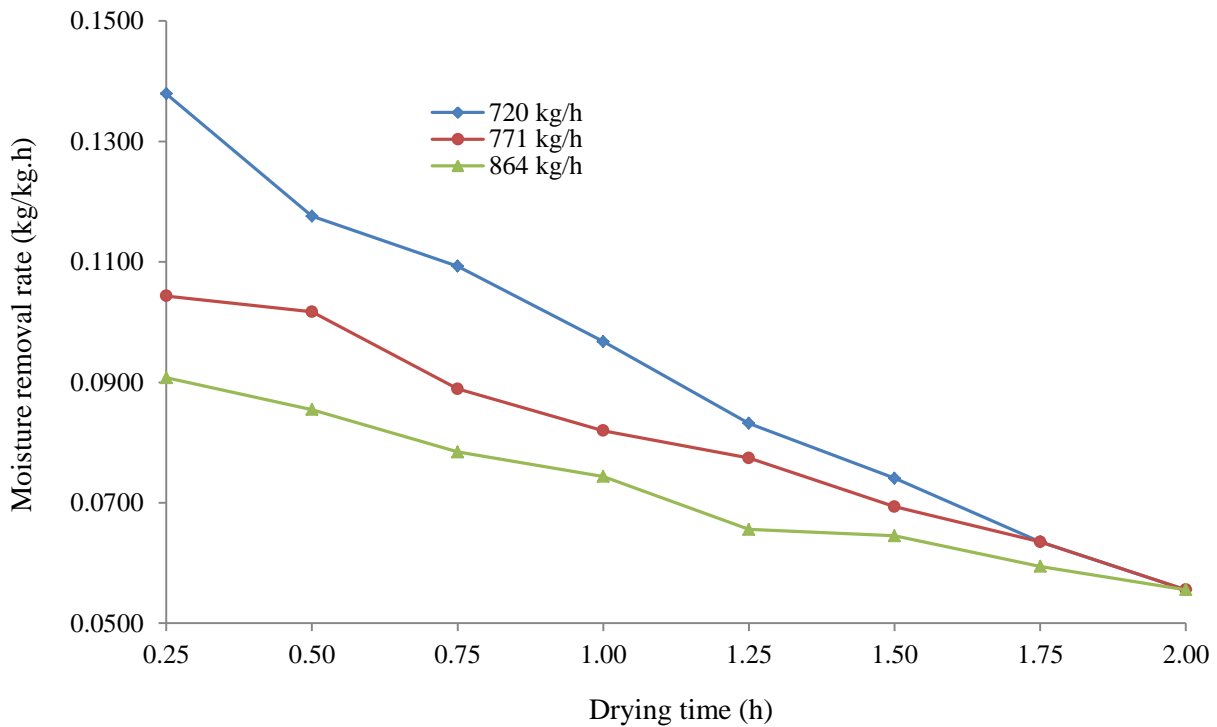


**Figure 4.9** Effect of mass flow rate on moisture removal rate in maize grain drying

The ANOVA results (Table D30, Appendix D) did not indicate any significant difference in the moisture removal rate (MRR) among the various controlled mass flow rate (MFR) levels. Furthermore, the Fisher's least significant difference ( $LSD_{5\%}$ ) results did not show any statistically significant differences in MRR between the MFR of 720 kg/h (0.1379 kg/kg.h to 0.0556 kg/kg.h) and 771 kg/h (0.1043 kg/kg.h to 0.0556 kg/kg.h), between 720 kg/h (0.1379 kg/kg.h to 0.0556 kg/kg.h) and 864 kg/h (0.0908 kg/kg.h to 0.0556 kg/kg.h), and between 771 kg/h (0.1043 kg/kg.h to 0.0556 kg/kg.h) and 864 kg/h (0.0908 kg/kg.h to 0.0556 kg/kg.h) (Table D31, Appendix D).

The energy used for drying of maize grain ( $E_a$ ) remained constant at 10.5 kWh across all controlled mass flow rate (MFR) levels (Table D26, Table D27, and Table D28, Appendix D). The plots of  $E_a$  variation with drying time for maize grain drying at controlled MFR of 720 kg/h, 771 kg/h, and 864 kg/h were overlapping and indistinguishable (Figure 4.10). This indicates that the MFR of maize grain did not have a considerable influence on the  $E_a$ .

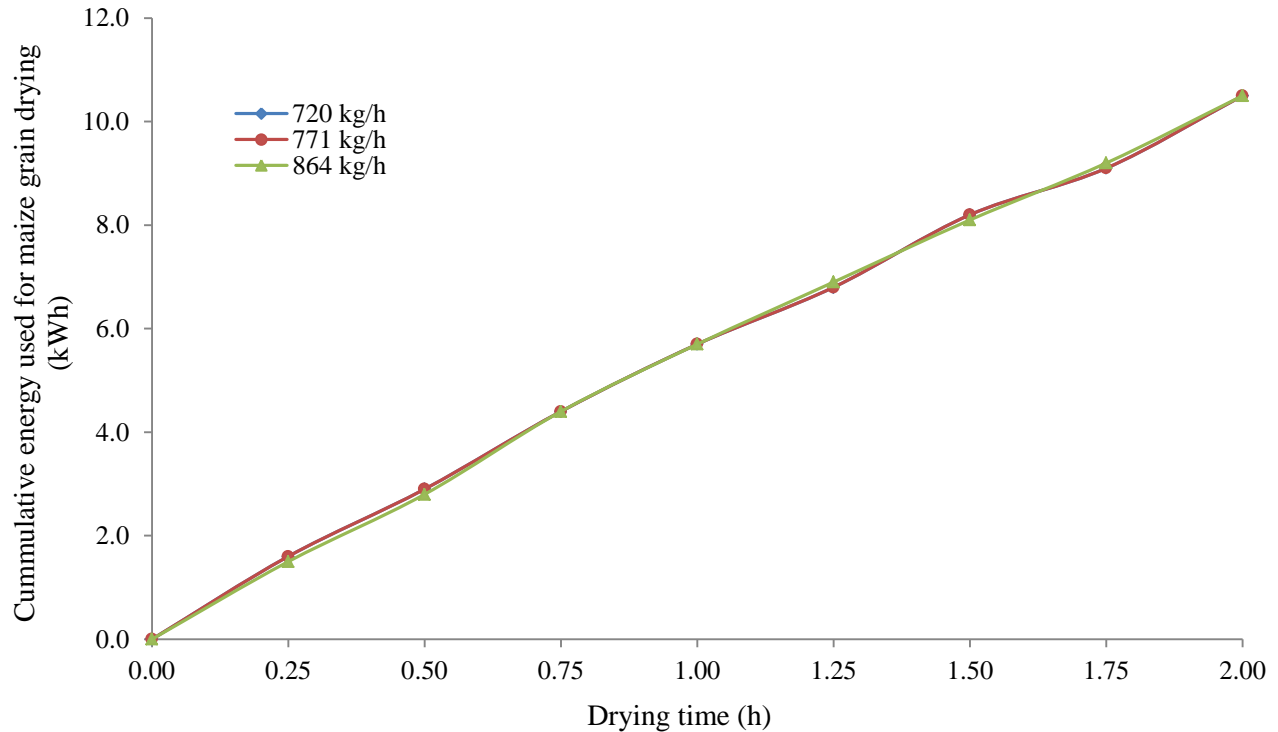


**Figure 4.10** Effect of mass flow rate on energy used for maize grain drying

The ANOVA results (Table D33, Appendix D) did not reveal any significant differences ( $P > 0.05$ ) in energy used for drying of maize grain ( $E_a$ ) across all the controlled mass flow rate (MFR) levels. Moreover, the Fisher's LSD5% results (Table D34, Appendix D) did not demonstrate any statistical differences in  $E_a$  between the MFR of 720 kg/h and 771 kg/h; 720 kg/h and 864 kg/h; 771 kg/h and 864 kg/h.

The energy used for transportation of maize grain ( $E_g$ ) during drying was 4.6 kWh (Table D26, Appendix D) for the grain mass flow rate (MFR) of 720 kg/h, 4.8 kWh (Table D27, Appendix D) for an MFR of 771 kg/h, and 5.4 kWh (Table D28, Appendix D) for an MFR of 864 kg/h. This indicates that the  $E_g$  for the MFR of 864 kg/h was 0.6 kWh and 0.8 kWh higher than that for 771 kg/h and 720 kg/h, respectively. This implies that the  $E_g$  increased with the grain MFR. In Figure 4.11, the variation of  $E_g$  with drying time is shown for maize grain drying at controlled MFRs of 720 kg/h, 771 kg/h, and 864 kg/h. The plots exhibit similar trends while being distinct from each other. This shows that the MFR of maize grain has an influence on the  $E_g$  during drying.

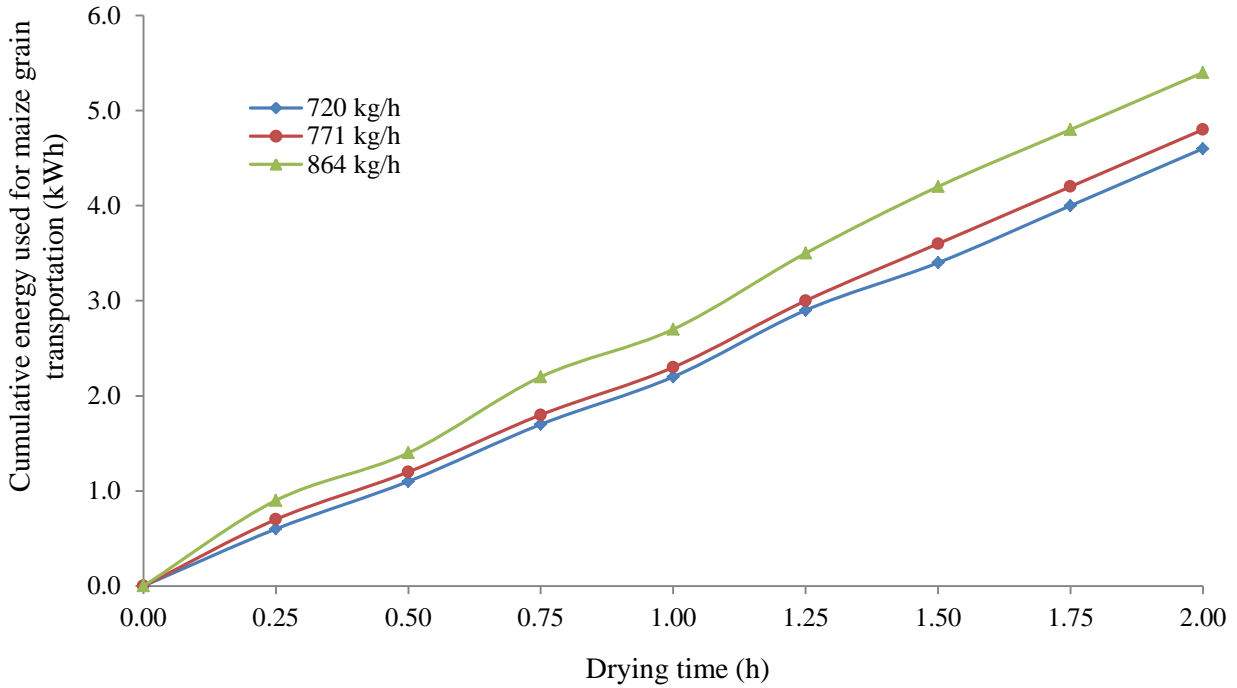


**Figure 4.11** Effect of mass flow rate on energy used for maize grain transportation

The ANOVA results (Table D36, Appendix D) did not reveal any significant differences ( $P > 0.05$ ) in the energy used for transportation of maize grain ( $E_g$ ) for all MFR levels. Similarly, the Fisher's  $LSD_{5\%}$  results (Table D37, Appendix D) did not indicate any statistical differences in  $E_g$  between the MFR of 720 kg/h (4.6 kWh) and 771 kg/h (4.8 kWh); 720 kg/h (4.6 kWh) and 864 kg/h (5.4 kWh); 771 kg/h (4.8 kWh) and 864 kg/h (5.4 kWh).

### 4.3 Optimisation of Energy Proportioned for Maize Grain Drying and Transportation

Table 4.1 presents moisture removal rates for various combinations of energy proportioned for drying and transportation of maize grain.

**Table 4.1** Moisture removal rate for various combinations of energy proportioned for maize grain drying and transportation

Experiment	$E_a$ (kWh)	$E_g$ (kWh)	Mean MRR (kg/kg.h)
1	3.4	2.2	0.0687 <sup>-23.3</sup>
2	3.4	2.4	0.0564 <sup>-25.0</sup>
3	3.4	2.8	0.0484 <sup>-26.3</sup>
4	5.5	2.2	0.0820 <sup>-21.7</sup>
5	5.5	2.4	0.0714 <sup>-22.9</sup>
6	5.5	2.8	0.0638 <sup>-23.9</sup>
<b>7</b>	<b>7.3</b>	<b>2.2</b>	<b>0.0965</b> <sup>-20.3</sup>
8	7.3	2.4	0.0844 <sup>-21.5</sup>
9	7.3	2.8	0.0734 <sup>-22.7</sup>

$E_a$  is energy proportioned for maize grain drying,  $E_g$  is energy proportioned for maize grain transportation, MRR is moisture removal rate, superscripts are signal to noise ratios for moisture removal rate (dB)

The highest moisture removal rate (MRR) of 0.0965 kg/kg.h was observed in experiment 7, which involved an energy combination of 7.3 kWh for  $E_a$  and 2.2 kWh for  $E_g$ . Conversely, the lowest MRR of 0.0484 kg/kg.h was recorded in experiment 3, where the energy combination included 3.4 kWh for  $E_a$  and 2.8 kWh for  $E_g$  (Table 4.1). Consequently, the  $E_a$  value in experiment 7 exceeded that in experiment 3 by 3.9 kWh, and the  $E_g$  value in experiment 3 was 0.6 kWh higher than that in experiment 7.

Moreover, a trend was observed indicating that the MRR in maize grain drying decreased with an increase in  $E_g$  while keeping  $E_a$  constant. This increase in  $E_g$  was associated with an elevated grain mass flow rate (MFR), resulting in a shorter residence time. Consequently, the reduced interaction time between the grain and drying air led to a decrease in MRR.

The experimental results of MRR in maize grain drying were transformed into signal to noise (S/N) ratios, as outlined in section 3.4. The corresponding S/N ratios for MRR are provided in superscripts within Table 4.1. The average S/N ratios for MRR in relation to different values of  $E_a$  were -24.8 dB for 3.4 kWh, -22.9 dB for 5.5 kWh, and -21.5 dB for 7.3 kWh. Similarly, the



average S/N ratios for MRR corresponding to various values of  $E_g$  were -21.8 dB for 2.2 kWh, -23.1 dB for 2.4 kWh, and -24.3 dB for 2.8 kWh (Table E12, Appendix E).

The mean of S/N ratios for MRR were plotted against each level of  $E_a$  and  $E_g$  using Minitab-19 software (Minitab Incorporated, USA for Windows®), as shown in Figure E2, Appendix E. The optimum levels of  $E_a$  and  $E_g$  were determined based on the larger is better criterion, aiming to maximise the mean of S/N ratios for achieving higher MRR.

The ANOVA results (Table E13, Appendix E) indicated a significant effect ( $P < 0.005$ ) of both  $E_a$  and  $E_g$  on the MRR. Moreover, it was observed that  $E_a$  had a more significant effect ( $F_{E_a,5\%} = 316.04 > F_{E_g,5\%} = 184.99$ ) on MRR compared to  $E_g$ . In general, when the F-value of a process parameter is higher, it signifies a greater influence of the variation of that parameter on the output (Nalbant *et al.*, 2007).

The analysis S/N ratios and ANOVA results (Table E13, Appendix E) revealed that the contributions of  $E_a$  and  $E_g$  to MRR in maize grain drying were 62.8% and 36.8%, respectively, with the remaining 0.4% attributed to residual error. Based on these analyses, the optimum levels of  $E_a$  and  $E_g$  for achieving the highest MRR in maize grain drying were determined to be 7.3 kWh (level 3) for  $E_a$  and 2.2 kWh (level 1) for  $E_g$  (Table 4.1).

The regression analysis results correlating  $E_a$  and  $E_g$  with respect to MRR in maize grain drying yielded equation 4.2:

$$MRR_1 = 0.0069E_a - 0.03252E_g + 0.1146 \quad (4.2)$$

$$\text{for } \left\{ \begin{array}{l} R^2 = 0.9701; \\ E_a \geq 3.5\text{kWh}; \\ E_g \geq 2.2\text{kWh}; \end{array} \right.$$

where,

$MRR_1$  is simulated moisture removal rate with respect to energy proportioned for drying and transportation of maize grain (kg/kg.h)

The simulated moisture removal rates ( $MRR_1$ ), based on equation 4.2, for various combinations of  $E_a$  and  $E_g$  are presented in Table E14, Appendix E.

Furthermore, the regression analysis did indicate a linear correlation between  $E_a$  and  $E_g$  with respect to signal to noise ratio for MRR given in equation 4.3:

$$S/N_{MRR1} = 0.8623E_a - 4.04E_g - 17.75 \quad (4.3)$$

$$\text{for } \left\{ \begin{array}{l} R^2 = 0.9702; \\ E_a \geq 3.5\text{kWh}; \\ E_g \geq 2.2\text{kWh}; \end{array} \right\}$$

where,

$S/N_{MRR1}$  is simulated signal to noise ratio for moisture removal rate regarding energy proportioned for drying and transportation of maize grain (dB)

The simulated S/N ratios ( $S/N_{MRR1}$ ) for moisture removal rate, using equation 4.3, for various combinations of  $E_a$  and  $E_g$  are presented in Table E15, Appendix E.

The utilization of the optimum energy proportioned of 7.3 kWh for  $E_a$  and 2.2 kWh for  $E_g$  resulted in MRR of 0.0965 kg/kg.h (Table 4.1). The simulation of MRR based on equation 4.2 yielded a value of 0.0935 kg/kg.h (Table E14, Appendix E). This confirms that the established optimum levels of  $E_a$  and  $E_g$  led to the highest MRR in maize grain drying. Consequently, this shows that a larger proportion of energy should be proportioned to the drying process compared to transportation of the grains. The agreement between the actual and simulated S/N ratios for MRR at the optimum  $E_a$  and  $E_g$  was -20.3 dB (Table E15, Appendix E), indicating consistency between the experimental and simulated results.

#### **4.4 Optimisation of Moisture Content, air Temperature and Mass Flow Rate in Maize Grain Drying**

Table 4.2 shows moisture removal rates and energy used in drying for various combinations of moisture content, air temperature and mass flow rate of maize grain.

**Table 4.2** Moisture removal rate and energy used in drying for various combinations of moisture content, air temperature and mass flow rate of maize grain

<b>Experiment</b>	<b>MC</b> <b>(%, wet basis)</b>	<b>T<sub>a</sub></b> <b>(°C)</b>	<b>MFR</b> <b>(kg/h )</b>	<b>Mean MRR</b> <b>(kg/kg.h)</b>	<b>Mean EU</b> <b>(kWh)</b>
1	20	60	720	0.0796 <sup>-22.0</sup>	6.1 <sup>-15.7</sup>
2	20	70	771	0.0828 <sup>-21.6</sup>	8.7 <sup>-18.8</sup>
3	20	80	864	0.0907 <sup>-20.8</sup>	11.1 <sup>-20.9</sup>
4	25	60	771	0.0635 <sup>-23.9</sup>	6.5 <sup>-16.2</sup>
5	25	70	864	0.0718 <sup>-22.9</sup>	9.3 <sup>-19.4</sup>
6	25	80	720	0.1086 <sup>-19.3</sup>	10.6 <sup>-20.5</sup>
7	30	60	864	0.0390 <sup>-28.2</sup>	7.1 <sup>-17.0</sup>
8	30	70	720	0.0860 <sup>-21.3</sup>	8.7 <sup>-18.8</sup>
9	30	80	771	0.1002 <sup>-20.0</sup>	11.0 <sup>-20.8</sup>

MC is moisture content, T<sub>a</sub> is air temperature, MFR is mass flow rate of maize grain, MRR is moisture removal rate, EU is energy used for maize grain drying and transportation, superscripts are signal to noise ratios for moisture removal rate and energy used (dB)

The experimental results indicated that the highest moisture removal rate (MRR) of 0.1086 kg/kg.h was observed in experiment 6, which involved a combination of 25% moisture content (MC), 80°C air temperature (T<sub>a</sub>), and 720 kg/h mass flow rate (MFR). Conversely, the lowest MRR of 0.0390 kg/kg.h was observed in experiment 7, which included 30% MC, 60°C T<sub>a</sub>, and 864 kg/h MFR. In all the experiments, the highest energy used in drying (EU) of 11.1 kWh was recorded in experiment 3, with 20% MC, 80°C T<sub>a</sub>, and 864 kg/h MFR. However, the lowest EU of 6.1 kWh was found in experiment 1, which had 20% MC, 60°C T<sub>a</sub>, and 720 kg/h MFR (Table 4.2).

The signal to noise (S/N) ratios for both moisture removal rate (MRR) and energy used in drying (EU) are presented in Table 4.2 with corresponding mean values for different levels of the process parameters. For MRR, the mean S/N ratios were -21.5 dB for 20% moisture content (MC), -22.0 dB for 25% MC, and -23.2 dB for 30% MC. With respect to air temperature (T<sub>a</sub>), the mean S/N ratios were -24.7 dB for 60°C, -21.9 dB for 70°C, and -20.0 dB for 80°C. When considering mass flow rate (MFR), the mean S/N ratios were -20.9 dB for 720 kg/h, -21.9 dB for

771 kg/h, and -24.0 dB for 864 kg/h. The mean S/N ratios for MRR were plotted against each level of the process parameters using the Minitab-19 software (Figure F3, Appendix F). The selection of the mean S/N ratios for MRR was based on the larger is better criterion.

The S/N ratios for energy used in drying (EU) are also presented in Table 4.2, along with the corresponding mean values for different levels of the process parameters. For EU, the mean S/N ratios were -18.5 dB for 20% moisture content (MC), -18.7 dB for 25% MC, and -18.9 dB for 30% MC. Regarding air temperature ( $T_a$ ), the mean S/N ratios were -16.3 dB for 60°C, -19.0 dB for 70°C, and -20.7 dB for 80°C. When considering mass flow rate (MFR), the mean S/N ratios were -18.3 dB for 720 kg/h, -18.6 dB for 771 kg/h, and -19.1 dB for 864 kg/h. The mean S/N ratios for EU were plotted against each level of the process parameters using the Minitab-19 software (Figure F4 in Appendix F). The selection of the mean S/N ratios for EU was based on the smaller is better criterion.

The ANOVA results at 5% level of significance (Table F15, Appendix F) showed that there was no significant effect ( $P > 0.05$ ) of moisture content (MC) and mass flow rate (MFR) on moisture removal rate (MRR), except for air temperature ( $T_a$ ) which had a significant effect ( $P < 0.05$ ) on MRR.

Similarly, the ANOVA results (Table F16, Appendix F) revealed that there was a significant effect ( $P < 0.05$ ) of MC,  $T_a$ , and MFR on energy used in drying (EU). The F-value for  $T_a$  ( $F_{T_a,5\%} = 12199.54$ ) was greater than that of MFR ( $F_{MFR,5\%} = 293.75$ ) and MC ( $F_{MC,5\%} = 71.88$ ), indicating that  $T_a$  had a more significant effect on EU compared to MFR and MC. This observation aligns with the general principle that a larger F-value signifies a greater effect of a variation in a process parameter on the output (Nalbant *et al.*, 2007). Generally, the ANOVA results highlight the importance of  $T_a$  in influencing both MRR and EU in the maize grain drying process, followed by MFR and MC.

According to the S/N ratios and ANOVA analyses, the contributions of  $T_a$ , MFR, and MC to MRR were 67.5%, 26.3%, and 3.9%, respectively, with a residual error contribution of 2.2% (Table F15, Appendix F). Similarly, for EU, the contributions of  $T_a$ , MFR, and MC were 97.1%, 2.3%, and 0.6%, respectively, with the remaining 0.6% attributed to the residual error (Table F16, Appendix F).

Based on these analyses, the optimum process parameters for attaining the highest MRR in maize grain drying were MC of 20% (level 1),  $T_a$  of 80°C (level 3), and MFR of 720 kg/h (level 1). Similarly, for EU, the optimum process parameters were MC of 20% (level 1),  $T_a$  of 60°C (level 1), and MFR of 720 kg/h (level 1). These results revealed the significance of controlling  $T_a$  and MFR of maize grain in achieving desired MRR and EU during maize grain drying processes.

The regression analysis results showed a linear correlation of MC,  $T_a$  and MFR with respect to MRR and EU as presented in equation 4.4 and 4.5, respectively:

$$\text{MRR}_2 = -0.00093\text{MC} + 0.00196T_a - 0.00016\text{MFR} + 0.0914 \quad (4.4)$$

$$\text{for } \left\{ \begin{array}{l} R^2 = 0.9700; \\ 20\% \leq \text{MC} \leq 30\%; \\ 60^\circ\text{C} \leq T_a \leq 80^\circ\text{C}; \\ 720\text{kg/h} \leq \text{MFR} \leq 864\text{kg/h}; \end{array} \right\}$$

where,

$\text{MRR}_2$  is simulated moisture removal rate in maize grain drying with respect to moisture content, air temperature, and mass flow rate (kg/kg.h)

The simulated moisture removal rates, using equation 4.4, for various combinations of MC,  $T_a$  and MFR are presented in Table F17, Appendix F.

$$\text{EU}_s = 0.033\text{MC} + 0.217T_a + 0.004\text{MFR} - 10.685 \quad (4.5)$$

$$\text{for } \left\{ \begin{array}{l} R^2 = 0.9974; \\ 20\% \leq \text{MC} \leq 30\%; \\ 60^\circ\text{C} \leq T_a \leq 80^\circ\text{C}; \\ 720\text{kg/h} \leq \text{MFR} \leq 864\text{kg/h}; \end{array} \right\}$$

where,

$\text{EU}_s$  is simulated energy used for drying and transportation of maize grain regarding moisture content, air temperature, and mass flow rate of the grain (kWh)

The simulated energy used for maize grain drying and transportation, based on equation 4.5, for various combinations of MC,  $T_a$  and MFR are given in Table F18, Appendix F.

Moreover, the regression analysis yielded a linear correlation of MC,  $T_a$  and MFR with respect to S/N ratio for MRR and EU as given in equation 4.6 and 4.7, respectively:

$$S/N_{MRR2} = -0.167MC + 0.233T_a - 0.021MFR - 18.03 \quad (4.6)$$

$$\text{for } \left\{ \begin{array}{l} R^2 = 0.9303; \\ 20\% \leq MC \leq 30\%; \\ 60^\circ C \leq T_a \leq 80^\circ C; \\ 720\text{kg/h} \leq MFR \leq 864\text{kg/h;} \end{array} \right\}$$

where,

$S/N_{MRR2}$  is simulated signal to noise ratio for moisture removal rate in maize grain drying with respect to moisture content, air temperature, and mass flow rate of the grain (dB)

The simulated signal to noise ratios for moisture removal rate, using on equation 4.6, for various combinations of MC,  $T_a$  and MFR are presented in Table F19, Appendix F.

$$S/N_{EUs} = -0.044MC - 0.221T_a - 0.005MFR + 1.72 \quad (4.7)$$

$$\text{for } \left\{ \begin{array}{l} R^2 = 0.9851; \\ 20\% \leq MC \leq 30\%; \\ 60^\circ C \leq T_a \leq 80^\circ C; \\ 720\text{kg/h} \leq MFR \leq 864\text{kg/h;} \end{array} \right\}$$

where,

$S/N_{EUs}$  is simulated signal to noise ratio for energy used for drying and transportation of maize grain with respect to moisture content, air temperature, and mass flow rate of the grain (dB)

The simulated signal to noise ratios for energy used for maize grain drying and transportation, based on equation 4.7, for various combinations of MC,  $T_a$  and MFR are given in Table F20, Appendix F.

The confirmatory test based on the optimum process parameters (MC of 20%,  $T_a$  of 80°C, and MFR of 720 kg/h) resulted in a mean actual moisture removal rate (MRR) of 0.1102 kg/kg.h (Table F21, Appendix F), while the simulated MRR using equation 4.4 was 0.1140 kg/kg.h. The

S/N ratio for the mean of actual MRR (0.1102 kg/kg.h) was -19.2 dB, and the simulated value (0.1140 kg/kg.h) based on equation 4.6 had a corresponding S/N ratio of -17.8 dB.

Similarly, the mean actual EU for the optimum process parameters (MC of 20%,  $T_a$  of 60°C, and MFR of 720 kg/h) was 6.1 kWh, while the simulated EU using equation 4.5 was 6.2 kWh. The S/N ratio for the mean actual EU (6.1 kWh) was -15.7 dB, and the S/N ratio for the simulated value (6.2 kWh) based on equation 4.7 was -16.0 dB. These comparisons indicate that the simulated values are considerably close to the actual values, indicating a good agreement between the experimental and simulated results for both MRR and EU under the optimum process parameters.

Table 4.3 shows constants and performance parameters of the selected drying models evaluated based on the optimum process parameters (MC of 20%,  $T_a$  of 80°C and MFR of 720 kg/h) for MRR in maize grain drying.

**Table 4.3** Constants and performance parameters of selected grain drying models

Model name	Model constant	Model performance parameters		
		SSE	R <sup>2</sup>	RMSE
Single term	a = 0.344; k = 0.9195	0.2494	0.9335	0.1888
Logarithmic	a = 0.4214; c = 0.5782; k = 8.673	0.0011	0.9928	0.0137
Modified Page I	k = 0.4422; n = 0.9935	0.1723	-0.1051	0.1569
Modified Page II	k = 0.0009449; n = 0.08885	0.0002	0.9984	0.0051
Verma	a = 0.6099; g = 12.46; k = 0.04071	0.0003	0.9978	0.0075
<b>Page</b>	<b>k = 0.5386; n = 0.08879</b>	<b>0.0002</b>	<b>0.9989</b>	<b>0.0049</b>
Thomson	a = -0.9736; b = 0.3684	0.0990	0.6240	0.1189
Two-Term	a = -7.868; b = 8.659; k <sub>1</sub> = 0.3248; k <sub>2</sub> = 0.3166	0.0850	0.4544	0.1304
Wang & Singh	a = 0.2885; b = -0.7573	0.0654	0.5802	0.0967

The Page model showed better performance with a higher coefficient of determination (R<sup>2</sup> = 0.9989) and lower root mean square error (RMSE = 0.0049) in comparison to the other tested

models (Table 4.5). The actual moisture ratios (MR) ranged from 1.0 to 0.56, while the MR predicted by the Page Model ranged from 1.0 to 0.57 (Table F22, Appendix F). The results of the Student's t-test (Table F23, Appendix F) indicated that there was no significant difference ( $t_{\text{stat}} = 0.651$ ;  $t_{\text{crit},5\%} = 1.860$ ) between the actual MR and those predicted by the Page model. This analyses implied that the Page model provided the best representation of the correlation between MR and time in maize grain drying.



## CHAPTER FIVE

### CONCLUSIONS AND RECOMMENDATIONS

This chapter summarizes the findings and gives recommendations derived from the research conducted. The research encompassed various research areas, which included the validation of simulation models for mass flow rate of maize grain through horizontal circular orifices, determination of the influence of moisture content, air temperature, and mass flow rate of maize grain on moisture removal rate and energy used during the drying process, optimisation of selected process parameters, and the evaluation of drying models for grains.

#### 5.1 Conclusions

The following were specific conclusions drawn from this research:

- (i) The mass flow rates of maize grain simulated by the Beverloo (BEV), British Code of Practice (BCP), and Tudor (TUD) models did not corroborate with the actual values. This discrepancy indicates that these three models were inadequate for accurately simulating the mass flow rates (MFR) of maize grain through horizontal orifices in the experimental vertical pneumatic dryer (PMGD). Conversely, the New model ( $Q_N$ ) showed congruence between its simulated MFR and the actual values. As a result, the  $Q_N$  model emerged as a more dependable and accurate option for simulating the mass flow rates of maize grain through horizontal circular orifices in the context of the PMGD, in comparison to the BEV, BCP, and TUD models.
- (ii) The moisture content (MC) of maize grain had a significant effect on the moisture removal rate (MRR) during the drying process. However, this MC did not show a significant influence on the energy used for both drying ( $E_a$ ) and transportation ( $E_g$ ) of maize grain. However, the drying air temperature had a significant effect on MRR and  $E_a$ , but its effect on  $E_g$  was not significant. The mass flow rate did not significantly affect MRR,  $E_a$ , and  $E_g$ .
- (iii) The optimum energy proportioned for drying ( $E_a$ ) and transportation ( $E_g$ ) of maize grain for moisture removal rate (MRR) were found to be 7.3 kWh and 2.2 kWh, respectively. The influence of the  $E_a$  on MRR was found to be more significant than that of  $E_g$ . Additionally, the contribution of  $E_a$  (62.8%) towards MRR was greater than that of  $E_g$  (36.8%).
- (iv) The optimum moisture content (MC), air temperature ( $T_a$ ) and mass flow rate of maize grain (MFR) for moisture removal rate (MRR) in drying were found to be 20%, 80°C and 720 kg/h, respectively. The effect of  $T_a$  on MRR was more significant than that of MFR and MC.

Moreover, the contribution of  $T_a$  (67.5%) to the variation in MRR was greater compared to MFR (26.3%) and MC (3.9%).

Similarly, the optimum MC,  $T_a$  and MFR for energy used for drying and transportation of maize grain (EU) were found to be 20%, 60°C and 720 kg/h. The influence of  $T_a$  on EU was more significant than MFR and MC. The contribution of  $T_a$  (97.1%) to the variation in EU exceeded that of MFR (2.3%) and MC (0.6%).

The difference between the Page model and actual moisture ratios (MR) was not significant, indicating the suitability of the Page model for accurately describing the drying process of maize grain.

## **5.2 Recommendations**

This research identified some key areas for industrial application or further investigation.

### **(a) Recommendations for Industry**

- (i) The New model showed higher reliability in comparison to the Beverloo, British Code of Practice, and Tudor models. Therefore, it is recommended to use the New model for simulating the mass flow rate of maize grain through horizontal circular orifices in various applications.
- (ii) To attain the highest moisture removal rate during maize grain drying more energy should be proportioned for the drying process compared to transportation. This prioritisation of energy allocation would contribute to efficient drying process and enhance the overall moisture removal rate.
- (iii) To achieve the highest moisture removal rate during maize grain drying, the optimum process parameters: moisture content of 20% (wet basis), air temperature of 80°C, and mass flow rate of maize grain of 720 kg/h should be employed. These conditions would lead to the most efficient moisture removal from the grain and maximise the effectiveness of the drying process.
- (iv) It is recommended to use the optimum process parameters namely: moisture content of 20% (wet basis), air temperature of 60°C, and mass flow rate of maize grain of 720 kg/h to minimise the energy used during maize grain drying. By employing these conditions, the overall energy used in the drying process would reduce.

(v) The Page model is the most appropriate and accurate for describing the variation of moisture ratios with time in maize grain drying. Therefore, it is recommended to use the Page model for modelling and simulating the moisture drying characteristics of maize grain over time.

**(b) Recommendations for Further Research**

- (i) The effect of variation of air mass flow rate on moisture removal rate and energy use in the experimental vertical pneumatic maize grain dryer should be investigated.
- (ii) In this research the process parameters in maize grain drying were optimised, therefore research aimed at determining optimum design parameters of the experimental dryer should be conducted.

## REFERENCES

- Abd-El-Rahman, A. M., & Youssef, M. E. S. (2008). A device for enhancement and controlling of the cohesive powder discharging without aeration. *Journal of Applied Sciences Research*, 4(2), 133-137.
- Agbetoye, L., & Ogunlowo, A. S. (2010). Modeling flow rate of egusi-melon (*colocynthis citrullus*) through circular horizontal hopper orifice. *Advances in Science and Technology*, 4(1), 35-44. <http://www.researchgate.net/publication/272685255>
- Aghbashlo, M., Kianmehr, M., Khani, S., & Ghasemi, M. (2009a). Mathematical modelling of thin-layer drying of carrot. *International Agrophysics*, 23(4), 313-317.
- Aghbashlo, M., Kianmehr, M. H., & Samimi-Akhijahani, H. (2009b). Evaluation of thin-layer drying models for describing drying kinetics of barberries (*barberries vulgaris*). *Journal of Food Process Engineering*, 32(2), 278-293. <https://doi.org/10.1111/j.1745-4530.2007.00216.x>
- Aghbashlo, M., Mobli, H., Rafiee, S., & Madadlou, A. (2013). A review on energy analysis of drying processes and systems. *Renewable and Sustainable Energy Reviews*, 22, 1-22. <https://doi.org/10.1016/j.rser.2013.01.015>
- Agrawal, P. K., Agrawal, B. D., Rao, P. V., & Singh, J. (1998). *Seed multiplication, conditioning and storage. Maize seed industries in developing countries*. Colorado, USA: Lynne Rienner Publishers Incorporated.
- Aguirre, M. A., De Schant, R., & Géminard, J.-C. (2014). Granular flow through an aperture: Influence of the packing fraction. *Physical Review* 90(1), 012203. <https://doi.org/10.1103/PhysRevE.90.012203>
- Aissa, W., El-Sallak, M., & Elhakem, A. (2014). Performance of solar dryer chamber used for convective drying of sponge-cotton. *Thermal Science*, 18(2), 451-462. <https://doi.org/10.2298/TSCI110710084A>
- Ajay, C., Orsunil, K., & Deepak, D. (2009). *Design of solar dryer with turbo ventilator and fireplace*. Paper presented at the International Solar Food Processing Conference.
- Akoko, P. O., Groote, H. D., Gathungu, E., & Ricker-Gilbert, J. (2021). Technical and economic analysis of small-scale maize dryers in Kenya.

- Akpinar, E. K. (2006). Mathematical modelling of thin layer drying process under open sun of some aromatic plants. *Journal of Food Engineering*, 77(4), 864-870. <https://doi.org/10.1016/j.jfoodeng.2005.08.014>
- Akpinar, E. K. (2011). Drying of parsley leaves in a solar dryer and under open sun: Modeling, energy and exergy aspects. *Journal of Food Process Engineering*, 34(1), 27-48. <https://doi.org/10.1111/j.1745-4530.2008.00335.x>
- Akpinar, E. K., Bicer, Y., & Cetinkaya, F. (2006). Modelling of thin layer drying of parsley leaves in a convective dryer and under open sun. *Journal of Food Engineering*, 75(3), 308-315. <https://doi.org/10.1016/j.jfoodeng.2005.04.018>
- Akpinar, E. K., Bicer, Y., & Midilli, A. (2003b). Modeling and experimental study on drying of apple slices in a convective cyclone dryer. *Journal of Food Process Engineering*, 26(6), 515-541. <https://doi.org/10.1111/j.1745-4530.2003.tb00654.x>
- Akpinar, E. K., Bicer, Y., & Yildiz, C. (2003a). Thin layer drying of red pepper. *Journal of Food Engineering*, 59(1), 99-104. <https://doi.org/10.1111/j.1745-4530.2003.tb00654.x>
- Al-mahasneh, M. A., Rababah, T. M., Al-shbool, M., & Yang, W. (2007). Thin-layer drying kinetics of sesame hulls under forced convection and open sun drying. *Journal of Food Process Engineering*, 30(3), 324-337. <https://doi.org/10.1111/j.1745-4530.2007.00119.x>
- Alonso, G., Del Del Valle, E., & Ramirez, J. R. (2020). *Desalination in nuclear power plants*: Woodhead Publishing. <https://doi.org/10.1016/B978-0-12-820021-6.09995-6>
- Amer, B. M. A. (1999). *Determination of drying rate of fruits as a function of the affecting factors under conditions suiting solar drying*. [Master's thesis, Agricultural Engineering Department, Faculty of Agriculture, Cairo University, Egypt].
- Anand, A., Curtis, J. S., Wassgren, C. R., Hancock, B. C., & Ketterhagen, W. R. (2008). Predicting discharge dynamics from a rectangular hopper using the discrete element method (dem). *Chemical Engineering Science*, 63(24), 5821-5830. <https://doi.org/10.1016/j.ces.2008.08.015>
- Anankware, J., Obeng-Ofori, D., Afreh-Nuamah, K., Oluwole, F., & Ansah, F. (2013). Use of the triple-layer hermetic bag against the maize weevil, *sitophilus zeamais* (mots) in three varieties of maize. *Journal of Biology, Agriculture and Healthcare*, 3(12), 67-73.
- ASAE. (2003). Flow of grain and seeds through orifices *American Society of Agricultural Engineers standards D274.1*. St. Joseph. MI 49085 – 9659. United States of America.

- ASAE, T. (1992). Moisture measurement unground grain and seeds. *American Society of Agricultural and Biological Engineering*, 1988, 2-4.
- Baeyens, J., Van Gauwbergen, D., & Vinckier, I. (1995). Pneumatic drying: The use of large-scale experimental data in a design procedure. *Powder Technology*, 83(2), 139-148. [https://doi.org/10.1016/0032-5910\(94\)02945-K](https://doi.org/10.1016/0032-5910(94)02945-K)
- Bains, M., Ramaswamy, H., & Lo, K. (1989). Tray drying of apple puree. *Journal of Food Engineering*, 9(3), 195-201. [https://doi.org/10.1016/0260-8774\(89\)90040-X](https://doi.org/10.1016/0260-8774(89)90040-X)
- Bakker-Arkema, F., DeBaerdemaeker, J., Amirante, P., Ruiz-Altisent, M., & Studman, C. (1999). *Agricultural Engineering International: CIGR handbook of agricultural engineering. Agro-processing engineering (Vol. 4)*: St Joseph MI.
- Bal, L. M., Kar, A., Satya, S., & Naik, S. N. (2010). Drying kinetics and effective moisture diffusivity of bamboo shoot slices undergoing microwave drying. *International Journal of Food Science & Technology*, 45(11), 2321-2328. <https://doi.org/10.1111/j.1365-2621.2010.02402.x>
- Bala, B. K. (1997). *Drying and storage of cereal grains*. Incorporated, Plymouth, United Kingdom: Science Publishers.
- Balbine, M., Marcel, E., Alexis, K., & Belkacem, Z. (2015). Experimental evaluation of the thermal performance of dryer airflow configuration. *International Journal of Energy Engineering*, 5(4), 80-86.
- Barnwal, P., & Tiwari, G. (2008). Grape drying by using hybrid photovoltaic-thermal greenhouse dryer: An experimental study. *Solar Energy*, 82(12), 1131-1144. <https://doi.org/10.1016/j.solener.2008.05.012>
- Basunia, M., & Abe, T. (2001). Moisture desorption isotherms of medium-grain rough rice. *Journal of Stored Products Research*, 37(3), 205-219. [https://doi.org/10.1016/S0022-474X\(00\)00022-9](https://doi.org/10.1016/S0022-474X(00)00022-9)
- Belegundu, A. D., & Chandrupatla, T. R. (2019). *Optimization concepts and applications in engineering*: Cambridge University Press.
- Bell, T. (1993). Measurement of powder flowability. *Advances in Powder Metallurgy & Particulate Materials--1993.*, 1, 169-180.

- Beverloo, W. A., Leniger, H. A., & Van de Velde, J. (1961). The flow of granular solids through orifices. *Chemical Engineering Science*, 15(3-4), 260-269. [https://doi.org/10.1016/0009-2509\(61\)85030-6](https://doi.org/10.1016/0009-2509(61)85030-6)
- Billiris, M. A., & Siebenmorgen, T. J. (2014). Energy use and efficiency of rice-drying systems ii. Commercial, cross-flow dryer measurements. *Applied Engineering in Agriculture*, 30(2), 217-226. <https://doi.org/10.13031/aea.30.10287>
- Biswajit, D., Roy, S., Rai, R., & Saha, S. (2016). Application of grey fuzzy logic for the optimization of milling parameters with multi-performance characteristics. *Engineering Science and Technology, an International Journal*, 19(2), 857-865. <https://doi.org/10.13031/aea.30.10287>
- Box, G. E., Hunter, W. H., & Hunter, S. (1978). *Statistics for experimenters (Vol. 664)*: John Wiley and sons New York.
- Brooker, D., Bakker-Arkema, F., & Hall, C. (1974). *Drying cereal grains*. Incorporated West Port, Connecticut, USA: AVI Publishing Company.
- Brooker, D., Bakker-Arkema, F., & Hall, C. W. (1992). *Drying and storage of grains and oil seeds*: Springer Science and Business Media.
- Brown, R. (1959). Exploratory study of the flow of granules through apertures. *Transactions of the Institution of Chemical Engineers*, 37, 108-119.
- Brown, R., & Richards, J. C. (1959). Exploratory study of the flow of granules through apertures. *Transactions of the Institution of Chemical Engineers*, 37, 108-119.
- Brown, R., & Richards, J. C. (1960). Profile of flow of granules through apertures. *Transactions of the Institution of Chemical Engineers*, 38, 243-256.
- Bruce, D. M. (1985). Exposed-layer barley drying: Three models fitted to new data up to 150 c. *Journal of Agricultural Engineering Research*, 32(4), 337-348. [https://doi.org/10.1016/0021-8634\(85\)90098-8](https://doi.org/10.1016/0021-8634(85)90098-8)
- Bunyawanchakul, P. (2006). *Development of a cyclone rice dryer*. [Doctoral dissertation, University of Tasmania]. [https://figshare.utas.edu.au/articles/thesis/Development\\_of\\_a\\_cyclone\\_rice\\_dryer/23235146/1](https://figshare.utas.edu.au/articles/thesis/Development_of_a_cyclone_rice_dryer/23235146/1)

- Cairns, J. E., Hellin, J., Sonder, K., Araus, J. L., MacRobert, J. F., Thierfelder, C., & Prasanna, B. (2013). Adapting maize production to climate change in sub-saharan africa. *Food Security*, 5(3), 345-360. <https://doi.org/10.1007/S12571-013-0256-X>
- Cardona, C., Hodges, R., & Farrell, G. (2004). *Common beans: Latin america (Vol. 2)*. Iowa: Blackwell Publishing Limited.
- Chakraverty, A., Mujumdar, A. S., & Ramaswamy, H. S. (2003). *Handbook of postharvest technology: Cereals, fruits, vegetables, tea, and spices (Vol. 93)*: Chemical Rubber Company Press.
- Chandra, P. K., & Singh, R. P. (2017). *Applied numerical methods for food and agricultural engineers*: Chemical Rubber Company Press.
- Chang, C., & Converse, H. (1988). Flow rates of wheat and sorghum through horizontal orifices. *Transactions of the American Society of Agricultural Engineers*, 31(1), 300-0304. <https://doi.org/10.13031/2013.30704>
- Chang, C., Converse, H., & Lai, F. (1984). Flow rate of corn through orifices as affected by moisture content. *Transactions of the American Society of Agricultural Engineers*, 27(5), 1586-1589. <https://doi.org/10.13031/2013.33008>
- Chang, C., Converse, H., & Steele, J. (1991). Flow rates of grain through various shapes of vertical and horizontal orifices. *Transactions of the American Society of Agricultural Engineers*, 34(4), 1789-1796. <https://doi.org/10.13031/2013.31802>
- Chapuis, A., Precoppe, M., Méot, J.-M., Ssiroth, K., & Tran, T. (2017). Pneumatic drying of cassava starch: Numerical analysis and guidelines for the design of efficient small-scale dryers. *Drying Technology*, 35(4), 393-408. <https://doi.org/10.1080/07373937.2016.1177537>
- Chen, J., Zhou, Y., Fang, S., Meng, Y., Kang, X., Xu, X., & Zuo, X. (2013). Mathematical modeling of hot air drying kinetics of momordica charantia slices and its color change. *Advance Journal of Food Science and Technology*, 5(9), 1214-1219.
- Coradi, P. C., Fernandes, C. H., Helmich, J. C., & Goneli, A. L. (2016). Effects of drying air temperature and grain initial moisture content on soybean quality (glycine max (l.) merrill). *Engenharia Agrícola*, 36, 866-876. <https://doi.org/10.1590/1809-4430-Eng.Agric.v36n5p866-876/2016>
- Crank, J. (1975). *The mathematics of diffusion* (pp. 21–24). London: Oxford University Press.



- Crapiste, G., & Rotstein, E. (1997). Design and performance evaluation of dryers. *Handbook of Food Engineering Practice*, 4, 125-165.
- Crewdson, B., Ormond, A. L., & Nedderman, R. (1977). Air-impeded discharge of fine particles from a hopper. *Powder Technology*, 16(2), 197-207. [https://doi.org/10.1016/0032-5910\(77\)87007-1](https://doi.org/10.1016/0032-5910(77)87007-1)
- Crowe, C. T., Schwarzkopf, J. D., Sommerfeld, M., & Tsuji, Y. (2011). *Multiphase flows with droplets and particles*: Chemical Rubber Company Press.
- Dandamrongrak, R., Young, G. & Mason, R. (2002). Evaluation of various pre-treatments for the dehydration of banana and selection of suitable drying models. *Journal of Food Engineering*, 55(2), 139-146. [https://doi.org/10.1016/S0260-8774\(02\)00028-6](https://doi.org/10.1016/S0260-8774(02)00028-6)
- Darıcı, S., & Şen, S. (2015). Experimental investigation of convective drying kinetics of kiwi under different conditions. *Heat and Mass Transfer*, 51(8), 1167-1176. <https://doi.org/10.1007/s00231-014-1487-x>
- Das, S., Das, T., Rao, P. S., & Jain, R. (2001). Development of an air recirculating tray dryer for high moisture biological materials. *Journal of Food Engineering*, 50(4), 223-227. [https://doi.org/10.1016/S0260-8774\(01\)00024-3](https://doi.org/10.1016/S0260-8774(01)00024-3)
- De Groote, H., Dema, G., Sonda, G. B., & Gitonga, Z. M. (2013). Maize for food and feed in east africa—the farmers’ perspective. *Field Crops Research*, 153, 22-36. <https://doi.org/10.1016/j.fcr.2013.04.005>
- Delgado, J., & de Lima, A. B. (2014). *Transport phenomena and drying of solids and particulate materials* (Vol. 48): Springer. <https://doi.org/10.1007/978-3-319-04054-7>
- Deming, W. E., & Mehring, A. L. (1929). The gravitational flow of fertilizers and other comminuted solids. *Industrial and Engineering Chemistry*, 21(7), 661-665. <https://doi.org/10.1021/ie50235a013>
- Demir, V., Gunhan, T., & Yagcioglu, A. (2007). Mathematical modelling of convection drying of green table olives. *Biosystems Engineering*, 98(1), 47-53. <https://doi.org/10.1016/j.biosystemseng.2007.06.011>
- Diamante, L. M., & Munro, P. A. (1993). Mathematical modelling of the thin layer solar drying of sweet potato slices. *Solar Energy*, 51(4), 271-276. [https://doi.org/10.1016/0038-092X\(93\)90122-5](https://doi.org/10.1016/0038-092X(93)90122-5)

- Dias, R. P., Teixeira, J. A., Mota, M. G., & Yelshin, A. I. (2004). Particulate binary mixtures: Dependence of packing porosity on particle size ratio. *Industrial and Engineering Chemistry Research*, 43(24), 7912-7919. <https://doi.org/10.1021/ie040048b>
- Dissa, A., Desmorieux, H., Bathiebo, J., & Koulidiati, J. (2008). Convective drying characteristics of amelie mango (*mangifera indica* l. Cv. 'Amelie') with correction for shrinkage. *Journal of Food Engineering*, 88(4), 429-437. <https://doi.org/10.1016/j.jfoodeng.2008.03.008>
- Doymaz, I. (2004). Drying kinetics of white mulberry. *Journal of Food Engineering*, 61(3), 341-346. [https://doi.org/10.1016/S0260-8774\(03\)00138-9](https://doi.org/10.1016/S0260-8774(03)00138-9)
- Doymaz, I. (2005). Sun drying of figs: An experimental study. *Journal of Food Engineering*, 71(4), 403-407. <https://doi.org/10.1016/j.jfoodeng.2004.11.003>
- Doymaz, I. (2006). Drying kinetics of black grapes treated with different solutions. *Journal of Food Engineering*, 76(2), 212-217. <https://doi.org/10.1016/j.jfoodeng.2005.05.009>
- Doymaz, I. (2007). Air-drying characteristics of tomatoes. *Journal of Food Engineering*, 78(4), 1291-1297. <https://doi.org/10.1016/j.jfoodeng.2005.12.047>
- Doymaz, I. (2008). Drying of leek slices using heated air. *Journal of Food Process Engineering*, 31(5), 721-737. <https://doi.org/10.1111/j.1745-4530.2007.00185.x>
- Doymaz, I., Gorel, O., & Akgun, N. A. (2004). Drying characteristics of the solid by-product of olive oil extraction. *Biosystems Engineering*, 88(2), 213-219. <https://doi.org/10.1016/j.biosystemseng.2004.03.003>
- Doymaz, I., & Ismail, O. (2010). Drying and rehydration behaviors of green bell peppers. *Food Science and Biotechnology*, 19(6), 1449-1455. <https://doi.org/10.1007/s10068-010-0207-7>
- Eissen, W., Muhlbauer, W., & Kutzbach, H. D. (1985). Solar drying of grapes. *Drying Technology*, 3 (1), 63-74. <https://doi.org/10.1080/07373938508916255>
- Ekechukwu, O. (1999). Review of solar-energy drying systems: An overview of drying principles and theory. *Energy Conversion and Management Journal*, 40(6), 593-613. [https://doi.org/10.1016/S0196-8904\(98\)00092-2](https://doi.org/10.1016/S0196-8904(98)00092-2)
- El-Behery, S. M., El-Askary, W. A., Hamed, M. H., & Ibrahim, K. A. (2012). Numerical simulation of heat and mass transfer in pneumatic conveying dryer. *Computers and Fluids*, 68 (2012), 159-167. <https://doi.org/10.1016/j.compfluid.2012.08.006>

- El-Beltagy, A., Gamea, G., & Essa, A. A. (2007). Solar drying characteristics of strawberry. *Journal of Food Engineering*, 78(2), 456-464.
- El-Sebaei, A., & Shalaby, S. (2013). Experimental investigation of an indirect-mode forced convection solar dryer for drying thymus and mint. *Energy Conversion and Management*, 74, 109-116. <https://doi.org/10.1016/j.enconman.2013.05.006>
- Erbay, Z., & Icier, F. (2010). A review of thin layer drying of foods: Theory, modeling, and experimental results. *Critical Reviews in Food Science and Nutrition*, 50(5), 441-464. <https://doi.org/10.1080/10408390802437063>
- Ewalt, D., & Buelow, F. (1963). Flow of shelled corn through orifices in bin walls. *Quarterly Bulletin of the Michigan Agricultural Experiment Station, Michigan State University, East Lansing, Michigan USA*, 46(1), 92-102.
- FAO. (1992). Maize in human nutrition. Rome (Italy): <http://www.fao.org/docrep/t0395e/T0395E00.htm#Contents>.
- FAO. (2011). *Rural structures in the tropics. Design and development*. Rome, Italy. <http://erepository.uonbi.ac.ke:8080/xmlui/handle/123456789/46813>
- FAOStat. (2021). Food and agriculture organization of the united nations-statistic. FAO, Rome. <http://www.fao.org/faostat>.
- FAOStat, F. (2014). Agricultural organization of the united nations, statistics division: <Http://faostat3.Fao.Org/browse/q/qc/e>.
- FAOStat, F. (2019). Food and agriculture organization of the united nations-statistic division <https://www.Fao.Org/faostat/en/#data:QC>.
- Fickie, K. E., Mehrabi, R., & Jackson, R. (1989). Density variations in a granular material flowing from a wedge-shaped hopper. *American Institute of Chemical Engineers*, 35(5), 853-855. <http://pascalfrancis.inist.fr/vibad/index.php?action=getRecordDetail&idt=7342147>
- Filková, I., & Mujumdar, A. S. (1995). Industrial spray drying systems. *Handbook of Industrial Drying, 1*, 263-308.
- Fohr, J., & Arnaud, G. (1992). Crape drying: From sample behaviour to the drier project. *Drying Technology*, 10(2), 445-465. <https://doi.org/10.1080/07373939208916445>

- Fortes, M., & Okos, M. R. (1981). Non-equilibrium thermodynamics approach to heat and mass transfer in corn kernels. *Transactions of the American Society of Agricultural Engineers*, 24(3), 761-769. <https://doi.org/10.13031/2013.34335>
- Fowler, R., & Glastonbury, J. R. (1959). The flow of granular solids through orifices. *Chemical Engineering Science*, 10(3), 150-156. [https://doi.org/10.1016/0009-2509\(59\)80042-7](https://doi.org/10.1016/0009-2509(59)80042-7)
- Frangopoulos, C., von Spakovsky, M., & Sciubba, E. (2002). A brief review of methods for the design and synthesis optimization of energy systems. *International Journal of Thermodynamics*, 5(4), 151-160. <https://dergipark.org.tr/en/pub/ijot/issue/5746/76638>
- Franklin, F., & Johanson, L. (1955). Flow of granular material through a circular orifice. *Chemical Engineering Science*, 4(3), 119-129. [https://doi.org/10.1016/0009-2509\(55\)80003-6](https://doi.org/10.1016/0009-2509(55)80003-6)
- Fyhr, C., & Rasmuson, A. (1997). Mathematical model of a pneumatic conveying dryer. *American Institute of Chemical Engineers*, 43(11), 2889-2902. <https://doi.org/10.1002/aic.690431102>
- Galedar, M. N., Tabatabaeefar, A., Jafari, A., Sharifi, A., Mohtasebi, S., & Fadaei, H. (2010). Moisture dependent geometric and mechanical properties of wild pistachio (*pistacia vera* l.) nut and kernel. *International Journal of Food Properties*, 13(6), 1323-1338. <https://doi.org/10.1080/10942910903062099>
- Gao, S., Ming, B., Li, L.-l., Xie, R.-z., Wang, K.-r., & Li, S.-k. (2021). Maize grain moisture content correction: From nonstandard to standard system. *Biosystems Engineering*, 204, 212-222. <https://doi.org/10.1016/j.biosystemseng.2021.01.013>
- García-Lara, S., & Serna-Saldivar, S. O. (2019). Corn history and culture (In: Serna-Saldivar, S.O. (Ed.), *Corn* (3rd Ed.) ed., pp. 1–18): AACC International Press, Oxford. <https://doi.org/10.1016/B978-0-12-811971-6.00001-2>
- Garcimartín, A., Mankoc, C., Janda, A., Arévalo, R., Pastor, J. M., Zuriguel, I., & Maza, D. (2009). Flow and jamming of granular matter through an orifice *Traffic and granular flow '07* (pp. 471-486): Springer. [https://doi.org/10.1007/978-3-540-77074-9\\_52](https://doi.org/10.1007/978-3-540-77074-9_52)
- Ghazanfari, A., Emami, S., Tabil, L., & Panigrahi, S. (2006). Thin-layer drying of flax fiber: II. Modeling drying process using semi-theoretical and empirical models. *Drying Technology*, 24(12), 1637-1642. <https://doi.org/10.1080/07373930601031463>

- Giner, S. A., & De Michelis, A. (1988). Evaluation of the thermal efficiency of wheat drying in fluidized beds: Influence of air temperature and heat recovery. *Journal of Agricultural Engineering Research*, 41(1), 11-23. [https://doi.org/10.1016/0021-8634\(88\)90199-0](https://doi.org/10.1016/0021-8634(88)90199-0)
- Glenn, T. L. (1978). *Dynamic analysis of grain drying system* [Doctoral thesis, Ohio State University, Ann Arbor, MI]
- Goldberg, D. E. (1989). Genetic algorithms in search, optimization and machine learning Addison-Wesley Publishing Company. Reading, MA.
- Golob, P., Farrel, G., & Orchard, J. (2002). *Crop post-harvest: Science and technology. Principles and practice. (Vol. 1):* Blackwell Science Limited. <https://doi.org/10.1002/9780470751015>
- Gregory, J. M., & Fedler, C. B. (1987). Equation describing granular flow through circular orifices *Transactions of the American Society of Agricultural Engineers*, 30(2), 529-532. <https://doi.org/10.13031/2013.31982>
- Guan, Z., Wang, X., Li, M., & Jiang, X. (2013). Mathematical modeling on hot air drying of thin-layer fresh tilapia fillets. *Polish Journal Food Nutrition Sciences*, 63(1), 25–34.
- Gunhan, T., Demir, V., Hancioglu, E., & Hepbasli, A. (2005). Mathematical modelling of drying of bay leaves. *Energy Conversion and Management*, 46(11-12), 1667-1679. <https://doi.org/10.1016/j.enconman.2004.10.001>
- Hanrahan, G., & Lu, K. (2006). Application of factorial and response surface methodology in modern experimental design and optimization. *Critical Reviews in Analytical Chemistry*, 36(3-4), 141-151. <https://doi.org/10.1080/10408340600969478>
- Harmens, A. (1963). Flow of granular material through horizontal apertures. *Chemical Engineering Science*, 18(5), 297-306. [https://doi.org/10.1016/0009-2509\(93\)80005-B](https://doi.org/10.1016/0009-2509(93)80005-B)
- Harold, F., Giles, J., John, R., & Wagner, J. (2013). *Extrusion*
- Hassan, B. H., & Hobani, A. I. (2000). Thin-layer drying of dates. *Journal of Food Process Engineering*, 23(3), 177-189. <https://doi.org/10.1111/j.1745-4530.2000.tb00510.x>
- Henderson, S. (1974). Progress in developing the thin layer drying equation. *Transactions of the American Society of Agricultural Engineers*, 17(6), 1167-1168.
- Henderson, S., & Pabis, S. (1961). Grain drying theory. I. Temperature effect on drying coefficients. *Journal of Agricultural Engineering Research*, 6, 169-174.

- Hidayat, M., & Rasmuson, A. (2007). Heat and mass transfer in u-bend of a pneumatic conveying dryer. *Chemical Engineering Research and Design*, 85(3), 307–319. <https://doi.org/10.1205/cherd06162>
- Hoffmann, F., & Pfister, G. (1997). Evolutionary design of a fuzzy knowledge base for a mobile robot. *International Journal of Approximate Reasoning*, 17(4), 447-469. [https://doi.org/10.1016/S0888-613X\(97\)00005-4](https://doi.org/10.1016/S0888-613X(97)00005-4)
- Holman, J. (1981). *Heat transfer*. McGraw-Hill, New York Pergamon.
- Hossain, M., & Bala, B. (2002). Thin-layer drying characteristics for green chilli. *Drying Technology*, 20(2), 489-505. <https://doi.org/10.1081/DRT-120002553>
- Hossain, M. A., Woods, J. L., & Bala, B. K. (2007). Single-layer drying characteristics and colour kinetics of red chilli. *International Journal of Food Science and Technology*, 42(11), 1367-1375. <https://doi.org/10.1111/j.1365-2621.2006.01414.x>
- Huntington, A., & Rooney, N. (1971). Discharge of granular materials from hoppers. *Project Report, Department of Chemical Engineering, University of Cambridge*.
- Husain, A., Chen, C., Clayton, J., & Whitney, L. (1972). Mathematical simulation of mass and heat transfer in high moisture foods. *Transactions of the American Society of Agricultural Engineers*, 15(4), 732-0736.
- Iguaz, A., Lopez, A., & Virseda, P. (2002). Influence of air recycling on the performance of a continuous rotary dryer for vegetable wholesale by-products. *Journal of Food Engineering*, 54(4), 289-297. [https://doi.org/10.1016/S0260-8774\(01\)00215-1](https://doi.org/10.1016/S0260-8774(01)00215-1)
- Ileleji, K., & Zhou, B. (2008). The angle of repose of bulk corn stover particles. *Powder Technology*, 187(2), 110-118. <https://doi.org/10.1016/j.powtec.2008.01.029>
- Indarto, A., Halim, Y., & Partoputro, P. (2007). Pneumatic drying of solid particle: Experimental and model comparison. *Experimental Heat Transfer*, 20(4), 277-287. <https://doi.org/10.1080/08916150701418252>
- Islam, M. T., Marks, B. P., & Bakker-Arkema, F. W. (2004). Optimization of commercial ear-corn dryers. *Agricultural Engineering International: CIGR Journal*, 6.
- Jafari, A., & Tabatabaefar, A. (2008). Some physical properties of wild pistachio [pistacia vera l.] nut and kernel as a function of moisture content. *International Agrophysics*, 22(1), 117-124. <https://agro.icm.edu.pl/agro/element/bwmeta1.element.agro-article-95831439-c28b-4928-acfe-23d36f990932>

- Jain, D., & Tiwari, G. (2003). Thermal aspects of open sun drying of various crops. *Energy*, 28(1), 37-54. [https://doi.org/10.1016/S0360-5442\(02\)00084-1](https://doi.org/10.1016/S0360-5442(02)00084-1)
- Jayaraman, K., & Gupta, D. D. (2014). Drying of fruits and vegetables *Handbook of industrial drying, fourth edition* (pp. 611-635): Chemical Rubber Company Press.
- Jazini, M., & Hatamipour, M. (2010). A new physical pretreatment of plum for drying. *Food and Bioproducts Processing Journal*, 88(2-3), 133-137. <https://doi.org/10.1016/j.fbp.2009.06.002>
- Jenike, A. (1967). Utah engineering experiment station. University of Utah, Salt Lake City. *Bulletin*, 108. <https://core.ac.uk/download/pdf/276282293.pdf>
- Jewell, D. C., Waddington, S., Ransom, J., & Pixley, K. (1995). *Maize research for stress environments*: International Maize and Wheat Improvement Center (CIMMYT).
- Jokiniemi, T., Kautto, K., Kokin, E., & Ahokas, J. (2011). Energy efficiency measurements in grain drying. *Agronomy Research Biosystem Engineering*, 1, 69-75.
- Kadam, D. M., & Dhingra, D. (2011). Mass transfer kinetics of banana slices during osmoconvective drying. *Journal of Food Process Engineering*, 34(2), 511-532. <https://doi.org/10.1111/j.1745-4530.2009.00373.x>
- Kahveci, K., & Cihan, A. (2008). *Drying of food materials: Transport phenomena*: Nova Science Publishers.
- Kaleemullah, S. (2002). *Studies on engineering properties and drying kinetics of chillies*. [Doctoral thesis Tamil Nadu Agricultural University; Coimbatore, India].
- Kaleemullah, S., & Kailappan, R. (2006). Modelling of thin-layer drying kinetics of red chillies. *Journal of Food Engineering*, 76(4), 531-537. <https://doi.org/10.1016/j.jfoodeng.2005.05.049>
- Kanali, C. L. (1997). Prediction of axle loads induced by sugarcane transport vehicles using statistical and neural-network models. *Journal of Agricultural Engineering Research*, 68(3), 207-213. <https://doi.org/10.1006/jaer.1997.0199>
- Karababa, E., & Coşkuner, Y. (2007). Moisture dependent physical properties of dry sweet corn kernels. *International Journal of Food Properties*, 10(3), 549-560. <https://doi.org/10.1080/10942910601003981>

- Karathanos, V. T. (1999). Determination of water content of dried fruits by drying kinetics. *Journal of Food Engineering*, 39(4), 337-344. [https://doi.org/10.1016/S0260-8774\(98\)00132-0](https://doi.org/10.1016/S0260-8774(98)00132-0)
- Kassem, A. (1998). *Comparative studies on thin layer drying models for wheat*. Paper presented at the 13th International Congress on Agricultural Engineering.
- Kayisoglu, S., & Ertekin, C. (2011). Vacuum drying kinetics of barbunya bean (*Phaseolus vulgaris* L. *Elipticus* Mart.). *The Philippine Agricultural Scientist*, 94(3).
- Keey, R. B. (2013). *Drying: Principles and practice (Vol. 13)*: Elsevier.
- Ketchum, M. S. (1919). *The design of walls, bins and grain elevators*: McGraw-Hill.
- Kingsly, A., Balasubramaniam, V., & Rastogi, N. (2009). Effect of high-pressure processing on texture and drying behavior of pineapple. *Journal of Food Process Engineering*, 32(3), 369-381. <https://doi.org/10.1111/j.1745-4530.2007.00221.x>
- Kirimi, L., Sitko, N., Jayne, T. S., Karin, F., Muyanga, M., Sheahan, M., Flock, J., & Bor, G. (2011). A farm gate-to-consumer value chain analysis of Kenya's maize marketing system. *Tegemeo Institute of Agricultural Policy and Development Working Paper*, 44.
- Kleinhans, M., Markies, H., De Vet, S., & Postema, F. (2011). Static and dynamic angles of repose in loose granular materials under reduced gravity. *Journal of Geophysical Research: Planets*, 116(E11).
- KNBS, G. (2020). Economic survey 2019. <https://doi.org/10.1029/2011JE003865>
- Korir, K., & Bii, C. (2012). Mycological quality of maize flour from aflatoxins "hot" zone eastern province—Kenya. *African Journal of Health Sciences*, 21, 143-146.
- Koua, K., B., Fassinou, W. F., Gbaha, P., & Toure, S. (2009). Mathematical modelling of the thin layer solar drying of banana, mango and cassava. *Energy*, 34(10), 1594-1602. <https://doi.org/10.1016/j.energy.2009.07.005>
- Krokida, M. K., Karathanos, V., Maroulis, Z., & Marinos-Kouris, D. (2003). Drying kinetics of some vegetables. *Journal of Food Engineering*, 59(4), 391-403. [https://doi.org/10.1016/S0260-8774\(02\)00498-3](https://doi.org/10.1016/S0260-8774(02)00498-3)
- Kudra, T. (2004). Energy aspects in drying. *Drying Technology*, 22(5), 917-932. <https://doi.org/10.1081/DRT-120038572>
- Kudra, T. (2008). Energy aspects in food dehydration. In C. Ratti (Ed.), *Advances in food dehydration* (pp. 423-445): Chemical Rubber Company Press.



- Kudra, T. (2012). Energy performance of convective dryers. *Drying Technology*, 30(11-12), 1190-1198. <https://doi.org/10.1080/07373937.2012.690803>
- Kumar, C., Karim, A., Joardder, M. U. H., & Miller, G. (2012). *Modeling heat and mass transfer process during convection drying of fruit*. Paper presented at the Proceedings of the 4th International Conference on Computational Methods. Queensland University of Technology, Australia.
- Lahsasni, S., Kouhila, M., Mahrouz, M., Idlimam, A., & Jamali, A. (2004a). Thin layer convective solar drying and mathematical modeling of prickly pear peel (*opuntia ficus indica*). *Energy*, 29(2), 211-224. <https://doi.org/10.1016/j.energy.2003.08.009>
- Lahsasni, S., Kouhila, M., Mahrouz, M., & Jaouhari, J. T. (2004b). Drying kinetics of prickly pear fruit (*opuntia ficus indica*). *Journal of Food Engineering*, 61(2), 173-179. [https://doi.org/10.1016/S0260-8774\(03\)00084-0](https://doi.org/10.1016/S0260-8774(03)00084-0)
- Lee, J. H., & Kim, H. J. (2009). Vacuum drying kinetics of asian white radish (*raphanus sativus* l.) slices. *LWT-Food Science and Technology*, 42(1), 180-186. <https://doi.org/10.1016/j.lwt.2008.05.017>
- Lemus-Mondaca, R., Betoret, N., Vega-Galv3ez, A., & Lara-Aravena, E. (2009). Dehydration characteristics of papaya (*carica pubescens*): Determination of equilibrium moisture content and diffusion coefficient. *Journal of Food Process Engineering*, 32(5), 645-663. <https://doi.org/10.1111/j.1745-4530.2007.00236.x>
- Lewis, A. M. (1992). Measuring the hydraulic diameter of a pore or conduit. *American Journal of Botany*, 79(10), 1158-1161. <https://doi.org/10.1002/j.1537-2197.1992.tb13712.x>
- Lewis, W. K. (1921). The rate of drying of solid materials. *Industrial & Engineering Chemistry*, 13(5), 427-432. <https://doi.org/10.1021/ie50137a021>
- LI, L.-l., Bo, M., Jun, X., Shang, G., Wang, K.-r., XIE, R.-z., Peng, H., & LI, S.-k. (2021). Difference in corn kernel moisture content between pre-and post-harvest. *Journal of Integrative Agriculture*, 20(7), 1775-1782. [https://doi.org/10.1016/S2095-3119\(20\)63245-2](https://doi.org/10.1016/S2095-3119(20)63245-2)
- Lin, T. R. (2002). Experimental design and performance analysis of Tin-coated carbide tool in face milling stainless steel. *Journal of Materials Processing Technology*, 127(1), 1-7. [https://doi.org/10.1016/S0924-0136\(02\)00026-2](https://doi.org/10.1016/S0924-0136(02)00026-2)

- Liu, Q., & Baker-Arkema, F. (1999). Capacity estimation of high-temperature grain dryers--a simplified calculation method. *Agricultural Engineering International: CIGR Journal*.
- López, R., De Ita, A., & Vaca, M. (2009). Drying of prickly pear cactus cladodes (*Opuntia ficus indica*) in a forced convection tunnel. *Energy Conversion and Management*, 50(9), 2119-2126. <https://doi.org/10.1016/j.enconman.2009.04.014>
- Lowe, D. R. (1976). Grain flow and grain flow deposits. *Journal of Sedimentary Research*, 46(1), 188-199. <https://doi.org/10.1306/212f6ef1-2b24-11d7-8648000102c1865d>
- Lui, X. (1995). *Energy conservation by recirculation of drying air*. [Doctoral dissertations, University of Tennessee, Knoxville, TN]. [https://trace.tennessee.edu/utk\\_graddiss/7529](https://trace.tennessee.edu/utk_graddiss/7529)
- Madamba, P. S. (2003). Thin layer drying models for osmotically pre-dried young coconut. *Drying Technology*, 21(9), 1759-1780. <https://doi.org/10.1081/DRT-120025507>
- Madamba, P. S., Driscoll, R. H., & Buckle, K. A. (1996). The thin-layer drying characteristics of garlic slices. *Journal of Food Engineering*, 29(1), 75-97. [https://doi.org/10.1016/0260-8774\(95\)00062-3](https://doi.org/10.1016/0260-8774(95)00062-3)
- Maier, D. E., & Bakker-Arkema, F. W. (2002). *Grain drying systems*. Paper presented at the Proceedings of the 2002 Facility Design Conference of the Grain Elevator and Processing Society, St. Charles, Illinois, United States of America, July.
- Mamtani, K. (2011). *Effect of particle shape on hopper discharge rate*. University of Florida.
- Marinos-Kouris, D., & Maroulis, Z. (2020). Transport properties in the drying of solids. *Handbook of Industrial Drying*, 2, 113-159.
- Matsumoto, S., & Pei, C. T. (1984). A mathematical analysis of pneumatic drying of grains – ii. Falling rate drying. *International Journal of Heat and Mass Transfer*, 27(6), 851-855. [https://doi.org/10.1016/0017-9310\(84\)90005-X](https://doi.org/10.1016/0017-9310(84)90005-X)
- McNeill, S. G., Thompson, S. A., & Montross, M. D. (2004). Effect of moisture content and broken kernels on the bulk density and packing of corn. *Applied Engineering in Agriculture*, 20(4), 475. <https://doi.org/10.13031/2013.16477>
- Meisami-Asl, E., Rafiee, S., Keyhani, A., & Tabatabaeefar, A. (2010). Determination of suitable thin layer drying curve model for apple slices (variety-golab). *Plant Omics*, 3(3), 103. <https://search.informit.org/doi/abs/10.3316/informit.123164921630722>

- Menges, H. O., & Ertekin, C. (2006). Mathematical modeling of thin layer drying of golden apples. *Journal of Food Engineering*, 77(1), 119-125. <https://doi.org/10.1016/j.jfoodeng.2005.06.049>
- Midilli, A., & Kucuk, H. (2003). Mathematical modeling of thin layer drying of pistachio by using solar energy. *Energy Conversion and Management*, 44(7), 1111-1122. [https://doi.org/10.1016/S0196-8904\(02\)00099-7](https://doi.org/10.1016/S0196-8904(02)00099-7)
- Midilli, A., Kucuk, H., & Yapar, Z. (2002). A new model for single-layer drying. *Drying Technology*, 20(7), 1503-1513. <https://doi.org/10.1081/DRT-120005864>
- Misha, S., Mat, A. S., Ruslan, M. H., Sopian, K., & Salleh, E. (2013). *The effect of drying air temperature and humidity on the drying kinetic of kenaf core*. Paper presented at the Applied Mechanics and Materials. <https://www.scientific.net/AMM.315.710>
- Mohsenin, N. (1986). Physical properties of plant and animal materials. Gordon and breach science publishers. *New York*.
- Montgomery, D. C. (2017). *Design and analysis of experiments*: John wiley & sons.
- Morris, W. (1981). Simplified techniques for designing natural convection collectors and estimating their performance. Final report: Morris (W. Scott), Santa Fe, NM (USA). <https://www.osti.gov/biblio/5353469>
- Morrison, G. L., Hall, K., Holste, J., Macek, M., Ihfe, L., DeOtte Jr, R., & Terracina, D. (1994). Comparison of orifice and slotted plate flowmeters. *Flow Measurement and Instrumentation*, 5(2), 71-77. [https://doi.org/10.1016/0955-5986\(94\)90039-6](https://doi.org/10.1016/0955-5986(94)90039-6)
- Moysey, E., Lambert, E., & Wang, Z. (1988). Flow rates of grains and oilseeds through sharp-edged orifices. *Transactions of American Society of Agricultural Engineers*, 31(1), 226-233. <https://doi.org/10.13031/2013.30693>
- Mrema, G. C., Gumbe, L. O., Chepete, H. J., & Agullo, J. O. (2012). *Rural structures in the tropics: Design and development*: Food and Agriculture Organization of the United Nations. <https://cgspace.cgiar.org/handle/10568/81085>
- Mujumdar, A. S. (2007). Book review: Handbook of industrial drying: A review of publisher: Chemical rubber company press. Boca raton, fl, 2007: Taylor & Francis. <https://doi.org/10.1080/07373930701399224>
- Mujumdar, A. S. (2014). *Principles, classification and selection of dryers*. In *handbook of industrial drying* (4 Ed.). Boca Raton, FL.: Chemical Rubber Company Press.

- Mujumdar, A. S., & Menon, A. S. (1995). Drying of solids: Principles, classification, and selection of dryers. *Handbook of Industrial Drying, 1*, 1-39.
- Mujumdar, A. S., & Menon, A. S. (2020). Drying of solids: Principles, classification, and selection of dryers *Handbook of industrial drying* (pp. 1-39): Chemical Rubber Company Press.
- Murthy, M. R. (2009). A review of new technologies, models and experimental investigations of solar driers. *Renewable and Sustainable Energy Reviews, 13*(4), 835-844. <https://doi.org/10.1016/j.rser.2008.02.010>
- Myers, M., & Sellers, M. (1978). Rate of discharge from wedge-shaped hoppers. *Project Report, Department of Chemical Engineering, University of Cambridge*.
- Myers, R. (1971). Response surface methodology, boston: Allyn and baron reprint 1976. *Ann Arbor, MI, Edwards Bros*.
- Naderinezhad, S., Etesami, N., Poormalek Najafabady, A., & Ghasemi Falavarjani, M. (2016). Mathematical modeling of drying of potato slices in a forced convective dryer based on important parameters. *Food Science and Nutrition, 4*(1), 110-118. <https://doi.org/10.1002/fsn3.258>
- Nalbant, M., Gökkaya, H., & Sur, G. (2007). Application of Taguchi method in the optimization of cutting parameters for surface roughness in turning. *Materials and Design, 28*(4), 1379-1385. <https://doi.org/10.1016/j.matdes.2006.01.008>
- Nedderman, R., & Tüzün, U. (1979). A kinematic model for the flow of granular materials. *Powder Technology, 22*(2), 243-253. [https://doi.org/10.1016/0032-5910\(79\)80030-3](https://doi.org/10.1016/0032-5910(79)80030-3)
- Nedderman, R., Tüzün, U., Savage, S., & Houlsby, G. (1982). Flow of granular materials-I. Discharge rates from hoppers. *Chemical Engineering Science, 37*(11). <https://www.osti.gov/etdeweb/biblio/6415193>
- Nelson, S. O. (1980). Moisture-dependent kernel-and bulk-density relationships for wheat and corn. *Transactions of the American Society of Agricultural Engineers, 23*(1), 139-0143. <https://doi.org/10.13031/2013.34540>
- Neter, J., Wasserman, W., & Kutner, M. H. (1990). Applied linear statistical models. In: Regression analysis of variance and experimental designs. *Richard D. Irwin Incorporated, USA*.

- Newton, R., Dunham, G., & Simpson, T. (1945). The tcc catalytic cracking process for motor gasoline production. *Transactions of the American Institute of Chemical Engineers*, 41(2), 215-232.
- Ng, K. C., & Li, Y. (1994). *Design of sophisticated fuzzy logic controllers using genetic algorithms*. Paper presented at the Proceedings of 1994 IEEE 3rd International Fuzzy Systems Conference. <https://ieeexplore.ieee.org/abstract/document/343598>
- Nian, C., Yang, W., & Tarng, Y. (1999). Optimization of turning operations with multiple performance characteristics. *Journal of Materials Processing Technology*, 95(1-3), 90-96. [https://doi.org/10.1016/S0924-0136\(99\)00271-X](https://doi.org/10.1016/S0924-0136(99)00271-X)
- Odal, I. (2005). *Method of determining rate of discharge from silo*. Paper presented at the TC15-Youth Imeko Symposium, Castrocaro Terme.
- Olwande, J., Ngigi, M., & Nguyo, W. (2009). Supply responsiveness of maize farmers in kenya: A farm-level analysis. <https://doi.org/10.22004/ag.econ.50786>
- Onyango, K., & Kirimi, L. (2017). Postharvest losses: A key contributor to food insecurity in kenya [Press release]
- Ostadi, M. (2019). *Mechanics of dry granular flow through an opening*. University of Alberta. <https://doi.org/10.7939/r3-yk7n-dm66>
- Otto, M. (1999). *Chemometrics: Statistics and computer application in analytical chemistry* wiley-vch. Chichester, UK.
- Overhults, D. G., White, G., Hamilton, H., & Ross, I. (1973). Drying soybeans with heated air. *Transactions of the American Society of Agricultural Engineers*, 16(1), 112.
- Özdemir, M., & Devres, Y. O. (1999). The thin layer drying characteristics of hazelnuts during roasting. *Journal of Food Engineering*, 42(4), 225-233. [https://doi.org/10.1016/S0260-8774\(99\)00126-0](https://doi.org/10.1016/S0260-8774(99)00126-0)
- Özilgen, M., & Özdemir, M. (2001). A review on grain and nut deterioration and design of the dryers for safe storage with special reference to turkish hazelnuts. *Critical Reviews in Food Science and Nutrition Journal*, 41(2), 95-132. <https://doi.org/10.1080/20014091091779>
- Pabis, S., Jayas, D. S., & Cenkowski, S. (1998). *Grain drying: Theory and practice*: John Wiley & Sons.

- Page, G. E. (1949). *Factors influencing the maximum rates of air drying shelled corn in thin layers*: Purdue University.
- Panchariya, P., Popovic, D., & Sharma, A. (2002). Thin-layer modelling of black tea drying process. *Journal of Food Engineering*, 52(4), 349-357. [https://doi.org/10.1016/S0260-8774\(01\)00126-1](https://doi.org/10.1016/S0260-8774(01)00126-1)
- Pandey, H., Sharma, H. K., Chauhan, R. C., Sarkar, B. C., & Bera, M. B. (2010). *Experiments in food process engineering*. . New Delhi: CBS Publisher and Distributors PVT.
- Pardeshi, I., Arora, S., & Borker, P. (2009). Thin-layer drying of green peas and selection of a suitable thin-layer drying model. *Drying Technology*, 27(2), 288-295. <https://doi.org/10.1080/07373930802606451>
- Parry, J. (1985). Mathematical modelling and computer simulation of heat and mass transfer in agricultural grain drying: A review. *Journal of Agricultural Engineering Research*, 32(1), 1-29. [https://doi.org/10.1016/0021-8634\(85\)90116-7](https://doi.org/10.1016/0021-8634(85)90116-7)
- Parti, M. (1993). Selection of mathematical models for drying grain in thin-layers. *Journal of Agricultural Engineering Research*, 54(4), 339-352. <https://doi.org/10.1006/jaer.1993.1026>
- Paulsen, M., & Thompson, T. (1973). Drying analysis of grain sorghum. *Transactions of the American Society of Agricultural Engineers*, 16(3), 537-0540. <https://doi.org/10.13031/2013.37563>
- Pelegrina, A., Elustondo, M., & Urbicain, M. (1999). Rotary semi-continuous drier for vegetables: Effect of air recycling. *Journal of Food Engineering*, 41(3-4), 215-219. [https://doi.org/10.1016/S0260-8774\(99\)00093-X](https://doi.org/10.1016/S0260-8774(99)00093-X)
- Pelegrina, A. H., & Crapiste, G. H. (2000). Modelling pneumatic drying of food. *Journal of Food Engineering*, 48(2001), 301-310.
- Pelegrina, A. H., & Crapiste, G. H. (2001). Modelling the pneumatic drying of food particles. *Journal of Food Engineering*, 48(4), 301-310. [https://doi.org/10.1016/S0260-8774\(00\)00170-9](https://doi.org/10.1016/S0260-8774(00)00170-9)
- Perez, N. E., & Schmalko, M. E. (2009). Convective drying of pumpkin: Influence of pretreatment and drying temperature. *Journal of Food Process Engineering*, 32(1), 88-103. <https://doi.org/10.1111/j.1745-4530.2007.00200.x>

- Precoppe, M., Chapuis, A., Müller, J., & Abass, A. (2015). Tunnel dryer and pneumatic dryer performance evaluation to improve small-scale cassava processing in tanzania. *Journal of Food Process Engineering*, 40(1), e12274. <https://doi.org/10.1111/jfpe.12274>
- Prvulovic, S., Tolmac, D., & Lambic, M. (2007). Convection drying in the food industry. *Agricultural Engineering International: the CIGR Ejournal*, 9, 1-12.
- Rafiee, S., Keyhani, A., & Jafari, A. (2008). Modeling effective moisture diffusivity of wheat (tajan) during air drying. *International Journal of Food Properties*, 11(1), 223-232. <https://doi.org/10.1080/10942910701291858>
- Rahmatinejad, B., Hosseinzadeh, H., Sharifi, O., & Rezazadeh, A. (2016). The effect of temperature and speed of wind on drying time of basil leaves in the solar-photovoltaic dryer. *International Journal of Biotechnology and Research*, 7(4), 432-437.
- Rajan, K. (2012). Simulation of pneumatic drying: Influence of particle diameter and solid loading ratio. *Simulation*, 4(4), 1633-1641.
- Randela, R. (2003). The incidence of post-harvest problems among small farmers surveyed in three regions of the limpopo province. *Agrekon*, 42(2), 163-180. <https://journals.co.za/doi/abs/10.10520/EJC18243>
- Rehman, Z. U. (2006). Storage effects on nutritional quality of commonly consumed cereals. *Food Chemistry*, 95(1), 53-57.
- Rembold, F., Hodges, R., Bernard, M., Knipschild, H., & Léo, O. (2011). The african postharvest losses information system (aphlis). Luxembourg: European Union.
- Resende, O., Arcanjo, R. V., Siqueira, V. C., & Rodrigues, S. (2009). Mathematical modeling for drying coffee (*coffea canephora pierre*) berry clones in concrete yard. *Acta Scientiarum. Agronomy*, 31, 189-196. <https://doi.org/10.1590/S1807-86212009000200001>
- Reyes, A., Alvarez, P., & Marquardt, F. (2002). Drying of carrots in a fluidized bed. I. Effects of drying conditions and modelling. *Drying Technology*, 20(7), 1463-1483. <https://doi.org/10.1081/DRT-120005862>
- Ribaut, J.-M., & Ragot, M. (2006). Marker-assisted selection to improve drought adaptation in maize: The backcross approach, perspectives, limitations, and alternatives. *Journal of Experimental Botany*, 58(2), 351-360. <https://doi.org/10.1093/jxb/erl214>
- Roberts, J. S., Kidd, D. R., & Padilla-Zakour, O. (2008). Drying kinetics of grape seeds. *Journal of Food Engineering*, 89(4), 460-465.

- Rose, H., & Tanaka, T. (1959). Rate of discharge of granular materials from bins and hoppers. *The Engineer*, 208, 465-469. <https://doi.org/10.1016/j.jfoodeng.2008.05.030>
- Ross, P. J. (1996). *Taguchi techniques for quality engineering: Loss function, orthogonal experiments, parameter and tolerance design*. <https://trid.trb.org/view/1182944>
- Sacilik. (2007). Effect of drying methods on thin-layer drying characteristics of hull-less seed pumpkin (*cucurbita pepo* L.). *Journal of Food Engineering*, 79(1), 23-30. <https://doi.org/10.1016/j.jfoodeng.2006.01.023>
- Sacilik, K., & Elicin, A. K. (2006). The thin layer drying characteristics of organic apple slices. *Journal of Food Engineering*, 73, 281–289. <https://doi.org/10.1016/j.jfoodeng.2005.03.024>
- Sacilik, K., Keskin, R., & Elicin, A. K. (2006). Mathematical modelling of solar tunnel drying of thin layer organic tomato. *Journal of Food Engineering*, 73(3), 231-238. <https://doi.org/10.1016/j.jfoodeng.2005.01.025>
- Sacilik, K., & Unal, G. (2005). Dehydration characteristics of kastamonu garlic slices. *Biosystems Engineering*, 92(2), 207-215. <https://doi.org/10.1016/j.biosystemseng.2005.06.006>
- Sangamithra, A., Gabriela, J. S., Prema, R. S., Nandini, K., Kannan, K., Sasikala, S., & Suganya, P. (2016). Moisture dependent physical properties of maize kernels. *International Food Research Journal*, 23(1), 109.
- Sarker, A., Islam, M., & Shaheb, M. (2012). A study on the drying behaviour of a local variety (lalpakri) of potato (*solanum tuberosum* L.). *Bangladesh Journal of Agricultural Research*, 37(3), 505-514.
- Sarsavadia, P. N., Sawhney, R. L., Pangavhane, D. R., & Singh, S. P. (1999). Drying behaviour of brined onion slices. *Journal of Food Engineering*, 40, 219–226. [https://doi.org/10.1016/S0260-8774\(99\)00058-8](https://doi.org/10.1016/S0260-8774(99)00058-8)
- Sawhney, R., Sarsavadia, P., Pangavhane, D., & Singh, S. (1999). Determination of drying constants and their dependence on drying air parameters for thin layer onion drying. *Drying Technology*, 17(1-2), 299-315. <https://doi.org/10.1080/07373939908917531>
- Seng, T. L., Khalid, M. B., & Yusof, R. (1999). Tuning of a neuro-fuzzy controller by genetic algorithm. *IEEE Transactions on Systems, Man, and Cybernetics, Part B (Cybernetics)*, 29(2), 226-236. <https://doi.org/10.1109/3477.752795>



- Sharaf-Eldeen, Y. I., Blaisdell, J. L., & Hamdy, M. Y. (1980). A model for ear corn drying. *Transaction of the American Society of Agricultural Engineers*, 23, 1261–1271.
- Sharma, P., & Fang, T. (2015). Spray and atomization of a common rail fuel injector with non-circular orifices. *Fuel*, 153, 416-430. <https://doi.org/10.1016/j.fuel.2015.02.119>
- Shi, J., Pan, Z., McHugh, T. H., Wood, D., Hirschberg, E., & Olson, D. (2008). Drying and quality characteristics of fresh and sugar-infused blueberries dried with infrared radiation heating. *LWT-Food Science and Technology*, 41(10), 1962-1972. <https://doi.org/10.1016/j.lwt.2008.01.003>
- Shittu, T., & Raji, A. (2011). Thin layer drying of african breadfruit (*treculia africana*) seeds: Modeling and rehydration capacity. *Food and Bioprocess Technology*, 4(2), 224-231. <https://doi.org/10.1007/s11947-008-0161-z>
- Singh, A., Datta, S., & Mahapatra, S. S. (2013). Application of a fuzzy inference system for the optimization of material removal rate and multiple surface roughness characteristics in the machining of gfrp polyester composites. *Decision Making in Manufacturing and Services*, 7. <https://doi.org/10.7494/dmms.2013.7.1.19>
- Sivanandam, S., Deepa, S., Sivanandam, S., & Deepa, S. (2008). Genetic algorithm optimization problems. *Introduction to Genetic Algorithms*, 165-209. [https://doi.org/10.1007/978-3-540-73190-0\\_2](https://doi.org/10.1007/978-3-540-73190-0_2)
- Slama, R. B., & Combarous, M. (2011). Study of orange peels dryings kinetics and development of a solar dryer by forced convection. *Solar Energy*, 85(3), 570-578. <https://doi.org/10.1016/j.solener.2011.01.001>
- Smale, M., Byerlee, D. & Jayne, T. (2011). *Maize revolutions in sub-saharan africa*: The World Bank. [https://doi.org/10.1007/978-94-007-5760-8\\_8](https://doi.org/10.1007/978-94-007-5760-8_8)
- Sobukola, O. P., Dairo, O. U., & Odunewu, A. V. (2008). Convective hot air drying of blanched yam slices. *International Journal of Food Science and Technology*, 43(7), 1233-1238. <https://doi.org/10.1111/j.1365-2621.2007.01597.x>
- Soponronnarit, S., & Prachayawarakorn, S. (1994). Optimum strategy for fluidized bed paddy drying. *Drying Technology*, 12(7), 1667-1686. <https://doi.org/10.1080/07373939408962192>
- Strumiłło, C., Jones, P. L., & Żyła, R. (2014). Energy aspects in drying *Handbook of industrial drying, fourth edition* (pp. 1077-1100): Chemical Rubber Company Press.

- Strumillo, C., & Kudra, T. (1986a). *Drying principles, applications and design*, Gordon and Breach Science Publishers, New York.
- Strumillo, C., & Kudra, T. (1986b). Heat and mass transfer in drying processes. *Drying: Principles, Applications and Design*.
- Sturm, B., Hofacker, W. C., & Hensel, O. (2012). Optimizing the drying parameters for hot-air-dried apples. *Drying Technology*, 30(14), 1570-1582. <https://doi.org/10.1080/07373937.2012.698439>
- Suarez, D., Pegram, B. L., & Frohlich, E. (1980). Systemic and regional haemodynamics in anterior hypothalamic hypertension in spontaneously hypertensive and wistar-kyoto rats. *Clinical Science (London, England: 1979)*, 59, 251s-253s. <https://doi.org/10.1042/cs059251s>
- Suleiman, R. A., & Kurt, R. A. (2015). *Current maize production, postharvest losses and the risk of mycotoxins contamination in Tanzania*. Paper presented at the 2015 American Society Agricultural Biological Engineers Annual International Meeting. <https://doi.org/10.13031/aim.20152189434>
- Suleiman, R. A., Rosentrater, K. A., & Bern, C. J. (2013, July 21-July 24). *Effects of deterioration parameters on storage of maize*, Kansas City, Missouri. <https://doi.org/10.13031/aim.20131593351>
- Taguchi, G. (1990). Introduction to quality engineering, tokyo. *Asian Productivity Organization*, 4(2), 10-15.
- Tanaka, F., Maeda, Y., Uchino, T., Hamanaka, D., & Atungulu, G. G. (2008). Monte carlo simulation of the collective behavior of food particles in pneumatic drying operation. *Food Science and Technology*, 41, 1567-1574. <https://doi.org/10.1016/j.lwt.2007.10.020>
- Tapani, J. (2016). *Energy efficiency in grain preservation*. [Doctoral thesis in agrotechnology, University of Helsinki, Helsinki, Finland]. <http://hdl.handle.net/10138/166973>
- Tefera, T., Mugo, S., & Likhayo, P. (2011). Effects of insect population density and storage time on grain damage and weight loss in maize due to the maize weevil *sitophilus zeamais* and the larger grain borer *prosthephanus truncatus*. *African Journal of Agricultural Research*, 6, 2249-2254. <https://doi.org/10.5897/AJAR11.179>

- Thakur, A. K., & Gupta, A. (2006). Two stage drying of high moisture paddy with intervening rest period. *Energy Conversion and Management Journal*, 47(18-19), 3069-3083. <https://doi.org/10.1016/j.enconman.2006.03.008>
- Thompson, T., Peart, R., & Foster, G. (1968). Mathematical simulation of corn drying a new model. *Transaction of the American Society of Agricultural Engineers*, 11(4), 582-586. <https://www.ars.usda.gov/ARSUserFiles/30200525/34MathematicalSimulationofCornDrying.pdf>
- Tiwari, G. N. (2002). *Solar energy: Fundamentals, design, modelling and applications*: Alpha Science International Limited.
- Toğrul, İ. T., & Pehlivan, D. (2003). Modelling of drying kinetics of single apricot. *Journal of Food Engineering*, 58(1), 23-32. [https://doi.org/10.1016/S0260-8774\(02\)00329-1](https://doi.org/10.1016/S0260-8774(02)00329-1)
- Tolmac, D. (1997). Contribution theory and drying practice: University in Novi Sad, Technical Faculty Mihajlo Pupin, Zrenjanin.
- Tolmac, D., & Lambic, M. (1997). Heat transfer through rotating roll of contact dryer. *International Communications in Heat and Mass Transfer Journal*, 24(4), 569-573. [https://doi.org/10.1016/S0735-1933\(97\)00042-0](https://doi.org/10.1016/S0735-1933(97)00042-0)
- Tolmač, D., Prvulović, S., & Radovanović, L. (2008). Effects of heat transfer on convection dryer with pneumatic transport of material. *Faculty of Mechanical Engineering Transactions*, 36(1), 45-49.
- Treybal, R. E. (1980). Mass transfer operations. *New York*, 466.
- Tscheuschner, H. D. (1987). Physical properties of plant and animal materials *Structure, physical characteristics and mechanical properties*. New York: Wiley Online Library. <https://doi.org/10.1002/food.19870310724>
- Tsotsas, E., & Mujumdar, A. S. (2008). Modern drying technology vol. 1 computational tools at different scales. <https://doi.org/10.1080/07373930802046559>
- Tudor, C., & Mieila, C. (2010). Theoretical development of a mathematical model to evaluate gravimetric flow rate of seeds through orifices. *UPB Scientific Bulletin, Serials D*, 72(4), 269-280. [https://www.scientificbulletin.upb.ro/rev\\_docs\\_arhiva/rez317.pdf](https://www.scientificbulletin.upb.ro/rev_docs_arhiva/rez317.pdf)
- Tupkari, H. M., & Vanalkar, A. (2015). Design and development of non-continuous type pneumatic conveying systems for ginning industries. *International Journal*, 2, 157-163.
- Twidell, J., & Weir, T. (2015). *Renewable energy resources*: Routledge.

- Tzempelikos, D. A., Vouros, A. P., Bardakas, A. V., Filios, A. E., & Margaritis, D. P. (2014). Case studies on the effect of the air drying conditions on the convective drying of quinces. *Case Studies in Thermal Engineering*, 3, 79-85. <https://doi.org/10.1016/j.csite.2014.05.001>
- Uluko, H., Kanali, C. L., Mailutha, J. T., & Shitanda, D. (2006). A finite element model for the analysis of temperature and moisture distribution in a solar grain dryer. *The Kenya Journal of Mechanical Engineering*, 2(1), 47–56.
- Vagenas, G., & Marinou-Kouris, D. (1991). The design and optimization of an industrial dryer for sultana raisins. *Drying Technology*, 9(2), 439-461. <https://doi.org/10.1080/07373939108916675>
- Valentin, F. H. (1985). *Draft code of practice for the design of silos, bins, bunkers and hoppers* (2nd ed.). United Kingdom. <https://www.osti.gov/etdeweb/biblio/6256343>
- Van't Land, C. (2011). *Drying in the process industry*: John Wiley & Sons.
- Vankanti, V. K., & Ganta, V. (2014). Optimization of process parameters in drilling of gfrp composite using Taguchi method. *Journal of Materials Research and Technology*, 3(1), 35-41. <https://doi.org/10.1016/j.jmrt.2013.10.007>
- Vega-Gálvez, A., Dagnino-Subiabre, A., Terreros, G., López, J., Miranda, M., & Di Scala, K. (2011). Mathematical modeling of convective air drying of quinoa-supplemented feed for laboratory rats. *Brazilian Archives of Biology and Technology*, 54(1), 161-171. <https://doi.org/10.1590/S1516-89132011000100021>
- Vega, A., Uribe, E., Lemus, R., & Miranda, M. (2007). Hot-air drying characteristics of aloe vera (*aloe barbadensis miller*) and influence of temperature on kinetic parameters. *LWT-Food Science and Technology*, 40(10), 1698-1707. <https://doi.org/10.1016/j.lwt.2007.01.001>
- Verghese, T., & Nedderman, R. (1995). The discharge of fine sands from conical hoppers. *Chemical Engineering Science*, 50(19), 3143-3153. [https://doi.org/10.1016/0009-2509\(95\)00165-2](https://doi.org/10.1016/0009-2509(95)00165-2)
- Verheye, W. (2010). Growth and production of maize: Traditional low-input cultivation *Land use, land cover and soil sciences*: United Nations Educational, Scientific and Cultural Organization-Encyclopedia of Life Support Systems Publishers.

- Verma, L. R. (1993). New methods for on-the-farm rice drying: Solar and biomass. *Food Science and Technology*, 275-275.
- Verma, L. R., Bucklin, R., Endan, J., & Wratten, F. (1985). Effects of drying air parameters on rice drying models. *Transactions of the American Society of Agricultural Engineers*, 28(1), 296-301. <https://doi.org/10.13031/2013.32245>
- Vijayaraj, B., Saravanan, R., & Renganarayanan, S. (2007). Studies on thin layer drying of bagasse. *International Journal of Energy Research*, 31(4), 422-437. <https://doi.org/10.1002/er.1237>
- Walker, T. H. (1992). *Drying cut fruits with recirculated air for energy savings*. [Master's thesis, University of Tennessee, Knoxville, United States of America]. [https://trace.tennessee.edu/utk\\_gradthes/7013/](https://trace.tennessee.edu/utk_gradthes/7013/)
- Wang, C., & Singh, R. (1978). A single layer drying equation for rough rice (pp. 33): American Society of Agricultural Engineers paper No. 78-3001.
- Whitaker, T., Barre, H., & Hamdy, M. (1969). Theoretical and experimental studies of diffusion in spherical bodies with a variable diffusion coefficient. *Transactions of the American Society of Agricultural Engineers*, 12(5), 668-672. <https://doi.org/10.13031/2013.38924>
- White, G., Bridges, T., Loewer, O., & Ross, I. (1980). Seed coat damage in thin-layer drying of soybeans. *Transactions of the American Society of Agricultural Engineers*, 23(1), 224-227. <https://doi.org/10.13031/2013.34559>
- White, K. P., & Ingalls, R. G. (2018). *The basics of simulation*. Paper presented at the 2018 Winter Simulation Conference. <https://doi.org/10.1109/WSC.2018.8632271>
- Wieghardt, K. (1952). Über einige versuche an strömungen in sand. *Ingenieur-Archiv*, 20(2), 109-115.
- Wongwises, S., & Thongprasert, M. (2000). Thin layer and deep bed drying of long grain rough rice. *Drying Technology*, 18(7), 1583-1599. <https://doi.org/10.1080/07373930008917794>
- Wu, C.-Y., Dihoru, L., & Cocks, A. C. (2003). The flow of powder into simple and stepped dies. *Powder Technology*, 134(1-2), 24-39. [https://doi.org/10.1016/S0032-5910\(03\)00130-X](https://doi.org/10.1016/S0032-5910(03)00130-X)
- Xie, X., & Puri, V. (2006). Uniformity of powder die filling using a feed shoe: A review. *Particulate Science and Technology*, 24(4), 411-426. <https://doi.org/10.1080/02726350600934663>

- Yagcioglu, A. (1999). *Drying characteristic of laurel leaves under different conditions*. Paper presented at the Proceedings of the 7th International Congress on Agricultural Mechanization and Energy, Faculty of Agriculture, Cukurova University. <https://cir.nii.ac.jp/crid/1571135649978749440>
- Yaldiz, Ertekin, C., & Uzun, H. I. (2001). Mathematical modeling of thin layer solar drying of sultana grapes. *Energy*, 26(5), 457-465. [https://doi.org/10.1016/S0360-5442\(01\)00018-4](https://doi.org/10.1016/S0360-5442(01)00018-4)
- Yaldiz, O., & Ertekin, C., (2001). Thin layer solar drying of some vegetables. *Drying Technology*, 19, 583–596. <https://doi.org/10.1081/DRT-100103936>
- Yang, W., & Tarnq, Y. (1998). Design optimization of cutting parameters for turning operations based on the Taguchi method. *Journal of Materials Processing Technology*, 84(1-3), 122-129. [https://doi.org/10.1016/S0924-0136\(98\)00079-X](https://doi.org/10.1016/S0924-0136(98)00079-X)
- Young, J., Tutor, J., & Cain Jr, G. (1990). Recirculation and solar energy collection to assist peanut drying. *Applied Engineering in Agriculture*, 6(3), 329-332.
- Young, J. H. (1969). Simultaneous heat and mass transfer in a porous, hygroscopic solid. *Transactions of the American Society of Agricultural Engineers*, 12(5), 720-0725. <https://doi.org/10.13031/2013.38936>
- Zenoozian, M. S., Feng, H., Razavi, S., Shahidi, F., & Pourreza, H. (2008). Image analysis and dynamic modeling of thin-layer drying of osmotically dehydrated pumpkin. *Food Processing and Preservation*, 32(1), 88-102. <https://doi.org/10.1111/j.1745-4549.2007.00167.x>
- Zhang, J., & Rudolph, V. (1991). Effect of shear friction on solid flow through an orifice. *Industrial and Engineering Chemistry Research*, 30(8), 1977-1981. <https://doi.org/10.1021/ie00056a047>
- Zuriguel, I., Pugnaroni, L. A., Garcimartin, A., & Maza, D. (2003). Jamming during the discharge of grains from a silo described as a percolating transition. *Physical Review E*, 68(3), 030301. <https://doi.org/10.1103/PhysRevE.68.030301>

## APPENDICES

### Appendix A: Detail Drawing of Experimental Vertical Pneumatic Maize Grain Dryer

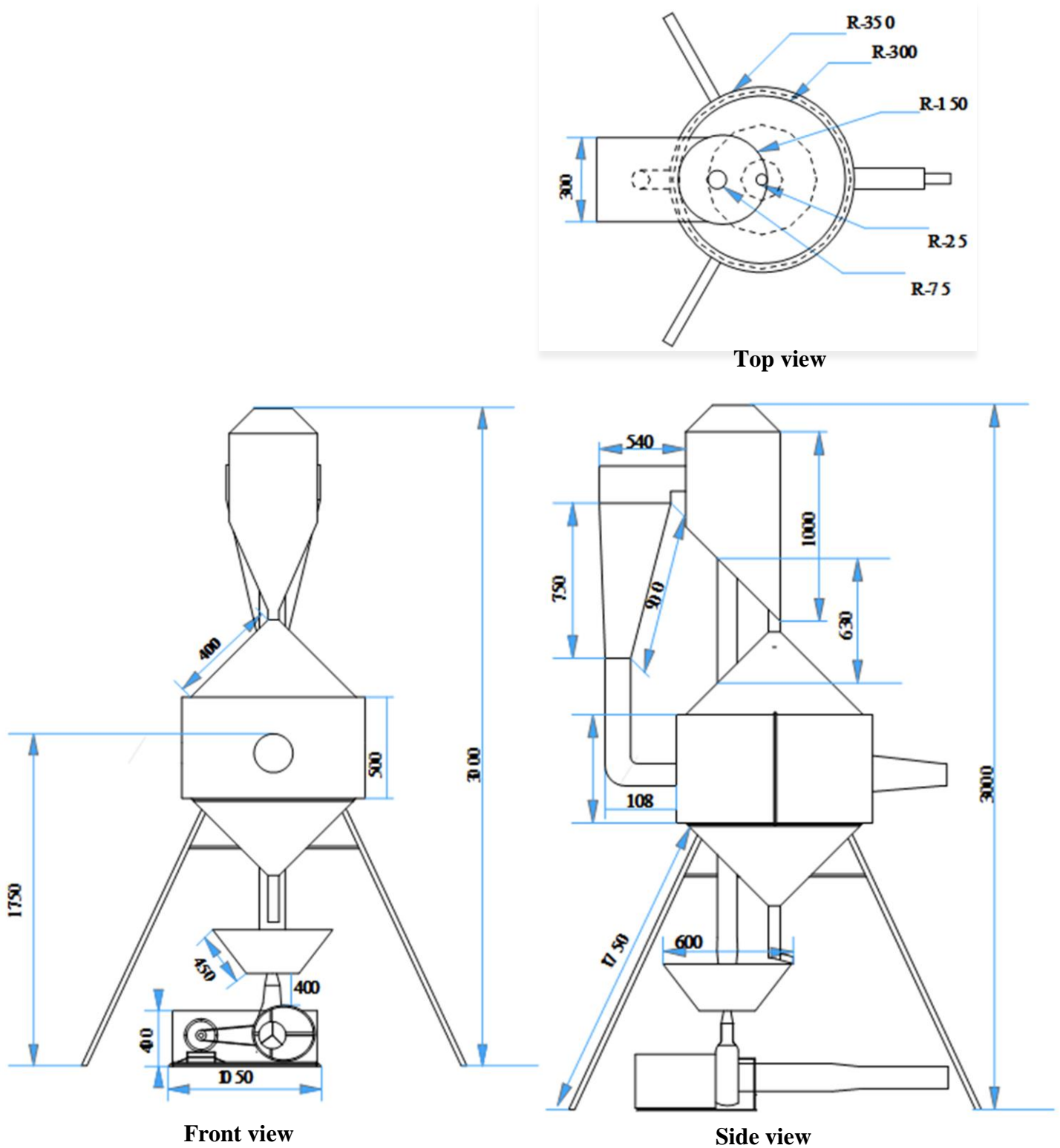


Figure A1 Detail drawing of experimental vertical pneumatic maize grain dryer

## Appendix B: Code and Graphic User Interface for Simulation Models

### Code for Simulation Models

'''

```
=====
PYTHON 3.8 MASS FLOW RATE SIMULATION MODELS FOR MAIZE GRAIN
-----
```

Model algorithms used [3]

- 1.Beverloo
- 2.BCP
- 3.Tudor

-----

The program also logs the O/P into a CSV and plots some plots for Visualisations

```
=====
```

'''

# Libraries and modules

```
import xlwt
```

```
from xlwt import Workbook
```

```
import openpyxl
```

```
from openpyxl.worksheet.table import Table, TableStyleInfo
```

```
from datetime import datetime
```

```
import math
```

```
from os import system
```

```
import os.path
```

```
import sympy
```

```
#=====
```

#Global variables and constants

```
g = 9.81 #g(m/s)
```

```
pi = round((22/7),4)
```

```
cd = 0.75 #Friction/discharge coefficient
```

```
models=['Beverloo','BCP','Tudor','Clear','Exit']
```

```
#MAIN FUNCTION
```





```

system('color 0D')
modes = ['1.Manual','2Automatic']
print('\n\n\t\t\tChoose a run Mode')
for model1_mode in modes:
    print(model1_mode)
u_input_2 = int(input())
if u_input_2 == 1:
    print('Manual Mode\n\n Enter the diameter of the orifice (m)')
    orifice_diameter = float(input())
    kp = 1.4
    rho = 760 #bulk density (kg/m`3)
    dg = 0.008512 #geometric mean diameter of grain (m)
    dh = orifice_diameter #hydraulic radius (m)
    #dh === orifice diameter
    de = dh - kp*dg
    ae = pi*pow(de,2)/4 #effective area of orifice (m`2)
    Q = cd*ae*(math.sqrt((g*de)))*3600*rho #Q is the mass flow rate (kg/kg.h)
        print(f'\n\n-----Grain mass flow rate for {orifice_diameter} m == {round(Q,0)}
        Kg/kg.h ')
    main()
elif u_input_2 == 2:
    start = float(input('\n\nEnter the lower limit (m): '))
    stop = float(input('Enter the upper limit (m): '))
    step = float(input('Enter the steps: '))
    result = []
    stop+=step
    def frange(start,stop,step):
        while start < stop:
            yield start
            start+=step
    for r in frange(start,stop,step):

```

```

kp = 1.4
rho = 760 #bulk density (kg/m`3)
dg = 0.008512 #geometric mean diameter of grain (m)
de = r - kp*dg
ae = pi*pow(de,2)/4 #effective area of orifice (m`2)
Q = cd*ae*(math.sqrt((g*de)))*3600*rho #Q is the mass flow rate (kg/kg.h)
print(f'\t-----Grain mass flow rate for {round(r,3)} m == {round(Q,0)} Kg/kg.h ')
Q1 = round(Q,0)
R = round(r,3)
entry = [R, Q1]
str(entry).replace(", ", "").replace(" ", "")
result.append(entry)
# print(result)
# add column headings. NB. these must be strings
ws.append(
    ['Diameter(m)', 'Mass flow rate (kg/kg.h)'])
for row in result:
    ws.append(row)
tab = Table(displayName="Table" +
    str({date_object.microsecond}), ref="A1:E5")
# Add a default style with striped rows and banded columns
    style = TableStyleInfo(name="TableStyleMedium9", showFirstColumn=False,
    showLastColumn=False, showRowStripes=True, showColumnStripes=True)
tab.tableStyleInfo = style
'''
Table must be added using ws.add_table() method to avoid duplicate names.
    Using this method ensures table name is unique through out defined names and all other
    table name.
'''
ws.add_table(tab)
wb.save("Model_reports.xlsx")

```

```

frange(start,stop,step)
print("\n\n\t\tA copy of the results has been saved!")
beverloo_model()
main()
# BCP model
elif u_input_1 == 2:
    system('color 0A')
print('\t#####')
#####')
print('\n\n\t\tRunning British Code of Practice model.....')
def bcp_model():
    modes = ['1.Manual','2.Automated']
    print("\n\n\n\t\tChoose a run Mode')
    for model1_mode in modes:
        print(model1_mode)
    u_input_3 = int(input())
    if u_input_3 == 1:
        print('Manual Mode\n\n\t\tEnter the Diameter of the orifice (m):')
        orifice_diameter = float(input())
        cd = 0.58 #friction/discharge coefficient
        rho = 760 #grain density kg/m`3
        kp = 1.0 #shape factor
        dg = 0.008512 #Geometric diameter of the grain
        Q = 3600*cd*rho*pow(g,0.5)*pow((orifice_diameter-(kp*dg)),2.5)
        print(f'Grain mass flow rate for {orifice_diameter} m == {round(Q,1)} Kg/kg.h ')
    main()
else:
    print('AUTOMATED MODE')
    start = float(input('\n\nEnter the lower limit (m): '))
    stop = float(input('Enter the upper limit (m): '))
    step = float(input('Enter the steps: '))

```

```

result = []
stop+=step
def frange(start,stop,step):
    while start < stop:
        yield start
        start+=step
for r in frange(start,stop,step):
    #automated BCP Model
    cd = 0.58 #friction/discharge coefficient
    rho = 760 #grain density kg/m`3
    kp = 1.0 #shape factor
    dg = 0.008512 #Geometric diameter of the grain
    Q = 3600*cd*rho*pow(g,0.5)*pow((r-(kp*dg)),2.5)
    print(f'-----Grain mass flow rate for {round(r,3)} m == {round(Q,0)} Kg/kg.h ')
    Q1 = round(Q,0)
    R = round(r,3)
    entry = [R, Q1]
    str(entry).replace("(", "").replace(")", "")
    result.append(entry)
# print(result)
# add column headings. NB. these must be strings
ws.append(
    ['Diameter(m)', 'Mass flow rate(kg/kg.h)'])
for row in result:
    ws.append(row)
tab = Table(displayName="Table" +
    str({ date_object.microsecond}), ref="A1:E5")
# Add a default style with striped rows and banded columns
style = TableStyleInfo(name="TableStyleMedium9", showFirstColumn=False,
showLastColumn=False, showRowStripes=True, showColumnStripes=True)
tab.tableStyleInfo = style

```

'''

Table must be added using ws.add\_table() method to avoid duplicate names.

Using this method ensures table name is unique through out defined names and all other table name.

'''

```
ws.add_table(tab)
```

```
wb.save("Model_reports.xlsx")
```

```
frange(start,stop,step)
```

```
print("\n\n\tA copy of the results has been saved!")
```

```
bcp_model()
```

```
main()
```

```
# Tudor Model
```

```
elif u_input_1 == 3:
```

```
system('color 0E')
```

```
print("\t#####  
#####')
```

```
print("\t\tRunning Tudor model...')
```

```
def tudor_model():
```

```
    modes = ['1.Manual','2.Automated']
```

```
    print("\n\n\t\tChoose a run Mode')
```

```
    for model1_mode in modes:
```

```
        print(model1_mode)
```

```
    u_input_4 = int(input())
```

```
    if u_input_4 == 1:
```

```
        print('Manual Mode\n\t\tEnter the Diameter of the orifice')
```

```
        orifice_diameter = float(input())
```

```
        cd = pi*math.sqrt(2)/6
```

```
        dg = 760 #grain density
```

```
        a = 0.3 #h/D
```

```
        u = 0.36 #t*g*phi sliding coefficient of friction
```

```
        #h is the height dome of granular material
```

```

#D is the orifice diameter
Q = 3600*cd*math.sqrt((g*a))*dg*pow(orifice_diameter,2.5)*math.sqrt((1-u))
print(f'\n\nGrain mass flow rate for {orifice_diameter} m == {round(Q,0)} Kg/kg.h ')
main()
else:
print('AUTOMATED MODE')
start = float(input('Enter the lower limit (m): '))
stop = float(input('Enter the upper limit (m): '))
step = float(input('Enter the steps: '))
result = []
stop+=step
def frange(start,stop,step):
while start < stop:
yield start
start+=step
for r in frange(start,stop,step):
cd = pi*math.sqrt(2)/6
dg = 760 #grain density
a = 0.3 #h/D
u = 0.36 #t*g*phi sliding coefficient of friction
#h is the height dome of granular materials
#D is the orifice diameter
Q = 3600*cd*math.sqrt((g*a))*dg*pow(r,2.5)*math.sqrt((1-u))
print(f'-----Grain mass flow rate for {round(r,3)} m == {round(Q,0)} Kg/kg.h ')
Q1 = round(Q,0)
R = round(r,3)
entry = [R, Q1]
str(entry).replace(", """).replace(")", "")
result.append(entry)
# print(result)
# add column headings. NB. these must be strings

```

```

ws.append(
    ['Diameter(m)', 'Mass flow rate(kg/kg.h)'])
for row in result:
    ws.append(row)
tab = Table(displayName="Table" +
    str({date_object.microsecond}), ref="A1:E5")
# Add a default style with striped rows and banded columns
style = TableStyleInfo(name="TableStyleMedium9", showFirstColumn=False,
    showLastColumn=False, showRowStripes=True, showColumnStripes=True)
tab.tableStyleInfo = style
'''
Table must be added using ws.add_table() method to avoid duplicate names.
    Using this method ensures table name is unique throughout defined names and all other
    table name.
'''
ws.add_table(tab)
wb.save("Model_reports.xlsx")
frange(start,stop,step)
print("\n\n\tA copy of the results has been saved!")
tudor_model()
main()
elif u_input_1 == 4:
    system('cls')
    main()
elif u_input_1 == 5:
    exit()
else:
    print("\n\n\n-----INVALID CHOICE-----')
    main()
main()

```



## Graphic User Interfaces for Simulation Models

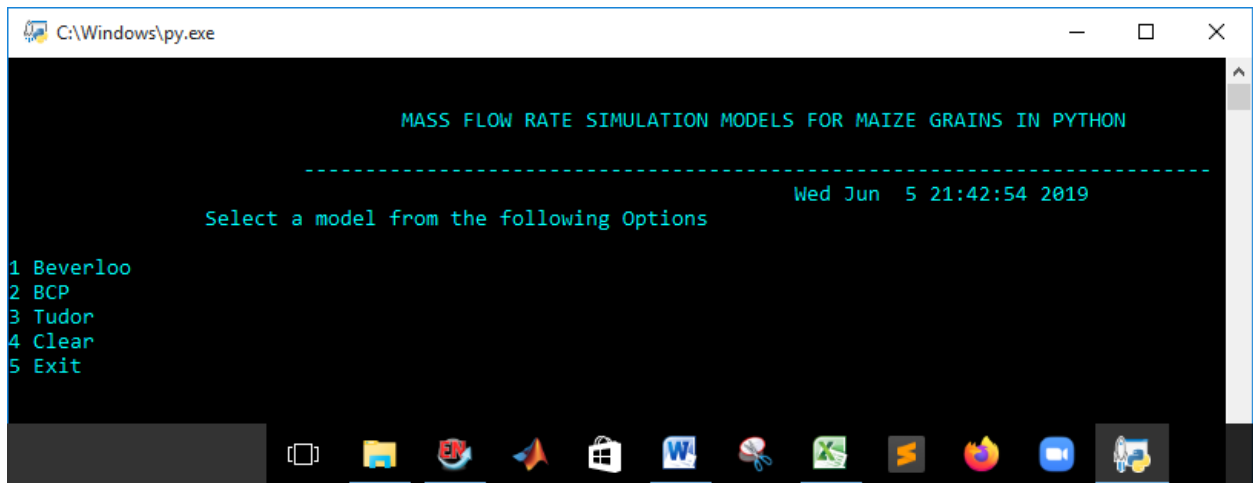


**Figure B1** Graphic user interface for selection of simulation models

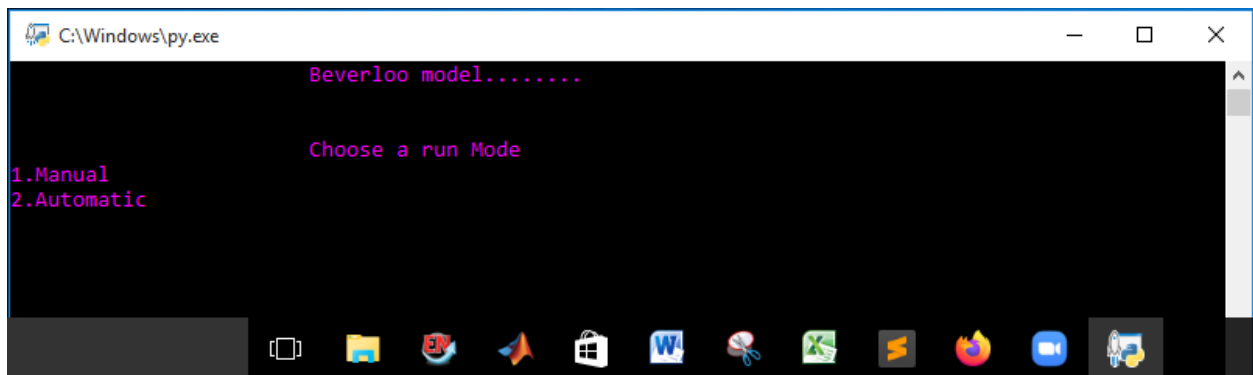


**Figure B2** Graphic user interface for selection of run mode for Beverloo model

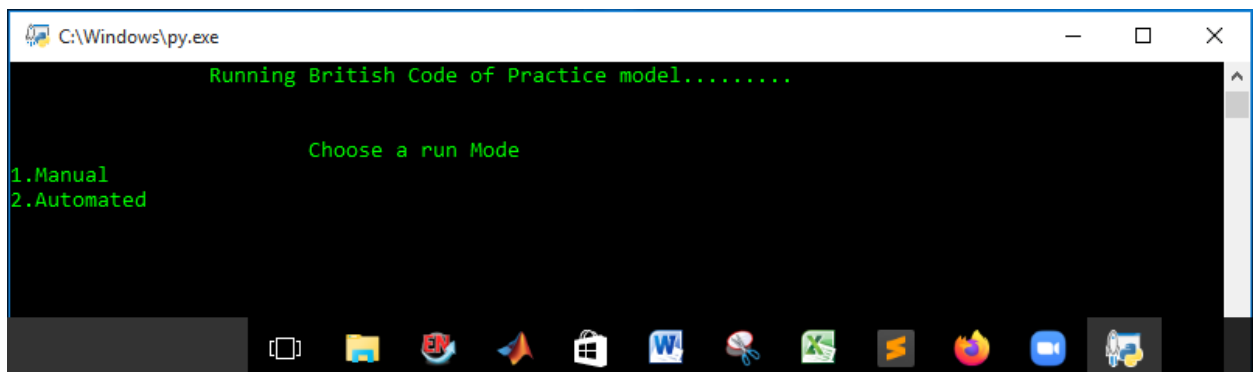


**Figure B3** Graphic user interface for selection of run mode for BCP model

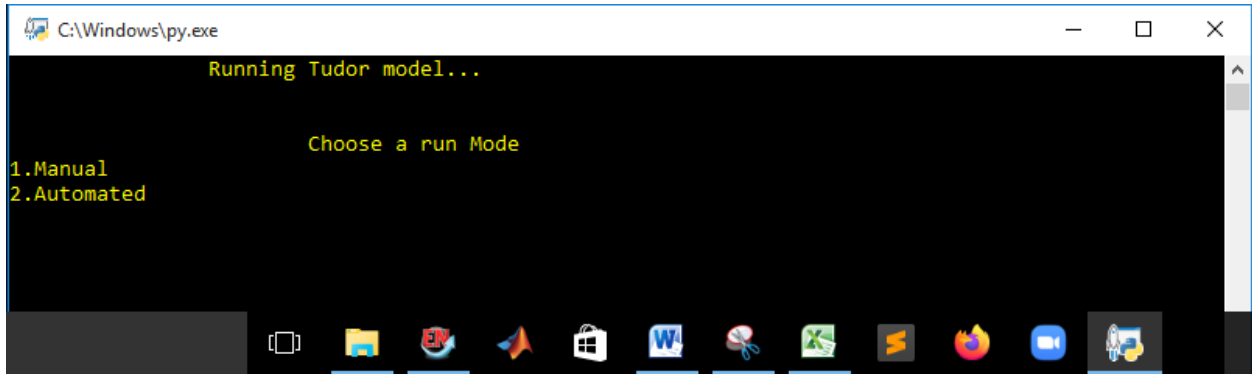


**Figure B4** Graphic user interface for selection of run mode for Tudor model

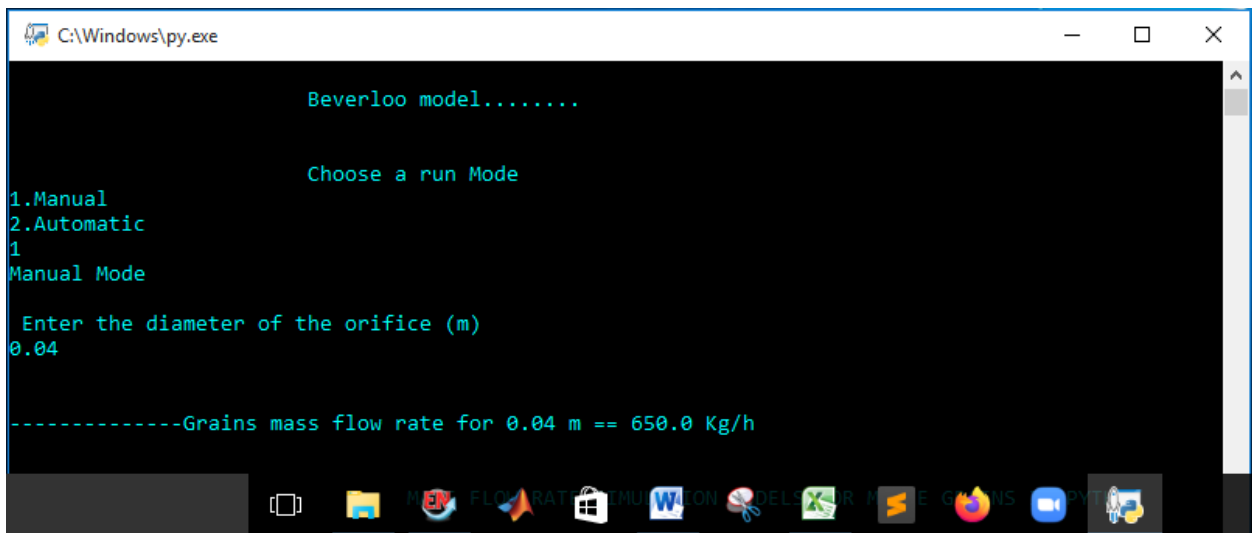


**Figure B5** Sample of Beverloo model output executed using manual mode

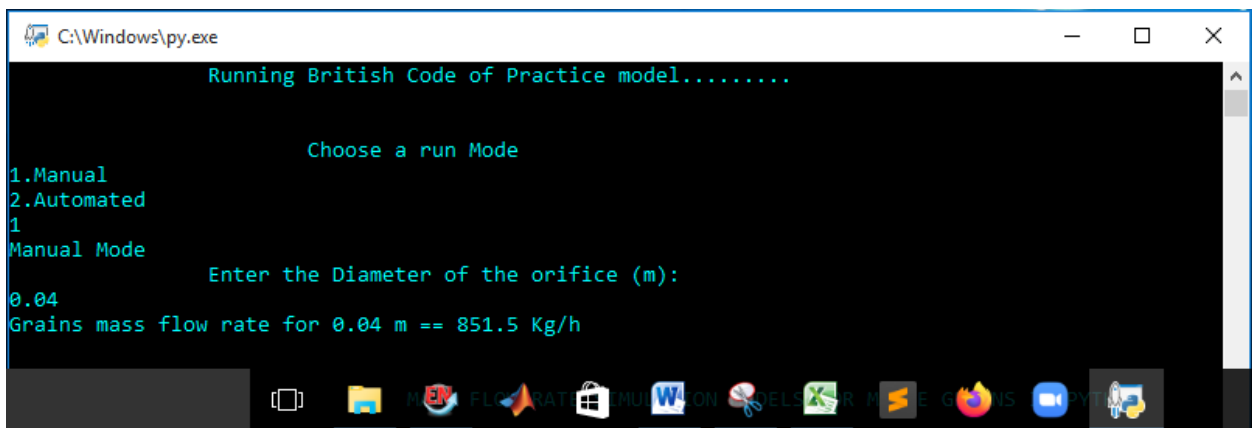


**Figure B6** Sample of BCP model output executed using manual mode

```
C:\Windows\py.exe
Running Tudor model...

Choose a run Mode
1.Manual
2.Automated
1
Manual Mode
Enter the Diameter of the orifice
0.04

Grains mass flow rate for 0.04 m == 890.0 Kg/h
```

Figure B7 Sample of Tudor model output executed using manual mode

```
C:\Windows\py.exe
Beverloo model.....

Choose a run Mode
1.Manual
2.Automatic
2

Enter the lower limit (m): 0.040
Enter the upper limit (m): 0.056
Enter the steps: 0.002
-----Grains mass flow rate for 0.04 m == 650.0 Kg/h
-----Grains mass flow rate for 0.042 m == 772.0 Kg/h
-----Grains mass flow rate for 0.044 m == 907.0 Kg/h
-----Grains mass flow rate for 0.046 m == 1055.0 Kg/h
-----Grains mass flow rate for 0.048 m == 1216.0 Kg/h
-----Grains mass flow rate for 0.05 m == 1392.0 Kg/h
-----Grains mass flow rate for 0.052 m == 1582.0 Kg/h
-----Grains mass flow rate for 0.054 m == 1786.0 Kg/h
-----Grains mass flow rate for 0.056 m == 2006.0 Kg/h
C:\Users\Admin\AppData\Local\Programs\Python\Python38-32\lib\site-packages\openpyxl\worksheet\wr
iter.py:273: UserWarning: File may not be readable: column headings must be strings.
  warn("File may not be readable: column headings must be strings.")

A copy of the results has been saved!
```

Figure B8 Beverloo model results executed using auto mode

```
C:\Windows\py.exe

Running British Code of Practice model.....

Choose a run Mode
1.Manual
2.Automated
2
AUTOMATED MODE

Enter the lower limit (m): 0.040
Enter the upper limit (m): 0.056
Enter the steps: 0.002
-----Grains mass flow rate for 0.04 m == 851.0 Kg/h
-----Grains mass flow rate for 0.042 m == 993.0 Kg/h
-----Grains mass flow rate for 0.044 m == 1148.0 Kg/h
-----Grains mass flow rate for 0.046 m == 1317.0 Kg/h
-----Grains mass flow rate for 0.048 m == 1500.0 Kg/h
-----Grains mass flow rate for 0.05 m == 1697.0 Kg/h
-----Grains mass flow rate for 0.052 m == 1909.0 Kg/h
-----Grains mass flow rate for 0.054 m == 2136.0 Kg/h
-----Grains mass flow rate for 0.056 m == 2378.0 Kg/h

A copy of the results has been saved!
```

Figure B9 BCP model results executed using auto mode option

```
C:\Windows\py.exe

Running Tudor model...

Choose a run Mode
1.Manual
2.Automated
2
AUTOMATED MODE
Enter the lower limit (m): 0.040
Enter the upper limit (m): 0.056
Enter the steps: 0.002
-----Grains mass flow rate for 0.04 m == 890.0 Kg/h
-----Grains mass flow rate for 0.042 m == 1006.0 Kg/h
-----Grains mass flow rate for 0.044 m == 1130.0 Kg/h
-----Grains mass flow rate for 0.046 m == 1262.0 Kg/h
-----Grains mass flow rate for 0.048 m == 1404.0 Kg/h
-----Grains mass flow rate for 0.05 m == 1555.0 Kg/h
-----Grains mass flow rate for 0.052 m == 1715.0 Kg/h
-----Grains mass flow rate for 0.054 m == 1885.0 Kg/h
-----Grains mass flow rate for 0.056 m == 2064.0 Kg/h

A copy of the results has been saved!
```

Figure B10 Tudor model results executed using auto mode option

## Appendix C: Key Data and Analysis for Objective One

**Table C1** Characteristic dimensions for maize grain

Sample	Characteristic dimensions for maize grain		
	Length (mm)	Width (mm)	Thickness (mm)
1	12.21	8.97	6.13
2	12.77	8.89	3.89
3	12.04	11.09	5.29
4	11.80	10.34	4.58
5	12.02	10.32	4.65
6	12.57	11.00	4.82
7	11.79	10.78	4.15
8	10.99	10.53	5.67
9	12.67	11.54	4.73
10	11.83	8.19	4.39
11	13.12	10.39	6.34
12	13.24	9.47	4.33
13	14.29	9.88	4.34
14	12.04	9.60	6.30
15	13.29	9.85	4.78
16	12.23	8.99	6.15
17	12.72	8.87	3.87
18	12.06	11.11	5.31
19	12.00	10.32	4.60
20	12.00	10.34	4.67
21	12.59	11.20	4.80
22	11.71	10.80	4.17
23	11.01	10.51	5.65
24	12.62	11.56	4.75
25	11.82	8.17	4.37
26	13.10	10.41	6.32
27	13.26	9.45	4.35

28	14.24	9.90	4.32
29	12.06	9.62	6.32
30	13.25	9.85	4.80
31	12.21	9.97	7.13
32	13.77	7.89	3.89
33	12.02	11.11	5.29
34	11.84	10.30	4.58
35	12.02	10.30	4.67
36	12.55	11.02	4.82
37	12.79	9.76	4.17
38	11.99	9.52	5.68
39	12.69	11.52	4.73
40	11.85	8.20	4.40
41	12.12	9.39	6.34
42	13.22	9.48	4.34
43	13.29	10.86	4.36
44	12.07	9.58	6.29
45	12.29	8.89	4.74
46	12.21	9.00	6.16
47	12.92	8.86	3.86
48	13.06	10.11	5.31
49	12.05	10.30	4.59
50	12.08	10.30	4.63
51	12.79	11.10	4.70
52	12.71	9.80	4.17
53	12.01	10.51	4.65
54	12.64	11.55	4.74
55	11.80	8.18	4.38
56	13.12	10.40	6.31
57	13.06	9.55	4.45
58	13.21	10.90	4.33

59	12.08	9.63	6.33
60	13.05	9.95	4.90
61	12.11	8.87	6.33
62	12.79	8.88	3.88
63	12.07	11.07	5.28
64	11.60	10.44	4.68
65	13.02	9.33	4.64
66	12.55	11.01	4.83
67	11.59	10.88	4.25
68	11.99	9.54	5.66
69	12.65	11.55	4.74
70	11.63	8.29	4.49
71	13.02	10.47	6.36
72	13.20	9.49	4.35
73	13.29	10.84	4.38
74	12.24	9.50	6.20
75	13.27	9.86	4.79
76	12.43	8.89	6.05
77	11.72	9.85	3.89
78	12.04	11.10	5.30
79	12.50	10.29	4.58
80	12.00	10.34	4.67
81	12.39	11.30	4.90
82	12.71	9.81	4.16
83	11.00	10.52	5.65
84	12.42	11.66	4.85
85	11.62	8.27	4.47
86	13.14	10.39	6.30
87	12.26	10.44	4.36
88	13.24	10.90	4.32
89	12.04	9.64	6.34

90	13.27	9.81	4.82
91	12.11	8.87	6.23
92	12.79	8.87	3.89
93	12.08	11.07	5.27
94	11.85	10.33	4.60
95	12.07	10.30	4.63
96	12.47	11.10	4.92
97	11.75	10.79	4.18
98	10.79	10.73	5.67
99	12.47	11.64	4.83
100	11.87	8.17	4.37
<b>Mean dimensions (mm)</b>	<b>12.41±0.12</b>	<b>10.5±0.17</b>	<b>4.96±0.14</b>
<b>Geometric mean diameter (mm)</b>	<b>8.52</b>		
<b>Arithmetic mean diameter (mm)</b>	<b>9.14</b>		
<b>Sphericity (%)</b>	<b>68.7</b>		

Mean values ± standard error

**Table C2** Initial moisture content of maize grain before rewetting in tap water

<b>Sample</b>	<b>Initial weight (g)</b>	<b>Final weight (g)</b>	<b>Moisture removed (g)</b>	<b>Moisture content (% wb)</b>
1	25.0	22.0	3.0	12.0
2	24.5	21.5	3.0	12.2
3	25.0	22.5	2.5	10.0
4	25.0	21.9	3.1	12.4
5	25.0	22.0	3.0	12.0
6	24.5	21.4	3.1	12.7
7	24.5	21.7	2.8	11.4
8	25.0	22.2	2.8	11.2
9	25.0	22.2	2.8	11.2
10	25.0	22.2	2.8	11.2



11	25.0	22.0	3.0	12.0
12	24.5	21.8	2.7	11.0
13	25.0	22.4	2.6	10.4
14	24.5	21.6	2.9	11.8
15	25.0	22.5	2.5	10.0
16	25.0	22.0	3.0	12.0
17	25.0	22.0	3.0	12.0
18	25.0	22.5	2.5	10.0
19	24.5	21.5	3.0	12.2
20	25.0	22.0	3.0	12.0
21	25.0	22.0	3.0	12.0
22	24.5	21.8	2.7	11.0
23	24.5	22.0	2.5	10.2
24	25.0	22.0	3.0	12.0
25	25.0	22.0	3.0	12.0
26	25.0	22.0	3.0	12.0
27	25.0	22.0	3.0	12.0
28	25.0	22.0	3.0	12.0
29	24.5	22.0	2.5	10.2
30	25.0	22.5	2.5	10.0

---

**Mean moisture content (% , wb) 11.4 ± 0.15**

---

Mean value ± standard error

**Table C3** Actual and simulation models mass flow rate of maize grain through horizontal circular orifices

<b>Actual and models mass flow rates of maize grain (kg/h)</b>				
<b>Horizontal orifice diameter (m)</b>	<b>Actual</b>	<b>Beverloo model</b>	<b>BCP model</b>	<b>Tudor model</b>
0.040	720 ± 10	650	851	867
0.042	771 ± 8	772	993	979
0.044	864 ± 10	907	1148	1100

0.046	1012 ± 11	1055	1317	1229
0.048	1085 ± 3	1216	1500	1367
0.050	1258 ± 2	1392	1697	1514
0.052	1397 ± 10	1582	1909	1670
0.054	1608 ± 30	1786	2136	1835
0.056	1735 ± 16	2006	2378	2010

Mean of actual values ± standard error

**Table C4** Actual and New model mass flow rates of maize grain through horizontal circular orifices

<b>Horizontal orifice diameter (m)</b>	<b>Actual MFR (kg/h)</b>	<b>New model MFR (kg/h)</b>
0.040	720 ± 10	706
0.042	771 ± 8	784
0.044	864 ± 10	877
0.046	1012 ± 11	986
0.048	1085 ± 3	1110
0.050	1258 ± 2	1249
0.052	1397 ± 10	1403
0.054	1608 ± 30	1572
0.056	1735 ± 16	1757

Mean of actual values ± standard error

**Table C5** Student's t-test results for Beverloo model and actual mass flow rates of maize grain through horizontal circular orifices

	<b>Beverloo model MFR</b>	<b>Actual MFR</b>
Mean	1262.889	1161.053
Variance	216629.861	132039.779
Observations	9	9
Pearson Correlation	0.997	
Hypothesized Mean Difference	0	
df	8	
t Stat	2.878	

P(T<=t) one-tail	0.010
t Critical one-tail	1.860
P(T<=t) two-tail	0.021
t Critical two-tail	2.306

---

MFR is mass flow rate of maize grain

**Table C6** Student's t-test results for Tudor model and actual mass flow rates of maize grain through horizontal circular orifices

	<b>Tudor model MFR</b>	<b>Actual MFR</b>
Mean	1396.778	1161.053
Variance	153598.444	132039.779
Observations	9	9
Pearson Correlation	0.996	
Hypothesized Mean Difference	0	
df	8	
t Stat	16.490	
P(T<=t) one-tail	0.000	
t Critical one-tail	1.860	
P(T<=t) two-tail	0.000	
t Critical two-tail	2.306	

---

MFR is mass flow rate of maize grain

**Table C7** Student's t-test results for BCP model and actual mass flow rates of maize grain through horizontal circular orifices

	<b>BCP model MFR)</b>	<b>Actual MFR</b>
Mean	1547.667	1161.053
Variance	274583.000	132039.779
Observations	9	9
Pearson Correlation	0.997	
Hypothesized Mean Difference	0	
df	8	

t Stat	7.073
P(T<=t) one-tail	0.000
t Critical one-tail	1.860
P(T<=t) two-tail	0.000
t Critical two-tail	2.306

---

MFR is mass flow rate of maize grain

**Table C8** Student's t-test results for Tudor and Beverloo model mass flow rates of maize grain through horizontal circular orifices

	<b>Tudor model MFR</b>	<b>Beverloo model MFR</b>
Mean	1396.778	1262.889
Variance	153598.444	216629.861
Observations	9	9
Pearson Correlation	1.000	
Hypothesized Mean Difference	0	
df	8	
t Stat	5.418	
P(T<=t) one-tail	0.000	
t Critical one-tail	1.860	
P(T<=t) two-tail	0.001	
t Critical two-tail	2.306	

---

MFR is mass flow rate of maize grain

**Table C9** Student's t-test results for British Code of Practice and Beverloo model mass flow rates of maize grain through horizontal circular orifices

	<b>BCP model</b>	<b>Beverloo model</b>
Mean	1547.667	1262.889
Variance	274583.000	216629.861
Observations	9	9
Pearson Correlation	1.000	
Hypothesized Mean Difference	0	

df	8
t Stat	14.552
P(T<=t) one-tail	0.000
t Critical one-tail	1.860
P(T<=t) two-tail	0.000
t Critical two-tail	2.306

---

BCP is British Code of Practice model

**Table C10** Student's t-test results for BCP and Tudor model mass flow rates of maize grain through horizontal circular orifices

	<b>BCP model</b>	<b>Tudor model</b>
Mean	1547.667	1396.778
Variance	274583.000	153598.444
Observations	9	9
Pearson Correlation	1.000	
Hypothesized Mean Difference	0	
df	8	
t Stat	3.423	
P(T<=t) one-tail	0.005	
t Critical one-tail	1.860	
P(T<=t) two-tail	0.009	
t Critical two-tail	2.306	

---

BCP is British Code of Practice model

**Table C11** Student's t-test results for actual and New model mass flow rates of maize grain through horizontal circular orifices

	<b>Actual</b>	<b>New Model</b>
Mean	1161.164	1160.259
Variance	132063.877	131678.188
Observations	9	9
Pearson Correlation	0.998	

Hypothesized Mean Difference	0
df	8
t Stat	0.126
P(T<=t) one-tail	0.452
t Critical one-tail	1.860
P(T<=t) two-tail	0.903
t Critical two-tail	2.306

**Table C12** Performance evaluation of the simulation models for mass flow rates of maize grain through horizontal circular orifices

Simulation model for mass flow rate	R <sup>2</sup>	χ <sup>2</sup>	RMSE	ε <sub>r</sub> (%)	η <sub>sim,10</sub> (%)
Beverloo	0.9950	-130.9	142.8	9.1	44
BCP	0.9943	-579.9	416.4	32.2	0
Tudor	0.9928	-353.6	239.2	21.3	0
<b>New</b>	<b>0.9965</b>	<b>1.2</b>	<b>24.8</b>	<b>0.6</b>	<b>100</b>

R<sup>2</sup> is coefficient of determination, χ<sup>2</sup> is reduced chi-square, RMSE is root mean square error, ε<sub>r</sub> is absolute residual error and η<sub>sim,10%</sub> is simulation performance at 10% residual error

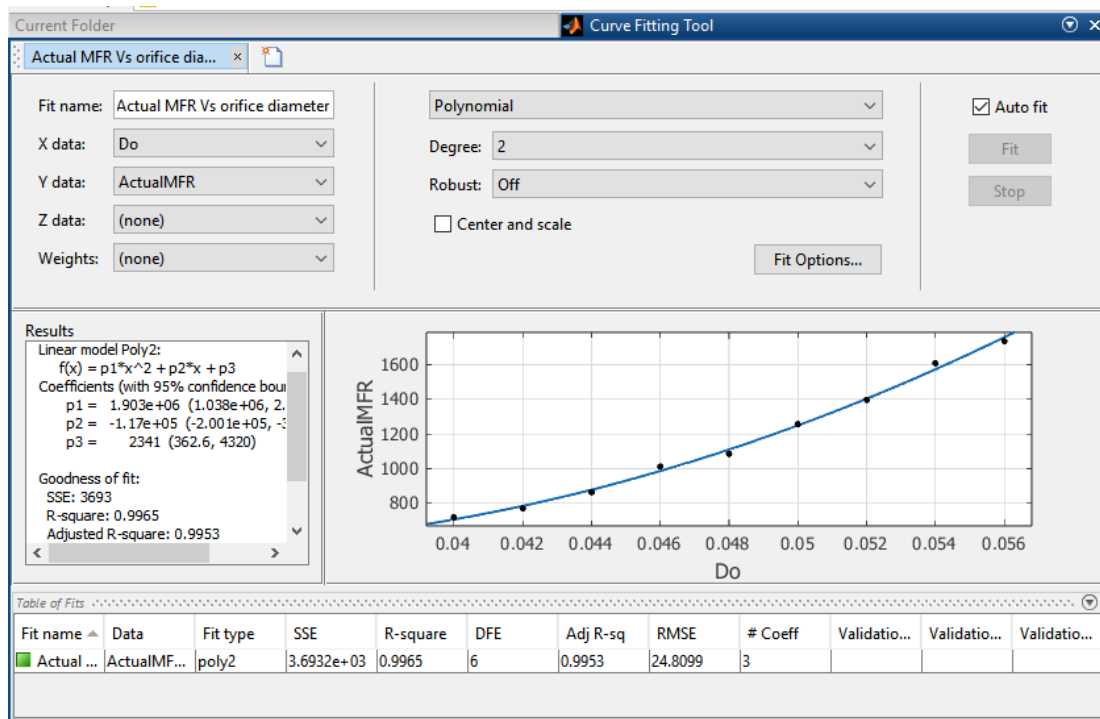


**Figure C1** Curve fitting using MATALAB R2019a software

### Appendix D: Key Data and Analysis for Objective Two

**Table D1** Variation of maize grain moisture content with time by rewetting in tap water at 18°C

<b>Time</b>		<b>Initial weight</b>	<b>Final weight</b>	<b>MC</b>	<b>Mean MC</b>
<b>(hr)</b>	<b>Replications</b>	<b>(g)</b>	<b>(g)</b>	<b>(%, wb)</b>	<b>(%, wb)</b>
0.00	R1	25.0	22.0	12.0	11.4
	R2	24.5	21.5	12.2	
	R3	25.0	22.5	10.0	
0.25	R1	25.0	20.5	18.0	18.7
	R2	25.0	20.0	20.0	
	R3	25.0	20.5	18.0	
0.50	R1	25.0	20.5	18.0	19.3
	R2	25.0	20.0	20.0	
	R3	25.0	20.0	20.0	
<b>0.75</b>	<b>R1</b>	<b>25.0</b>	<b>20.0</b>	<b>20.0</b>	<b>20.0</b>
	R2	25.0	20.0	20.0	
	R3	25.0	20.0	20.0	
1.00	R1	25.0	20.0	20.0	22.5
	R2	25.0	19.0	24.0	
	R3	25.5	19.5	23.5	
1.25	R1	25.0	19.0	24.0	23.3
	R2	25.0	19.5	22.0	
	R3	25.0	19.0	24.0	
1.50	R1	25.0	19.0	24.0	24.7
	R2	25.0	18.5	26.0	
	R3	25.0	19.0	24.0	
<b>1.75</b>	<b>R1</b>	<b>25.0</b>	<b>18.5</b>	<b>26.0</b>	<b>25.3</b>
	R2	25.0	19.0	24.0	
	R3	25.0	18.5	26.0	
2.00	R1	25.0	18.5	26.0	26.3
	R2	25.5	18.5	27.5	
	R3	25.5	19.0	25.5	

2.25	R1	25.0	18.3	26.8	26.4
	R2	25.5	18.9	25.9	
	R3	25.5	18.7	26.7	
2.50	R1	25.0	18.3	27.0	26.5
	R2	25.5	19.0	25.5	
	R3	25.5	18.6	27.1	
2.75	R1	25.0	18.5	26.0	26.6
	R2	25.5	18.7	26.7	
	R3	25.5	18.6	27.1	
3.00	R1	25.0	18.5	26.0	26.7
	R2	25.0	18.0	28.0	
	R3	25.0	18.5	26.0	
3.25	R1	25.0	18.4	26.4	27.1
	R2	25.0	18.1	27.6	
	R3	25.0	18.2	27.2	
3.50	R1	25.0	18.2	27.2	27.3
	R2	25.0	18.2	27.2	
	R3	25.0	18.1	27.6	
3.75	R1	24.5	17.5	28.6	27.9
	R2	25.0	18.0	28.0	
	R3	25.5	18.6	27.1	
4.00	R1	24.5	18.0	26.5	28.0
	R2	25.0	18.0	28.0	
	R3	25.5	18.0	29.4	
4.25	R1	24.5	17.5	28.6	28.4
	R2	25.0	17.9	28.4	
	R3	25.5	18.3	28.2	
4.50	R1	24.5	17.2	29.8	28.7
	R2	25.0	17.8	28.8	
	R3	25.5	18.5	27.5	
4.75	R1	25.0	17.8	28.8	29.1



	R2	25.0	17.7	29.2	
	R3	25.0	17.7	29.2	
5.00	R1	25.0	18.0	28.0	29.3
	R2	25.0	17.5	30.0	
	R3	25.0	17.5	30.0	
5.25	R1	25.0	17.5	30.0	29.7
	R2	25.0	17.6	29.6	
	R3	25.0	17.6	29.6	
5.50	R1	25.0	17.4	30.4	29.9
	R2	25.0	17.7	29.2	
	R3	25.0	17.5	30.0	
<b>5.75</b>	<b>R1</b>	<b>25.0</b>	<b>17.3</b>	<b>30.8</b>	<b>30.0</b>
	R2	25.5	17.9	29.8	
	R3	25.5	18.0	29.4	
6.00	R1	25.0	17.5	30.0	30.3
	R2	25.5	18.0	29.4	
	R3	25.5	17.5	31.4	
6.25	R1	25.4	17.5	31.1	30.6
	R2	25.5	18.0	29.4	
	R3	25.5	17.5	31.4	
6.50	R1	25.5	17.5	31.4	30.8
	R2	25.8	18.0	30.2	
	R3	25.3	17.5	30.8	
6.75	R1	25.3	17.5	30.8	31.0
	R2	26.2	18.0	31.3	
	R3	25.3	17.5	30.8	
7.00	R1	25.0	17.0	32.0	31.3
	R2	25.0	17.0	32.0	
	R3	25.0	17.5	30.0	
7.25	R1	24.8	17.0	31.5	31.6
	R2	25.5	17.0	33.3	

	R3	25.0	17.5	30.0	
7.50	R1	24.9	17.0	31.7	31.8
	R2	24.9	17.0	31.7	
	R3	25.0	17.0	32.0	
7.75	R1	25.0	17.2	31.2	31.9
	R2	25.0	16.9	32.4	
	R3	25.0	17.0	32.0	
8.00	R1	25.0	17.0	32.0	32.0
	R2	25.0	17.0	32.0	
	R3	25.0	17.0	32.0	
8.25	R1	25.0	16.9	32.4	32.3
	R2	25.0	16.9	32.4	
	R3	25.0	17.0	32.0	
8.50	R1	25.0	16.8	32.8	32.4
	R2	25.0	16.9	32.4	
	R3	25.0	17.0	32.0	
8.75	R1	25.0	16.9	32.4	32.5
	R2	25.0	16.8	32.8	
	R3	25.0	16.9	32.4	
9.00	R1	25.0	16.5	34.0	32.7
	R2	25.0	16.5	34.0	
	R3	25.0	17.5	30.0	

**Table D2** Variation of moisture removal rate and energy used with time for maize grain with moisture content of 20% (wet basis) dried at constant air temperature of 70°C and maize grain mass flow rate of 771 kg/h

Time (h)	Moisture can	Empty can (g)	Can + wet grain (g)	Can + dry grain (g)	Mean MRR (kg/kg.h)	Mean MR	E <sub>a</sub> (kWh)	E <sub>g</sub> (kWh)
0.00	0A	51.5	76.5	71.5	0.0000	1.00	0.0	0.0
	0B	46.5	71.5	66.5				

	0C	49.5	74.5	69.4				
0.25	15A	49.5	74.5	70.0	0.0914	0.89	1.6	0.6
	15B	49.5	74.5	70.0				
	15C	48.0	73.0	68.3				
0.50	30A	55.0	80.0	76.0	0.0832	0.81	2.9	1.1
	30B	54.5	79.5	75.5				
	30C	49.0	74.0	69.5				
0.75	45A	48.5	73.5	69.5	0.0756	0.771	4.4	1.7
	45B	45.5	70.5	67.0				
	45C	52.5	77.5	73.5				
1.00	60A	49.5	74.5	71.0	0.0641	0.77	5.7	2.1
	60B	53.5	78.5	75.0				
	60C	47.5	72.5	68.5				
1.25	75A	54.5	79.5	76.0	0.0524	0.76	6.8	2.9
	75B	47.0	72.0	68.5				
	75C	53.0	78.0	74.1				
1.50	90A	54.0	79.0	75.5	0.0447	0.76	8.1	3.4
	90B	47.0	72.0	68.2				
	90C	47.0	72.0	68.5				
1.75	105A	47.0	72.0	68.5	0.0408	0.75	9.1	4.0
	105B	54.0	79.0	75.5				
	105C	50.0	75.0	71.5				
2.00	120A	48.5	73.5	70.0	0.0357	0.74	10.5	4.6
	120B	53.0	78.5	75.0				
	120C	54.0	78.5	75.0				

---

MRR is moisture removal rate, MR is moisture ratio,  $E_a$  is energy for maize grain drying,  $E_g$  is energy for maize grain transportation

**Table D3** Variation of moisture removal rate and energy used with time for maize grain with moisture content of 25% (wet basis) dried at constant drying air temperature of 70°C and maize grain mass flow rate of 771 kg/h

Time (h)	Moisture in can	Empty can (g)	Can +	Can +	Mean	Mean MR	E <sub>a</sub> (kWh)	E <sub>g</sub> (kWh)
			wet grain (g)	dry grain (g)	MRR (kg/kg.h)			
0.00	0A	51.5	76.5	70.0	0.0000	1.00	0.0	0.0
	0B	46.5	71.5	65.0				
	0C	49.5	74.5	68.5				
0.25	15A	49.5	74.5	68.5	0.1043	0.90	1.6	0.7
	15B	49.5	74.5	68.5				
	15C	48.0	73.0	67.5				
0.50	30A	55.0	80.0	75.0	0.1017	0.80	2.9	1.2
	30B	54.5	79.5	74.0				
	30C	49.0	74.0	68.5				
0.75	45A	48.5	73.5	69.0	0.0889	0.74	4.4	1.8
	45B	45.5	70.5	65.5				
	45C	52.5	77.5	72.0				
1.00	60A	49.5	74.5	70.0	0.0820	0.68	5.7	2.3
	60B	53.5	78.5	74.0				
	60C	47.5	72.5	67.5				
1.25	75A	54.5	79.5	75.5	0.0774	0.62	6.8	3.0
	75B	47.0	72.0	67.5				
	75C	53.0	78.0	73.5				
1.50	90A	54.0	79.0	74.5	0.0693	0.59	8.2	3.6
	90B	47.0	72.0	68.0				
	90C	47.0	72.0	68.0				
1.75	105A	47.0	72.0	68.5	0.0635	0.56	9.1	4.2
	105B	54.0	79.0	74.5				
	105C	50.0	75.0	71.0				

2.00	120A	48.5	73.5	69.5	0.0556	0.56	10.5	4.8
	120B	53.0	78.5	74.0				
	120C	54.0	78.5	75.0				

MRR is moisture removal rate, MR is moisture ratio,  $E_a$  is energy for drying and  $E_g$  is energy for maize transportation

**Table D4** Variation of moisture removal rate and energy used with time for maize grain with moisture content of 30% (wet basis) dried at constant drying air temperature of 70°C and maize grain mass flow rate of 771 kg/h

Time (hr)	Moisture can	Empty can (g)	Can +	Can +	Mean	Mean MR	$E_a$ (kWh)	$E_g$ (kWh)
			wet grain (g)	dry grain (g)	MRR (kg/kg.h)			
0.00	0A	51.5	76.5	68.5	0.0000	1.00	0.0	0.0
	0B	46.5	71.5	64.4				
	0C	49.5	74.5	67.0				
0.25	15A	49.5	74.5	67.0	0.1185	0.90	1.7	0.8
	15B	49.5	74.5	67.5				
	15C	48.0	73.0	66.5				
0.50	30A	55.0	80.0	73.5	0.1117	0.81	2.9	1.3
	30B	54.5	79.5	73.0				
	30C	49.0	74.0	67.5				
0.75	45A	48.5	73.5	67.5	0.1076	0.74	4.4	1.9
	45B	45.5	70.5	64.5				
	45C	52.5	77.5	71.5				
1.00	60A	49.5	74.5	69.0	0.0966	0.68	5.8	2.4
	60B	53.5	78.5	73.0				
	60C	47.5	72.5	66.5				
1.25	75A	54.5	79.5	74.0	0.0895	0.62	6.9	3.2
	75B	47.0	72.0	67.0				
	75C	53.0	78.0	72.5				

1.50	90A	54.0	79.0	73.5	0.0796	0.59	8.3	3.8
	90B	47.0	72.0	66.5				
	90C	47.0	72.0	67.5				
1.75	105A	47.0	72.0	67.5	0.0756	0.56	9.1	4.4
	105B	54.0	79.0	74.0				
	105C	50.0	75.0	70.0				
2.00	120A	48.5	73.5	68.5	0.0705	0.56	10.6	5.0
	120B	53.0	78.0	73.5				
	120C	54.0	79.0	74.5				

MRR is moisture removal rate, MR is moisture ratio,  $E_a$  is energy for and  $E_g$  is energy for maize transportation

**Table D5** Summary of ANOVA results for effect of moisture content on moisture removal rate in pneumatic maize grain drying

Moisture content level (% , wet basis)	Count	Sum	Average	Variance
20	8	0.4877	0.0610	0.0004
25	8	0.6427	0.0803	0.0003
30	8	0.7495	0.0937	0.0003

**Table D6** ANOVA results for effect of moisture content on moisture removal rate in maize grain drying

Source of variation	S.S.	D.F.	M.S.	$F_{\text{computed}}$	P-value	$F_{\text{critical}}$
Moisture content	0.0043	2	0.0022	6.153	0.0079	3.467
Residual	0.0074	21	0.0004			
Total	0.0117	23				

**Table D7** Fisher's LSD results for effect of moisture content of levels on moisture removal rate in pneumatic maize grain drying

Alpha	DFW	MSW	Student's t-distribution	Fisher's $LSD_{5\%}$	ABSMD	MC (% , wb)
0.05	21	0.0004	2.0796	0.0195	0.0194	20 and 25
					0.0327	20 and 30
					0.0133	25 and 30

**Table D8** Summary of ANOVA results for effect of moisture content on energy used for maize grain drying

Moisture content level (% , wb)	Count	Sum	Average	Variance
20	9	49.1	6.1375	9.4827
25	9	49.2	6.1500	9.5400
30	9	49.7	6.2125	9.6013

**Table D9** ANOVA results for effect of moisture content on energy used for maize grain drying

Source of variation	S.S.	D.F.	M.S.	F <sub>computed</sub>	P-value	F <sub>critical</sub>
Moisture content	0.0258	2	0.0129	0.0014	0.9986	3.4668
Residual	200.3675	21	9.5413			
Total	200.3933	23				

**Table D10** Fisher's LSD results for effect of moisture content on energy used for maize grain drying

Alpha	DFW	MSW	Student's t-distribution	Fisher's LSD <sub>5%</sub>	ABSMD	MC (% , wb)
0.05	21	9.5413	2.0796	3.2119	0.0125	20 and 25
					0.0750	20 and 30
					0.0625	25 and 30

**Table D11** Summary of ANOVA results for effect moisture content on energy used for maize grain transportation in pneumatic drying

Moisture content level (% , wb)	Count	Sum	Average	Variance
20	8	20.4	2.5500	1.9971
25	8	21.5	2.6875	2.1241
30	8	22.8	2.8500	2.2514

**Table D12** ANOVA results for effect of moisture content on energy used for maize grain transportation in drying

Source of variation	S.S.	D.F.	M.S.	F <sub>computed</sub>	P-value	F <sub>critical</sub>
Moisture content	0.3608	2	0.1804	0.0849	0.9189	3.4668
Residual	44.6088	21	2.1242			
Total	44.9696	23				

**Table D13** Fisher's LSD results for effect of moisture content on energy used for maize grain transportation in drying

Alpha	DFW	MSW	Student's t-distribution	Fisher's LSD <sub>5%</sub>	ABSMD	MC (% , wb)
0.05	21	2.1242	2.0796	1.5155	0.1375	20 and 25
					0.3000	20 and 30
					0.1625	25 and 30

**Table D14** Variation of moisture removal rate and energy used with drying time for air temperature of 60°C, maize grain moisture content of 25% (wet basis) and mass flow rate of 771 kg/h

Time (hr)	Moisture can	Empty can (g)	Can +	Can +	Mean	Mean MR	E <sub>a</sub> (kWh)	E <sub>g</sub> (kWh)
			wet grain (g)	dry grain (g)	MRR (kg/kg.h)			
0.00	0A	51.5	76.5	70.5	0.0000	1.00	0	0
	0B	46.5	71.5	64.5				
	0C	49.5	74.5	68.5				
0.25	15A	49.5	74.5	68.0	0.0702	0.93	1.1	0.7
	15B	49.5	74.5	69.0				
	15C	48.0	73.0	67.0				
0.50	30A	55.0	80.0	74.0	0.0690	0.86	1.8	1.3
	30B	54.5	79.5	74.0				
	30C	49.0	74.0	68.5				
0.75	45A	48.5	73.5	68.5	0.0678	0.80	2.4	1.8
	45B	45.5	70.5	65.0				
	45C	52.5	77.5	72.0				
1.00	60A	49.5	74.5	70.0	0.0667	0.74	3.4	2.4
	60B	53.5	78.5	73.0				
	60C	47.5	72.5	67.5				
1.25	75A	54.5	79.5	74.5	0.0595	0.71	4.4	3
	75B	47.0	72.0	67.5				



	75C	53.0	78.0	73.0				
1.50	90A	54.0	79.0	74.0	0.0596	0.65	5.0	3.6
	90B	47.0	72.0	67.5				
	90C	47.0	72.0	68.0				
1.75	105A	47.0	72.0	68.5	0.0594	0.59	5.7	4.2
	105B	54.0	79.0	74.5				
	105C	50.0	75.0	70.5				
2.00	120A	48.5	73.5	69.0	0.0556	0.56	6.6	4.8
	120B	53.0	78.0	74.5				
	120C	54.0	79.0	75.0				

MRR is moisture removal rate, MR is moisture ratio,  $E_a$  is energy for maize grain drying,  $E_g$  is energy for maize grain transportation

**Table D15** Variation of moisture removal rate and energy used with drying time for air temperature of 70°C, maize grain moisture content of 25% (wet basis) and mass flow rate of 771 kg/h

Time (h)	Moistur e can	Empty can (g)	Can +	Can +	Mean	Mean MR	$E_a$ (kWh)	$E_g$ (kWh)
			wet grain (g)	dry grain (g)	MRR (kg/kg.h )			
0.00	0A	51.5	76.5	70.0	0.0000	1.00	0.0	0.0
	0B	46.5	71.5	65.0				
	0C	49.5	74.5	68.5				
0.25	15A	49.5	74.5	68.5	0.1043	0.90	1.6	0.7
	15B	49.5	74.5	68.5				
	15C	48.0	73.0	67.5				
0.50	30A	55.0	80.0	75.0	0.1017	0.80	2.9	1.2
	30B	54.5	79.5	74.0				
	30C	49.0	74.0	68.5				
0.75	45A	48.5	73.5	69.0	0.0889	0.74	4.4	1.8
	45B	45.5	70.5	65.5				

	45C	52.5	77.5	72.0				
1.00	60A	49.5	74.5	70.0	0.0820	0.68	5.7	2.3
	60B	53.5	78.5	74.0				
	60C	47.5	72.5	67.5				
1.25	75A	54.5	79.5	75.5	0.0774	0.62	6.8	3.0
	75B	47.0	72.0	67.5				
	75C	53.0	78.0	73.5				
1.50	90A	54.0	79.0	74.5	0.0693	0.59	8.2	3.6
	90B	47.0	72.0	68.0				
	90C	47.0	72.0	68.0				
1.75	105A	47.0	72.0	68.5	0.0635	0.56	9.1	4.2
	105B	54.0	79.0	74.5				
	105C	50.0	75.0	71.0				
2.00	120A	48.5	73.5	69.5	0.0556	0.56	10.5	4.8
	120B	53.0	78.5	74.0				
	120C	54.0	78.5	75.0				

MRR is moisture removal rate, MR is moisture ratio,  $E_a$  is energy for maize grain drying,  $E_g$  is energy for maize grain transportation

**Table D16** Variation of moisture removal rate and energy used with drying time for air temperature of 80°C, maize grain moisture content of 25% (wet basis) and mass flow rate of 771 kg/h

Time (h)	Moisture can	Empty can (g)	Can +	Can +	Mean	Mean MR	$E_a$ (kWh)	$E_g$ (kWh)
			wet grain (g)	dry grain (g)	MRR (kg/kg.h)			
0.00	0A	51.5	76.5	70.0	0.0000	1.00	0.0	0.0
	0B	46.5	71.5	65.5				
	0C	49.5	74.5	68.0				
0.25	15A	49.5	74.5	69.5	0.1379	0.87	2.1	0.6
	15B	49.5	74.5	68.5				

	15C	48.0	73.0	67.0				
0.50	30A	55.0	80.0	75.0	0.1333	0.74	3.9	1.2
	30B	54.5	79.5	74.5				
	30C	49.0	74.0	69.0				
0.75	45A	48.5	73.5	68.5	0.1093	0.68	6.1	1.7
	45B	45.5	70.5	66.0				
	45C	52.5	77.5	73.0				
1.00	60A	49.5	74.5	70.5	0.0968	0.62	7.3	2.4
	60B	53.5	78.5	74.0				
	60C	47.5	72.5	68.0				
1.25	75A	54.5	79.5	75.0	0.0889	0.56	9.5	2.9
	75B	47.0	72.0	68.5				
	75C	53.0	78.0	74.0				
1.50	90A	54.0	79.0	75.0	0.0741	0.56	10.7	3.5
	90B	47.0	72.0	68.5				
	90C	47.0	72.0	67.5				
1.75	105A	47.0	72.0	68.5	0.0635	0.56	12.4	4.1
	105B	54.0	79.0	74.5				
	105C	50.0	75.0	71.0				
2.00	120A	48.5	73.5	69.0	0.0556	0.56	13.8	4.8
	120B	53.0	78.0	74.5				
	120C	54.0	79.0	75.0				

MRR is moisture removal rate, MR is moisture ratio,  $E_a$  is energy for maize grain drying,  $E_g$  is energy for maize grain transportation

**Table D17** Summary of ANOVA results for effect of air temperature on moisture removal rate in maize grain drying

Air temperature level (°C)	Count	Sum	Average	Variance
60	8	0.507715	0.063464	3.05E-05
70	8	0.642699	0.080337	0.000305
80	8	0.759339	0.094917	0.000935

**Table D18** ANOVA results for effect of air temperature on moisture removal rate in maize grain drying

Source of variation	S.S.	D.F.	M.S.	F <sub>computed</sub>	P-value	F <sub>critical</sub>
Drying air temperature	0.003964	2	0.0020	4.6804	0.0208	3.4668
Residual	0.008893	21	0.0004			
Total	0.012857	23				

**Table D19** Fisher's LSD results for effect of air temperature on moisture removal rate in maize grain drying

Alpha	DFW	MSW	Student's t-distribution	Fisher's LSD <sub>5%</sub>	ABSMD	T <sub>a</sub> (°C)
0.05	21	0.0004	2.0796	0.0214	0.0169	60 and 70
					0.0315	60 and 80
					0.0146	70 and 80

**Table D20** SUMMARY of ANOVA results for effect of air temperature on energy used for maize grain drying

Drying air temperature (°C)	Count	Sum	Average	Variance
60	8	30.4000	3.8000	3.8086
70	8	49.2000	6.1500	9.5400
80	8	65.8000	8.2250	16.8364

**Table D21** ANOVA results for effect of air temperature on energy for maize grain drying

Source of variation	S.S.	D.F.	M.S.	F <sub>computed</sub>	P-value	F <sub>critical</sub>
Drying air temperature	78.4233	2	39.2117	3.8971	0.0364	3.4668
Residual	211.2950	21	10.0617			
Total	289.7183	23				

**Table D22** Fisher's LSD results for effect of air temperature on energy used in maize grain drying

Alpha	DFW	MSW	Student's t-distribution	LSD <sub>5%</sub>	ABSMD	T <sub>a</sub> (°C)
0.05	24	10.0617	2.0796	3.2983	2.3500	60 and 70
					4.4250	60 and 80
					2.0750	70 and 80

**Table D23** Summary of ANOVA results for effect of air temperature on maize grain transportation in pneumatic maize grain drying

Drying air temperature (°C)	Count	Sum	Average	Variance
60	8	21.7000	2.7125	2.0013
70	8	21.6000	2.7000	2.1114
80	8	21.2000	2.6500	2.1114

**Table D24** ANOVA results for effect of air temperature on transportation of maize grain in drying

Source of variation	S.S.	D.F.	M.S.	F <sub>computed</sub>	P-value	F <sub>critical</sub>
Drying air temperature	0.0175	2	0.0087	0.0042	0.9958	3.4668
Residual	43.5688	21	2.0747			
Total	43.5863	23				

**Table D25** Fisher's LSD results for effect of air temperature on transportation of maize grain in drying

Alpha	DFW	MSW	Student's t-distribution	LSD <sub>5%</sub>	ABSMD	T <sub>a</sub> (°C)
0.05	21	2.0747	2.0796	1.4977	0.0125	60 and 70
					0.0625	60 and 80
					0.0500	70 and 80

**Table D26** Variation of moisture removal rate and energy used with drying time for maize grain mass flow rate of 720 kg/h, moisture content of 25% (wet basis) and drying air temperature of 70°C

Time (hr)	Moisture can	Empty can (g)	Can +	Can +	Mean	Mean MR	E <sub>a</sub> (kWh)	E <sub>g</sub> (kWh)
			wet grain (g)	dry grain (g)	MRR (kg/kg.h)			
0.00	0A	51.5	76.5	70.5	0.0000	1.00	0.0	0.0
	0B	46.5	71.5	65.0				
	0C	49.5	74.5	68.0				
0.25	15A	49.5	74.5	68.5	0.1379	0.87	1.6	0.6

	15B	49.5	74.5	69.0				
	15C	48.0	73.0	67.5				
0.50	30A	55.0	80.0	74.5	0.1176	0.77	2.9	1.1
	30B	54.5	79.5	74.5				
	30C	49.0	74.0	69.0				
0.75	45A	48.5	73.5	69.0	0.1093	0.68	4.4	1.7
	45B	45.5	70.5	66.0				
	45C	52.5	77.5	72.5				
1.00	60A	49.5	74.5	70.5	0.0968	0.62	5.7	2.2
	60B	53.5	78.5	74.0				
	60C	47.5	72.5	68.0				
1.25	75A	54.5	79.5	76.0	0.0832	0.59	6.8	2.9
	75B	47.0	72.0	67.5				
	75C	53.0	78.0	73.5				
1.50	90A	54.0	79.0	75.0	0.0741	0.56	8.2	3.4
	90B	47.0	72.0	68.0				
	90C	47.0	72.0	68.0				
1.75	105A	47.0	72.0	68.0	0.0635	0.56	9.1	4.0
	105B	54.0	79.0	75.0				
	105C	50.0	75.0	71.0				
2.00	120A	48.5	73.5	70.0	0.0556	0.56	10.5	4.6
	120B	53.0	78.5	74.0				
	120C	54.0	78.5	74.5				

---

MRR is moisture removal rate, MR is moisture ratio,  $E_a$  is energy for maize grain drying,  $E_g$  is energy for maize transportation

**Table D27** Variation of moisture removal rate and energy used with drying time for maize grain mass flow rate of 771 kg/h, moisture content of 25% (wet basis) and drying air temperature of 70°C

Time (hr)	Moisture in can	Empty can (g)	Can +	Can +	MRR (kg/kg.h )	Mean MR	E <sub>a</sub> (kWh)	E <sub>g</sub> (kWh)
			wet grain (g)	dry grain (g)				
0.00	0A	51.5	76.5	70.0	0.0000	1.00	0.0	0.0
	0B	46.5	71.5	65.0				
	0C	49.5	74.5	68.5				
0.25	15A	49.5	74.5	68.5	0.1043	0.90	1.6	0.7
	15B	49.5	74.5	68.5				
	15C	48.0	73.0	67.5				
0.50	30A	55.0	80.0	75.0	0.1017	0.80	2.9	1.2
	30B	54.5	79.5	74.0				
	30C	49.0	74.0	68.5				
0.75	45A	48.5	73.5	69.0	0.0889	0.74	4.4	1.8
	45B	45.5	70.5	65.5				
	45C	52.5	77.5	72.0				
1.00	60A	49.5	74.5	70.0	0.0820	0.68	5.7	2.3
	60B	53.5	78.5	74.0				
	60C	47.5	72.5	67.5				
1.25	75A	54.5	79.5	75.5	0.0774	0.62	6.8	3.0
	75B	47.0	72.0	67.5				
	75C	53.0	78.0	73.5				
1.50	90A	54.0	79.0	74.5	0.0693	0.59	8.2	3.6
	90B	47.0	72.0	68.0				
	90C	47.0	72.0	68.0				
1.75	105A	47.0	72.0	68.5	0.0635	0.56	9.1	4.2
	105B	54.0	79.0	74.5				
	105C	50.0	75.0	71.0				

2.00	120A	48.5	73.5	69.5	0.0556	0.56	10.5	4.8
	120B	53.0	78.5	74.0				
	120C	54.0	78.5	75.0				

MRR is moisture removal rate, MR is moisture ratio,  $E_a$  is energy for maize grain drying,  $E_g$  is energy for maize grain transportation

**Table D28** Variation of moisture removal rate and energy used with drying time for maize grain mass flow rate of 864 kg/h, moisture content of 25% and drying air temperature of 70°C

Time (hr)	Moisture can	Empty can (g)	Can +	Can +	MRR (kg/kg.h)	Mean MR	$E_a$ (kWh)	$E_g$ (kWh)
			wet grain (g)	dry grain (g)				
0.00	0A	51.5	76.5	70.5	0.0000	1.00	0.0	0.0
	0B	46.5	71.5	65.0				
	0C	49.5	74.5	68.0				
0.25	15A	49.5	74.5	68.5	0.0908	0.90	1.5	0.9
	15B	49.5	74.5	68.5				
	15C	48.0	73.0	67.5				
0.50	30A	55.0	80.0	74.5	0.0855	0.83	2.8	1.4
	30B	54.5	79.5	74.0				
	30C	49.0	74.0	68.5				
0.75	45A	48.5	73.5	68.5	0.0784	0.77	4.4	2.2
	45B	45.5	70.5	65.0				
	45C	52.5	77.5	72.5				
1.00	60A	49.5	74.5	69.5	0.0744	0.71	5.7	2.7
	60B	53.5	78.5	74.0				
	60C	47.5	72.5	67.5				
1.25	75A	54.5	79.5	75.5	0.0656	0.68	6.9	3.5
	75B	47.0	72.0	67.0				
	75C	53.0	78.0	73.0				
1.50	90A	54.0	79.0	74.5	0.0645	0.62	8.1	4.2



	90B	47.0	72.0	68.0				
	90C	47.0	72.0	67.5				
1.75	105A	47.0	72.0	68.0	0.0594	0.59	9.2	4.8
	105B	54.0	79.0	75.0				
	105C	50.0	75.0	70.5				
2.00	120A	48.5	73.5	69.5	0.0556	0.56	10.5	5.4
	120B	53.0	78.0	74.5				
	120C	54.0	79.0	74.5				

MRR is moisture removal rate, MR is moisture ratio,  $E_a$  is energy used maize grain drying,  $E_g$  is energy for maize transportation

**Table D29** Summary of ANOVA results for effect of mass flow rate of maize grain on moisture removal rate in drying

Groups	Count	Sum	Average	Variance
720 kg/h	8	0.7379	0.0922	0.0008
771 kg/h	8	0.6427	0.0803	0.0003
864 kg/h	8	0.5741	0.0718	0.0002

**Table D30** ANOVA results for effect of mass flow rate of maize grain on moisture removal rate in drying

Source of Variation	S.S.	D.F.	M.S.	$F_{\text{computed}}$	P-value	$F_{\text{critical}}$
Mass flow rate	0.0017	2	0.0008	2.0034	0.1598	3.4668
Residual	0.0089	21	0.0004			
Total	0.0106	23				

**Table D31** Fisher's LSD results for effect of mass flow rate of maize grain on moisture removal rate in drying

Alpha	DFW	MSW	Student's t-distribution	Fisher's $LSD_{5\%}$	ABSMD	MFR (kg/h)
0.05	21	0	2.0796	0.0729	0.0119	720 and 771
					0.0205	720 and 864
					0.0086	771 and 864

**Table D32** Summary of ANOVA results for effect mass flow rate of maize grain on energy used in drying

Groups	Count	Sum	Average	Variance
720 kg/h	8	49.2	6.1500	9.5400
771 kg/h	8	49.2	6.1500	9.5400
864 kg/h	8	49.1	6.1375	9.8141

**Table D33** ANOVA results for effect of mass flow rate of maize grain on energy used in drying

Source of Variation	S.S.	D.F.	M.S.	F <sub>computed</sub>	P-value	F <sub>critical</sub>
Mass flow rate	0.0008	2	0.0004	0.00004	1.0000	3.4668
Residual	202.2588	21	9.6314			
Total	202.2596	23				

**Table D34** Fisher's LSD results for effect of mass flow rate of maize grain on energy used in drying

Alpha	DFW	MSW	Student's t-distribution	LSD <sub>5%</sub>	ABSMD	MFR (kg/h)
0.05	21	0	2.0796	1.3012	0.00004	720 and 771
					0.0125	720 and 864
					0.0125	771 and 864

**Table D35** Summary of ANOVA results for effect mass flow rate of maize grain on energy used for transportation in drying

Groups	Count	Sum	Average	Variance
720 kg/h	8	20.5	2.5625	1.9855
771 kg/h	8	21.6	2.7000	2.1114
864 kg/h	8	25.1	3.1375	2.6055

**Table D36** ANOVA results for effect of mass flow rate of maize grain on the energy used for transportation in drying

Source of Variation	S.S.	D.F.	M.S.	F <sub>computed</sub>	P-value	F <sub>critical</sub>
Mass flow rate	1.4425	2	0.7212	0.3228	0.7276	3.4668
Residual	46.9175	21	2.2342			

Total

48.36

23

**Table D37** Fisher's LSD results for effect of mass flow rate of maize grain on the energy used for transportation in drying

Alpha	DFW	MSW	Student's t-distribution	Fisher's LSD <sub>5%</sub>	ABSMD	MFR (kg/h)
0.05	21	2.2342	2.0796	0.9585	0.1375	720 and 771
					0.5750	720 and 864
					0.4375	771 and 864

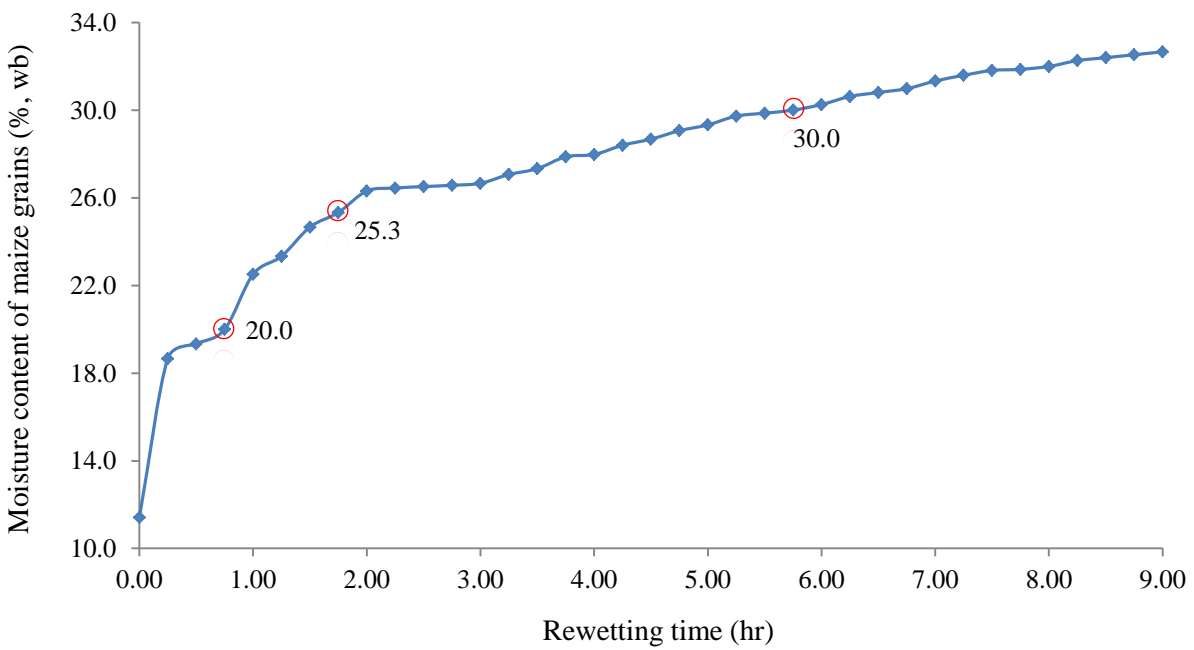


**Figure D1** Variation of maize grain moisture content with rewetting time



**Plate D1** Rewetting of dry maize grain using tap water

**Appendix E: Key Data and Analysis for Objective Three**

**Table E1** Taguchi L9 experiment design with factor levels of energy proportioned for maize grain drying and transportation

Experiment t	Factor levels of energy used for drying	
	Energy used for maize grain drying	Energy used for maize grain transportation
1	1	1
2	1	2
3	1	3
4	2	1
5	2	2
6	2	3
7	3	1
8	3	2
9	3	3

**Table E2** Moisture removal rate and energy proportioned for maize grain drying and transportation with air temperature of 60°C, mass flow rate of 720 kg/h, moisture content of 25% (wet basis) and air mass flow rate of 547 kg/h

Time (hr)	Moisture can	Empty can (g)	Can + wet grain (g)	Can + dry grain (g)	Mean MRR (kg/kg.h)	E <sub>a</sub> (kWh)	E <sub>g</sub> (kWh)
0.00	0A	51.5	76.5	70.0	0.0000	0.0	0.0
	0B	46.5	71.5	64.5			
	0C	49.5	74.5	69.0			
0.25	15A	49.5	74.5	68.5	0.1043	1.0	0.5
	15B	49.5	74.5	69.0			
	15C	48.0	73.0	67.0			
0.50	30A	55.0	80.0	74.5	0.1017	1.8	1.1
	30B	54.5	79.5	74.5			
	30C	49.0	74.0	68.5			

0.75	45A	48.5	73.5	68.5	0.0889	2.3	1.5
	45B	45.5	70.5	65.5			
	45C	52.5	77.5	72.5			
1.00	60A	49.5	74.5	70.0	0.0744	3.5	2.1
	60B	53.5	78.5	73.5			
	60C	47.5	72.5	67.5			
1.25	75A	54.5	79.5	75.0	0.0656	4.3	2.7
	75B	47.0	72.0	67.5			
	75C	53.0	78.0	73.0			
1.50	90A	54.0	79.0	74.5	0.0645	5.1	3.3
	90B	47.0	72.0	67.5			
	90C	47.0	72.0	68.0			
1.75	105A	47.0	72.0	68.0	0.0635	5.7	3.9
	105B	54.0	79.0	75.0			
	105C	50.0	75.0	71.0			
2.00	120A	48.5	73.5	69.5	0.0556	6.5	4.5
	120B	53.0	78.0	74.0			
	120C	54.0	79.0	75.0			
<b>Mean</b>					<b>0.0687</b>	<b>3.4</b>	<b>2.2</b>

MRR is moisture removal rate,  $E_a$  is energy used for maize grain drying,  $E_g$  is energy for maize grain transportation

**Table E3** Moisture removal rate and energy proportioned for maize grain drying and transportation with air temperature of 60°C, mass flow rate of 771 kg/h, moisture content of 25% (wet basis) and air mass flow rate of 547 kg/h

Time (hr)	Moisture can	Empty can (g)	Can +	Can +	Mean	$E_a$ (kWh)	$E_g$ (kWh)
			wet grain (g)	dry grain (g)	MRR (kg/kg.h)		
0.00	0A	51.5	76.5	70.5	0.0000	0.0	0.0
	0B	46.5	71.5	64.5			
	0C	49.5	74.5	68.5			

0.25	15A	49.5	74.5	68.0	0.0702	1.1	0.7
	15B	49.5	74.5	69.0			
	15C	48.0	73.0	67.0			
0.50	30A	55.0	80.0	74.0	0.0690	1.8	1.3
	30B	54.5	79.5	74.0			
	30C	49.0	74.0	68.5			
0.75	45A	48.5	73.5	68.5	0.0678	2.4	1.8
	45B	45.5	70.5	65.0			
	45C	52.5	77.5	72.0			
1.00	60A	49.5	74.5	70.0	0.0667	3.4	2.4
	60B	53.5	78.5	73.0			
	60C	47.5	72.5	67.5			
1.25	75A	54.5	79.5	74.5	0.0595	4.4	3.0
	75B	47.0	72.0	67.5			
	75C	53.0	78.0	73.0			
1.50	90A	54.0	79.0	74.0	0.0596	5.0	3.6
	90B	47.0	72.0	67.5			
	90C	47.0	72.0	68.0			
1.75	105A	47.0	72.0	68.5	0.0594	5.7	4.2
	105B	54.0	79.0	74.5			
	105C	50.0	75.0	70.5			
2.00	120A	48.5	73.5	69.0	0.0556	6.6	4.7
	120B	53.0	78.0	74.5			
	120C	54.0	79.0	75.0			
<b>Mean</b>					<b>0.0564</b>	<b>3.4</b>	<b>2.4</b>

---

MRR is moisture removal rate,  $E_a$  is energy used for maize grain drying,  $E_g$  is energy used for maize grain transportation

**Table E4** Moisture removal rate and energy proportioned for maize grain drying and transportation with air temperature of 60°C, mass flow rate of 864 kg/h, moisture content of 25% (wet basis) and air mass flow rate of 547 kg/h

Time (hr)	Moisture can	Empty can (g)	Can +	Can +	Mean	E <sub>a</sub> (kWh)	E <sub>g</sub> (kWh)
			wet grain (g)	dry grain (g)	MRR (kg/kg.h)		
0.00	0A	51.5	76.5	70.0	0.0000	0.0	0.0
	0B	46.5	71.5	65.0			
	0C	49.5	74.5	68.5			
0.25	15A	49.5	74.5	68.5	0.0650	1.1	0.9
	15B	49.5	74.5	68.0			
	15C	48.0	73.0	67.0			
0.50	30A	55.0	80.0	73.5	0.0606	1.9	1.5
	30B	54.5	79.5	73.5			
	30C	49.0	74.0	69.0			
0.75	45A	48.5	73.5	68.0	0.0570	2.4	2.1
	45B	45.5	70.5	65.0			
	45C	52.5	77.5	72.0			
1.00	60A	49.5	74.5	69.5	0.0549	3.4	2.7
	60B	53.5	78.5	73.0			
	60C	47.5	72.5	67.5			
1.25	75A	54.5	79.5	74.0	0.0533	4.3	3.4
	75B	47.0	72.0	67.5			
	75C	53.0	78.0	73.0			
1.50	90A	54.0	79.0	74.0	0.0496	5.1	4.2
	90B	47.0	72.0	67.0			
	90C	47.0	72.0	67.5			
1.75	105A	47.0	72.0	67.0	0.0468	5.7	4.8
	105B	54.0	79.0	74.5			
	105C	50.0	75.0	70.5			
2.00	120A	48.5	73.5	69.0	0.0484	6.5	5.4



120B	53.0	78.0	73.5
120C	54.0	79.0	75.0

**Mean** **0.0484**    **3.4**    **2.8**

MRR is moisture removal rate,  $E_a$  is energy used for maize grain drying,  $E_g$  is energy used for maize grain transportation

**Table E5** Moisture removal rate and energy proportioned for maize grain drying and transportation with air temperature of 70°C, maize grain mass flow rate of 720 kg/h, moisture content of 25% (wet basis) and air mass flow rate of 547 kg/h

Time (hr)	Moisture can	Empty can (g)	Can +	Can +	Mean	$E_a$ (kWh)	$E_g$ (kWh)
			wet grain (g)	dry grain (g)	MRR (kg/kg.h)		
0.00	0A	51.5	76.5	70.5	0.0000	0.0	0.0
	0B	46.5	71.5	65.0			
	0C	49.5	74.5	68.0			
0.25	15A	49.5	74.5	68.5	0.1379	1.6	0.6
	15B	49.5	74.5	69.0			
	15C	48.0	73.0	67.5			
0.50	30A	55.0	80.0	74.5	0.1176	2.9	1.1
	30B	54.5	79.5	74.5			
	30C	49.0	74.0	69.0			
0.75	45A	48.5	73.5	69.0	0.1093	4.4	1.7
	45B	45.5	70.5	66.0			
	45C	52.5	77.5	72.5			
1.00	60A	49.5	74.5	70.5	0.0968	5.7	2.2
	60B	53.5	78.5	74.0			
	60C	47.5	72.5	68.0			
1.25	75A	54.5	79.5	76.0	0.0832	6.8	2.9
	75B	47.0	72.0	67.5			
	75C	53.0	78.0	73.5			
1.50	90A	54.0	79.0	75.0	0.0741	8.2	3.4

	90B	47.0	72.0	68.0			
	90C	47.0	72.0	68.0			
1.75	105A	47.0	72.0	68.0	0.0635	9.1	4.0
	105B	54.0	79.0	75.0			
	105C	50.0	75.0	71.0			
2.00	120A	48.5	73.5	70.0	0.0556	10.5	4.6
	120B	53.0	78.5	74.0			
	120C	54.0	78.5	74.5			
<b>Mean</b>					<b>0.820</b>	<b>5.5</b>	<b>2.3</b>

MRR is moisture removal rate,  $E_a$  is energy for maize grain drying,  $E_g$  is energy for maize grain transportation

**Table E6** Moisture removal rate and energy proportioned for maize grain drying and grain transportation with air temperature of 70°C, mass flow rate of 771 kg/h, moisture content of 25% (wet basis) and air mass flow rate of 547 kg/h

Time (hr)	Moisture can	Empty can (g)	Can +	Can +	Mean	$E_a$ (kWh)	$E_g$ (kWh)
			wet grain (g)	dry grain (g)	MRR (kg/kg.h)		
0.00	0A	51.5	76.5	70.0	0.0000	0.0	0.0
	0B	46.5	71.5	65.0			
	0C	49.5	74.5	68.5			
0.25	15A	49.5	74.5	68.5	0.1043	1.6	0.7
	15B	49.5	74.5	68.5			
	15C	48.0	73.0	67.5			
0.50	30A	55.0	80.0	75.0	0.1017	2.9	1.2
	30B	54.5	79.5	74.0			
	30C	49.0	74.0	68.5			
0.75	45A	48.5	73.5	69.0	0.0889	4.4	1.8
	45B	45.5	70.5	65.5			
	45C	52.5	77.5	72.0			
1.00	60A	49.5	74.5	70.0	0.0820	5.7	2.3

	60B	53.5	78.5	74.0			
	60C	47.5	72.5	67.5			
1.25	75A	54.5	79.5	75.5	0.0774	6.8	3.0
	75B	47.0	72.0	67.5			
	75C	53.0	78.0	73.5			
1.50	90A	54.0	79.0	74.5	0.0693	8.2	3.6
	90B	47.0	72.0	68.0			
	90C	47.0	72.0	68.0			
1.75	105A	47.0	72.0	68.5	0.0635	9.1	4.2
	105B	54.0	79.0	74.5			
	105C	50.0	75.0	71.0			
2.00	120A	48.5	73.5	69.5	0.0556	10.5	4.8
	120B	53.0	78.5	74.0			
	120C	54.0	78.5	75.0			
<b>Mean</b>					<b>0.0714</b>	<b>5.5</b>	<b>2.4</b>

MRR is moisture removal rate,  $E_a$  is energy used for maize grain drying,  $E_g$  is energy used for maize grain transportation

**Table E7** Moisture removal rate and energy proportioned for maize grain drying and transportation with air temperature of 70°C, mass flow rate of 864 kg/h, moisture content of 25% (wet basis) and air mass flow rate of 547 kg/h

Time (hr)	Moisture can	Empty can (g)	Can +	Can +	Mean	$E_a$ (kWh)	$E_g$ (kWh)
			wet grain (g)	dry grain (g)	MRR (kg/kg.h)		
0.00	0A	51.5	76.5	70.5	0.0000	0.0	0.0
	0B	46.5	71.5	65.0			
	0C	49.5	74.5	68.0			
0.25	15A	49.5	74.5	68.5	0.0908	1.5	0.9
	15B	49.5	74.5	68.5			
	15C	48.0	73.0	67.5			
0.50	30A	55.0	80.0	74.5	0.0855	2.8	1.4

	30B	54.5	79.5	74.0			
	30C	49.0	74.0	68.5			
0.75	45A	48.5	73.5	68.5	0.0784	4.4	2.2
	45B	45.5	70.5	65.0			
	45C	52.5	77.5	72.5			
1.00	60A	49.5	74.5	69.5	0.0744	5.7	2.7
	60B	53.5	78.5	74.0			
	60C	47.5	72.5	67.5			
1.25	75A	54.5	79.5	75.5	0.0656	6.9	3.5
	75B	47.0	72.0	67.0			
	75C	53.0	78.0	73.0			
1.50	90A	54.0	79.0	74.5	0.0645	8.1	4.2
	90B	47.0	72.0	68.0			
	90C	47.0	72.0	67.5			
1.75	105A	47.0	72.0	68.0	0.0594	9.2	4.8
	105B	54.0	79.0	75.0			
	105C	50.0	75.0	70.5			
2.00	120A	48.5	73.5	69.5	0.0556	10.5	5.4
	120B	53.0	78.0	74.5			
	120C	54.0	79.0	74.5			
<b>Mean</b>					<b>0.0638</b>	<b>5.5</b>	<b>2.8</b>

MRR is moisture removal rate,  $E_a$  is energy used for maize grain drying,  $E_g$  is energy for maize grain transportation

**Table E8** Moisture removal rate and energy proportioned for maize grain drying and transportation with air temperature of 80°C, mass flow rate of 720 kg/h, moisture content of 25% (wet basis) and air mass flow rate of 547 kg/h

Time (hr)	Moisture can	Empty can (g)	Can +	Can +	Mean	$E_a$ (kWh)	$E_g$ (kWh)
			wet grain (g)	dry grain (g)	MRR (kg/kg.h)		
0.00	0A	51.5	76.5	70.5	0.0000	0.0	0.0

	0B	46.5	71.5	65.0			
	0C	49.5	74.5	68.0			
0.25	15A	49.5	74.5	69.5	0.2034	2.0	0.5
	15B	49.5	74.5	69.0			
	15C	48.0	73.0	67.5			
0.50	30A	55.0	80.0	74.5	0.1495	3.8	1.0
	30B	54.5	79.5	74.5			
	30C	49.0	74.0	69.0			
0.75	45A	48.5	73.5	68.5	0.1295	6.1	1.5
	45B	45.5	70.5	65.5			
	45C	52.5	77.5	73.0			
1.00	60A	49.5	74.5	70.5	0.1040	7.4	2.1
	60B	53.5	78.5	74.5			
	60C	47.5	72.5	68.0			
1.25	75A	54.5	79.5	75.5	0.0889	9.5	2.6
	75B	47.0	72.0	68.0			
	75C	53.0	78.0	74.0			
1.50	90A	54.0	79.0	75.5	0.0741	10.8	3.3
	90B	47.0	72.0	68.0			
	90C	47.0	72.0	67.5			
1.75	105A	47.0	72.0	68.0	0.0635	12.4	3.8
	105B	54.0	79.0	75.0			
	105C	50.0	75.0	71.0			
2.00	120A	48.5	73.5	69.5	0.0556	13.7	4.5
	120B	53.0	78.0	74.0			
	120C	54.0	79.0	75.0			
	<b>Mean</b>				<b>0.0965</b>	<b>7.3</b>	<b>2.1</b>

---

MRR is moisture removal rate,  $E_a$  is energy used for maize grain drying,  $E_g$  is energy for maize grain transportation

**Table E9** Moisture removal rate and energy proportioned for maize grain drying and transportation with air temperature of 80°C, mass flow rate of 771 kg/h, moisture content of 25% (wet basis) and air mass flow rate of 547 kg/h

Time (hr)	Moisture can	Empty can (g)	Can +	Can +	Mean	E <sub>a</sub> (kWh)	E <sub>g</sub> (kWh)
			wet grain (g)	dry grain (g)	MRR (kg/kg.h)		
0.00	0A	51.5	76.5	70.0	0.0000	0.0	0.0
	0B	46.5	71.5	65.5			
	0C	49.5	74.5	68.0			
0.25	15A	49.5	74.5	69.5	0.1379	2.1	0.6
	15B	49.5	74.5	68.5			
	15C	48.0	73.0	67.0			
0.50	30A	55.0	80.0	75.0	0.1333	3.9	1.2
	30B	54.5	79.5	74.5			
	30C	49.0	74.0	69.0			
0.75	45A	48.5	73.5	68.5	0.1093	6.1	1.7
	45B	45.5	70.5	66.0			
	45C	52.5	77.5	73.0			
1.00	60A	49.5	74.5	70.5	0.0968	7.3	2.4
	60B	53.5	78.5	74.0			
	60C	47.5	72.5	68.0			
1.25	75A	54.5	79.5	75.0	0.0889	9.5	2.9
	75B	47.0	72.0	68.5			
	75C	53.0	78.0	74.0			
1.50	90A	54.0	79.0	75.0	0.0741	10.7	3.5
	90B	47.0	72.0	68.5			
	90C	47.0	72.0	67.5			
1.75	105A	47.0	72.0	68.5	0.0635	12.4	4.1
	105B	54.0	79.0	74.5			
	105C	50.0	75.0	71.0			
2.00	120A	48.5	73.5	69.0	0.0556	13.8	4.8

120B	53.0	78.0	74.5
120C	54.0	79.0	75.0

**Mean** **0.0844**    **7.3**    **2.4**

MRR is moisture removal rate,  $E_a$  is energy used for maize grain drying,  $E_g$  is energy for maize grain transportation

**Table E10** Moisture removal rate and energy proportioned for maize grain drying and transportation with air temperature of 80°C, mass flow rate of 864 kg/h, moisture content of 25% (wet basis) and air mass flow rate of 547 kg/h

Time (hr)	Moisture can	Empty can (g)	Can +	Can +	Mean	$E_a$ (kWh)	$E_g$ (kWh)
			wet grain (g)	dry grain (g)	MRR (kg/kg.h)		
0.00	0A	51.5	76.5	70.5	0.0000	0.0	0.0
	0B	46.5	71.5	65.0			
	0C	49.5	74.5	68.0			
0.25	15A	49.5	74.5	69.0	0.1043	2.1	0.8
	15B	49.5	74.5	68.5			
	15C	48.0	73.0	67.0			
0.50	30A	55.0	80.0	74.5	0.1017	3.8	1.5
	30B	54.5	79.5	74.0			
	30C	49.0	74.0	69.0			
0.75	45A	48.5	73.5	68.5	0.0992	6.1	2.1
	45B	45.5	70.5	66.0			
	45C	52.5	77.5	72.5			
1.00	60A	49.5	74.5	70.0	0.0894	7.3	2.7
	60B	53.5	78.5	73.5			
	60C	47.5	72.5	68.5			
1.25	75A	54.5	79.5	75.0	0.0774	9.6	3.4
	75B	47.0	72.0	68.0			
	75C	53.0	78.0	73.5			
1.50	90A	54.0	79.0	75.0	0.0693	10.8	3.5

	90B	47.0	72.0	68.0			
	90C	47.0	72.0	67.5			
1.75	105A	47.0	72.0	68.0	0.0635	12.4	4.7
	105B	54.0	79.0	74.5			
	105C	50.0	75.0	71.5			
2.00	120A	48.5	73.5	69.0	0.0556	13.7	5.4
	120B	53.0	78.0	74.0			
	120C	54.0	79.0	75.5			
<b>Mean</b>					<b>0.0734</b>	<b>7.3</b>	<b>2.7</b>

MRR is moisture removal rate,  $E_a$  is energy used for maize grain drying,  $E_g$  is energy used for maize grain transportation

**Table E11** Mean moisture removal rate for each level of energy used for maize grain drying and transportation

<b>Energy levels</b>	<b>Mean MRR for each level of energy proportioned for maize grain drying (kg/kg.h)</b>	<b>Mean MRR for each level of energy proportioned for maize grain transportation (kg/kg.h)</b>
1 (3.4 kWh, 2.2 kWh)	0.06	0.08
2 (5.5 kWh, 2.4 kWh)	0.07	0.07
3 (7.3 kWh, 2.8 kWh)	0.08	0.06
$\Delta$ (max-min)	0.03	0.02
Rank	1	2

**Table E12** Mean S/N ratio for moisture removal rate for each level of energy proportioned for maize grain drying and transportation

<b>Level</b>	<b>S/N ratios for MRR factors</b>	
	<b>Mean S/N ratio for <math>E_a</math> (dB)</b>	<b>Mean S/N ratio for <math>E_g</math> (dB)</b>
1 (3.4 kWh, 2.2 kWh)	-24.8	-21.8
2 (5.5 kWh, 2.4 kWh)	-22.9	-23.1
3 (7.3 kWh, 2.8 kWh)	-21.5	-24.3



$\Delta$ (max-min)	3.4	2.5
Rank	1	2

**Table E13** ANOVA results for optimisation of energy proportioned for maize grain drying and transportation with respect to moisture removal rate

Source of variation	d.f.	s.s.	m.s.	F-value	P-value	Contribution (%)
E <sub>a</sub>	2	1.09E-03	5.44E-04	316.04	<.001	62.8
E <sub>g</sub>	2	6.37E-04	3.19E-04	184.99	<.001	36.8
Residual	4	6.89E-06	1.72E-06			0.4
Total	8	1.73E-03				

**Table E14** Actual and simulated moisture removal rate for various combinations of energy proportioned for maize grain drying and transportation

Experiment	Actual MRR (kg/kg.h)	Simulated MRR (kg/kg.h)
1	0.0687	0.0665
2	0.0564	0.0600
3	0.0484	0.0470
4	0.0820	0.0810
5	0.0714	0.0745
6	0.0638	0.0615
7	0.0965	0.0935
8	0.0844	0.0869
9	0.0734	0.0739

**Table E15** Actual and simulated S/N ratios for moisture removal rate for various combinations energy proportioned for maize grain drying and transportation

Experiment	Actual S/N ratio for MRR (dB)	Simulated S/N ratio for MRR (dB)
1	-23.3	-23.7
2	-25.0	-24.5
3	-26.3	-26.1
4	-21.7	-21.9
5	-22.9	-22.8

6	-23.9	-24.3
7	-20.3	-20.3
8	-21.5	-21.2
9	-22.7	-22.8

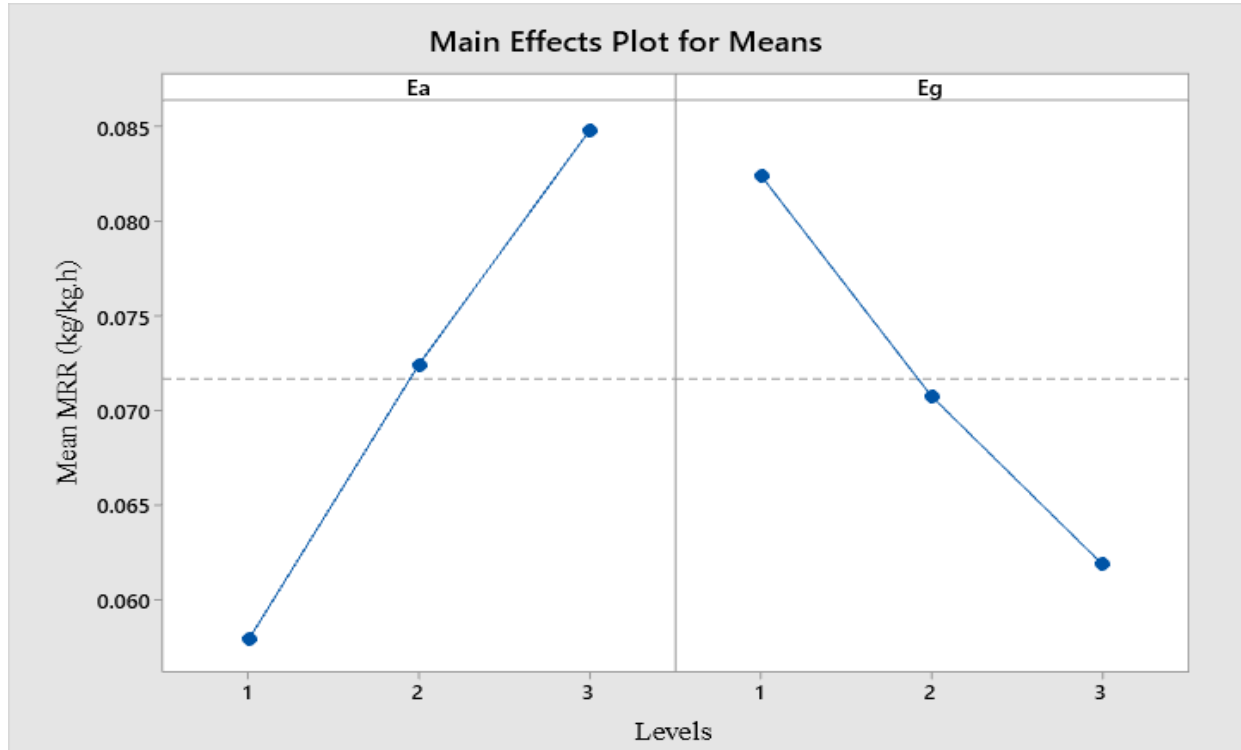


**Figure E1** Mean moisture removal rate for each level of energy proportioned for maize grain drying and transportation

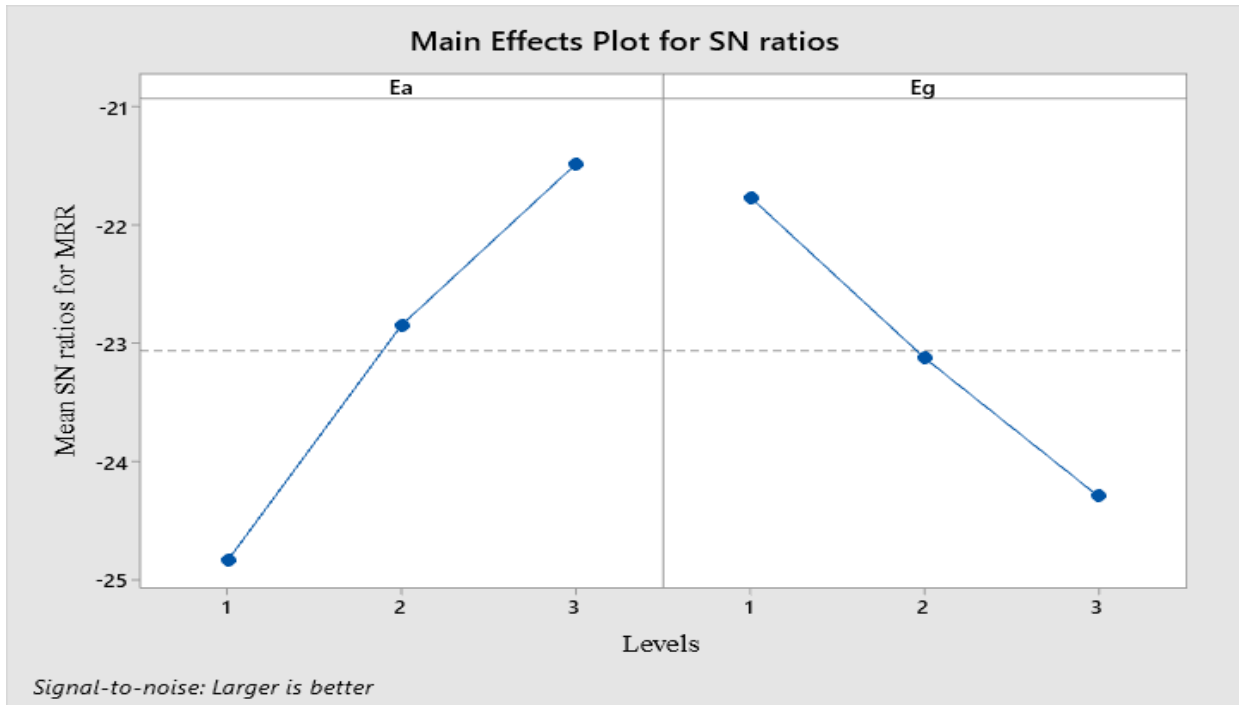


**Figure E2** Mean S/N ratios for moisture removal rate with respect to levels of energy proportioned for maize grain drying and transportation

### Appendix F: Key Data and Analysis for Objective Four

**Table F1** Taguchi L9 orthogonal design of experiment with factor levels for optimisation of moisture content, air temperature and mass flow rate of maize grain with respect to moisture removal rate and energy used in drying

Experiment	Levels of selected process parameters		
	MC	T <sub>a</sub>	MFR
1	1	1	1
2	1	2	2
3	1	3	3
4	2	1	2
5	2	2	3
6	2	3	1
7	3	1	3
8	3	2	1
9	3	3	2

**Table F2** Moisture removal rate and energy used with respect to moisture content of 20% (wet basis) air temperature of 60°C and maize grain mass flow rate of 720 kg/h in drying

Time (hr)	Moisture can	Empty can (g)	Can + wet grain (g)	Can + dry grain (g)	Mean	
					MRR (kg/kg.h)	EU (kWh)
0.00	0A	51.5	76.5	71.4	0.0000	0.0
	0B	46.5	71.0	65.9		
	0C	49.5	75.0	70.0		
0.25	15A	49.5	74.5	70.0	0.1543	1.4
	15B	49.5	74.5	70.2		
	15C	48.0	73.0	69.0		
0.50	30A	55.0	80.0	76.1	0.1046	2.8
	30B	54.5	79.5	75.5		
	30C	49.0	74.0	70.0		
0.75	45A	48.5	73.5	70.0	0.0875	3.7

	45B	45.5	70.5	66.5		
	45C	52.5	77.5	74.0		
1.00	60A	49.5	74.5	71.0	0.0800	5.5
	60B	53.5	78.5	75.5		
	60C	47.5	72.5	69.0		
1.25	75A	54.5	79.5	76.5	0.0663	6.9
	75B	47.0	72.0	68.7		
	75C	53.0	78.0	74.5		
1.50	90A	54.0	79.0	76.0	0.0552	8.2
	90B	47.0	72.0	69.0		
	90C	47.0	72.0	68.2		
1.75	105A	47.0	72.0	68.7	0.0473	9.4
	105B	54.0	79.0	76.0		
	105C	50.0	75.0	71.5		
2.00	120A	48.5	73.5	70.0	0.0414	10.8
	120B	53.0	78.0	75.0		
	120C	54.0	79.0	75.7		
<b>Mean</b>					<b>0.0796</b>	<b>6.1</b>

MRR is moisture removal rate and EU is energy used for maize grain drying and transportation

**Table F3** Moisture removal rate and energy used with respect to moisture content of 20% (Wet basis), air temperature of 70°C and maize grain mass flow rate of 771 kg/h in drying

Time (hr)	Moisture can	Empty can (g)	Can + wet grain (g)	Can + dry grain (g)	Mean	
					MRR (kg/kg.h)	EU (kWh)
0.00	0A	51.5	76.5	71.5	0.0000	0.0
	0B	46.5	71.5	66.5		
	0C	49.5	74.5	69.4		
0.25	15A	49.5	74.5	70.0	0.1664	2.2
	15B	49.5	74.5	70.5		
	15C	48.0	73.0	69.0		

0.50	30A	55.0	80.0	76.0	0.1134	4.0
	30B	54.5	79.5	76.0		
	30C	49.0	74.0	70.0		
0.75	45A	48.5	73.5	70.0	0.0951	6.1
	45B	45.5	70.5	67.0		
	45C	52.5	77.5	74.0		
1.00	60A	49.5	74.5	71.4	0.0813	7.8
	60B	53.5	78.5	75.3		
	60C	47.5	72.5	69.0		
1.25	75A	54.5	79.5	76.0	0.0650	9.7
	75B	47.0	72.0	69.0		
	75C	53.0	78.0	74.7		
1.50	90A	54.0	79.0	75.6	0.0542	11.6
	90B	47.0	72.0	68.7		
	90C	47.0	72.0	68.9		
1.75	105A	47.0	72.0	69.0	0.0465	13.1
	105B	54.0	79.0	75.6		
	105C	50.0	75.0	71.6		
2.00	120A	48.5	73.5	70.0	0.0406	15.1
	120B	53.0	78.5	75.2		
	120C	54.0	78.5	75.5		
<b>Mean</b>					<b>0.0828</b>	<b>8.7</b>

MRR is moisture removal rate and EU is energy used for maize grain drying and transportation

**Table F4** Moisture removal rate and energy used with respect to moisture content of 20% (wet basis), air temperature of 80°C and maize grain mass flow rate of 864 kg/h in drying

Time (hr)	Moisture can	Empty can (g)	Can + wet grain (g)	Can + dry grain (g)	Mean	
					MRR (kg/kg.h)	EU (kWh)
0.00	0A	51.5	76.5	71.5	0.0000	0.0
	0B	46.5	71.5	66.4		

	0C	49.5	74.5	69.5		
0.25	15A	49.5	74.5	70.5	0.1968	2.8
	15B	49.5	74.5	70.5		
	15C	48.0	73.0	69.0		
0.50	30A	55.0	80.0	76.5	0.1426	5.2
	30B	54.5	79.5	76.0		
	30C	49.0	74.0	70.5		
0.75	45A	48.5	73.5	70.0	0.0989	8.1
	45B	45.5	70.5	67.2		
	45C	52.5	77.5	74.0		
1.00	60A	49.5	74.5	71.0	0.0813	9.9
	60B	53.5	78.5	75.0		
	60C	47.5	72.5	69.7		
1.25	75A	54.5	79.5	76.5	0.0650	12.8
	75B	47.0	72.0	69.0		
	75C	53.0	78.0	74.2		
1.50	90A	54.0	79.0	76.0	0.0542	14.1
	90B	47.0	72.0	69.0		
	90C	47.0	72.0	68.2		
1.75	105A	47.0	72.0	68.6	0.0465	16.9
	105B	54.0	79.0	75.6		
	105C	50.0	75.0	72.0		
2.00	120A	48.5	73.5	70.0	0.0406	18.8
	120B	53.0	78.0	75.1		
	120C	54.0	79.0	75.6		
	<b>Mean</b>				<b>0.0907</b>	<b>11.1</b>

---

MRR is moisture removal rate and EU is energy used for maize grain drying and transportation

**Table F5** Moisture removal rate and energy used with respect to moisture content of 25% (wet basis), air temperature of 60°C and maize grain mass flow rate of 771 kg/h in drying

Time (hr)	Moisture can	Empty can (g)	Can + wet grain (g)	Can + dry grain (g)	Mean	
					MRR (kg/kg.h)	EU (kWh)
0.00	0A	76.5	70.5	6.0	0.0000	0.0
	0B	71.5	64.5	7.0		
	0C	74.5	68.5	6.0		
0.25	15A	74.5	68.0	6.5	0.0702	1.8
	15B	74.5	69.0	5.5		
	15C	73.0	67.0	6.0		
0.50	30A	80.0	74.0	6.0	0.0690	3.1
	30B	79.5	74.0	5.5		
	30C	74.0	68.5	5.5		
0.75	45A	73.5	68.5	5.0	0.0678	4.2
	45B	70.5	65.0	5.5		
	45C	77.5	72.0	5.5		
1.00	60A	74.5	70.0	4.5	0.0667	5.8
	60B	78.5	73.0	5.5		
	60C	72.5	67.5	5.0		
1.25	75A	79.5	74.5	5.0	0.0595	7.4
	75B	72.0	67.5	4.5		
	75C	78.0	73.0	5.0		
1.50	90A	79.0	74.0	5.0	0.0596	8.6
	90B	72.0	67.5	4.5		
	90C	72.0	68.0	4.0		
1.75	105A	72.0	68.5	3.5	0.0594	9.9
	105B	79.0	74.5	4.5		
	105C	75.0	70.5	4.5		
2.00	120A	73.5	69.0	4.5	0.0556	11.3
	120B	78.0	74.5	3.5		



**Mean**

**0.0635**

**6.5**

MRR is moisture removal rate and EU is energy used for maize grain drying and transportation

**Table F6** Moisture removal rate and energy used with respect to moisture content of 25% (wet basis), air temperature of 70°C and maize grain mass flow rate of 864 kg/h in drying

<b>Time (hr)</b>	<b>Moisture can</b>	<b>Empty can (g)</b>	<b>Can + wet grain (g)</b>	<b>Can + dry grain (g)</b>	<b>Mean</b>	
					<b>MRR (kg/kg.h)</b>	<b>EU (kWh)</b>
0.00	0A	51.5	76.5	70.5	0.0000	0.0
	0B	46.5	71.5	65.0		
	0C	49.5	74.5	68.0		
0.25	15A	49.5	74.5	68.5	0.0908	2.4
	15B	49.5	74.5	68.5		
	15C	48.0	73.0	67.5		
0.50	30A	55.0	80.0	74.5	0.0855	4.2
	30B	54.5	79.5	74.0		
	30C	49.0	74.0	68.5		
0.75	45A	48.5	73.5	68.5	0.0784	6.6
	45B	45.5	70.5	65.0		
	45C	52.5	77.5	72.5		
1.00	60A	49.5	74.5	69.5	0.0744	8.4
	60B	53.5	78.5	74.0		
	60C	47.5	72.5	67.5		
1.25	75A	54.5	79.5	75.5	0.0656	10.4
	75B	47.0	72.0	67.0		
	75C	53.0	78.0	73.0		
1.50	90A	54.0	79.0	74.5	0.0645	12.3
	90B	47.0	72.0	68.0		
	90C	47.0	72.0	67.5		
1.75	105A	47.0	72.0	68.0	0.0594	14.0
	105B	54.0	79.0	75.0		

	105C	50.0	75.0	70.5		
2.00	120A	48.5	73.5	69.5	0.0556	15.9
	120B	53.0	78.0	74.5		
	<b>Mean</b>				<b>0.0718</b>	<b>9.3</b>

MRR is moisture removal rate and EU is energy used for maize grain drying and transportation

**Table F7** Moisture removal rate and energy used with respect to moisture content of 25% (wet basis), air temperature of 80°C and maize grain mass flow rate of 720 kg/h in drying

Time (hr)	Moisture can	Empty can (g)	Can + wet grain (g)	Can + dry grain (g)	Mean	
					MRR (kg/kg.h)	EU (kWh)
0.00	0A	51.5	76.5	70.5	0.0000	0.0
	0B	46.5	71.5	65.0		
	0C	49.5	74.5	68.0		
0.25	15A	49.5	74.5	69.5	0.2034	2.5
	15B	49.5	74.5	69.0		
	15C	48.0	73.0	67.5		
0.50	30A	55.0	80.0	74.5	0.1495	4.8
	30B	54.5	79.5	74.5		
	30C	49.0	74.0	69.0		
0.75	45A	48.5	73.5	68.5	0.1295	7.6
	45B	45.5	70.5	65.5		
	45C	52.5	77.5	73.0		
1.00	60A	49.5	74.5	70.5	0.1040	9.5
	60B	53.5	78.5	74.5		
	60C	47.5	72.5	68.0		
1.25	75A	54.5	79.5	75.5	0.0889	12.1
	75B	47.0	72.0	68.0		
	75C	53.0	78.0	74.0		
1.50	90A	54.0	79.0	75.5	0.0741	14.1
	90B	47.0	72.0	68.0		

	90C	47.0	72.0	67.5		
1.75	105A	47.0	72.0	68.0	0.0635	16.2
	105B	54.0	79.0	75.0		
	105C	50.0	75.0	71.0		
2.00	120A	48.5	73.5	69.5	0.0556	18.2
	120B	53.0	78.0	74.0		
<b>Mean</b>					<b>0.1086</b>	<b>10.6</b>

MRR is moisture removal rate and EU is energy used for maize grain drying and transportation

**Table F8** Moisture removal rate and energy used with respect to moisture content of 30% (wet basis), air temperature of 60°C and maize grain mass flow rate of 864 kg/h in drying

Time (hr)	Moisture can	Empty can (g)	Can + wet grain (g)	Can + dry grain (g)	Mean	
					MRR (kg/kg.h)	EU (kWh)
0.00	0A	51.5	76.5	69.0	0.0000	0.0
	0B	46.5	71.5	64.0		
	0C	49.5	74.5	67.0		
0.25	15A	49.5	74.5	67.5	0.0452	2.2
	15B	49.5	74.5	67.0		
	15C	48.0	73.0	65.6		
0.50	30A	55.0	80.0	72.6	0.0410	3.5
	30B	54.5	79.5	72.5		
	30C	49.0	74.0	67.0		
0.75	45A	48.5	73.5	66.2	0.0406	4.6
	45B	45.5	70.5	64.0		
	45C	52.5	77.5	70.4		
1.00	60A	49.5	74.5	67.2	0.0402	6.2
	60B	53.5	78.5	72.0		
	60C	47.5	72.5	66.0		
1.25	75A	54.5	79.5	72.5	0.0377	7.9
	75B	47.0	72.0	65.6		

	75C	53.0	78.0	71.5		
1.50	90A	54.0	79.0	72.5	0.0360	9.5
	90B	47.0	72.0	65.0		
	90C	47.0	72.0	66.0		
1.75	105A	47.0	72.0	66.0	0.0357	10.7
	105B	54.0	79.0	73.0		
	105C	50.0	75.0	68.0		
2.00	120A	48.5	73.5	67.0	0.0354	12.2
	120B	53.0	78.0	71.0		
<b>Mean</b>					<b>0.0390</b>	<b>7.1</b>

MRR is moisture removal rate and EU is energy used for maize grain drying and transportation

**Table F9** Moisture removal rate and energy used with respect to moisture content of 30% (wet basis), air temperature of 70°C and maize grain mass flow rate of 720 kg/h in drying

Time (hr)	Moisture can	Empty can (g)	Can + wet grain (g)	Can + dry grain (g)	Mean	
					MRR (kg/kg.h)	EU (kWh)
0.00	0A	51.5	76.5	68.5	0.0000	0.0
	0B	46.5	71.5	64.5		
	0C	49.5	74.5	67.0		
0.25	15A	49.5	74.5	67.5	0.0967	2.1
	15B	49.5	74.5	67.3		
	15C	48.0	73.0	66.0		
0.50	30A	55.0	80.0	73.5	0.0909	4.0
	30B	54.5	79.5	73.0		
	30C	49.0	74.0	67.0		
0.75	45A	48.5	73.5	67.5	0.0900	6.0
	45B	45.5	70.5	64.3		
	45C	52.5	77.5	71.0		
1.00	60A	49.5	74.5	68.5	0.0870	7.8
	60B	53.5	78.5	73.0		

	60C	47.5	72.5	66.5		
1.25	75A	54.5	79.5	74.0	0.0845	9.7
	75B	47.0	72.0	66.5		
	75C	53.0	78.0	72.7		
1.50	90A	54.0	79.0	74.0	0.0833	11.8
	90B	47.0	72.0	67.0		
	90C	47.0	72.0	67.0		
1.75	105A	47.0	72.0	67.5	0.0794	13.2
	105B	54.0	79.0	74.5		
	105C	50.0	75.0	70.0		
2.00	120A	48.5	73.5	69.0	0.0766	15.2
	120B	53.0	78.0	74.0		
	120C	54.0	79.0	74.5		
<b>Mean</b>					<b>0.0860</b>	<b>8.7</b>

MRR is moisture removal rate and EU is energy used for maize grain drying and transportation

**Table F10** Moisture removal rate and energy used with respect to moisture content of 20% (wb), air temperature of 60°C and maize grain mass flow rate of 720 kg/h in drying

<b>Time (hr)</b>	<b>Moisture can</b>	<b>Empty can (g)</b>	<b>Can + wet grain (g)</b>	<b>Can + dry (g)</b>	<b>MRR (kg/kg.h)</b>	<b>EU (kWh)</b>
0.00	0A	51.5	76.5	68.7	0.0000	0.0
	0B	46.5	71.5	64.1		
	0C	49.5	74.5	67.1		
0.25	15A	49.5	74.5	67.0	0.1185	2.8
	15B	49.5	74.5	67.5		
	15C	48.0	73.0	66.5		
0.50	30A	55.0	80.0	73.5	0.1117	5.2
	30B	54.5	79.5	73.0		
	30C	49.0	74.0	67.5		
0.75	45A	48.5	73.5	67.0	0.1076	8.0
	45B	45.5	70.5	64.5		

	45C	52.5	77.5	72.0		
1.00	60A	49.5	74.5	68.5	0.1043	9.9
	60B	53.5	78.5	73.0		
	60C	47.5	72.5	67.5		
1.25	75A	54.5	79.5	74.5	0.1013	12.5
	75B	47.0	72.0	67.0		
	75C	53.0	78.0	73.0		
1.50	90A	54.0	79.0	74.0	0.0893	14.4
	90B	47.0	72.0	67.5		
	90C	47.0	72.0	67.0		
1.75	105A	47.0	72.0	67.5	0.0885	16.7
	105B	54.0	79.0	74.5		
	105C	50.0	75.0	71.0		
2.00	120A	48.5	73.5	69.0	0.0808	18.8
	120B	53.0	78.0	74.0		
<b>Mean</b>					<b>0.1002</b>	<b>11.0</b>

MRR is moisture removal rate and EU is energy used for maize grain drying and transportation

**Table F11** Mean moisture removal rates for each level of moisture content, air temperature and maize grain mass flow rate in drying

Level	Mean of MRR for each level of process parameters (kg/kg.h)		
	MC	T <sub>a</sub>	MFR
1 (20%, 60°C, 720 kg/h)	0.084	0.061	0.091
2 (25%, 70°C, 771 kg/h)	0.081	0.080	0.082
3 (30%, 80°C, 864 kg/h)	0.075	0.100	0.067
Δ (Max-min)	0.009	0.039	0.024
Rank	3	1	2

MRR is moisture removal rate, MC is moisture content, T<sub>a</sub> air temperature, MFR is mass flow rate of maize grain

**Table F12** Mean energy used for each level of moisture content, air temperature and maize grain mass flow rate in drying

Level	Mean of EU for each level of process parameters (kWh)		
	MC	T <sub>a</sub>	MFR
1 (20%, 60°C, 720 kg/h)	8.6	6.6	8.5
2 (25%, 70°C, 771 kg/h)	8.8	8.9	8.8
3 (30%, 80°C, 864 kg/h)	9.0	10.9	9.2
Δ (Max-min)	0.3	4.3	0.7
Rank	3	1	2

EU is energy used for maize grain drying and transportation, MC is moisture content, T<sub>a</sub> air temperature, MFR is mass flow rate of maize grain

**Table F13** Mean S/N ratios for moisture removal rate for each level of moisture content, air temperature and maize grain mass flow rate in drying

Level	Mean S/N ratio for MRR for each level of process parameters (dB)		
	MC (% , wb)	T <sub>a</sub> (°C)	MFR (kg/h)
1 (20%, 60°C, 720 kg/h)	-21.5	-24.7	-20.9
2 (25%, 70°C, 771 kg/h)	-22.0	-21.9	-21.9
3 (30%, 80°C, 864 kg/h)	-23.2	-20.0	-24.0
Δ (Max-min)	1.7	4.7	3.1
Rank	3	1	2

MRR is moisture removal rate, MC is moisture content, T<sub>a</sub> air temperature, MFR is mass flow rate of maize grain

**Table F14** Mean S/N ratios for energy used for each level of moisture content, air temperature and mass flow rate

Level	Mean S/N for EU for each level of process parameters (dB)		
	MC (% , wb)	T <sub>a</sub> (°C)	MFR (kg/h)
1 (20%, 60°C, 720 kg/h)	-18.5	-16.3	-18.3
2 (25%, 70°C, 771 kg/h)	-18.7	-19.0	-18.6
3 (30%, 80°C, 864 kg/h)	-18.9	-20.7	-19.1
Δ (Max-min)	0.4	4.4	0.8
Rank	3	1	2

EU is energy used for maize drying and transportation, MC is moisture content, T<sub>a</sub> air temperature, MFR is mass flow rate of maize grain

**Table F15** ANOVA results for optimisation of moisture content, air temperature and maize grain mass flow rate with respect to moisture removal rate in drying

Source of variation	d.f.	s.s.	m.s.	F-value	P-value	Contribution (%)
MC	2	0.00013392	0.00006696	1.78	0.360	3.9
T <sub>a</sub>	2	0.00230132	0.00115066	30.60	0.032	67.5
MFR	2	0.00089687	0.00044843	11.92	0.077	26.3
Residual	2	0.00007521	0.00003761			2.2
Total	8	0.00340732				

**Table F16** ANOVA results for optimisation of moisture content, air temperature and maize grain mass flow rate with respect to energy used in drying

Source of variation	d.f.	s.s.	m.s.	F-value	P-value	Contribution (%)
MC	2	0.16722	0.08361	71.88	0.014	0.6
T <sub>a</sub>	2	28.38087	14.19043	12199.54	<.001	97.1
MFR	2	0.68337	0.34168	293.75	0.003	2.3
Residual	2	0.00233	0.00116			0.0
Total	8	29.23379				



**Table F17** Actual and simulated moisture removal rates for various combinations of moisture content, air temperature and maize grain mass flow rate in drying

<b>Experiment</b>	<b>Actual MRR (kg/kg.h)</b>	<b>Simulated MRR (kg/kg.h)</b>
1	0.0796	0.0748
2	0.0828	0.0890
3	0.0908	0.0909
4	0.0635	0.0647
5	0.0718	0.0667
6	0.1086	0.1094
7	0.0390	0.0424
8	0.0860	0.0851
9	0.1003	0.0993

MRR is moisture removal rate

**Table F18** Actual and simulated energy used for various combinations of moisture content, air temperature and maize grain mass flow rate in drying

<b>Experiment</b>	<b>Actual EU (kWh)</b>	<b>Simulated EU (kWh)</b>
1	6.1	6.2
2	8.7	8.5
3	11.1	11.2
4	6.5	6.5
5	9.3	9.2
6	10.6	10.7
7	7.1	7.2
8	8.7	8.7
9	11.0	11.0

EU is energy used for maize grain drying and transportation

**Table F19** Actual and simulated S/N ratios for moisture removal rate for various combinations of moisture content, air temperature and maize grain mass flow rate in drying

<b>Experiment</b>	<b>Actual S/N ratio for MRR (dB)</b>	<b>Simulated S/N ratio for MRR (dB)</b>
1	-21.9840	-22.4820
2	-21.6380	-20.8620
3	-20.8430	-20.8390
4	-23.9490	-24.0290
5	-22.8820	-24.0060
6	-19.2870	-18.6470
7	-28.1790	-27.1730
8	-21.3060	-21.8140
9	-19.9790	-20.1940

S/N is signal to noise ratio and MRR is moisture removal rate

**Table F20** Actual and simulated S/N ratios for energy used for maize grain drying and transportation for various combinations of moisture content, air temperature and maize grain mass flow rate in drying

<b>Experiment</b>	<b>Actual S/N ratio for EU (dB)</b>	<b>Simulated S/N ratio for EU (dB)</b>
1	-15.7066	-15.9650
2	-18.79039	-18.3440
3	-20.90646	-21.0950
4	-16.25827	-16.3530
5	-19.36966	-19.1040
6	-20.50612	-20.6140
7	-17.02517	-17.1120
8	-18.79039	-18.6220
9	-20.82785	-21.0020

S/N is signal to noise ratio and EU is energy used for maize grain drying and transportation

**Table F21** Confirmatory experiment for optimum combination of moisture content, air temperature, maize grain mass flow rate with respect to moisture removal rate in drying

<b>Time (hr)</b>	<b>Moisture can</b>	<b>Empty can (g)</b>	<b>Can + wet grain (g)</b>	<b>Can + dry (g)</b>	<b>MRR (kg/kg.h)</b>	<b>EU (kWh)</b>
0.00	0A	51.5	76.5	71.4	0.0000	0.0
	0B	46.5	71.5	66.5		
	0C	49.5	74.5	69.5		
0.25	15A	49.5	74.5	71.2	0.3082	2.8
	15B	49.5	74.5	71.2		
	15C	48.0	73.0	69.5		
0.50	30A	55.0	80.0	76.5	0.1569	5.2
	30B	54.5	79.5	76.5		
	30C	49.0	74.0	70.5		
0.75	45A	48.5	73.5	70.3	0.1103	8.0
	45B	45.5	70.5	67.2		
	45C	52.5	77.5	74.3		
1.00	60A	49.5	74.5	71.3	0.0855	9.9
	60B	53.5	78.5	75.4		
	60C	47.5	72.5	69.3		
1.25	75A	54.5	79.5	76.5	0.0698	12.5
	75B	47.0	72.0	68.9		
	75C	53.0	78.0	74.7		
1.50	90A	54.0	79.0	76.0	0.0579	14.4
	90B	47.0	72.0	69.0		
	90C	47.0	72.0	68.6		
1.75	105A	47.0	72.0	68.9	0.0497	16.7
	105B	54.0	79.0	75.7		
	105C	50.0	75.0	72.0		
2.00	120A	48.5	73.5	70.5	0.0434	18.8
	120B	53.0	78.0	75.0		
<b>Mean</b>					<b>0.1102</b>	<b>10.3</b>

MRR is moisture removal rate and EU is energy used for drying and transportation

**Table F22** Comparison of actual and Page model moisture ratios

<b>Time (h)</b>	<b>Actual MR</b>	<b>Page model MR</b>
0.00	1.00	1.00
0.25	0.62	0.62
0.50	0.61	0.60
0.75	0.59	0.59
1.00	0.58	0.58
1.25	0.57	0.58
1.50	0.57	0.57
1.75	0.57	0.57
2.00	0.57	0.56

MR is moisture ratio

**Table F23** Student's test results for difference in means between actual and Page model moisture ratios

	<b>Page model MR</b>	<b>Actual MR</b>
Mean	0.631	0.630
Variance	0.019	0.020
Observations	9	9
Pearson Correlation	0.999	
Hypothesized Mean Difference	0	
df	8	
t Stat	0.651	
P(T<=t) one-tail	0.267	
t Critical one-tail	1.860	
P(T<=t) two-tail	0.533	
t Critical two-tail	2.306	

MR is moisture ratio

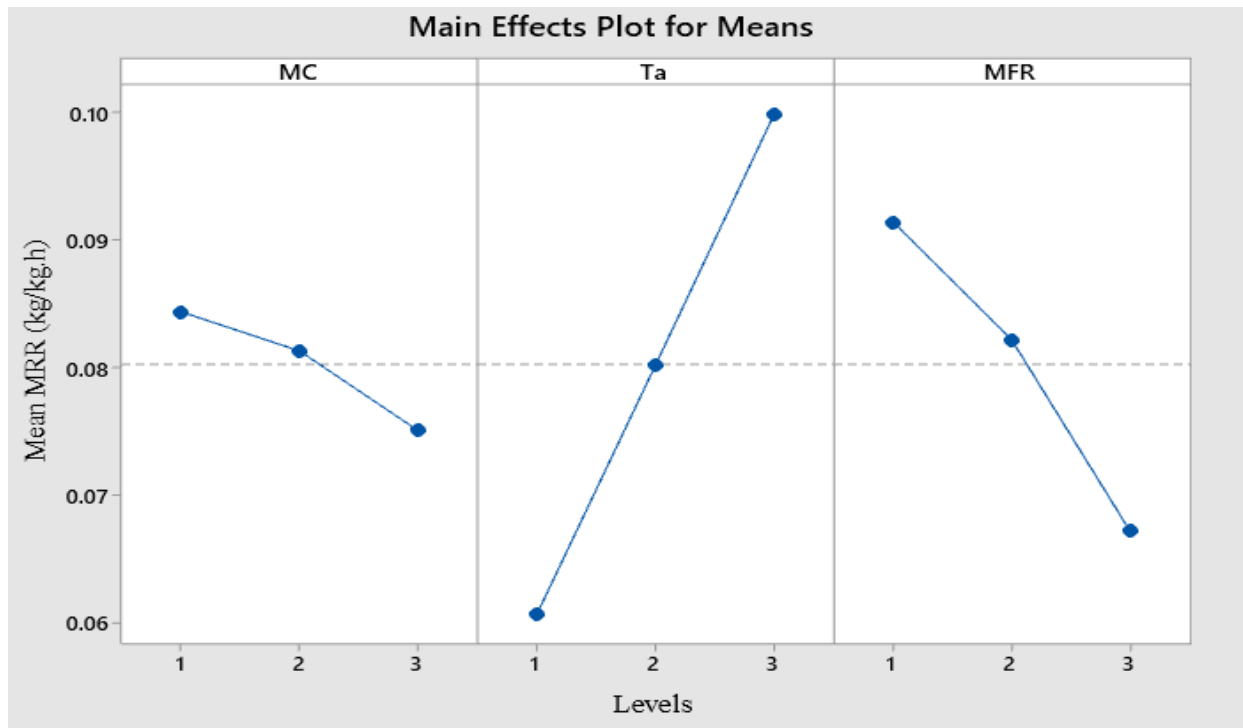


**Figure F1** Mean of moisture removal rates in maize drying with respect to moisture content, air temperature and mass flow rate levels

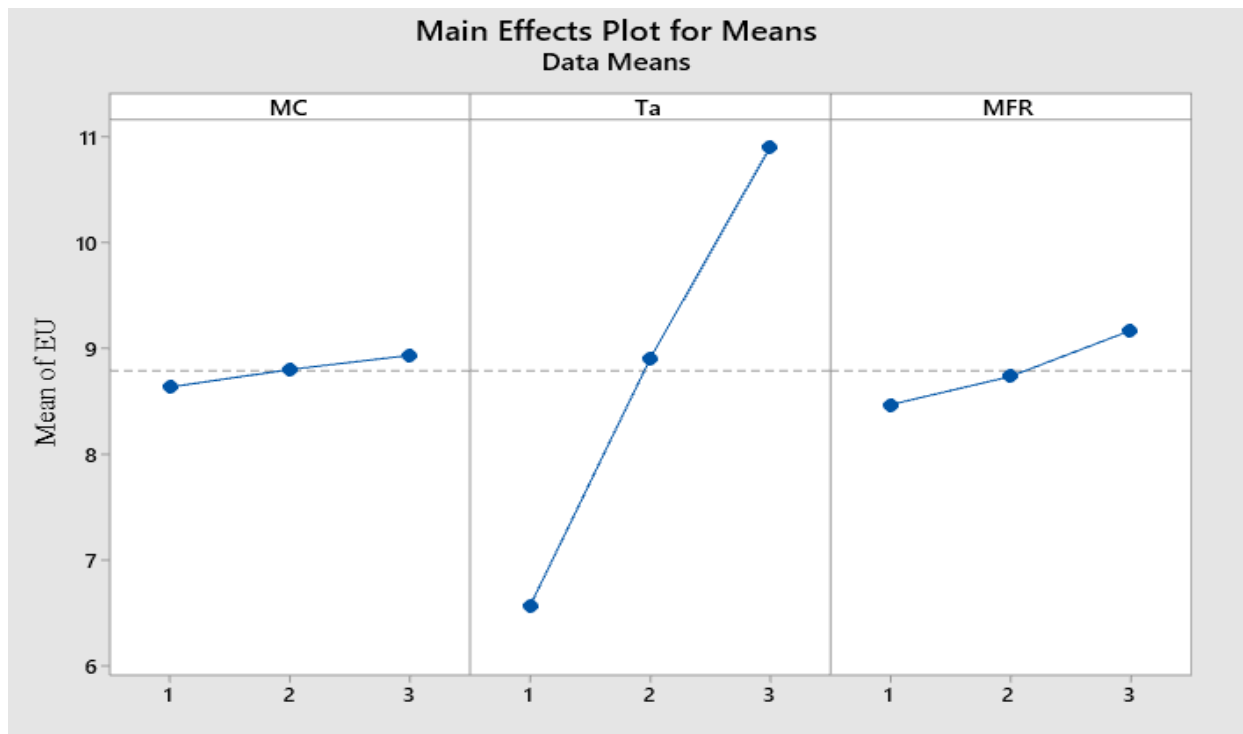


**Figure F2** Mean of energy used in maize grain drying with respect to moisture content, air temperature and mass flow rate levels

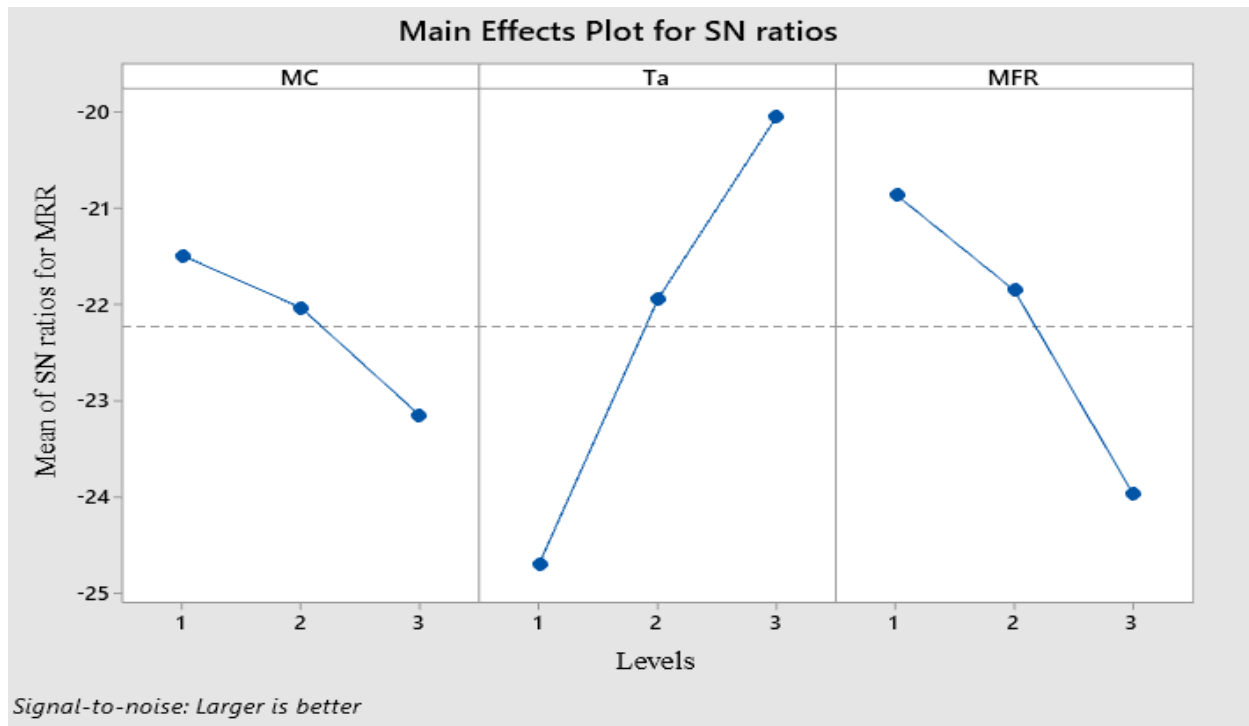


**Figure F3** Mean of S/N ratios for moisture removal rate in maize grain drying with respect to moisture content, air temperature and maize grain mass flow rate levels

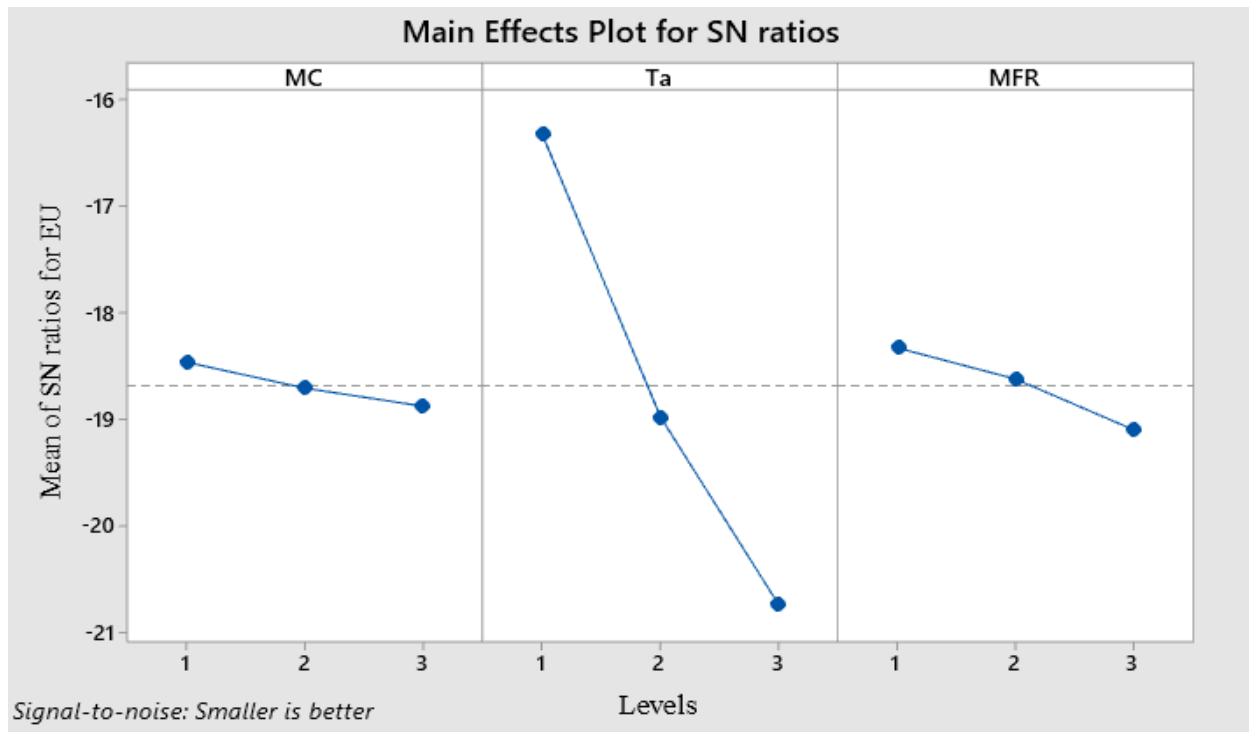


**Figure F4** Mean of S/N ratios for energy used in maize grain drying with respect to moisture content, air temperature and maize grain mass flow rate levels

## Appendix G: Published Paper on Objective One

Korir, M. K., Njue, M. R., & Nyaanga, D. M. (2022). Validation of Simulation Models for Mass Flow Rate of Maize Grain Through Horizontal Circular Orifices. *Bioprocess Engineering*, 6(2), 40-45.

---

### Bioprocess Engineering

2022; 6(2): 40-45

<http://www.sciencepublishinggroup.com/j/be>

doi: 10.11648/j.be.20220602.16

ISSN: 2578-8698 (Print); ISSN: 2578-8701 (Online)



---

## Validation of Simulation Models for Mass Flow Rate of Maize Grain Through Horizontal Circular Orifices

Meshack Kipruto Korir<sup>\*</sup>, Musa Rugiri Njue, Daudi Mongeri Nyaanga

Department of Agricultural Engineering, Faculty of Engineering and Technology, Egerton University, Nakuru, Kenya

### Email address:

meshack.korir@egerton.ac.ke (Meshack Kipruto Korir), mrugiri@egerton.ac.ke (Musa Rugiri Njue),

dmnyaanga@egerton.ac.ke (Daudi Mongeri Nyaanga)

<sup>\*</sup>Corresponding author

### To cite this article:

Meshack Kipruto Korir, Musa Rugiri Njue, Daudi Mongeri Nyaanga. Validation of Simulation Models for Mass Flow Rate of Maize Grain Through Horizontal Circular Orifices. *Bioprocess Engineering*. Vol. 6, No. 2, 2022, pp. 40-45. doi: 10.11648/j.be.20220602.16

Received: October 30, 2022; Accepted: November 28, 2022; Published: December 8, 2022

---

**Abstract:** The mass flow rate (MFR) of maize grain is essential in determining appropriate size of orifice for flow control. There are several simulation models for MFR that have been developed. However, there is need for a reliable simulation model for MFR of maize grain through horizontal circular orifices. In this paper, the Beverloo, British Code of Practice (BCP) and Tudor simulation models for MFR were validated. The experimental results used in validation were obtained by discharging 12.0 kg of maize grain (Hybrid 614 variety) through horizontal circular orifices with diameters ranging from 0.040 m to 0.056 m. The time taken for the grain to flow through the orifices was recorded and MFR determined. The moisture content of the maize grain used was 11.4%, wet basis. The actual MFR ranged from 720 kg/h to 1735 kg/h, 650 kg/h to 2006 kg/h for Beverloo, 851 kg/h to 2378 kg/h for BCP and 867 kg/h to 2010 kg/h for Tudor model. The data analysis showed that none of the simulation models results best fitted the experimental. Therefore, New model was established based on MATLAB R2019a curve fitting tool. The New model results corroborated with the experimental. In addition, the models performance evaluation results showed that the New model had higher coefficient of determination ( $R^2 = 0.9965$ ), lower root mean square error ( $RMSE = 24.8$  kg/h), lower absolute residual error ( $\epsilon_r = 0.6\%$ ) and higher simulation performance at 10% residual error ( $\eta_{sim,10\%} = 100\%$ ) than Beverloo, BCP and Tudor model. This implied that the New model was more reliable for simulating MFR of maize grain through horizontal circular orifices compared with Beverloo, BCP and Tudor model.

**Keywords:** Validation, Simulation Models, Mass Flow Rate, Maize Grain, Horizontal Circular Orifices

---

## Appendix H: Published Paper on Objective Two

Korir, M. K., Njue, M. R., & Nyaanga, D. M. (2022). Effect of Initial Moisture Content of Maize Grain on Moisture Removal Rate and Energy Used in Experimental Vertical Pneumatic Dryer. *Bioprocess Engineering*, 6(2), 34-39.

---

### Bioprocess Engineering

2022; 6(2): 34-39

<http://www.sciencepublishinggroup.com/j/be>

doi: 10.11648/j.be.20220602.15

ISSN: 2578-8698 (Print); ISSN: 2578-8701 (Online)

---



## Effect of Initial Moisture Content of Maize Grain on Moisture Removal Rate and Energy Used in Experimental Vertical Pneumatic Dryer

Meshack Kipruto Korir\*, Musa Rugiri Njue, Daudi Mongeri Nyaanga

Department of Agricultural Engineering, Faculty of Engineering and Technology, Egerton University, Nakuru, Kenya

### Email address:

meshack.korir@egerton.ac.ke (Meshack Kipruto Korir), mrugiri@egerton.ac.ke (Musa Rugiri Njue),

dmnyaanga@egerton.ac.ke (Daudi Mongeri Nyaanga)

\*Corresponding author

### To cite this article:

Meshack Kipruto Korir, Musa Rugiri Njue, Daudi Mongeri Nyaanga. Effect of Initial Moisture Content of Maize Grain on Moisture Removal Rate and Energy Used in Experimental Vertical Pneumatic Dryer. *Bioprocess Engineering*. Vol. 6, No. 2, 2022, pp. 34-39.

doi: 10.11648/j.be.20220602.15

**Received:** October 28, 2022; **Accepted:** November 28, 2022; **Published:** December 8, 2022

---


**Abstract:** Maize is a staple food and source of income in Kenya. However, postharvest losses are estimated at 12% to 20% of the national total output primarily due to high moisture storage. Drying to safe level of 13.5% before storage is essential. One of the main factors which influence drying process is initial moisture content (MC) of the grain. Therefore, this paper presents the effect of initial MC of maize grain on moisture removal rate (MRR) and energy used in drying. The experiments were based on selected initial MC levels of 20%, 25% and 30%, wet basis (wb). The first experiment involved loading experimental vertical pneumatic dryer with 70.0 kg of wet maize grain with initial MC of 20%. The grain was then dried for 2 hours as MRR and energy used monitored at an interval of 15 minutes. The grain and drying air mass flow rate was controlled at 771 kg/h and 547 kg/h, respectively. The plenum chamber air temperature was maintained at 70°C using proportional integral derivative controller. The maize grain variety used was hybrid 614 sourced from a farmer in Njoro sub-County, Nakuru County, Kenya. Similar experiments were repeated but using maize grain with initial MC of 25% and 30%, wb. The MC of 20%, 25% and 30% were obtained by rewetting maize grain with initial MC of 11.4% (wb) in tap water at a temperature of 18°C for 0.75 hours, 1.75 hours and 5.75 hours, respectively. The MRR results ranged from 0.0914 kg/kg.h to 0.0357 kg/kg.h for maize grain with initial MC of 20%, 0.1043 kg/kg.h to 0.0556 kg/kg.h for 25% and 0.1185 kg/kg.h to 0.0705 kg/kg.h for 30%. The energy used for air heating ( $E_a$ ) for each level of MC was 10.5 kWh. The energy used for grain transportation ( $E_g$ ) was 4.6 kWh for MC of 20%, 4.8 kWh for 25% and 5.0 kWh for 30%. Data analysis results showed that the initial MC of the maize grain had significant effect ( $P < 0.05$ ) on MRR. However, the effect of initial MC on  $E_a$  and  $E_g$  was not significant ( $P > 0.05$ ).

**Keywords:** Initial Moisture Content, Maize Grain, Moisture Removal Rate, Energy Used in Drying, Pneumatic Dryer

---




# Appendix I: Research Permit

  
REPUBLIC OF KENYA

**Ref No: 497618**


**RESEARCH LICENSE**




**This is to Certify that Mr.. Meshack Kipruto Korir of Egerton University, has been licensed to conduct research in Nakuru on the topic: Optimisation of drying rate and energy use in an experimental vertical pneumatic maize dryer for the period ending : 26/April/2022.**

**License No: NACOSTI/P/21/10264**

**497618**  
**Applicant Identification Number**

  
**Director General**  
**NATIONAL COMMISSION FOR SCIENCE, TECHNOLOGY & INNOVATION**

**Verification QR Code**



**NOTE: This is a computer generated License. To verify the authenticity of this document, Scan the QR Code using QR scanner application.**